

**ENHANCED DISTORTION INTERACTIVE VIEWER  
FOR GRIDS (EDIG)**

BY

**Badr Mohammed Al Harbi**

A Thesis Presented to the  
DEANSHIP OF GRADUATE STUDIES

**KING FAHD UNIVERSITY OF PETROLEUM & MINERALS**

DHAHRAN, SAUDI ARABIA

In Partial Fulfillment of the  
Requirements for the Degree of

**MASTER OF SCIENCE**

In

**COMPUTER SCIENCE**

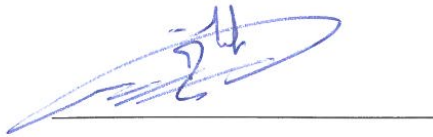
**May 2016**

KING FAHD UNIVERSITY OF PETROLEUM & MINERALS

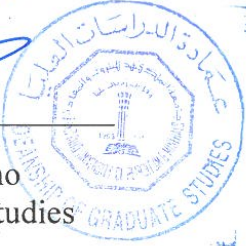

DHAHRAN- 31261, SAUDI ARABIA

**DEANSHIP OF GRADUATE STUDIES**

This thesis, written by Badr Mohammed Al Harbi under the direction of his thesis advisor and approved by his thesis committee, has been presented and accepted by the Dean of Graduate Studies, in partial fulfillment of the requirements for the degree of the Master of Science (MS) in Computer Science.

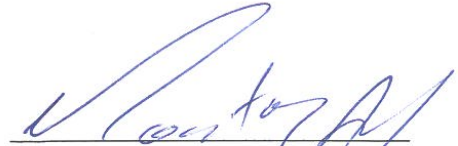


Dr. Khalid A. Aljasser  
Department Chairman



Dr. Salam A. Zummo  
Dean of Graduate Studies

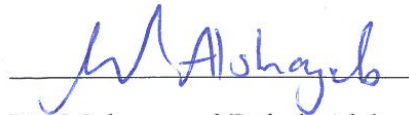
4/1/17  
Date



Dr. Moataz Ahmed  
(Committee Chairman)



Dr. Adel Fadhl Ahmed  
(Advisor)



Dr. Mohammad Rabah Alshayeb  
(Member)



Dr. Musab Alturki  
(Member)



Dr. Ali Alturki  
(Member)

© Badr Mohammed Al Harbi

2016



IN THE NAME OF ALLAH, THE MOST GRACIOUS, THE MOST MERCIFUL



I dedicate this thesis

To my parents whom I look up to

To my wife who has gave me courage and support

To my children Hala, Albarra, and Ghala whom are the joy in my life

And to all supporting people in my life.

## ACKNOWLEDGMENTS

Imagining and shaping this research was a long and intensive effort. Nevertheless, it was a gratifying journey due to the guidance and support provided by many talented individuals and generous institutions that I am happy to acknowledge them here.

I would like to express my sincere appreciation to my Committee Chairman Dr. Adel Fadhil Ahmed. He has been the catalyst for providing the initial idea, the mentor on the progression of the research to tackle larger scope, and the guide during venturing in a new frontier.

I also wish to thank my advisor Dr. Moataz Ahmed for his consistent effort to maintain a high level of quality. I appreciate the time he gave me from his busy schedule to review progress and provide support and contribution to the research.

I would also like to express my deep appreciation to my thesis committee members. Dr. Mohammad Rabah Alshayeb for his helpful insight in the process of developing the study metrics and validation process. Dr. Musab Alturki for his helpful feedback and comments throughout the research and the implementation. Dr. Ali Alturki for his valuable contribution in the technical writing of the thesis and the input on the application of this research in the Petroleum Engineering domain.

In addition, I would like to thank my friend Dr. Mubarak Dossary for his helpful assistance.

I also thank Reservoir Simulation Systems Division management and personnel in Saudi Aramco for their support. I am thankful for all the support I have received from King Fahad University of Petroleum & Minerals in completing all work required for this thesis.

# TABLE OF CONTENTS

ACKNOWLEDGMENTS .....	VI
TABLE OF CONTENTS .....	VII
LIST OF TABLES .....	XII
LIST OF FIGURES .....	XVI
LIST OF ABBREVIATIONS .....	XXXII
ABSTRACT .....	XXXIII
ملخص الرسالة.....	XXXV
CHAPTER 1 INTRODUCTION .....	1
1.1 Motivation.....	2
1.1.1 Analysis of massive data sizes .....	3
1.1.2 Reveal.....	3
1.1.3 Aesthetics for Scientific Visualization .....	4
1.1.4 Detailed view in Global context .....	4
1.2 Objective .....	5
1.3 Contribution .....	6
1.3.1 Visualization Survey.....	6
1.3.2 Detail-in-Context implementation .....	7
1.3.3 Visual and Aesthetics Measurement .....	7
1.3.4 Developing a workflow to perform aesthetics optimization .....	8
1.3.5 Real Time Interactive rendering using GPGPU .....	8

1.4	Organization of The Thesis .....	9
<b>CHAPTER 2 LITERATURE REVIEW .....</b>		<b>10</b>
2.1	Data Revealing Visualization .....	11
2.2	Detail-in-Context Visualization.....	18
2.3	Perception and Design Principles .....	25
2.3.1	Perception levels .....	25
2.3.2	Perception Principles .....	26
2.3.3	Norman Principles .....	29
2.3.4	Design and Guidelines for Displaying Quantitative Information .....	32
2.4	Metrics and Visualizations .....	33
2.5	Validation for Graph Aesthetics Metrics.....	38
<b>CHAPTER 3 METHODOLOGY AND APPROACH .....</b>		<b>40</b>
3.1	The Research Process.....	40
3.2	Methodology .....	40
3.3	Approach .....	41
3.4	Research Flow.....	42
3.5	Research design .....	45
3.6	Input Data Visualization.....	45
3.7	Analysis data .....	45
3.8	Experiments.....	45
3.9	Possible threat to validity .....	46
<b>CHAPTER 4 IMPLEMENTATION .....</b>		<b>47</b>
4.1	Visual Access .....	47
4.1.1	Displacement Function .....	48



4.1.2	Distortion Function .....	48
4.1.3	Focus and Pivot Point.....	49
4.1.4	Camera Position and Direction.....	50
4.2	ENHANCED DISTORTION INTERACTIVE VIEWER FOR GRIDS (EDIG) .....	50
4.2.1	3D Detail-In-Context Techniques.....	50
4.2.2	Focus Area and distance of the affected area .....	51
4.2.3	Stacked Cells.....	51
4.2.4	Focus Emphasizing Function.....	51
4.3	Optimization Framework .....	52
4.3.1	Generate Combinations .....	52
4.3.2	Visualize using eDIG Viewer .....	52
4.3.3	Metrics .....	53
4.3.4	Optimization & Results .....	53
4.3.5	Data Extractions and Reports.....	53
4.4	Aesthetic and Utility Metrics.....	54
4.4.1	Face Conformal Energy (FCE).....	54
4.4.2	Visible Cells.....	57
4.5	Ratio of Used Space (RUS).....	60
4.5.1	Average Relative Change of Mean Curvature (RCMC).....	61
4.5.2	Combined RUS & RCMC .....	61
<b>CHAPTER 5 EXPERIMENTS &amp; RESULTS .....</b>		<b>63</b>
5.1	Hydrocarbon Reservoir Dataset .....	63
5.2	Experiment Setup .....	63
5.3	Lenses Included in The Experiments.....	64
5.4	Results.....	65

5.5	Discussion .....	66
5.5.1	Base Case Analysis .....	66
5.5.2	Number of visible cells (NVC) .....	67
5.5.3	Face Conformal Energy Metric (FCE).....	70
5.5.4	Ratio of Used Space (RUS).....	72
5.5.5	Average Relative Change of Mean Curvature (RCMC).....	73
5.5.6	Combined Ratio of Used Space & Average Relative Change of Mean Curvature .....	74
5.6	Summary of Results .....	77
5.6.1	Highest Correlation Values.....	77
5.6.2	Highest objective function results .....	78
5.6.3	Observation on the input parameters .....	79
<b>CHAPTER 6 SURVEY &amp; VALIDATION.....</b>		<b>82</b>
6.1	Questionnaire.....	82
6.2	Survey results and Analysis .....	83
6.3	Distance and Camera Angles .....	83
6.4	Z Axis Exaggeration .....	83
6.5	XY & XYZ Displacement Function .....	84
6.6	Distortion Function .....	84
6.7	Number of Visible Cells (NVC) .....	85
6.8	Ratio of Used Space (RUS).....	85
6.9	Curvature Analysis (FCE & RCMC).....	86
6.10	Combined Metric (RUS & RCMC) .....	86
6.11	View Automation.....	87
<b>CHAPTER 7 CONCLUSION .....</b>		<b>88</b>

<b>REFERENCES.....</b>	<b>90</b>
<b>APPENDIX.....</b>	<b>98</b>
<b>VITAE.....</b>	<b>174</b>

## LIST OF TABLES

Table 1: Literature Review Summary of Detail-in-context volumetric visualization lenses.....	24
Table 2: Default Lens Parameters.....	64
Table 3: Base Case Analysis.....	65
Table 4: Summary of highest correlation values between the objective function and input parameters.....	77
Table 5: Summary of highest results obtained from objective functions and input parameters.....	78
Table 6: The Gaussian parameter & Number of Visible Cells Correlation per experiment .....	98
Table 7: The Gaussian parameter & Number of Visible Cells Min Max per experiment	98
Table 8: Camera Distance & Number of Visible Cells Correlation per experiment .....	101
Table 9: Camera Distance & Number of Visible Cells Min Max per experiment .....	101
Table 10: Z Exaggeration & Number of Visible Cells Correlation per experiment.....	104
Table 11: Z Exaggeration & Number of Visible Cells Min Max per experiment .....	104
Table 12: XY Displacement & Number of Visible Cells Correlation per experiment...	107
Table 13: XY Displacement & Number of Visible Cells Min Max per experiment .....	107
Table 14: XYZ Displacement & Number of Visible Cells Correlation per experiment	110
Table 15: XYZ Displacement & Number of Visible Cells Min Max per experiment....	110
Table 16: The Gaussian parameter & Face Conformal Energy Correlation per experiment .....	113



Table 17: The Gaussian parameter & Face Conformal Energy Min Max per experiment .....	113
Table 18: Camera Distance & Face Conformal Energy Correlation per experiment .....	116
Table 19: Camera Distance & Face Conformal Energy Min Max per experiment .....	116
Table 20: Z Exaggeration & Face Conformal Energy Correlation per experiment.....	119
Table 21: Z Exaggeration & Face Conformal Energy Min Max per experiment.....	119
Table 22: XY Displacement & Face Conformal Energy Correlation per experiment....	122
Table 23: XY Displacement & Face Conformal Energy Min Max per experiment.....	122
Table 24: XYZ Displacement & Face Conformal Energy Correlation per experiment .	125
Table 25: XYZ Displacement & Face Conformal Energy Min Max per experiment ....	125
Table 26: The Gaussian parameter & Ratio of Used Space Correlation per experiment	128
Table 27: The Gaussian parameter & Ratio of Used Space Min Max per experiment ..	128
Table 28: Camera Distance & Ratio of Used Space Correlation per experiment.....	131
Table 29: Camera Distance & Ratio of Used Space Min Max per experiment.....	131
Table 30: Z Exaggeration & Ratio of Used Space Correlation per experiment .....	134
Table 31: Z Exaggeration & Ratio of Used Space Min Max per experiment.....	134
Table 32: XY Displacement & Ratio of Used Space Correlation per experiment .....	137
Table 33: XY Displacement & Ratio of Used Space Min Max per experiment.....	137
Table 34: XYZ Displacement & Ratio of Used Space Correlation per experiment.....	140
Table 35: XYZ Displacement & Ratio of Used Space Min Max per experiment .....	140
Table 36: The Gaussian parameter & Average Relative Change of Mean Curvature Correlation per experiment.....	143

Table 37: The Gaussian parameter & Average Relative Change of Mean Curvature Min Max per experiment .....	143
Table 38: Camera Distance & Average Relative Change of Mean Curvature Correlation per experiment .....	146
Table 39: Camera Distance & Average Relative Change of Mean Curvature Min Max per experiment .....	146
Table 40: Z Exaggeration & Average Relative Change of Mean Curvature Correlation per experiment .....	149
Table 41: Z Exaggeration & Average Relative Change of Mean Curvature Min Max per experiment .....	149
Table 42: XY Displacement & Average Relative Change of Mean Curvature Correlation per experiment .....	152
Table 43: XY Displacement & Average Relative Change of Mean Curvature Min Max per experiment .....	152
Table 44: XYZ Displacement & Average Relative Change of Mean Curvature Correlation per experiment .....	155
Table 45: XYZ Displacement & Average Relative Change of Mean Curvature Min Max per experiment .....	155
Table 46: The Gaussian parameter & Combined Ratio of Used Space & Average Relative Change of Mean Curvature Correlation per experiment .....	158
Table 47: The Gaussian parameter & Combined Ratio of Used Space & Average Relative Change of Mean Curvature Min Max per experiment .....	159

Table 48: Camera Distance & Combined Ratio of Used Space & Average Relative	
Change of Mean Curvature Correlation per experiment .....	161
Table 49: Camera Distance & Combined Ratio of Used Space & Average Relative	
Change of Mean Curvature Min Max per experiment.....	162
Table 50: Z Exaggeration & Combined Ratio of Used Space & Average Relative	
Change of Mean Curvature Correlation per experiment .....	164
Table 51: Z Exaggeration & Combined Ratio of Used Space & Average Relative	
Change of Mean Curvature Min Max per experiment.....	165
Table 52: XY Displacement & Combined Ratio of Used Space & Average Relative	
Change of Mean Curvature Correlation per experiment .....	167
Table 53: XY Displacement & Combined Ratio of Used Space & Average Relative	
Change of Mean Curvature Min Max per experiment.....	168
Table 54: XYZ Displacement & Combined Ratio of Used Space & Average Relative	
Change of Mean Curvature Correlation per experiment .....	170
Table 55: XYZ Displacement & Combined Ratio of Used Space & Average Relative	
Change of Mean Curvature Min Max per experiment.....	171

## LIST OF FIGURES

Figure 1 Sample 3D Hydrocarbon Reservoir Grid Data Set colored by depth.....	2
Figure 2 Full Reservoir Simulation Grid .....	12
Figure 3 The left image shows a raw slice, middle image shows a column, and the image on the right shows a layer.....	13
Figure 4 Visual Access Method being applied from different angles .....	23
Figure 5 Graph Layout on the left is a random graph layout and on the right is a graph layout that minimize edge crossing.....	34
Figure 6 Approach Flow Chart .....	43
Figure 7 Sample 3D Hydrocarbon Reservoir Grid Data Set colored by depth.....	47
Figure 8 Displacement Function.....	48
Figure 9 Distortion Function.....	48
Figure 10 Visual Access Method.....	49
Figure 11 on the left is a corner view of the data and on the right is the same view after applying distortion and displacement .....	49
Figure 12 Developed Framework .....	52
Figure 13 The left figure present the delta Tangent at a curve and the right figure shows the principle curveture .....	54
Figure 14 The FCE metric uses the curvature analysis, on the left is the original data in the middle is the data colored by principle curvature, and on the right is the 2D color map.....	55
Figure 15 Face Energy Conformal Process. The curvature analysis is used to compute the energy applied to change the shape.....	57



Figure 16 (a) shows the frustum in action while (b) shows how rays trace cover the data in the space .....	58
Figure 17 These figures shows how the new algorithm of shadow casting works.....	59
Figure 18 Visible Cells Test (b) shows the results of visibility test on connected surface and (c) and (d) shows visibility test on disconnected surface .....	60
Figure 19 Ratio of Used Space: (a) shows the full space is used while (b) shows that part of the space is used .....	61
Figure 20 X & Y Angle, The Gaussian parameter,X Angle,Y Angle, Number of Visible Cells.....	68
Figure 21 X & Y Angle, Z Exaggeration, X Angle, Y Angle, Number of Visible Cells .	69
Figure 22 X & Y Angle, Camera Distance, X Angle, Y Angle, using Ratio of Used Space .....	73
Figure 23 X & Y Angle, The Gaussian parameter, X Angle, Y Angle, Combined Ratio of Used Space & Average Relative Change of Mean Curvature .....	75
Figure 24 X & Y Angle, XYZ Displacement, X Angle, Y Angle, Combined Ratio of Used Space & Average Relative Change of Mean Curvature .....	76
Figure 25 Z Axis Exaggeration.....	80
Figure 26 Survey Results .....	87
Figure 27: Top & 45: The Gaussian parameter & Number of Visible Cells .....	99
Figure 28: X & Y Angles The Gaussian parameter & Number of Visible Cells.....	99
Figure 29: 3D Case 1: Top, The Gaussian parameter, Number of Visible Cells.....	100
Figure 30: 3D Case 2: Top, The Gaussian parameter, Number of Visible Cells.....	100
Figure 31: 3D Case 1: 45, The Gaussian parameter, Number of Visible Cells .....	100

Figure 32: 3D Case 2: 45, The Gaussian parameter, Number of Visible Cells .....	100
Figure 33: 3D Case 1: X & Y Angle, The Gaussian parameter, X Angle, Y Angle, Number of Visible Cells .....	101
Figure 34: 3D Case 2: X & Y Angle, The Gaussian parameter, X Angle, Y Angle, Number of Visible Cells .....	101
Figure 35: Top & 45: Camera Distance & Number of Visible Cells.....	102
Figure 36: X & Y Angles Camera Distance & Number of Visible Cells.....	102
Figure 37: 3D Case 1: Top, Camera Distance, Number of Visible Cells .....	103
Figure 38: 3D Case 2: Top, Camera Distance, Number of Visible Cells.....	103
Figure 39: 3D Case 1: 45, Camera Distance, Number of Visible Cells.....	103
Figure 40: 3D Case 2: 45, Camera Distance, Number of Visible Cells.....	103
Figure 41: 3D Case 1: X & Y Angle, Camera Distance, X Angle, Y Angle, Number of Visible Cells .....	104
Figure 42: 3D Case 2: X & Y Angle, Camera Distance, X Angle, Y Angle, Number of Visible Cells .....	104
Figure 43: Top & 45: Z Exaggeration & Number of Visible Cells .....	105
Figure 44: X & Y Angles Z Exaggeration & Number of Visible Cells.....	105
Figure 45: 3D Case 1: Top, Z Exaggeration, Number of Visible Cells.....	106
Figure 46: 3D Case 2: Top, Z Exaggeration, Number of Visible Cells.....	106
Figure 47: 3D Case 1: 45, Z Exaggeration, Number of Visible Cells .....	106
Figure 48: 3D Case 2: 45, Z Exaggeration, Number of Visible Cells .....	106
Figure 49: 3D Case 1: X & Y Angle, Z Exaggeration, X Angle, Y Angle, Number of Visible Cells.....	107

Figure 50: 3D Case 2: X & Y Angle, Z Exaggeration, X Angle, Y Angle, Number of Visible Cells.....	107
Figure 51: Top & 45: XY Displacement & Number of Visible Cells .....	108
Figure 52: X & Y Angles XY Displacement & Number of Visible Cells.....	108
Figure 53: 3D Case 1: Top, XY Displacement, Number of Visible Cells.....	109
Figure 54: 3D Case 2: Top, XY Displacement, Number of Visible Cells.....	109
Figure 55: 3D Case 1: 45, XY Displacement, Number of Visible Cells .....	109
Figure 56: 3D Case 2: 45, XY Displacement, Number of Visible Cells .....	109
Figure 57: 3D Case 1: X & Y Angle, XY Displacement, X Angle, Y Angle, Number of Visible Cells .....	110
Figure 58: 3D Case 2: X & Y Angle, XY Displacement, X Angle, Y Angle, Number of Visible Cells .....	110
Figure 59: Top & 45: XYZ Displacement & Number of Visible Cells.....	111
Figure 60: X & Y Angles XYZ Displacement & Number of Visible Cells .....	111
Figure 61: 3D Case 1: Top, XYZ Displacement, Number of Visible Cells .....	112
Figure 62: 3D Case 2: Top, XYZ Displacement, Number of Visible Cells .....	112
Figure 63: 3D Case 1: 45, XYZ Displacement, Number of Visible Cells.....	112
Figure 64: 3D Case 2: 45, XYZ Displacement, Number of Visible Cells.....	112
Figure 65: 3D Case 1: X & Y Angle, XYZ Displacement, X Angle, Y Angle, Number of Visible Cells .....	113
Figure 66: 3D Case 2: X & Y Angle, XYZ Displacement, X Angle, Y Angle, Number of Visible Cells .....	113
Figure 67: Top & 45: The Gaussian parameter & Face Conformal Energy.....	114

Figure 68: X & Y Angles The Gaussian parameter & Face Conformal Energy .....	114
Figure 69: 3D Case 1: Top, The Gaussian parameter, Face Conformal Energy .....	115
Figure 70: 3D Case 2: Top, The Gaussian parameter, Face Conformal Energy .....	115
Figure 71: 3D Case 1: 45, The Gaussian parameter, Face Conformal Energy .....	115
Figure 72: 3D Case 2: 45, The Gaussian parameter, Face Conformal Energy .....	115
Figure 73: 3D Case 1: X & Y Angle, The Gaussian parameter, X Angle, Y Angle, Face Conformal Energy .....	116
Figure 74: 3D Case 2: X & Y Angle, The Gaussian parameter, X Angle, Y Angle, Face Conformal Energy .....	116
Figure 75: Top & 45: Camera Distance & Face Conformal Energy .....	117
Figure 76: X & Y Angles Camera Distance & Face Conformal Energy .....	117
Figure 77: 3D Case 1: Top, Camera Distance, Face Conformal Energy .....	118
Figure 78: 3D Case 2: Top, Camera Distance, Face Conformal Energy .....	118
Figure 79: 3D Case 1: 45, Camera Distance, Face Conformal Energy .....	118
Figure 80: 3D Case 2: 45, Camera Distance, Face Conformal Energy .....	118
Figure 81: 3D Case 1: X & Y Angle, Camera Distance, X Angle, Y Angle, Face Conformal Energy .....	119
Figure 82: 3D Case 2: X & Y Angle, Camera Distance, X Angle, Y Angle, Face Conformal Energy .....	119
Figure 83: Top & 45: Z Exaggeration & Face Conformal Energy .....	120
Figure 84: X & Y Angles Z Exaggeration & Face Conformal Energy .....	120
Figure 85: 3D Case 1: Top, Z Exaggeration, Face Conformal Energy .....	121
Figure 86: 3D Case 2: Top, Z Exaggeration, Face Conformal Energy .....	121

Figure 87: 3D Case 1: 45, Z Exaggeration, Face Conformal Energy .....	121
Figure 88: 3D Case 2: 45, Z Exaggeration, Face Conformal Energy .....	121
Figure 89: 3D Case 1: X & Y Angle, Z Exaggeration, X Angle, Y Angle, Face Conformal Energy .....	122
Figure 90: 3D Case 2: X & Y Angle, Z Exaggeration, X Angle, Y Angle, Face Conformal Energy .....	122
Figure 91: Top & 45: XY Displacement & Face Conformal Energy .....	123
Figure 92: X & Y Angles XY Displacement & Face Conformal Energy .....	123
Figure 93: 3D Case 1: Top, XY Displacement, Face Conformal Energy.....	124
Figure 94: 3D Case 2: Top, XY Displacement, Face Conformal Energy.....	124
Figure 95: 3D Case 1: 45, XY Displacement, Face Conformal Energy .....	124
Figure 96: 3D Case 2: 45, XY Displacement, Face Conformal Energy .....	124
Figure 97: 3D Case 1: X & Y Angle, XY Displacement, X Angle, Y Angle, Face Conformal Energy .....	125
Figure 98: 3D Case 2: X & Y Angle, XY Displacement, X Angle, Y Angle, Face Conformal Energy .....	125
Figure 99: Top & 45: XYZ Displacement & Face Conformal Energy.....	126
Figure 100: X & Y Angles XYZ Displacement & Face Conformal Energy .....	126
Figure 101: 3D Case 1: Top, XYZ Displacement, Face Conformal Energy .....	127
Figure 102: 3D Case 2: Top, XYZ Displacement, Face Conformal Energy .....	127
Figure 103: 3D Case 1: 45, XYZ Displacement, Face Conformal Energy.....	127
Figure 104: 3D Case 2: 45, XYZ Displacement, Face Conformal Energy.....	127

Figure 105: 3D Case 1: X & Y Angle, XYZ Displacement, X Angle, Y Angle, Face Conformal Energy.....	128
Figure 106: 3D Case 2: X & Y Angle, XYZ Displacement, X Angle, Y Angle, Face Conformal Energy.....	128
Figure 107: Top & 45: The Gaussian parameter & Ratio of Used Space.....	129
Figure 108: X & Y Angles The Gaussian parameter & Ratio of Used Space .....	129
Figure 109: 3D Case 1: Top, The Gaussian parameter, Ratio of Used Space .....	130
Figure 110: 3D Case 2: Top, The Gaussian parameter, Ratio of Used Space .....	130
Figure 111: 3D Case 1: 45, The Gaussian parameter, Ratio of Used Space.....	130
Figure 112: 3D Case 2: 45, The Gaussian parameter, Ratio of Used Space.....	130
Figure 113: 3D Case 1: X & Y Angle, The Gaussian parameter, X Angle, Y Angle, Ratio of Used Space.....	131
Figure 114: 3D Case 2: X & Y Angle, The Gaussian parameter, X Angle, Y Angle, Ratio of Used Space.....	131
Figure 115: Top & 45: Camera Distance & Ratio of Used Space .....	132
Figure 116: X & Y Angles Camera Distance & Ratio of Used Space .....	132
Figure 117: 3D Case 1: Top, Camera Distance, Ratio of Used Space.....	133
Figure 118: 3D Case 2: Top, Camera Distance, Ratio of Used Space.....	133
Figure 119: 3D Case 1: 45, Camera Distance, Ratio of Used Space .....	133
Figure 120: 3D Case 2: 45, Camera Distance, Ratio of Used Space .....	133
Figure 121: 3D Case 1: X & Y Angle, Camera Distance, X Angle, Y Angle, Ratio of Used Space.....	134

Figure 122: 3D Case 2: X & Y Angle, Camera Distance, X Angle, Y Angle, Ratio of Used Space.....	134
Figure 123: Top & 45: Z Exaggeration & Ratio of Used Space.....	135
Figure 124: X & Y Angles Z Exaggeration & Ratio of Used Space .....	135
Figure 125: 3D Case 1: Top, Z Exaggeration, Ratio of Used Space .....	136
Figure 126: 3D Case 2: Top, Z Exaggeration, Ratio of Used Space .....	136
Figure 127: 3D Case 1: 45, Z Exaggeration, Ratio of Used Space.....	136
Figure 128: 3D Case 2: 45, Z Exaggeration, Ratio of Used Space.....	136
Figure 129: 3D Case 1: X & Y Angle, Z Exaggeration, X Angle, Y Angle, Ratio of Used Space.....	137
Figure 130: 3D Case 2: X & Y Angle, Z Exaggeration, X Angle, Y Angle, Ratio of Used Space.....	137
Figure 131: Top & 45: XY Displacement & Ratio of Used Space.....	138
Figure 132: X & Y Angles XY Displacement & Ratio of Used Space .....	138
Figure 133: 3D Case 1: Top, XY Displacement, Ratio of Used Space .....	139
Figure 134: 3D Case 2: Top, XY Displacement, Ratio of Used Space .....	139
Figure 135: 3D Case 1: 45, XY Displacement, Ratio of Used Space.....	139
Figure 136: 3D Case 2: 45, XY Displacement, Ratio of Used Space.....	139
Figure 137: 3D Case 1: X & Y Angle, XY Displacement, X Angle, Y Angle, Ratio of Used Space.....	140
Figure 138: 3D Case 2: X & Y Angle, XY Displacement, X Angle, Y Angle, Ratio of Used Space.....	140
Figure 139: Top & 45: XYZ Displacement & Ratio of Used Space .....	141

Figure 140: X & Y Angles XYZ Displacement & Ratio of Used Space.....	141
Figure 141: 3D Case 1: Top, XYZ Displacement, Ratio of Used Space.....	142
Figure 142: 3D Case 2: Top, XYZ Displacement, Ratio of Used Space.....	142
Figure 143: 3D Case 1: 45, XYZ Displacement, Ratio of Used Space .....	142
Figure 144: 3D Case 2: 45, XYZ Displacement, Ratio of Used Space .....	142
Figure 145: 3D Case 1: X & Y Angle, XYZ Displacement, X Angle, Y Angle, Ratio of Used Space.....	143
Figure 146: 3D Case 2: X & Y Angle, XYZ Displacement, X Angle, Y Angle, Ratio of Used Space.....	143
Figure 147: Top & 45: The Gaussian parameter & Average Relative Change of Mean Curvature.....	144
Figure 148: X & Y Angles The Gaussian parameter & Average Relative Change of Mean Curvature .....	144
Figure 149: 3D Case 1: Top, The Gaussian parameter, Average Relative Change of Mean Curvature .....	145
Figure 150: 3D Case 2: Top, The Gaussian parameter, Average Relative Change of Mean Curvature .....	145
Figure 151: 3D Case 1: 45, The Gaussian parameter, Average Relative Change of Mean Curvature .....	145
Figure 152: 3D Case 2: 45, The Gaussian parameter, Average Relative Change of Mean Curvature.....	145
Figure 153: 3D Case 1: X & Y Angle, The Gaussian parameter, X Angle, Y Angle, Average Relative Change of Mean Curvature .....	146



Figure 154: 3D Case 2: X & Y Angle, The Gaussian parameter, X Angle, Y Angle, Average Relative Change of Mean Curvature .....	146
Figure 155: Top & 45: Camera Distance & Average Relative Change of Mean Curvature.....	147
Figure 156: X & Y Angles Camera Distance & Average Relative Change of Mean Curvature.....	147
Figure 157: 3D Case 1: Top, Camera Distance, Average Relative Change of Mean Curvature.....	148
Figure 158: 3D Case 2: Top, Camera Distance, Average Relative Change of Mean Curvature.....	148
Figure 159: 3D Case 1: 45, Camera Distance, Average Relative Change of Mean Curvature.....	148
Figure 160: 3D Case 2: 45, Camera Distance, Average Relative Change of Mean Curvature.....	148
Figure 161: 3D Case 1: X & Y Angle, Camera Distance, X Angle, Y Angle, Average Relative Change of Mean Curvature.....	149
Figure 162: 3D Case 2: X & Y Angle, Camera Distance, X Angle, Y Angle, Average Relative Change of Mean Curvature.....	149
Figure 163: Top & 45: Z Exaggeration & Average Relative Change of Mean Curvature.....	150
Figure 164: X & Y Angles Z Exaggeration & Average Relative Change of Mean Curvature.....	150

Figure 165: 3D Case 1: Top, Z Exaggeration, Average Relative Change of Mean Curvature.....	151
Figure 166: 3D Case 2: Top, Z Exaggeration, Average Relative Change of Mean Curvature.....	151
Figure 167: 3D Case 1: 45, Z Exaggeration, Average Relative Change of Mean Curvature.....	151
Figure 168: 3D Case 2: 45, Z Exaggeration, Average Relative Change of Mean Curvature.....	151
Figure 169: 3D Case 1: X & Y Angle, Z Exaggeration, X Angle, Y Angle, Average Relative Change of Mean Curvature.....	152
Figure 170: 3D Case 2: X & Y Angle, Z Exaggeration, X Angle, Y Angle, Average Relative Change of Mean Curvature.....	152
Figure 171: Top & 45: XY Displacement & Average Relative Change of Mean Curvature.....	153
Figure 172: X & Y Angles XY Displacement & Average Relative Change of Mean Curvature.....	153
Figure 173: 3D Case 1: Top, XY Displacement, Average Relative Change of Mean Curvature.....	154
Figure 174: 3D Case 2: Top, XY Displacement, Average Relative Change of Mean Curvature.....	154
Figure 175: 3D Case 1: 45, XY Displacement, Average Relative Change of Mean Curvature.....	154

Figure 176: 3D Case 2: 45, XY Displacement, Average Relative Change of Mean Curvature.....	154
Figure 177: 3D Case 1: X & Y Angle, XY Displacement, X Angle, Y Angle, Average Relative Change of Mean Curvature.....	155
Figure 178: 3D Case 2: X & Y Angle, XY Displacement, X Angle, Y Angle, Average Relative Change of Mean Curvature.....	155
Figure 179: Top & 45: XYZ Displacement & Average Relative Change of Mean Curvature.....	156
Figure 180: X & Y Angles XYZ Displacement & Average Relative Change of Mean Curvature.....	156
Figure 181: 3D Case 1: Top, XYZ Displacement, Average Relative Change of Mean Curvature.....	157
Figure 182: 3D Case 2: Top, XYZ Displacement, Average Relative Change of Mean Curvature.....	157
Figure 183: 3D Case 1: 45, XYZ Displacement, Average Relative Change of Mean Curvature.....	157
Figure 184: 3D Case 2: 45, XYZ Displacement, Average Relative Change of Mean Curvature.....	157
Figure 185: 3D Case 1: X & Y Angle, XYZ Displacement, X Angle, Y Angle, Average Relative Change of Mean Curvature .....	158
Figure 186: 3D Case 2: X & Y Angle, XYZ Displacement, X Angle, Y Angle, Average Relative Change of Mean Curvature .....	158

Figure 187: Top & 45: The Gaussian parameter & Combined Ratio of Used Space & Average Relative Change of Mean Curvature .....	159
Figure 188: X & Y Angles The Gaussian parameter & Combined Ratio of Used Space & Average Relative Change of Mean Curvature .....	159
Figure 189: 3D Case 1: Top, The Gaussian parameter, Combined Ratio of Used Space & Average Relative Change of Mean Curvature .....	160
Figure 190: 3D Case 2: Top, The Gaussian parameter, Combined Ratio of Used Space & Average Relative Change of Mean Curvature .....	160
Figure 191: 3D Case 1: 45, The Gaussian parameter, Combined Ratio of Used Space & Average Relative Change of Mean Curvature .....	160
Figure 192: 3D Case 2: 45, The Gaussian parameter, Combined Ratio of Used Space & Average Relative Change of Mean Curvature .....	160
Figure 193: 3D Case 1: X & Y Angle, The Gaussian parameter, X Angle, Y Angle, Combined Ratio of Used Space & Average Relative Change of Mean Curvature.....	161
Figure 194: 3D Case 2: X & Y Angle, The Gaussian parameter, X Angle, Y Angle, Combined Ratio of Used Space & Average Relative Change of Mean Curvature.....	161
Figure 195: Top & 45: Camera Distance & Combined Ratio of Used Space & Average Relative Change of Mean Curvature.....	162
Figure 196: X & Y Angles Camera Distance & Combined Ratio of Used Space & Average Relative Change of Mean Curvature .....	162

Figure 197: 3D Case 1: Top, Camera Distance, Combined Ratio of Used Space & Average Relative Change of Mean Curvature .....	163
Figure 198: 3D Case 2: Top, Camera Distance, Combined Ratio of Used Space & Average Relative Change of Mean Curvature .....	163
Figure 199: 3D Case 1: 45, Camera Distance, Combined Ratio of Used Space & Average Relative Change of Mean Curvature .....	163
Figure 200: 3D Case 2: 45, Camera Distance, Combined Ratio of Used Space & Average Relative Change of Mean Curvature .....	163
Figure 201: 3D Case 1: X & Y Angle, Camera Distance, X Angle, Y Angle, Combined Ratio of Used Space & Average Relative Change of Mean Curvature .....	164
Figure 202: 3D Case 2: X & Y Angle, Camera Distance, X Angle, Y Angle, Combined Ratio of Used Space & Average Relative Change of Mean Curvature .....	164
Figure 203: Top & 45: Z Exaggeration & Combined Ratio of Used Space & Average Relative Change of Mean Curvature.....	165
Figure 204: X & Y Angles Z Exaggeration & Combined Ratio of Used Space & Average Relative Change of Mean Curvature .....	165
Figure 205: 3D Case 1: Top, Z Exaggeration, Combined Ratio of Used Space & Average Relative Change of Mean Curvature .....	166
Figure 206: 3D Case 2: Top, Z Exaggeration, Combined Ratio of Used Space & Average Relative Change of Mean Curvature .....	166
Figure 207: 3D Case 1: 45, Z Exaggeration, Combined Ratio of Used Space & Average Relative Change of Mean Curvature .....	166

Figure 208: 3D Case 2: 45, Z Exaggeration, Combined Ratio of Used Space & Average Relative Change of Mean Curvature .....	166
Figure 209: 3D Case 1: X & Y Angle, Z Exaggeration, X Angle, Y Angle, Combined Ratio of Used Space & Average Relative Change of Mean Curvature .....	167
Figure 210: 3D Case 2: X & Y Angle, Z Exaggeration, X Angle, Y Angle, Combined Ratio of Used Space & Average Relative Change of Mean Curvature .....	167
Figure 211: Top & 45: XY Displacement & Combined Ratio of Used Space & Average Relative Change of Mean Curvature .....	168
Figure 212: X & Y Angles XY Displacement & Combined Ratio of Used Space & Average Relative Change of Mean Curvature .....	168
Figure 213: 3D Case 1: Top, XY Displacement, Combined Ratio of Used Space & Average Relative Change of Mean Curvature .....	169
Figure 214: 3D Case 2: Top, XY Displacement, Combined Ratio of Used Space & Average Relative Change of Mean Curvature .....	169
Figure 215: 3D Case 1: 45, XY Displacement, Combined Ratio of Used Space & Average Relative Change of Mean Curvature .....	169
Figure 216: 3D Case 2: 45, XY Displacement, Combined Ratio of Used Space & Average Relative Change of Mean Curvature .....	169
Figure 217: 3D Case 1: X & Y Angle, XY Displacement, X Angle, Y Angle, Combined Ratio of Used Space & Average Relative Change of Mean Curvature.....	170

Figure 218: 3D Case 2: X & Y Angle, XY Displacement, X Angle, Y Angle, Combined Ratio of Used Space & Average Relative Change of Mean Curvature.....	170
Figure 219: Top & 45: XYZ Displacement & Combined Ratio of Used Space & Average Relative Change of Mean Curvature .....	171
Figure 220: X & Y Angles XYZ Displacement & Combined Ratio of Used Space & Average Relative Change of Mean Curvature .....	171
Figure 221: 3D Case 1: Top, XYZ Displacement, Combined Ratio of Used Space & Average Relative Change of Mean Curvature .....	172
Figure 222: 3D Case 2: Top, XYZ Displacement, Combined Ratio of Used Space & Average Relative Change of Mean Curvature .....	172
Figure 223: 3D Case 1: 45, XYZ Displacement, Combined Ratio of Used Space & Average Relative Change of Mean Curvature .....	172
Figure 224: 3D Case 2: 45, XYZ Displacement, Combined Ratio of Used Space & Average Relative Change of Mean Curvature .....	172
Figure 225: 3D Case 1: X & Y Angle, XYZ Displacement, X Angle, Y Angle, Combined Ratio of Used Space & Average Relative Change of Mean Curvature.....	173
Figure 226: 3D Case 2: X & Y Angle, XYZ Displacement, X Angle, Y Angle, Combined Ratio of Used Space & Average Relative Change of Mean Curvature.....	173

## LIST OF ABBREVIATIONS

<b>GPGPU</b>	:	General Purpose Graphical Processing Unit
<b>OpenGL</b>	:	Open Graphics Library
<b>OpenCL</b>	:	Open Computing Language
<b>CPU</b>	:	Central Processing Unit
<b>CFD</b>	:	Computational Fluid Dynamics
<b>HCI</b>	:	Human Computer Interface
<b>SD</b>	:	Standard Deviation



## ABSTRACT

Full Name : Badr Mohammed Al Harbi  
Thesis Title : enhanced Distortion Interactive viewer for Grids (eDIG)  
Major Field : Data Analysis and Visualization  
Date of Degree : May 2016

In the field of scientific data visualization, the use of detail-in-context visualization methods, metrics, and improving perceptions are among the topmost challenges. In this research work, an implementation of a detail-in-context method with five controlling variables using general-purpose graphical processing units (GPGPU) on 3D hydrocarbon reservoir simulation data is presented. We implemented and identified a set of, carefully selected, aesthetics metrics based on perception and design guideline with utility metrics. These metrics are designed to improve perception and enrich the user understanding of the presentation. An optimization framework is introduced to evaluate the performance of the detail-in-context visualization method using the designed metrics. Such an optimization framework is meant to assist in evaluating the metrics and identify whether they can be used to quantify the results of scientific visualization methods. This approach empowered us with the ability to identify which of the metrics had the biggest impact on visualization results and which metrics had the highest correlation to the controlling variables. The conducted experiments in this research identified that the lens parameters with the highest impact on the metrics are XYZ Displacement, Z Axis Exaggeration, and Camera Distance. In addition, shape and space utilization metrics have the highest correlation which help in creating of views that are both relatable to original data set and reduction of unused space.

The conducted survey distinguishes the highly sought visualization features; view optimization, efficient space utilization, and maximization of displayed data and present their limitation.

## ملخص الرسالة

الاسم الكامل: بدر محمد صالح الحربي

عنوان الرسالة: تحويل التصور للبيانات في برنامج تفاعلي

التخصص: علوم وهندسة الحاسب الآلي

تاريخ الدرجة العلمية: مايو 2015

من بين التحديات في مجال التصور العلمي اولا استخدام أساليب التصور بطريقة عرض التفاصيل في سياق البيانات وثانيا قياس أداء طرق التصور العلمي وثالثا تحسين الإدراك الحسي للمعلومات المعروضة. في هذا العمل البحثي، قمنا بتنفيذ طريقة عرض التفاصيل في سياق البيانات مع خمسة متغيرات من خصائص أسلوب العرض باستخدام وحدات المعالجة الرسومية للأغراض العامة (GPGPU) على نموذج الحقول الهيدروكربونية ثلاثية الأبعاد (3D). نفذنا وحددنا مجموعة من المقاييس الجمالية مختارة بعناية، استناداً إلى المبدأ الإدراك الحسي وإرشادات التصميم مع اثنان من المقاييس المساعدة. ونحن قد نفذنا إطار لتقييم أداء أسلوب التصور من التفاصيل في سياق استخدام المقاييس المصممة. وهذا يساعد في تقييم طريقة العرض والمقاييس وتحديد ما إذا كان يمكن استخدامها لقياس نتائج أساليب التصور العلمي. هذا النهج يخول لنا تحديد أثر المقاييس على نتائج التصور. هذه المقاييس مصممة لتحسين الإدراك وإثراء فهم المستخدم وتحسين الإدراك الحسي.

# CHAPTER 1

## INTRODUCTION

The 21<sup>st</sup> century witnessed a tremendous expansion of knowledge and data over the previous centuries. It became necessary to view the collection of data in new ways to link, synthesize and analyze the message faster. Visualization is a set of algorithms and techniques that generate computer images for the purpose of displaying and understanding many types of data; Scientific and engineering data is no exception [1]. Scientific visualizations (SciViz) are the techniques used to display realistic data types for scientists in their respective fields such as medical imagery, pharmaceutical chemistry compounds and computational fluid dynamics (CFD) [1], [2].

Since the advancement of parallel computation, scientific 3D and 4D data produced by measurement tools, such as CAT scan equipment or computer simulators, has increased dramatically in size, and that increase is proportional to the effort and time it takes to analyze and visualize the data. For example, hydrocarbon simulation models have recently reached billion cell model sizes [3]. In addition, the basic way to visualize Computational Fluid Dynamics CFD data is inefficient and ineffective to process massive amount of data and new visualization methods are needed to be developed [4]. Figure 1 is a visualization of a reservoir grid targeted as the sample data for this research.

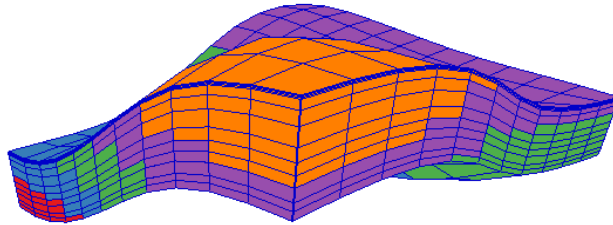


**Figure 1 Sample 3D Hydrocarbon Reservoir Grid Data Set colored by depth**

Scientific visualization is considered a new field since its initial introduction in National Science Foundation report in 1987 [5]. Johnson in 2004 has outlined a set of guidelines and presented several elements that should be considered when designing and developing a new scientific visualization [6]. The purpose of this visualization research is to provide the most effective way to deliver the data to the user. This thesis research targets improving the effectiveness of visualizing massive CFD model data types.

## **1.1 Motivation**

The motivation of pursuing a research in visualization for CFD data originated primarily from the need to reveal more of the relevant data in an effective and efficient manner [6]. Secondly, visualization is a holistic process and even while focusing on view details the full view is needed to have a better perspective of the area of interest. CFD dynamic data is spacious while changes are both locally and globally. In this case, it becomes inconvenient to switch between zoomed view and full view thus, detailed in-context

visualization is needed[6]. Thirdly, scientific visualization is not influenced by aesthetics design principles. New visualization methods exist that uses aesthetics principles that can be applied to improve visual comprehension for scientific data [6]. Fourthly, the model sizes are becoming tremendously large which, adversely, impacts the analysis time. An efficient analysis ways and means are needed [3], [6]. These motivation aspects are discussed in details in this section.

### **1.1.1 Analysis of massive data sizes**

In a visualization of CFD grid data, there are  $I * J * K$  number of gridblocks (cells) to visualize. Typically, views consist of visualizing layers and cross-sections. In the case of layers,  $K$  number of layers are created to view the data. Cross-sectional  $I$  or  $J$  slices are created to view north-south or east-west vertical sections of the grid. To view the full fluid/reservoirs, it takes  $I * J * K$  number of views which is unfeasible due to the huge number of layers or cross-sections in displaying massive model sizes. Thus, a new visualization method is needed for scientific data to increase valuable displayed data.

### **1.1.2 Reveal**

Volumetric data as CAT scan, 3D or 4D seismic volumetric cubes, and CFD 3D models are dense by nature and contains internal valuable information to extract. The basic visualization method is to view the data as a whole grid or as cross-sections views of the whole volumetric data. Whole grid visualization does not present the changes within the CFD volume data, for example. Cross-sections can only present fraction of the full data at a certain time stamp, thus requiring the user to go through all of the sections views to build a representative mental image of the data. Another visualization method is to view sub-cubes of the data showing only a portion of the data (volume). Other researchers have

applied various methods such as data reduction and transparency in an attempt to visualize the data in an efficient manner for analysis. These approaches have proven to reveal limited information, which is becoming more inconvenient and inefficient as data size increases; That is due to the fact that the percentage of revealed data is reduced. Therefore, it is necessary to develop techniques to see the relevant internal and sub data in proper context [6]. In this research, we are investigating various methods to reveal the inner of volumetric data, which is an active research area for scientific and engineering visualization researchers.

### **1.1.3 Aesthetics for Scientific Visualization**

“What is beautiful is usable”, the more appealing the visualization, the more attention it receives [7]. This is applicable for graph and information visualization [8]. On the other hand, scientific visualization is a direct representation of the data that does not utilize design algorithms for automated layout generation. However, the addition of any new visualization method for scientific data for the purpose of maximizing usability of the visualization can benefit from the use of perception and cognition-based principles for visual appeal. Therefore, these principles can be applied to improve the aesthetic appeal of the scientific data in designing visual views that improve reveal and provide detail-in-context visualization.

### **1.1.4 Detailed view in Global context**

CFD data are scientific in nature and they have a shape that simulate the intended target for example aerodynamic simulation or in this case hydrocarbon reservoirs. The data used here consist of static shape and dynamic properties that change in time. Moreover, CFD time dependent data have complex interrelations and are locally and globally change in the

view. To convey the benefit of a detailed simulation data, full grid visualization is required to comprehend the available data in context, for example the complex fluid dynamics near a wellbore at an area of heterogeneous rock properties or bypassing oil due to using low-resolution of the original data [3]. Hence, details of the flow dynamics changes are essential in for small or large scale visual analysis. The purpose of pursuing this visualization method is not to convey the same cell size in 3D space; nonetheless, it is to convey the shape and relation between the focus areas and the neighboring cells in semi sphere.

## **1.2 Objective**

Scientific grid visualization has three main limitations to achieve an efficient analysis time for massive data: does not capitalize on detail in-context methods, low information revealing factor, and perceptual principles have limited usage in designing visualization algorithms, as presented earlier. The objective is to research visualization methods that can improve perception and understanding for CFD visualization for efficient CFD data analysis. The main visualization approach that this research is focusing on implementing is a suitable detail-in-context visualization for CFD grids. In addition, the implemented method should result in improving the reveal ratio of CFD grids and data it encompasses. The second main part of this work is research and study of suitable perceptual principles to implement aesthetics measurements for improving aesthetics aspects of the visualization method. To the best of our knowledge, this is the first research utilizing aesthetics measurements to optimize detail-in-context techniques for scientific grid visualization [6].



This research work is attempting in testing and proving the hypothesis: “if aesthetic quality heuristics are used to measure detail-in-context visualization then it will affect the perceptibility of CFD grids, which in turn can impact understandability”.

### **1.3 Contribution**

The main contribution of this thesis consists of four main aspects. First, present a survey on the visualization method used for CFD grids, the different detail-in-context methods and perceptual principles used for visualization. Second, select and implement a detail-in-context method on 3D reservoir simulation grids. Third, implement a set of aesthetics metrics based on human perception to optimize the aesthetics aspect of the detail-in-context method. The selection, implementation, and analysis of the metrics is the main contribution in this research. Finally, general-purpose graphical processing units (GPGPU) programming languages will be utilized in the implementation of this visualization method.

#### **1.3.1 Visualization Survey**

There are multiple visualization methods developed to reveal data. This work surveys the standard and complex visualization methods in the research to reveal hidden data/information. In addition, the survey will also include the different perceptual designs that are used in information visualization for the purpose of providing improved visual qualities. It has been shown in the literature that the more appealing the visualization the better the understanding is going to be [7].

### **1.3.2 Detail-in-Context implementation**

In this work, Visual Access, a grid detail-in-context method that was developed by Carpendale [9], is selected as the bases for this visualization research and investigated thoroughly for the applicability on scientific data. This method is selected due to the two main functions. First property, the capability to reveal the concealed area of interest within the gridblocks by using a displacement function. The second property is the applied scaling and lens function that provides detail-in-context ability. Carpendale's method is reexamined for the effect of distortion and scaling on the CFD data for scientific visualization to convey data accurately. This research work extends the Visual Access process through the incorporation of design principles and aesthetics measurements to control the transfer functions and to tailor the method for scientific visualization.

### **1.3.3 Visual and Aesthetics Measurement**

In Human Computer Interface (HCI) research area, researchers have concluded that what is beautiful is usable [7]. This principle is applied on visualization perception and spatial graphs layout algorithms. Perceptual principles and aesthetics measurements are minimally used in designing visualization algorithms for scientific data [6]. In this research work, a suitable and optimized set of measurements to optimize aesthetics properties of detail-in-context visualization is studied and developed to improve the performance of grid scientific visualization with visual appeal bases. The development of these measurements is derived from a selection of suitable perceptual and design principles that are applicable for detail-in-context, grid and scientific visualization criteria. Moreover, this research establishes and implements aesthetics measurements based on the selected and developed perceptual and design principles. The visual measurements are combined to form an aesthetics

measurement that provides a unique value for grid visualization. The aesthetics measurement is applied to maximize the visual aesthetics properties of the detail-in-context visualization.

#### **1.3.4 Developing a workflow to perform aesthetics optimization**

A number of optimization experiments are conducted to evaluate various grid visualizations against the multiple visual and aesthetic measurements in this research. The displacement and lens functions are the two visual properties of Visual Access method that are the main focus for aesthetics optimization against perceptual and design principles. In addition, cross-functional evaluation of the aesthetically optimized visualization is conducted to determine the effectiveness and usability. The workflow is a step toward automation of generation of optimal views.

#### **1.3.5 Real Time Interactive rendering using GPGPU**

Massive data visualization is considered one of the top challenges in scientific visualization. This scientific visualization research, GPGPU is used to address the performance of handling massive data [33]. The proposed work is to implement an interactive detail-in-context visualization using the open graphical language (OpenGL) and provide constant efficiency by utilizing the parallel capability of GPGPU for performance enhancement using open computational library (OpenCL). The visual measurements will be implemented in either CPU or GPGPU depending the on measurement needs.

## **1.4 Organization of The Thesis**

The structure of the theses as follows: Chapter 2 is the literature review that goes over visualization lenses, aesthetics, and design guidelines. Chapter 3 discusses the methodology followed in this research and Chapter 4 goes in details over the implementation. Chapter 5 presents the results and explains the analysis whereas Chapter 6 presents the conducted survey and its analysis followed by the conclusion Chapter 7.

## **CHAPTER 2**

### **LITERATURE REVIEW**

This literature review investigates the scientific visualization methods that are used for revealing hidden or concealed data. It covers in depth detail-in-context visualization methods for 2D and 3D data. This is in addition to perception theory and design guidelines and metrics implemented to improve aesthetics. Chapter 2 covers the main uses of aesthetics in visualization. These specific topics are directly related to the objective of this research. The visualization that we are aiming to improve consists of 3D grid data that contains hundreds of layers, columns, and rows which can form a massive billion cell hydrocarbon reservoir simulation [3], [4]. Thus, is the need to focus on methods that reveal covered data. Researchers have proposed many visualization methods, named as lenses that are introduced to address viewing and interacting with these data. These lenses are reviewed in the following sections.

These lenses are introduced in the process or pipeline to visualize the data. The standard visualization pipeline, as defined by Card et al [10], follows a simple process starting from a loading data source to restructure the data to create the virtual world then to fit the visualization method then to specify display area to visualize the selected content and then to a visualization view. The use of lenses requires adding to the visualization pipeline a new step. This step is between data restructuring and specifying the display area to be viewed. The lens alters the original location of the data. The way the lens alters the data depends on the implementation of the lenses and the type of the data.

In addition, this research investigates the perception principles and aesthetics to identify metrics that can be used with 3D detail-in-context lens.

## **2.1 Data Revealing Visualization**

Visualization is a massive research area that consists of many fields that includes information visualization, scientific visualization, data visualization, knowledge visualization, visual communication, and visual analytics [11]–[14]. In this research we are focusing on scientific visualization method that targets revealing hidden data. Multiple techniques address this issue. These methods include transparency, cutaways, and exploded views. In addition, we examine Flow visualization, which is a different paradigm that are used with simulation model.

The increase in the size of the data to be visualized introduced the issue of time it takes to complete interactive tasks. There are seven common interactive tasks defined as select the data, explore, reconfigure, encode, elaborate, filter and connect [15], [16]. All of these tasks involve searching for data, and in a massive data set it will be similar to searching for a needle in a haystack. In this research, the focus is on exploration of the data.

The type of data used in this research is a structured discrete models such as grids are used in reservoir simulation studies to, spatially, represent the object of interest in a 3D space [17]. The used grid consists of gridblocks (cells) that are accessed logically or visualized separately using 3D indices. These gridblocks (cells) contains valuable information that are either static such as permeability and porosity rock properties or dynamic (time-dependent) pressure and saturation data. Both static and dynamic data feeds in to

understanding fluid flow in porous media (hydrocarbon reservoirs) that is generated by scientific applications as Computational Fluid Dynamics CFD methods [3].

The industry standard to visualize the content of a simulation grid is in the following way. First is to visualize it as a whole as seen in **Figure 2 Full Reservoir Simulation Grid**. Second, is with a basic slice and dice method where the model is visualized as single or multiple rows, column, layers, or any combination of the three using logical indices as seen in **Figure 3**. It also can be visualized in X, Y and Z axes planes by using cross-sections. This is in addition to sub-volume [4]. The user supposedly synthesis a mental image to construct a relation between these cross-sections and the properties distribution using the layer and cross section method. This visualization method is effective with small data set [4].

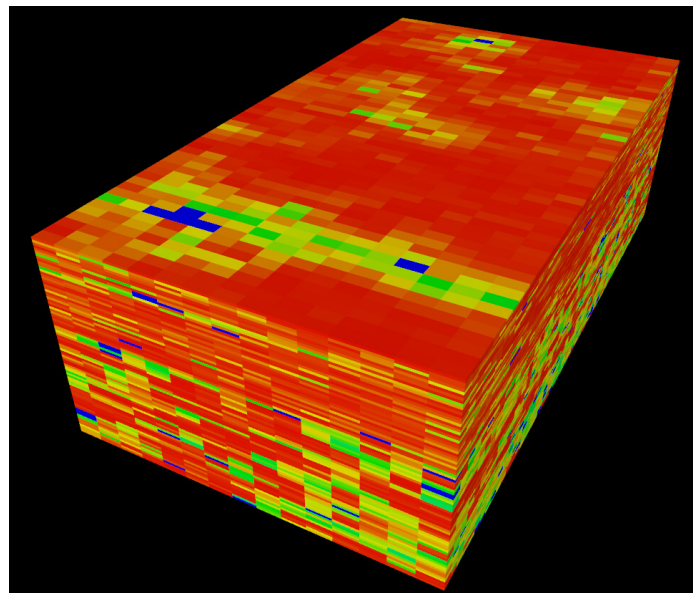


**Figure 2 Full Reservoir Simulation Grid**

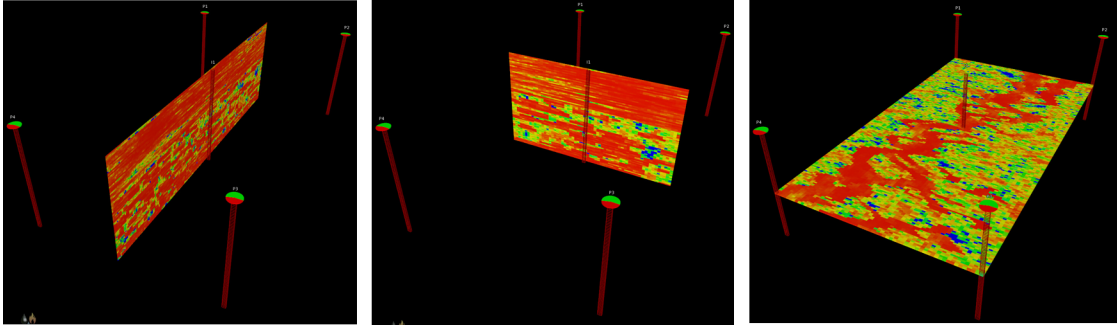


**Figure 3** The left image shows a raw slice, middle image shows a column, and the image on the right shows a layer. In order to focus on the volume of concern, an additional feature is to filter data based on a threshold of volume or from any cross-section [4]. 3D visualization application provides another visualization feature to utilize is transparency that can be applied on the grid layers which are not effective in 3D grid data, specifically, if different colors are required to represent cells properties [9]. Moreover, Iso-Surfaces [18] are also used in hydrocarbon reservoir simulation[4]. Iso-surface is data extracting and surface generation method generated by setting iso-value/thresholds on the active properties to search the equivalent values in active cells to generate the surfaces [18]. Iso-surface visualization is used to follow value changes in volume of data like tracking oil movement in the gridblocks. However, this method still occludes valuable information above and below it as it is concerned with specific thresholds. Streamlines [19] is another data extraction and visualize method for CFD data [4]. It has been developed on top of velocity vector field to focus more on the behavior of fluids flow in a grid. However, visualizing the streamlines requires to hide the grid which in turns reduce awareness of the context. Streamlines-based stream surfaces are also extracted form grid data to provide a better shape of data of interest despite the fact that these surfaces are highly self-occluding. The new illustrative stream surface approach [20], [21] does provide an enhanced visual comprehension of the stream



surface. The use of streamlines and stream surfaces only provide a portion of a wealth of data comprised by the grid [22].

Scientific visualization does not only provide accurate representation of the data, it also supports comprehension to obtain insight. There are multiple methods implemented with many variations. In this review, the main set of methodology are covered with highlighting the important differences. 3D cut-away or peel techniques are another form that represents hidden information in grids and solid 3D objects [23], [24]. These approaches specify the way the objects or layers are cut beforehand. As a rule, it should distinguish front side of a layer from the backside of it. The visual rules also include the inner objects in which it should always be visible from any angle. Another similar approach is the Section Views [25], where half space is utilized to view the hidden objects or data. A half space can be represented by a cutoff slicing plane in which exterior structures of the solid data that hide the interior are removed to show the inside of the occluding objects with respect to the viewing angle. The methodology of cutaway means that a set of the data is removed from the display to show the inner part. Also, for cut-away views it assumes that there are logical distinguish of the layers or surfaces and it requires supporting meta information per occluding layers [23], [26]–[29].

Ghosted Views is yet another approach that extensively utilizes semi-transparency [24],[30]–[32]. The visual rules are specified in a way that handles level of transparency between several objects. The important rules are that inner object must shine through. In this case, transparency is less at the edges of the transparent objects. These approaches derived from illustrative drawing. These methods are better suited for building designs, mechanical structures, or human organs visualization where objects have unique

identifiable shapes that are hidden or occluded by skin or encompassing structures of polygonal nature. The mostly used approaches for the 3D grid is the section view where the user can hide any number of layers and cross-sections by slicing planes in a primitive manner. These methods suffers from requirement such as pre-definition of what should be visible and not visible. ClearView is a developed method that circumvent this issue by providing the end-user with minimal parameters during run time such as focus point size and location, degree of transparency, and color for the area. From the example provided in this method, there are a maximum two layered data set that has been used and this might not work when dealing with hundreds of layers [3], [33].

Exploded view is a technique utilized mainly for presenting assembly of objects. A proposed method by [34]–[36] is presented for creating instructions of effective assembly. Usually the exploded views utilize a preset direction for aesthetic reasons as presenting the objects in the clearest orientation. Hierarchy of operations and objects composes an assembly. Then through a timely sequenced animation it shows the assembly of parts in the same hierarchy or at a lower level. This visual enhancement method is mainly used in mechanical objects [34]–[36]. This method requires pre-definition of the parts and how it is assembled. This method works with parts that has constant shapes over time. If this method is applied on the grid data such as reservoir simulation, it could be implemented as displacement on logical layers or it could be implemented as properties. However, due to the nature of the dynamic properties of the cells in the model it will change location over time. This might cause undesirable results of cell changes as the variation of the properties in the cells can change drastically at source of change similar to oil well produces or water well injectors [37].

Splitting the volume [38] is yet another distortion method used for medical and scientific data. The technique is implemented on data with multiple iso-surfaces or layers such as car frame, structure and mechanical parts, or human organs in a predefined manner. The layers are logically split and moved away from the view revealing the last surface in the data viewable to the user. Another splitting method developed by Islam et al is splitting the volume geometrically into two half's and move them half way apart to reveal the sections [38], [39]. He has presented two different approaches, the first is explicit split where an object is spatially split into components and implicit split where a new set of movable objects compromises of the original object. Both of these methods require pre-definition by the users and it would introduce a large overhead when used with large number of simulation models. The McGuffin method is applied on data with logically distinct such as car frame and sub mechanical car parts. This real time method allows for structures to be split and removed based on user browsing and active view of data [40]. Barmbilla et al. have presented a hierarchical splitting method for surface based flow data. The data revealing methods are called cuts on specific values of the surfaces [41].

Deformation is a manipulation method for exaggerating selected or important data without displacement. Various techniques such as magic lenses, fish-eye views, or perspective wall are methods developed for 2D data such as maps and graphs or text document to highlight important area or to provide an in context zoom [42]. These techniques change the data shape to highlight the focus area [40], [43]. Keahey has applied deformation method on high dimensional clusters of data. Due to the problem the researcher is addressing, there was no implementation of displacement as there is no data being occluded [44]. This method only works if the data is sparse and thus it cannot be applied to grid data.

Visualization of data flow is an active research area for scientific simulation applications. Many methods have been developed that tackle effectiveness of visualizations to improve understanding of the data, there is not a specific flow visualization method that is significantly better than the other [45]. These methods summarize the CFD generated data to show direction of flow as either vector fields or streamlines [46]–[49], [19], [50]. These methods do not focus on revealing hidden data as much as on visualization only the summarized flow information. Stream-surface is the next generation for flow visualization as it aggregates the streamlines to depict the shape of the flow [20], [21], [51]. This method also suffers from data loss of context. Schlemmer et al. have implemented a method that highlights the important area of the streamline by increasing the density of the streamlines [52]. This implementation provides a form of details within the context by giving detailed streamlines versus sparse streamlines in the rest of the visualization. This method only applies to data that have sparse areas that can be visible from different angles. In a 3D grid data set it will not highlight occluded information. However, it can be used for 2D plots. In general, the use of streamlines reduces the information of the grid to the most dominant flow instead of showing all of the flow.

Illustrative Context-Preserving [53], [54] is an example of combining the power of GPU into providing a visual access to internal data to be revealed while maintaining context information by specifying the focus area with threshold for the context region of interest. This lens requires manual selection of interior and exterior layers and user input to select the opacity level. Another similar method is an importance-aware composition [55]; it is a technique that calculates an importance value such as intensity, extinction coefficient,

gradient magnitude and silhouette-ness to generate a real time image from a single pass of front-to-back rendering. This lens has been presented with three layers only.

## **2.2 Detail-in-Context Visualization**

The Detail-in-Context lenses were introduced to resolve the issue of viewing high level details in context of the data. Many variations of these lenses have been implemented covering aspects beyond the scope of this work [16]. The purpose of these lenses is not only to magnify the selected area but also to remove the occluding cluster of data points that hides the desired data. This should be achieved with minimal and smooth changes on the data. These lenses have been applied on different data types. there are applied on geo, tabular format, flow data, maps, graph, city models [16]. The interest of this research is to find lenses that can also displays occluded area on volumetric data.

Researchers has looked into different aspects of detail-in-context lenses. Appert et al, has focused on improving the exploration and object selection when using lenses in 2D maps. They have not explored their implementation in 3D space volumes data [56]. Cignoni et al, developed the first 3D lens that uses semi-transparency on the external element in the spherical volume of interest which require manual classification of the data types. This method is combined with multi resolution filters, edge emphasize, and magnifier of internal data [57]. This method is more on show inner data than fisheye view and it is an extension of the Magic lens developed by Bier in 1993 [58].

Viega et al has extended the implementation of the magic lens and introduced cubic shaped transparent lenses [59]. They have implemented three 3D lenses. The first reduces the displaced data sets by culling the dens data inside the lens. The second method was named

X Ray Vision, which removes the outer layer. The third method named The Worlds in Miniature that is a duplication of the displayed virtual environment with an interactive capability. They have also presented the means to combine these lenses. However, this implementation uses clipping planes and it does not cover many layered data nether it does distortion or displacement.

Wang et al has developed the magic lens as a method that is based on geometric optics. The used lenses can be circular, square, or arbitrary shapes for magnifying the focused point to have any shape or to the shape of a specific feature in the data. this method also supports angular lenses that camera fisheye [60].

Mendez et al, has used the x-ray vision method as a context-sensitive lens that is implemented as part of the scene graph structure [61]. This lens resolve to a certain degree the manual configuration of setting up on which parts of the scene to be influenced by the x-ray lenses.

Ropinski and Hinrichs has developed a lens that address that manual classification of outer and inner layers by filter outs the outer layer using two depth tests. This method is implemented on polygonal datasets with multiple filters being used. The approach requires three rendering passes. The first is to what is beyond focus of the lens. The second is to render the occluded data or what is in the lens. The third is to render occluder differently. They have rendered the occluder as wireframe or as a transparent and have used two shapes of lenses: a sphere and a box shape. There have been no details on how to work with more than three layers of data [62].

Yang et al has focused their implementation on the use of depth, view angle, and camera parameters in designing the lens. Their method deforms the shape of the selected area to a fisheye lens however it does not show details rather than it enlarges the view. The deformation happens as an image processing in 2D dimension rather than in the 3D rendering pipeline [63].

Researchers have also looked in mixing stereoscopic 3D rendering with transparency for the purpose of viewing occluded data [64]. Shaw et al, have used this on volumetric datasets. The shape of the lens are rectangle and can be in any arbitrary orientation. The method requires two visualization rendering passes: the first for the data and the second one for what is inside the lens. This method was not implement on dense volume data that naturally occlude the insides of the grid and displacement or distortion were not used.

Lamar et al. method focuses on deformation on the model for the purpose of magnification. This method does not utilize displacement to enable viewing occluded data however it allows it to view occluded data by means of a adding a clipping plane [65].

The Gimlenses method is an extension of the cut lenses by introducing nested multi 3D views showing the details of the selected region [66]. Each of these views are referenced back on the original location by pointed lines. This method still requires manual definition of how to cut each layer. However, the nested drill down can address the multi-layer limitation.

In the area of streamlines, researchers have applied multiple concepts of detail-in-context methods [19], [67], [48], [48], [68], [52], [52]. Fuhrmann and Groller has presented dashtubes method to resolve occluded distant details and lack of depth hints, and

directional information [69]. The method provides an animated streamline with transparency being added when needed. This method uses non-transparent cube occluded layer and to indicate the existing of the focus area. This does not apply on the 3D volume data. Mattausch et al has extended the lenses on streamlines by introducing multiple enhancements [68]. They have introduced the use of spotlights, flow direction arrows, depth cuing and color-coded depth. The method only works on streamlines and not volume data.

The BalloonProbe is fish-eye lens that provide detail-in-context visualization [70]. This method focused on virtual 3D environment such as cityscape where the lens displaces the objects within the vicinity of the balloon toward the surface of the balloon. This method can be applied on 3D volumes however it was not conducted in this paper. This method uses wireframe of the displaced objects to represent the original location of the data. This might cause more confusion as it adds more over lapping data.

The undistorted lens is a hierarchical view of a zoomed area on top of a distortion lens [71]. This is done to provide more details on very large datasets that otherwise does not get benefit from the standard distortion lens. This method was only implemented on images and geo-spatial maps.

Wang et al have developed a focus-in-context method that maintain minimal distortion in the unwanted areas by utilizing bounding volumes to select areas of interest. this method has been implemented on 3D volumes and it does not provide a see-through means to occluded data [72]. The conformal magnifier by Zhao et al has used angle preserving function when using the magnification lens. this method requires user input to manually



select the important features to be preserved. This lens has been applied on 2D, geospatial maps, and 3D volumes [73]. This method does provide detail-in-context lens however; it does not provide a mean to visualize occluded data.

Several researches have only applied fisheye views on 3D volume data that combine non-geometric distortion such as transparency and drawing wireframe layers [74], [75]. Their work has been developed on top of Winch [76] fisheye on 3D data work, these method hides the inner data and only focus on deforming the external layer. Illustrative deformation is another Focus+Context (F+C) method that provide user controls to explore data by combining hand illustrative technique with deformation methods. Deformation is used to emphasize the important part and peel and cut-away the illustrative technique. This method is not applicable to grids with massive sizes as it produces a large empty spaces [77], [78].

In alternative implementation of the detail-in-context lenses Doleisch et al. have implemented detail-in-context lens in the area of simulation data [79]. This lens is a feature based. The feature-based visualizations are type of lenses that highlights important features to the users by eliminating bulk of the data. Their proposed method is a semi-automated one. In reservoir simulation data the use of data filtering is a standard feature in most packages. Piringer et al. have introduce the use of linked visualization in for 3D scatter data using detail-in-context lenses [80]. Linked views is where a selected sub dataset gets displayed on adjacent view. They reason the use of the need for the linked view is due to the massive scatter points will reduce perception and interaction without going into details on how it does. This method is designed for scatter data points only and cannot be applied on dense 3D models. Doleisch et al. have combined the linked views and the feature based detail-in-context method in a research application named SimVis. They have extended the

feature-based lens to support time-dependent grids. This has been applied on 3D scatter dataset and not on 3D grids [81].

Carpendale [9],[82] proposed a novel approach in providing a detail-in-context view of 3D data. The proposed approach accesses the internal information in 3D grids by applying a distortion function. The method reveals internals (innards/ look for more) that is hidden when viewing the 3D grid by utilizing the line of sight that rearranges the cells at focus point. Her work is an extension of the 2D distortion viewing techniques. Her proposed method is compared against basic 3D distortion viewing. The resulted visualization is both understandable and appealing. Figure 4 Visual Access Method shows the visual access method developed to reveal the internals of the grid using fisheye method. This is the lens we have selected for the research objective and experiments.

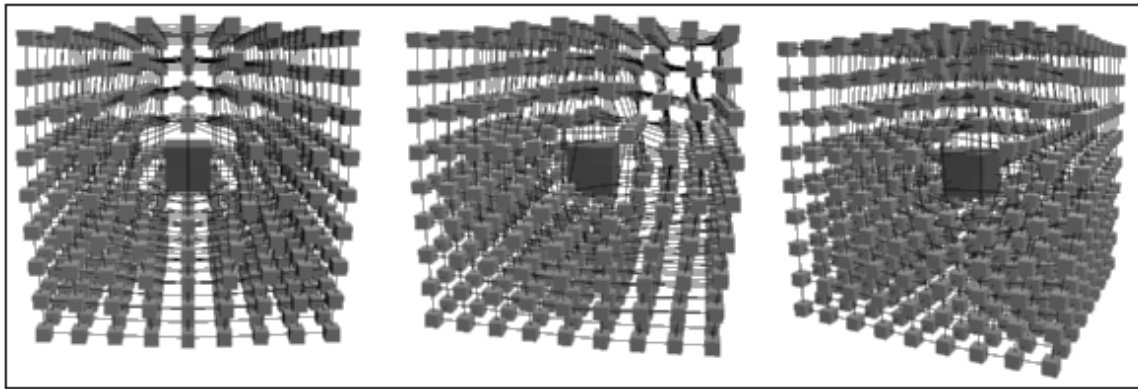


**Figure 4 Visual Access Method being applied from different angles**

Table 1 shows a summary of visualization lenses that targets detail-in-context visualization. There are large similarities between these lenses, however the results of the method vary due to slight differences in the implementation.

**Table 1: Literature Review Summary of Detail-in-context volumetric visualization lenses**

	Disp	Magn	Dist	Trans	Cutaway	Num Layers	Shape	Auto
Diepstraten et al(2)				Y	Y	3	Axis/FF	Y
McGuffin et al			Y			5	Arbitrary	
Kruger et al				Y		3	Circle	Y
Bruckner,	Y					4	Axis	
Li					Y	4	M Axis	
Islam et al (2)	Y		Y			2	Arbitrary	
Elmqvist et al				Y		4	FF	
Agrawala et al	Y					5	M Axis	
Brambilla et al	Y				Y	5	M Axis	
Correa et al			Y			10+	Arbitrary	
Cignoni,Viega		Y	Y	Y	Y	2	Sphere	
Wang		Y		Y		2	Arbitrary	Y
Carpendale et al	Y	Y	Y			10+	Bell Shape	Y
Ropinski et al					Y	4	Arbitrary	
Yang et al		Y	Y			1	Sphere	
Lamar et al		Y	Y			1	Multiple	Y
Pindat et al		Y				4	Arbitrary	
Elmqvist et al			Y			1	Sphere	Y
Wang et al		Y	Y			1	Sphere	Y
Zaho et al		Y	Y			1	Sphere	Y
Lue et al (2)		Y		Y		2	Arbitrary	

Winch et al		Y	Y			1	Sphere	Y
-------------	--	---	---	--	--	---	--------	---

## 2.3 Perception and Design Principles

Perception is a mental process to understanding the information reaching the sensors through organization, identification and interpretation. To achieve better perception of the data it is Perception principles have been researched and experimented by Norman to explain what we like or dislike products in order to improve design [83], [84]. Researchers have applied Norman’s perception processing stages to design visual measurements of graph layout [8]. In addition, it has been investigated by Norman that understandability is also linked to the visual properties of the displayed data [83].

In this section, we discuss the perception and design principles that are applied on the visual properties of the scientific data that can be used to develop aesthetics measurements.

### 2.3.1 Perception levels

Phycology researchers have studied human perception extensively [85], [86]. Perception processing has been classified to three main stages. The first two, visceral and behavior, stages happen involuntary just as the information reaches the brain sensors while the third stages, reflective, is a higher cognitive level.

#### Visceral Processing

Perception in the visceral level is the initial impression the viewer has of the product, either it is appealing or not. This process happens involuntarily once the light travel to the eyes and transfers to the sensors then the mental processes translate the light to objects [86]. In this level the visual properties of the objects are perceived. These properties include

curvature, collinearity, symmetry, parallelism, and cotermination [85]. The result of this level is the recognition of shape, size and color by the viewer [85], [86]. In scientific visualization, the visceral processes are responsible for organizing the laid out data to recognize the different properties. Norman has stated that the attractive the object is the easier for mental processes to recognize it [83]. In visualization, the same analogy can be applied, the appealing the visuals to the viewer then the data is understandable and usable.

### **Behavioral Processing**

The part of the brain that manages every data behavior controls the behavioral visual processing [87]. This level is processed at the brain in a subconscious manner where perceived actions on the observed objects are assumed. This level takes the result of the visceral processing and analyzes the function, usability, performance and physical feel of the viewed object. An example of behavioral processing is driving and while thinking where driving is a behavioral operation and thinking is a higher level processing [87].

### **Reflective Processing**

Reflective processing is a conscious mental and thought stimulating process. The viewer is reflecting back at the design and functional use of the observed objects. In this stage the user is looking into how do it make him feel using or owning such object. This has a personal impact on the users influenced by his experience priorities and personality. Culture and environment also have an impact on how the user perceives the object. This is observed on why some might value design over function or vice versa [87].

## **2.3.2 Perception Principles**

Utilizing mental capability to distinguish form and recognize objects allows for design and development of lenient algorithms to visualize scientific data and provide a recognizable

and understandable visualization. The perception principles explain mental forming phenomena from different perspectives. Psychology researchers observed during perception that several features about the objects recognized. Identifying these features leads to designing visualization that are easier to process which lead to better visualization and these features are consistency, grouping and contrast [85], [86]. Gestalt principles are a detailed study of the perception-grouping feature and are about grouping as in "the whole is greater than the sum" [88].

### **Constancy**

Psychology researcher identified a mental capability named as perceptual constancy that can recognize the object to be the same within a range of change in distance, angle and context [89]. Size, shape and distance constancy have slight variation between them. Size constancy refers to perceiving the object to have the same size even if there is a slight difference in distance. Shape constancy is the mental ability to recognize the object from different sides. An example of this is looking at a mobile phone from several angles. Distance constancy points to the constancy perceiving of the distance between the viewer and the objects real distance or apparent distance. Another variation of constancy is perception of constant location of far objects due to the parallax illusion [90]. In example for this the location of the mountain stays the same when even if the car is traveling. Perceptual constancy states that slight changes in size, shape or distance can be still recognized during the perception process as the same [89], [91], [92].

### **Grouping/gestalt**

The perception capability of the human mind to recognize a group of objects and form a single entity or certain order has been extensively studied at Berlin school and has been named as Gestalt psychology [91], [93]. There are four main properties of observed

emergence, reification, multistability and invariance [94]. Emergence is the name of the mental ability to form objects from sub parts. reification refers to the forming of shapes due to contour parts. Multistability is the perception ability to perceive objects as two or more shapes and this is due to the semi-instability of crossing multiple illusions based on the different perception properties. Invariance is related to size and shape constancy where objects are perceived to be the same under a range of modification such as scale, sheer and rotation [93], [94].

Researchers have addressed these properties and more and set principles/laws that predict grouping perception and allow to capitalize on them to create images and plots [95]. These laws are Proximity, Similarity, Closure, Continuation, Common Fate, Good Form and Good Gestalt [95]. Proximity law, objects that are close to each other considered to be the in the same group. Similarity law, groups that have similar shape or color are perceived as part of the same group. Law of closure, the mind has the ability to connect the dots, lines and curves to complete the missing shapes. For example, the ability to identify the circle and the square even when there are missing lines and curves. Continuation law states that occluded part of the object can still be grouped as a single object. Law of common fate states that objects moving along the same path are grouped together. This is observed on a flock of birds moving in the same direction. Law of good form or gestalt states that objects that have elements in common are grouped to be similar as a collection of water bottles that share a common theme. Researchers have identified that past experience does have an effect on how objects can be perceived to belong in the same group. For example experience hand writing reader can read faster versus a beginner [95].

The principles under this category can be applied on the type of data this research is targeting. Although the expectation of the benefit gained from maximizing these features are principles is low.

### **Contrast**

The third perception principle is contract perception. This means that objects are perceived differently compared to others in different context in shape, color and contrast. This translates to objects appeal can be enhanced or reduced if placed in certain context relative to normal or standard [96], [97]. In scientific visualization there is minimal use of contrast where we only distinguish foreground from background using a high contrast background color also color legends are used to identify the value color range of the data [98].

### **2.3.3 Norman Principles**

Bennett reasoned that visualization of data is perceptually processed on the same three levels and measurements heuristics can be designed on all three levels as presented in his survey heuristics [99]. Norman has discussed in his book emotional design: why we love (or hate) everyday things that properties of a product is processed and analyzed by the viewer in three levels or dimensions that designers should consider; attractiveness, behavioral and the impression a product have on the viewer [87]. These three levels explain the different mental processes that happen when the viewer sees, uses and remember from using a product.

The same mental activities can be applied to visualization. The emotion side of perception can be used to guide product or visualization design. They have an effect on the experience of using products or visualization. The design aspects on each of these three levels are discussed here.



## **Visceral Design**

Seeking appealing forms in objects is a natural human instinct [87]. Norman argued that designing for visceral attractiveness transcends cultural differences [87]. As mentioned, visceral processing recognizes these main primitive properties: symmetrical, curvature, collinearity, parallelism and cotermination. Designing visualization to optimize the attractiveness at the visceral level require focusing on having an easy to recognize shapes by optimizing the form of the data using the shape properties. Researchers in graph aesthetics have developed multiple heuristics that targets visceral level attractiveness.

Edge identification of properties is the main factor in forming the shape of the objects. Collinearity, identifies edges so if straight lines are identified then it can be considered easy to identify the shape of the objects. Curvature or smoothed edges properties, the visceral level processing identifies the curvilinearity properties of the object if it has a smooth edge. This translates to the clearer the curvature property is the easier it is to identifying the edges of the objects [100]. Parallelism, similar or parallel curvature or lines leads to identify objects better. In addition, cotermination that is the edge point between two edges also easily identifies the shape of the objects [85].

Symmetrical properties, researcher for graph layout has identified that the more symmetrical the layout is the easier the shape of the object to be recognized and the more appealing it is to the users [86], [100]. Although, others have pointed out that focusing on aesthetics does not necessary provide a better usability [101]. Maximizing symmetry does have an impact on visual appeal but it does not have an impact to usability, thus it will be not be included in this research.

### **Behavioral Design**

Improving the mental processing for the behavioral processing of visualization requires optimizing these important properties function, performance and usability [83]. For function optimization, the visualization needs to achieve the desired goal. If the visualization goal is to view more data, then the more data it shows the better the visualization [102]. One interpretation of performance is how will does the visualization achieve the goal. Usability optimization, what is the learnability of the visualization method and who efficient can the user uses it. The usability metric has been empirical evaluated for graph layout [103].

### **Reflective Design**

Designers that address design in this level of processing will have to pick and select users. There are users that are looking artistic design rather than precise function and visa versa. This has to do with many factors such as culture and meaning of the objects or the target. Due to the different meaning each design have to the users at this level it becomes hard to pin point measurement of what is better. Thus it is not possible to have a direct relation between an aesthetics measurements and reflective level design [83].

Designing visualization with focusing on data revealing is the main derive of this research. The selection of detail-in-context visualization affects the users mainly in the reflective level. Scientific visualization purpose is focusing on function and initial reaction of the image, which is accurate representation of the data [104]. The addition of detail-in-focus does in this research conflict with the definition of scientific visualization and this might affect the acceptance in the scientific community how values change and enhancements over reduction in full accuracy.

### **2.3.4 Design and Guidelines for Displaying Quantitative Information**

Edward Tufte have discussed in his book “Visual Display of Quantitative information” several design and guidelines with measures to ensure the excellence and integrity of the visualization [105]. The graph representation of data according to Tufte should show the data, focus the view on data substance and optimize data display. These guidelines and measurements were developed for statistical data. Several of these measurements can be used for scientific data.

#### **Lie Factor**

The Lie factor has been explained in Tufte’s book as a measure to determine the amount of the distorting in visualization. Tufte argue that distortion should used should be minimize in graphs that reflects the numerical data. The use of distortion can affect the perceived visuals. The lie factor measures the ratio of the distortion effect in graphics against to the size of data [105].

#### **Data Density**

Density in visualization is the amount of displayed data over the area of the data graphic. This approach is derived from a research that state the eyes can differentiate up to 625 points in a one square inch [106], [107]. This translate that visualization can pack a large amount of data and the human perception can still distinguish the data point. The data density can be measured using the number of total data used in relation to the area of the visualization [105].

### **Data-Ink**

The data-ink measurement is the efficiency of the visualization in terms of data verses the shown presented visuals. This measure has minimum impact as this scientific visualization uses minimum visual aid [105].

### **Visualizing Emptiness**

Visualizing Emptiness is researched by Dimitri Mortelmans [108]. The research indicated that minimal use of the display space could not only provide clean visualization but also provide better result. The research suggest that the more information is displayed the less value is perceived. This is also related to the minimalist design principles where it state less is more. In scientific visualization, this design factor means that minimal data should be displayed to provide the minimal needed information.

## **2.4 Metrics and Visualizations**

In the area of visualizations, graph layout researches have used perception to design aesthetic metrics to improve layout heuristics and to evaluate results [99]. Designing layouts in graph visualization is one of the main challenging tasks in research. This is an active area with recent work up to 2016 [109]. In this section, we are reviewing the highly used aesthetics and metrics in graph layout. As far as we have searched, we have not identified 3D scientific visualizations that have incorporated the use of aesthetics in lens design and evaluation.

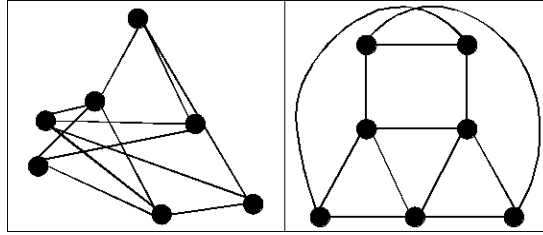


**Figure 5 Graph Layout on the left is a random graph layout and on the right is a graph layout that minimize edge crossing**

Graph visualization is the discipline of generating illustration of nodes and edges between them as presented in Figure 5 [110]. There has been numerous drawing algorithm to generate graph layouts surveyed by Bennett et al., and Herman et al., and Battista et al. have conducted surveys on the graph drawing algorithms [99], [111], [112]. Laying out the graph focuses on node placements, edge length/location and, shape. In this section, we are focusing on the used aesthetics to define the graph layout. Bennett et al. have stated that the commonly used perceptions are good figure, similarity, continuation, proximity and connectedness, these are in addition to symmetry, orientation, and contour [99]. These perception and aesthetics are used in designing the visualization of graph information as a means to arrange the data [8], [113].

By definition graph data consist of nodes and edges typically without initial information on where the nodes are located. The aesthetic measurements used in graph layout are based on perception and design principles to improve comprehension. Wong [114] have used in his research extensive set of perception principles to design UML layout as an extension to graph drawing algorithms. Good figure, similarity, continuation, proximity, connectedness, familiarity, symmetry, orientation and contour are the set of perceptual principles used to optimize the location of the nodes in relation to each other. They are also used to set the placement of the edges [8], [114]. Harel and Davidson have used symmetry

and even node distribution to improve visual appeal [115], [116]. Wetherell et al [117] have designed a tree drawing algorithms based on two main aesthetics rules. The first rule, nodes should be in the same level i.e should be in the same horizontal lines. This means that the nodes should not be overlapping. The second rule is that nodes should be symmetrical around its parent where edges should not create a cross [117]. Purchase has developed node placement metric by maximizing node orthogonally [118]. Researchers have also targeted to reduce edge crossing that reduces clutter. Overlapping edges can cause misinterpretations [100], [117]–[120]. Edge with shape bends is perceived as two objects and this is why others have used metrics to minimize edge bends [120]. Researchers have also applied symmetry on both global and local scales to improve aesthetics [118], [120]. Researchers have applied a combination of metrics to improve the overall layout, for example node separation and edge length [118]. Maximizing convex is a metric developed by Tamassia and co to optimize overall layout [110]. Figure 5 Graph Layout shows a graph before and after applying aesthetics metrics for layout design.

Baum have identified and selected aesthetics properties through interviewing users to improve a visualization method [121]. This is done in the area of software visualization. He has defined aesthetics properties as: “Aesthetics are visual properties of a visualization that are observable for human readers as well as directly measurable.” Baum has interviewed users to identify aesthetics properties of a specific visualization technique called recursive disk metaphor that represent software classes. These were used to update the software visualization method to address the short comings and improve readability. This method only works with data that has hierarchal and adjacent relationship. It does not scale to 3D column data [121].

Metrics often contradict with each other, Huang et al. have proposed drawing algorithms that compromise between the standard aesthetics metrics for perceiving the shortest path [122]. Additional metrics have been used such as the non-adjacent vertex proximity which maximizes the distance between non-adjacent vertices to improve readability [123].

Huang et al. have used seven (7) 2D metrics to evaluate BIANGLER, proposed drawing algorithm. These metrics are number of edge crossings, average size of crossing angles, standard deviation of crossing angles, average of edge lengths, standard deviation of edge lengths, angular resolution, and average of standard deviations of angular resolution. They have evaluated the result of the new graph with a user survey. The metrics are not used as optimization criteria [122].

Beck et al. has added in his research aesthetics that can evaluate multiple graph visualizations for dynamic data [124]. These are readability metrics for the number of visible vertices, edges, and sub-sequent graphs. They have confirmed that these metrics are conflicting and thus not all three should be used in the same time. The conflicting ones are the readability for vertices against the readability of sub-graphs. The only metrics that can be used in 3D visualization is the readability of vertices.

The use of multi-objective optimization has been researched in the area of special graph drawing, business process diagrams (BPDs) [125]. Zilinskas and Varoneckas, have utilized aesthetic metrics as a form of optimizing graph drawing using multi-objective functions to lay out business processes diagrams [125]. This approach draws the edges between the nodes and assumes that the node locations are fixed and the flow is defined. The used aesthetic criteria are minimum total length, minimum total number of bends, and minimum

neighborship. They have provided a deterministic approach using linear programming; however, for large data sizes it is too slow thus they have developed a heuristics optimization. The used criteria do not fit with the data type at hand as this method focuses on the length of the edges, number of bend in the edges and closeness of the edges and uses straight lines only. In case of the detail-in-context method these have minimum relativity. Researchers has concluded that single pareto front can be obtained however for large sized graphs the use of heuristics to obtain acceptable results is more efficient. These cannot be used for 3D data.

Huang et al. have used four aggregated normalized metrics to find the graph quality visualization for optimizing graph drawing [109]. These metrics are minimal edge crossing, maximum crossing angle resolution, maximum node angular resolution and uniform edge length. These metrics cannot be used on 3D data. The following list is the result of Bennett et al. survey on the metrics used to evaluate graph layout [99]:

- Minimize changes of nodes location over time to maintain stability
- Minimize the need for cognitive effort to analyze dynamic data
- Reduce the use of the same location for different nodes over the same time.
- Minimal edge bends
- Minimal edge length
- Symmetry of nodes
- Aspect ratio of the plot / new
- Maximize angle between edges
- Minimize area of drawing



- Node separation
- Minimize overlap

The surveyed metrics cannot be applied on 3D scientific data or detail in focus lenses.

## **2.5 Validation for Graph Aesthetics Metrics**

Recently researchers have started evaluating and validating graph layout algorithms instead on relating directly on intuition. Ware et al. have developed metrics based on perceptual principles then verified the results based on user survey [83]. The result concluded that good continuation and edge crossing are has good impact in understandability of the graph by finding the correct answers about the graph. Edge crossing importance scored high in multiple surveys that targeted users of graph visualization.

Multiple studies showed that high symmetry, minimizing edge length and bends has a positive effect on task performance in graph visualization [76][83]. In UML diagrams orthogonality, minimum edge crossing had a high impact and minimum drawing width improved task performance [86].

Purchase and co has evaluated the use of aesthetics to directly affect comprehension of automatic generated UML diagrams. The study was conducted between pre-measured hand-designed aesthetic of a UML layout against computer measurements. The algorithm did not capture the measurements correctly and provided inconsistent results. The use of hand-designed graph in a user survey did provided conclusive results that only minimal edge bends have direct effect on the comprehension [60]. In a later study by Purchase focusing on social network, with high edge crossing grouped/clustered layout performed

better than radial or hierarchical layout. In addition, the central positioning of important points is preferred by the users [86].

In 2011 Burch et al. has evaluated tree multiple diagrams against radial diagrams using eye-tracking method. The result concluded that tree structure is faster in exploration and finding the desired node from another [82]. Huang et al. have also used eye-tracking method revealed that distracting edges and dense cluster requires longer time for task completion [87].

Isenberg et al. have conducted a systematic review on 581 papers to identify the shared evaluating objectives for visualization. The methods used by researchers focuses on the rendered images and performance of the algorithms and recently participants were added to the research studies for either reviewing performance and for qualitative evaluation. They have identified that validation area used to identify the correctness of the model whereas verification used to know if the implementation of the algorithm is correct.

None of the evaluated method has target the use of quantitative aesthetics metrics.

## **CHAPTER 3**

### **METHODOLOGY AND APPROACH**

#### **3.1 The Research Process**

This research topic is primarily selected to address an issue related to the use of the detail-in-context visualization method in the field of hydrocarbon reservoir simulation. The first reason why we selected this area is this field have been using basic volumetric visualization features in most of the industry packages and we want to introduce the detail-in-context method [104]. The second reason is a personnel interest is to investigate the possibility to optimizing the view of the selected method. This is done to identify the best possible view given a set of data and point of interest.

#### **3.2 Methodology**

This work will use the following steps to achieve the results of this research.

1. Identify the area of the study we will investigate and research literature for all previous work related to visualization methods, perception theory and metrics.
2. Build our hypothesis and formulate it as a research question with aim and objectives.
3. Develop and conduct experiments to generate the evidence needed to support or reject the hypothesis.
4. Conduct a survey to cross- validate the selection of metrics and validate results.

### 3.3 Approach

This research work will investigate the hypothesis that the use of metrics based on aesthetics and guidelines can improve the output of the detail-in-context method. In order to proof this relation, this research investigates the properties of the detail-in-context method in terms of the impact it has on the results of the view. The work will focus on the cause and effect of the parameters have on the results affect how the data is presented and most likely how it would be perceived. This is done in this work by selecting a specific data to work with then selecting a specific visualization method to implement then selecting and implementing a set of metrics.

The aim in this work is to answer the following research question RQ1: Can aesthetic and guidelines metrics be used to measure and describe the different aspects of detail-in-context visualization for the purpose of optimizing the view on scientific grid data? This aim is split into the following several objectives. First is to find perception principles that can be applied to 3D data. Second, is to identify the metrics that can be used based on perception principles. Third objective, is to use the metrics to optimize the visualization. Fourth, is to validate the results.

In conducting the literature review, we will look into journals, conferences, and books in the areas of visualizations, perceptions, and metrics. The literature review will start with investigating open problems in scientific visualization as it is in the professional interest of the researcher. We will look into different visualization method researched that exposes the internal part of data. We will research the different implementations of detail-in-context visualizations as identify what was implemented on scientific data. Then will we research

the perception theory and the different principles that explains theories behind shape comprehension. In addition, we will look into design guidelines to identify what can be applied to 3D grid data. Moreover, in the literature reviews research we will also search for work that implements metrics that target visualization view optimization and lens designs. The selected topics are directly related to the research at hand.

In order to validate the results of the experiments will generate, we are going to conduct a survey. This survey will be an interactive session where an interactive application will be presented to a user with a questionnaire targeting the usefulness and benefit of both the detail-in-context method and the implemented metrics. The survey will target experts and users of visualization application for hydrocarbon reservoir simulation data.

### **3.4 Research Flow**

This section presents the flow of the research. it goes over all the steps that the research has will go through to address the research problem. Figure 6 represents the flow of the developed approach.

The research starts by researching visualization methods that reveals data, which is the objective of this work. The review also covers perception and design principles. This is meant to identify lenses and metrics that can be applied on volumetric data.

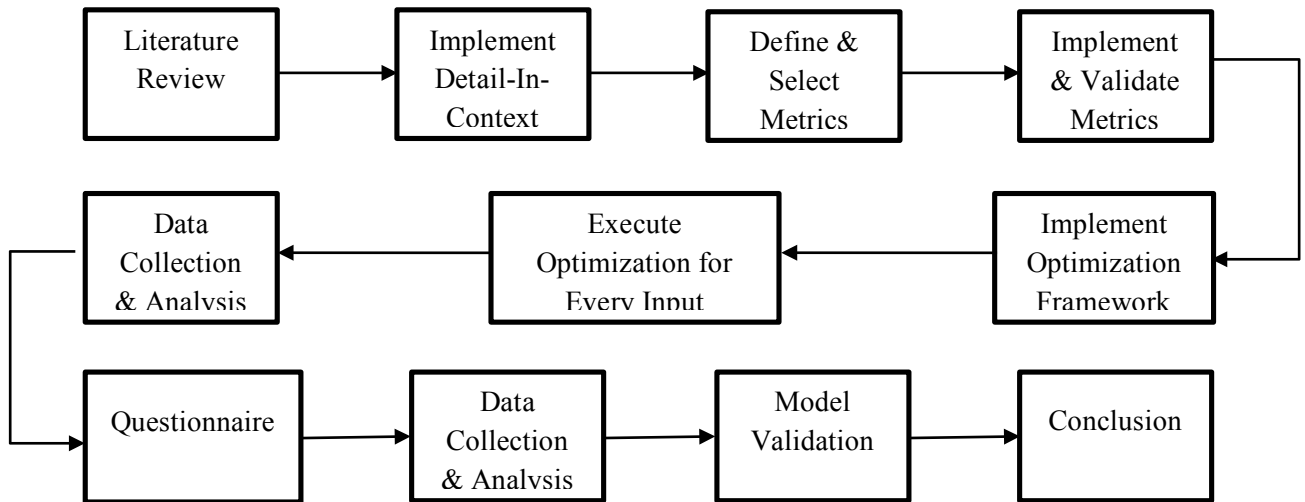


Figure 6 Approach Flow Chart

Then, the selected lens is implement on hydrocarbon reservoir simulation data which lacks in the area of advance lenses [126]. The implementation of these methods will be in C++ OpenGL/OpenCL for performance and real-time visualization. The selection of a low-level API is to have a total control in the development which is required due to the change of the data location on the fly.

After that, from the researched perception, metrics, and guidelines a selected set will be implemented. The metric selection is based on what can be applied on volumetric data and the selected lenses. These metrics are linked to a guideline or to a defined perception theory. These metrics evaluate the generated visualization against the perception and guidelines.

Then, we will adopt and implement these metrics to work on the data type at hand integrated with the visualization application. The implementation has enable automation to be used in a workflow.

Then, a manual test will be conducted to ensure the validity of the process. This testing evolves verification of the generated results either numerically or visually.

After that, an optimization library is added for the purpose of optimizing the result of the view based on the metrics. The optimization will change the input parameters to achieve an optimal view by maximizing or minimizing objective function based on the designed metrics.

After that, we will implement a framework to evaluate all input parameters against each objective function. This is to find what is the top results of each of the metrics. The framework will link the visualization with the objective function to automate the experiments and generate the results.

Then, the data generated will be conducted. The collection will be automated, as the results of the objective functions will be exported as part of the automated framework and sorted by the optimization library.

After that, we will conduct analysis on the results of the metrics for two datasets. The analysis will include correlation study of input parameters values versus the results of the metrics.

This is to get a sense on the direct relation of the impact of the metric on the resulted images. These steps would conclude the experimental analysis.

Next we will conduct a survey to verify the importance of the usage of lenses and usefulness of the metrics in real life. Finally, we will combine the analysis and conclude the research.

### **3.5 Research design**

This research specifically is the study of cause-and-effect of the input parameters of the detail-in-context method on the implemented metrics. This is why need to conduct experiments that uses quantitative metrics to have an in-depth analysis of the relationship between the input and the metrics.

### **3.6 Input Data Visualization**

The selected data to conduct the experiments is volumetric hydrocarbon reservoir data. The size of these datasets can go up to multi-billion cells. The selected datasets are a sample of what would a reservoir look like. These would serve as the basis conducting the optimization runs for the purpose of generating the primary data used for the analysis.

### **3.7 Analysis data**

The analysis in this research will be conducted on the results of the optimization runs. The data that will be generated will be in a table format. The columns in the results will contain the values for the inputs and output of the experiments. Each row will represent the value of input parameter and the results of the metric associated with it. This provides the data in a format that allows to processing to find the correlation between the input and output.

### **3.8 Experiments**

The experiments in this research is designed to thoroughly cover all of the possible one to one configuration. This will be a controlled experiment having one of the input parameters



changing at a time. In addition, two data sets will be used and the analysis of the study will be conducted on the average of the results of the objective functions.

### **3.9 Possible threat to validity**

The shared results of the optimization only show the top of the results. This will not show all of the ranges of the input parameter. This means if the objective function is a maximization then the minimum values will not be included. The reason behind selecting this method for showing the results in this research because identifying the minimum in the case of maximization is not part of the objective. However, this might impact the correlation results as it eliminates input parameters values that will generate low results. For further work in this area, researchers might want to consider all possible input values rather than the top results.

## CHAPTER 4

### IMPLEMENTATION

Chapter 4 discusses the implementation of the visualization application and the metrics. In the first section, Visual Access method is presented followed by a presentation of some of the variation that was added to adapt it to be an interactive viewer. The third section, is on the developed optimization framework. Metrics and their implementation are detailed in the fourth section.

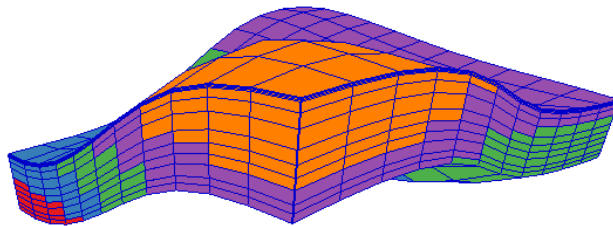


Figure 7 Sample 3D Hydrocarbon Reservoir Grid Data Set colored by depth

#### 4.1 Visual Access

The proposed approach by Carpendale and co requires the use of several techniques to produce the final output [82]. The techniques are applied on the different aspects that control visualization. These techniques include the following: displacement function,

distorting function area of influence, point of view, and focus exaggeration. Figure 7 presents the original grid data.

#### 4.1.1 Displacement Function

Displacement provides a mechanism for viewing grid cells inside the volume. The cell displacement step disperses the cells apart from each other in the three main axes. This allows for occluded cells to be revealed as seen by this Figure 8 Displacement Function.

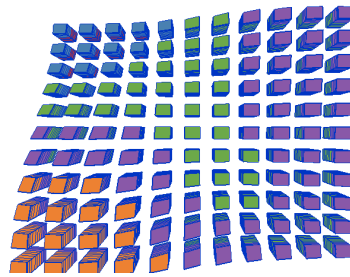


Figure 8 Displacement Function

#### 4.1.2 Distortion Function

Distortion still needs proper continuity to be perceived as whole. Visual access has used the normal distribution shape for the distortion function. Two main variables control the bell shape of the normal distribution, and width and height of the bell curve.

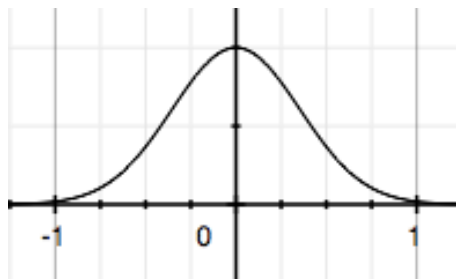
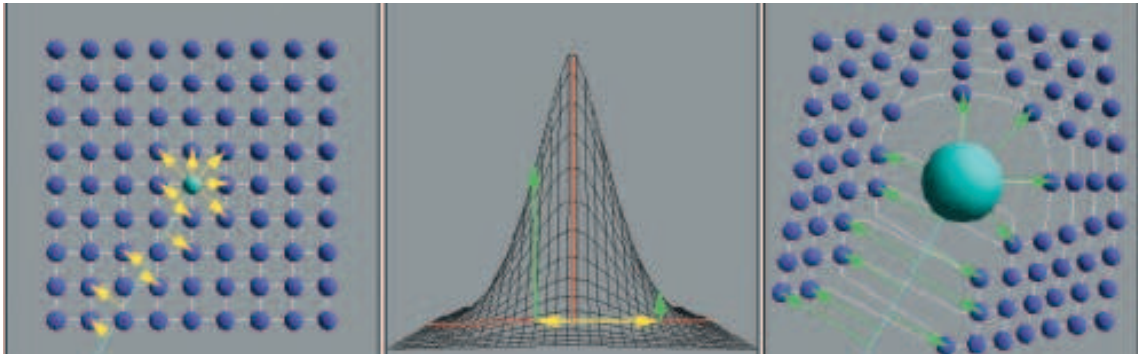


Figure 9 Distortion Function

The height of the function is the displacement coefficient corresponding to the view direction. The width of the function is the displacement coefficient perpendicular to the view direction. The following Figure 9 Distortion Function shows the used Gaussian profile used in Visual Access lens.



**Figure 10 Visual Access Method**

This work we are implementing here is based on the Visual Access method developed by Carpendale [127]. Figure 10 presented how the Gaussian function is implemented. Figure 11 shows the effect of the displacement and distortion on the original data.

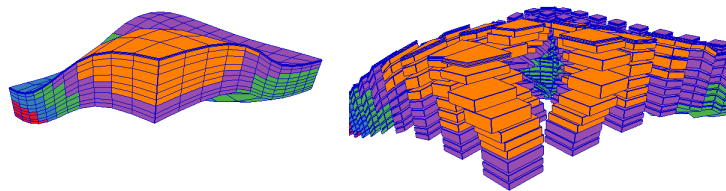


**Figure 11 on the left is a corner view of the data and on the right is the same view after applying distortion and displacement**

### **4.1.3 Focus and Pivot Point**

The focus point is a primary property associated with the lens; it is the focal of the detail-in-context effect. It can be a single cell or a group of cells representing a volume/area of

interest. Pivot Point, is the camera's center of rotation. In this visualization lens, the pivot is the same as the focus point for convenience.

#### **4.1.4 Camera Position and Direction**

Visual access method uses the camera-position/viewers-eye as a facilitator for the distortion lens. It can change the result of the distortion as it follows the line of sight. Some viewpoints reveal more/higher number of cells than others.

## **4.2 ENHANCED DISTORTION INTERACTIVE VIEWER FOR GRIDS (EDIG)**

The implementation of this work is done using OpenGL for interactive rendering and OpenCL for executing the detail-in-context in real-time. Applying the Visual Access method on the hydrocarbon reservoir simulation grid requires changing some of the default parameters. In this section we are introducing these changes.

### **4.2.1 3D Detail-In-Context Techniques**

The research work is capitalizing on the Visual Access method and applying few changes to it. Start from initial conditions, no displacement or distortion. The camera distance is set to optimal.

The visualization process of the eDig:

1. Select the set of data to be viewed from subset to a full field.
2. Select the focus point, line or curve interactively.
3. Apply displacement on all cells.

4. Apply distortion everywhere except the selected focus point.
5. Apply highlight method, if needed.
6. Set initial optimal camera location.

#### **4.2.2 Focus Area and distance of the affected area**

In this method, the viewer is allowed the ability to select single or multiple cells to focus on, interactively, during the visualization. The interactive capability allows for smooth curve selection with full editing.

#### **4.2.3 Stacked Cells**

Direct implementation of the visual access methods resulted in several limitations when distorting the cells in place. The method exaggerates the difference between each cell in the distance from the line of sight toward the cell direction. If the line of sight is too minimal then the direction values is minimal the distortion does not look correct.

#### **4.2.4 Focus Emphasizing Function**

Emphasizing the important area of the visualization can be achieved by exaggeration or highlighting. According to the design guidelines, lie factors should be reduced to bare minimum and according to the constancy perception minimum changes of the size might not be noticeable. In this implementation of the detail-in-context method we are not going to use any technique to emphasize the focus area. However, this method ignores distortion/displacement for the focused area. This means that a selected set of cells will be used as is that the distortion and displacement will not affect it.

### 4.3 Optimization Framework

In this section, the developed framework that enables the optimization is presented. This framework encompasses scripts, executable, results extraction, and correlation and report generation. This developed framework enables the optimization of the detail-in-context visualization. Figure 12 illustrates the process of the developed framework.

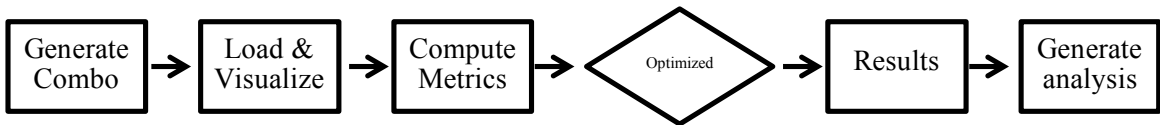


Figure 12 Developed Framework

#### 4.3.1 Generate Combinations

The first step on this framework is to develop managing tool that automate generation of all the combination of the input and metrics to be executed by the eDig viewer with the pre-created dataset. This was developed in python and it creates all the needed input for the viewer. These included, the selected dataset, parameters to optimize, metrics to be used, the applied default values for the rest of the controlling parameters, and the location for the output files. Then it passes these as command line arguments for the viewer.

#### 4.3.2 Visualize using eDIG Viewer

A visualization application is developed to view hydrocarbon reservoir simulation results. this application enables the use of the detail-in-context visualization method in two modes. An interactive mode where it allows the user to change any parameter on the fly. The second mode is a batch mode where it allows for the optimizations to be triggered. This application is developed with OpenGL and OpenCL. In batch mode, the viewer loads the selected dataset and prepare the view.

### **4.3.3 Metrics**

All the metrics selected in this work are implemented as part of the eDig 3D visualization tool for streamlining the optimization. It is implemented this way to reduce development time, as all of the dataset is loaded and ready.

### **4.3.4 Optimization & Results**

An optimization library is integrated with the viewer and connected with the metrics in a way that it enables the selection of the used metric to be dynamic and configurable at the execution time. The library is a global optimization PyGMO/PaGMO and the used method is self-adaptive differential evolution [128]. The library allows to define new optimization problem as an extension to the library and allow for compare all optimization algorithm to be used for comparison [128]. This library can be used with C++ and Python projects. The optimization identifies from the input space the rightly ranked metric results. These results will be analyzed. During the development, there were many iteration of the structure of the framework. The main aim is to develop an extendable framework that can accept and handle many input parameters and metrics with minimal integration effort.

### **4.3.5 Data Extractions and Reports**

An additional python script is developed that extract all the results from the experiments, generate correlation values, and place them into tables and charts. The generated analysis are covariance values between input and metric output. These results are exported as Microsoft PowerPoint slides and Word document.



## 4.4 Aesthetic and Utility Metrics

Five metrics are selected in this study. Two curvature analysis, two utility metrics, and a combined metric.

### 4.4.1 Face Conformal Energy (FCE)

This metric measures the curvature of the outcome of the visualization method. According to the grouping visual principles objects that follow curves appear to be viewed as a whole [88]. In this work we have implemented the real-time method to analyze curvature presented by Griffin et al [129]. The results of the method generate the principle curvatures per vertex.  $K_1$  is the maximum curvature at point  $p$  and  $K_2$  is the minimum curvature at point  $p$ . In plan curves the curvature at point  $p$  is the rate of change of its tangent vector. Figure 13 is showing the detail of tangent at point  $p$  at the left figure. It is the means to quantify the degree of curviness along a curve. In 3D surfaces, the curvature at point  $p$  have many curvature values along all directions. However, there are two main principle direction the maximum  $K_1$  and minimum  $K_2$  at it shows in the right picture of Figure 13. Detailed explanation of the principle curvature and how to generate them is beyond the scope of this work.

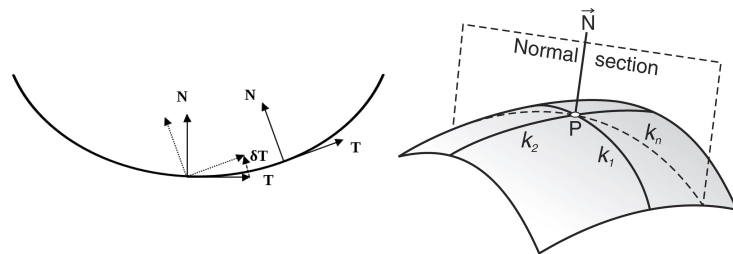
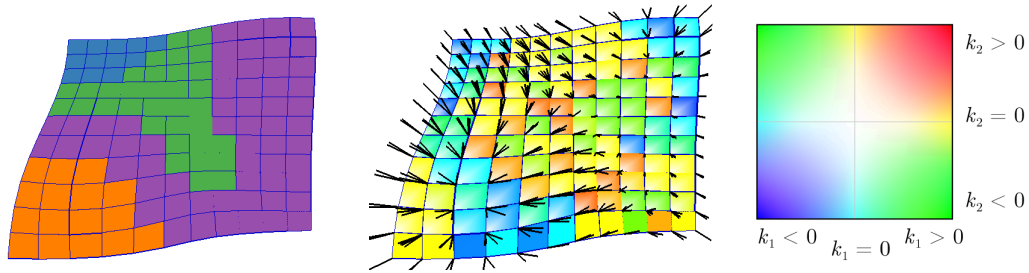


Figure 13 The left figure present the delta Tangent at a curve and the right figure shows the principle curvature

Figure 14 shows the curvature analysis for the first layer in the left image. The middle image shows the data colored by the principle curvature and the black lines represent the average normal of the vertices shared between triangles. The right image shows the 2D color map used which was generated by Griffin et al [129].



**Figure 14** The FCE metric uses the curvature analysis, on the left is the original data in the middle is the data colored by principle curvature, and on the right is the 2D color map.

Curvature analysis provides a value per point and this cannot be used as an objective function. Eigensatz et al developed a method to apply advanced shape editing on the curvature domain of the surface. This method allows direct editing on surface curvature values instead of the standard editing vertices positions. The new shape will be generated by rebuilding the shape using an optimization framework [130], [131].

The building block in this method is the evaluation of the surface curvature. Eigensatz et al have developed three different approaches to quantify curvature energy between the original shapes and the new deformed one. The first metric measures the vertex area curvature energy change named as Face Conformal Energy. Curvature analysis is computed on vertices. The vertex curvature energy is also computed on the vertex level. The vertex area is computed using the barycentric area, this can be seen in equation (5.1). The second method measures the energy changes in the edges of the polygons. This targets the difference of edge length before and after applying the lens. The barycentric areas of

the edge are used to normalize the effect of each edge. The third metric measures the deviation of the shape of the polygon by computing the differences in the angles. This metric is useful to determine how much change the area between the cells [130], [131].

$$E_c = \sum_{vi=V}^n A_{vi} [(K'_{1,i} - K_{1,i})^2 + (K'_{2,i} - K_{2,i})^2] \quad (5.1)$$

In this work, we have used Face Conformal Energy. To compute it in the optimization framework we auto set the base case and generate the principle curvature per vertex. Then for every variation on the shape we have by using the lens we generate the new principle curvature. From this we use equation (5.1) to find the absolute energy change. Figure 15 Face Energy Conformal Process shows the process from start to end. Figure (a) presents the base case and (b) shows the curvature, (d) shows the same grid with applying the distortion lens on it. The principle curvature from after the distortion effect is shown in (c), (e) and (f) and. The results of the FCE of this change is an absolute energy of 286.

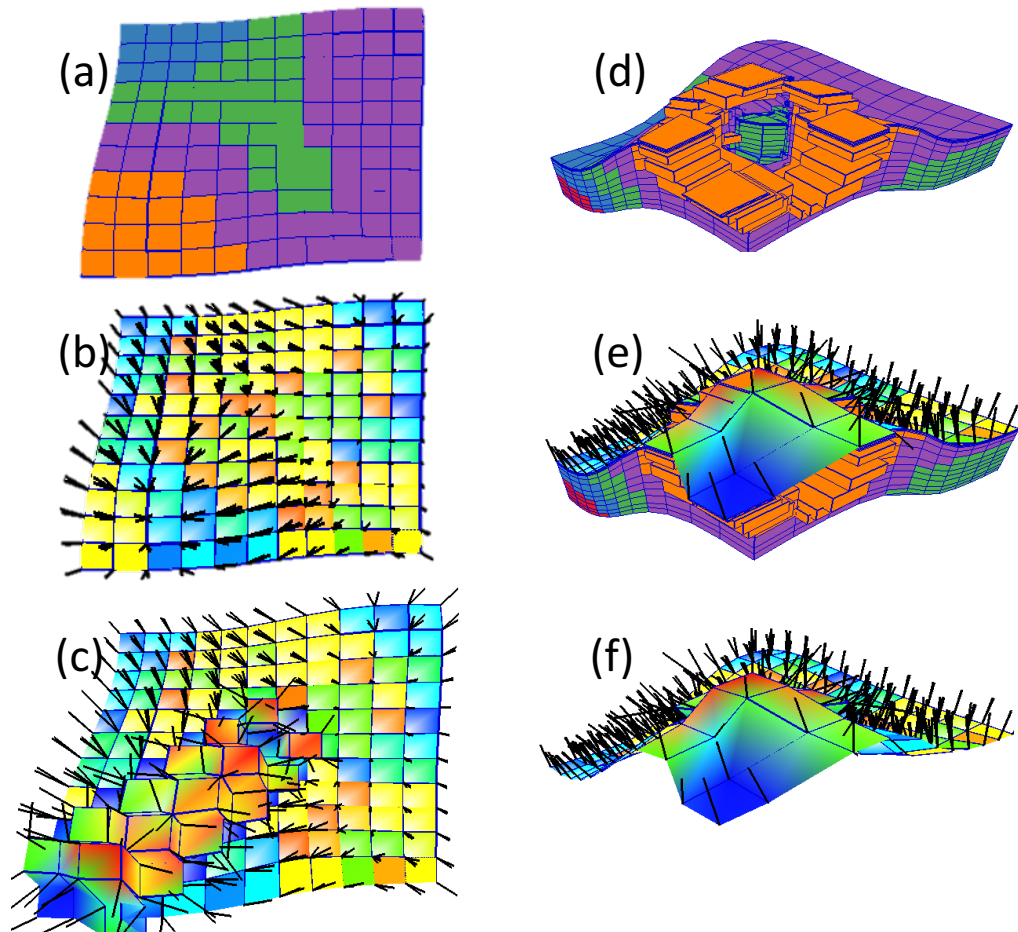


**Figure 15 Face Energy Conformal Process.** The curvature analysis is used to compute the energy applied to change the shape.

In this implementation, we are comparing the old surface curvature energy with the new one computed after applying the fish-eye lens effect on the data.

#### **4.4.2 Visible Cells**

This is a quantitative metric used for the purpose of reporting the visible cells in the view. This metrics will be used to evaluate the each of the aesthetics metrics for effectiveness. One aspect of the fisheye visualization is to improves the data visibility. This is achieved

by applying the displacement and distortion on the data volume. Figure 11 shows the shape of the data before and after applying the detail-in-context method. It is clear that more data is visible. With this finding, we are using the number of visible cells as a metric to measure the effectiveness of applying detail-in-context on the data.

Due to type of the data used and the current implementation of OpenGL/OpenCL libraries we customized and developed an approximation algorithm to create the number of visible cells metric. It is a software method mixing casting shadow algorithms (Frustum) and the ray casting method developed by Amanatides and Woo called “A Fast Voxel Traversal Algorithm for Ray Tracing”. We have adopted it to 3D space and used technique to build up the culling frustum as we traverse the grid cells [132].

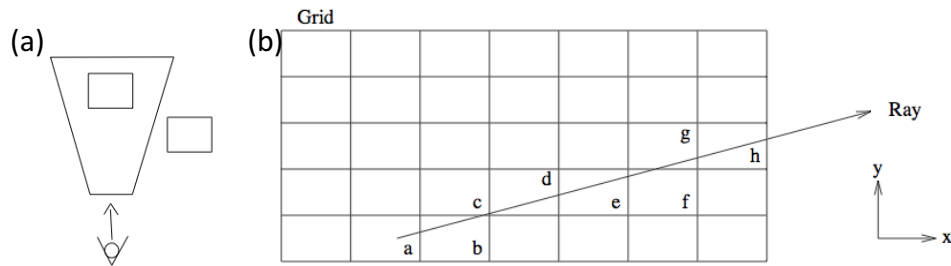


**Figure 16 (a) shows the frustum in action while (b) shows how rays trace cover the data in the space**

Figure 16 (a) shows a frustum test, any cells inside the frustum is visible and any cells outside the frustum is not. The following is the process we use to generate create compute the number of visible cells.

1. Create a spatial structure using loose grids
2. Sort cells in block based on distance from camera
3. Select the closest corner to start from
4. Ray trace the blocks in the path Figure 16(b)

5. For all the blocks
  - a. Select the closest cell
  - b. Find all adjacent if any
  - c. Create a frustum Figure 17 (a) , (d) and (f)
  - d. Use the Frustum on all cells in the block in the path Figure 17 (b)
    - i. If cell inside, then flag
    - ii. If cell intersect then set flag visible, rebuild Frustum by adding this cell, and continue Figure 17 (e) shows how the frustum is rebuild

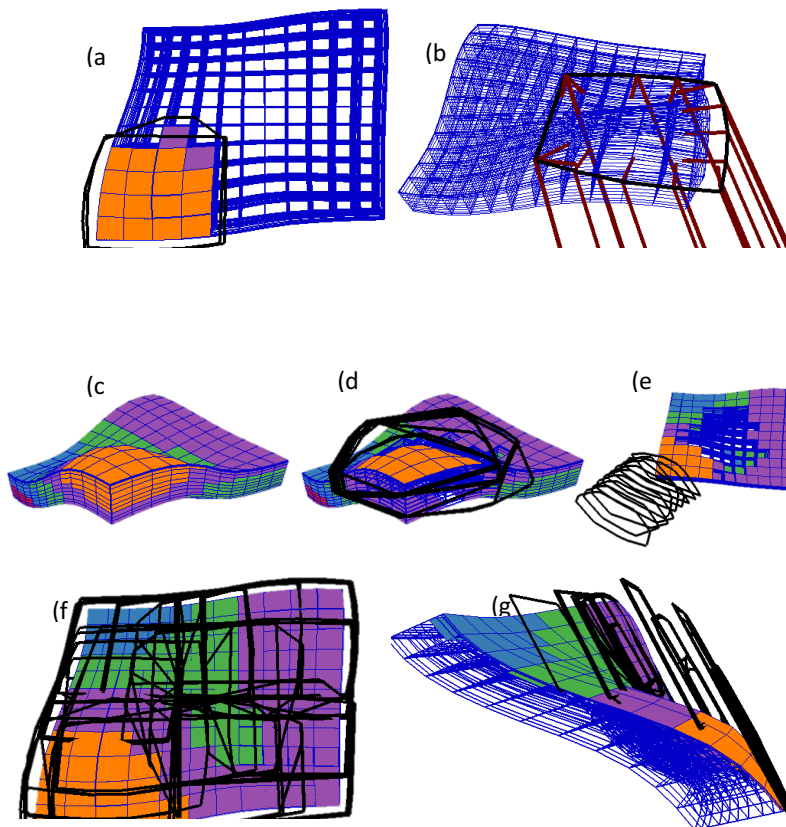


**Figure 17** These figures shows how the new algorithm of shadow casting works

The new developed method should work with data that uses polygons as the underline structure. Figure 18 shows how the implemented visibility test works on the grid data. (a)

and (b) shows that the algorithm works on a connected surface by identifying neighboring cells to create a connected cull surface and test the cells in the ray path. (b) shows that the same algorithm will work on cell by cell.

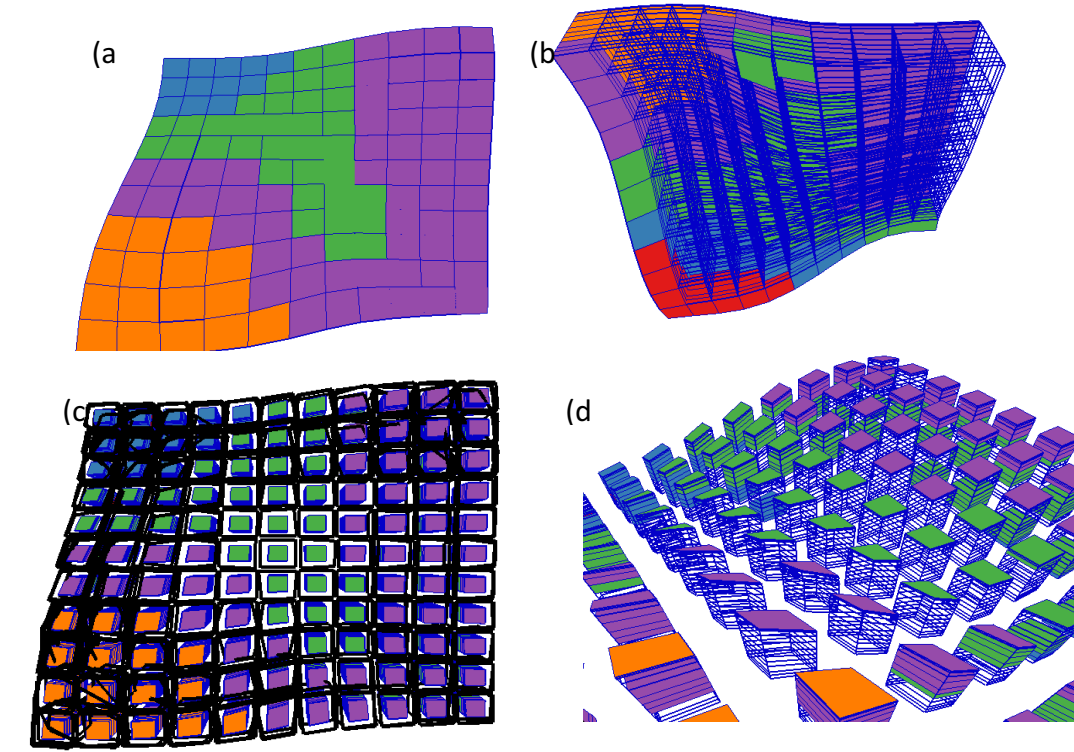
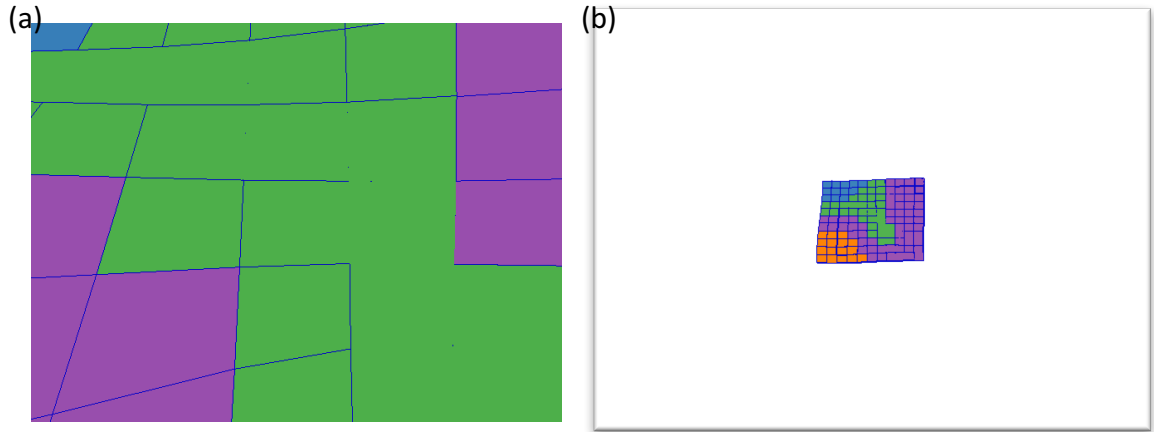


Figure 18 Visible Cells Test (b) shows the results of visibility test on connected surface and (c) and (d) shows visibility test on disconnected surface

### 4.5 Ratio of Used Space (RUS)

This metric focus on how much space is used after applying the detail-in-context method. This is to maximize the display area and to reduce unutilized space. It is simply computed as the number of used pixels over the total number of pixels in the display area. It is based on Tufte's [133] guideline of maximizing the usage of display area. Figure 19 shows the difference that the Ratio of Used Space compute.



**Figure 19 Ratio of Used Space:** (a) shows the full space is used while (b) shows that part of the space is used

### 4.5.1 Average Relative Change of Mean Curvature (RCMC)

This metric indicates the relative change of the shape represented by the overall averaged mean curvature  $H$  (1). The mean curvature is computed from the principle curvature at every vertex. It is based on the same data used for FCE. The computation of the curvature we have implemented the method presented by [129]. This is applied on one layer.

$$ARMC = 1/n\{\sum_{i=0}^n |H - H'|/\max(H, H')\} \quad (2)$$

Equation (5.2) is used as the objective function. This metric aims to minimize the change to the results of the detail-in-context visualization method to maintain relative relationship to the original shape that translate to better recognition. This is developed on top of the generated curvature. In Figure 15 we have computed the RCMC which is a relative value of .180.

### 4.5.2 Combined RUS & RCMC

To simplify the optimization, we have combined both of the objective function into a single minimization problem. Equation (5.3) shows the combined functions. During the



experiments of the combined metric the weights for each of the objective function were under evaluation to achieve the most appealing view.

$$\textit{Combined} = .3 * \textit{RUS} + -.7 * \textit{RCMC} \quad (3)$$

## **CHAPTER 5**

### **EXPERIMENTS & RESULTS**

In Chapter 5, we describe the used dataset, the setup for each experiment, the results generated from the experiments, and discussion and analysis of resulted data.

#### **5.1 Hydrocarbon Reservoir Dataset**

In this study, we are using geocellular 3D grids as the datasets. It is consisting of voxels/cells. There are two datasets used for the experiments in this study the results of the studies are averaged. Both of the sizes of the data set is  $11*11*11$  total size of 1331 cells. These datasets are from hydrocarbon numerical reservoirs simulation models. The datasets are aerially larger (x and y) axis in comparison to the depth axis and therefore. The depth axis is exaggerated by a default scale of 50 for visualization purposes.

#### **5.2 Experiment Setup**

The experiments conducted in this research is to evaluate all the input parameter against all objective functions. The experiments are prepared in this manner to find relation between changing the input parameter and the objective functions. We have used three camera setups for these experiments. The camera setups are as follows. The first and the second are the top view and 45-degree view. The third setup is using the camera X and Y angle as parameters to be optimized by the objective functions.

The following is the list of used objective functions that was detailed in Chapter 4:

1. Number of Visible Cells
2. Face Conformal Energy
3. Ratio of Used Space
4. Average Relative Change of Mean Curvature
5. Combined Ratio of Used Space & Average Relative Change of Mean Curvature

**Table 2: Default Lens Parameters**

	Min	Max	Default
Gaussian Parameter	0	2.0	.5
Z-Axis Exaggeration	0	200	50
Camera distance	1	5	2.5
Camera X& Y Angle	0	359	0
XY Displacement	0	5	1
XYZ Displacement	0	5	1

Table 2: Default Lens Parameters shows the default parameters used for all experiments. In every experiment, we use the default value of each of the input parameters and changes the targeted parameter through linear optimization. There are five objective functions and five input parameters with three different camera setups and two datasets that leads to 150 executed experiments.

### **5.3 Lenses Included in The Experiments**

Visual access method consists of distortion and displacement features in addition to the interactive parameters. The use of displacement parameter on 3D by itself is similar to multiple lenses. Such as cutaway lenses [23], [26], [27].

The use of distortion function without displacement on 3D data is similar to these two such as fisheye methods [75], [76]. As part of the experiment, we have conducted each of these features separately to see their effect of metrics.

Ghost and transparent lens implementation was applied on 3D data with limited size of layers [32]. It cannot be easily applied on simulation data without creating clutter. However, a modified version might resolve the clutter issue and be part of future research.

The balloon lens is a form of distortion function. It was not used on scientific data due to the potential of sever amount of displacement from the original location that can create clutter. Even with the help of the ghost objects remaining in the original the visualization will be confusing with so many cells displaced in a balloon shape in the view [70]. A proper evaluate of this lens can be part of future work.

## 5.4 Results

In this section, we present the results of the conducted 150 experiments. Then we analyze and discuss the results. The starting of the experiments is executing the base case with the default values. The results are summarized in Table 3.

The next section highlights the major findings of the experiments. The second section contains the results of the objective functions. The third section presents the highest correlation values between the input parameters and the objective functions.

**Table 3: Base Case Analysis**

Name	Case	Top	45	X &Y
# of Vis Cells	Case 1	668	646	958

	Case 2	654	700	1121
	Avg	661	673	1039
Face Conformal Energy (FCE)	Avg	0	0	0
Ratio of Used Space (RUS)	Case 1	0.3546	.3793	0.4745
	Case 2	.39	.42	.5
	Avg	0.372	0.399	.487
Average Relative Change of Mean Curvature (RCMC)	Avg	0	0	0
Combined RUS & RCMC	Case 1	0.5405	0.5578	0.6121
	Case 2	0.5566	0.5834	0.6189
	Avg	0.5485	0.5706	0.6155

The detailed results for all of the 150 experiments are summarized in tabular format and listed in the Appendix.

## 5.5 Discussion

In this section, the results are explained. Starting with the base cases analysis then going over the results grouped by objective function and presenting the impact of the input parameters per objective function.

### 5.5.1 Base Case Analysis

In the analysis of the base case we evaluate both of the datasets against the objective functions without optimizations on any of the input parameters except the X & Y parameters. The results in the X & Y column is a search for the best angle viewing angle using one of the objective functions. This provides an understanding of the dataset at hand and serve as a base for comparison with the experiments. The summary of the base case analysis is presented at Table 3.

The outcome of the first objective function, the number of visible cells, using the default parameters for the top view is 661 cells while the outcome for the 45-degree view is 673 cells. The visible cell test is highly impacted by the viewing angle, as the maximum visible cells found are 1039. This means the users of this lens need to keep looking for the best angle to get the most of this lens. In practice, users will require more time to find it. Manual experiments have been conducted to verify that the primary cause for the initial high number of visible cells is due to the displacement function. The second objective function, the ratio of used space is also impacted by the viewing angle, where the maximum ratio found was 48%. The top view has 37% where the 45-degree view had 39% used display area. This means when forcing a specific data size and camera distance the shape of the can determine the utilization. In both of the test cases, the data is aerially and finding a proper angle can cover the space. However, it is not that significant. The third and fourth metric, the face conformal energy and average relative change of mean curvature (RCMC) objective functions are a comparison metrics and thus the results shows zero changes because there are not changes on the input parameters. This means that these metrics only benefit lenses that change the shape of the data. The Combined RUS & RCMC provides a sense shape and used space. This allowed for maximization of space usage when identifying the optimal viewing angle.

### **5.5.2 Number of visible cells (NVC)**

NVC is a utility metric that shows the practical benefit of displaying data. Using NVC as an objective will maximize the visible cells.

### **Gaussian parameter**

Top and 45-degree views did not present changes to the results of the visible cells. The Viewing angle did provide a marginal improve result at 4% with a value of 1081 which is at 81%. The  $R^2$  correlation value indicates that there is no direct correlation between Gaussian parameter and the number of visible cells objective function. Figure 20 presents the results for optimizing the view on both cases. Due to displacement, the amount required to apply distortion is minimal view the hidden cells.

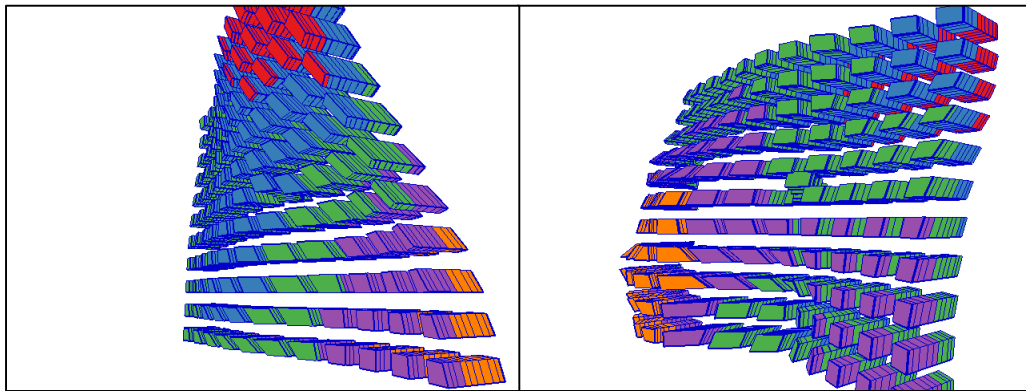


Figure 20 X & Y Angle, The Gaussian parameter,X Angle,Y Angle, Number of Visible Cells

### **Camera Distance**

The change on top view is minimal. Whereas the 45-degree view provided a change of 31.5% on average of the two cases. The result of the number of visible cells is also limited when optimizing for X & Y parameters. On the top view. Camera distance in general has a minimal correlation on the number of visible cells with a maximum  $R^2$  value of .3 for the top view on the first case only. The other camera setup has less that  $R^2$  value of .15. if the camera distance is close then few cells would show up. If the distance allows for full view, then only cells at the outer area will be visible.

### **Z Axis Exaggeration**

Over all this parameter did have an impact on the number of visible cells. The top view has a change of 11% compared to base case. The 45-degree view resulted in a 9% increase of visible cells. The average gain of cells when optimizing the view for the optimal X&Y values is 5%. The maximum visible cells in using Z exaggeration reached 84% of the data. The second case has showed the highest correlation of  $R^2$  value of .3 when optimizing for the camera angle and 19% more visible cells other than that, there is no noticeable correlation. When optimizing with the X and Y angle parameter the results showed 9% more cells as seen in Figure 21. The maximum correlation of the XY with the NVC was in the first case with an  $R^2$  value of .8 for the top view and the average  $R^2$  value is .45.

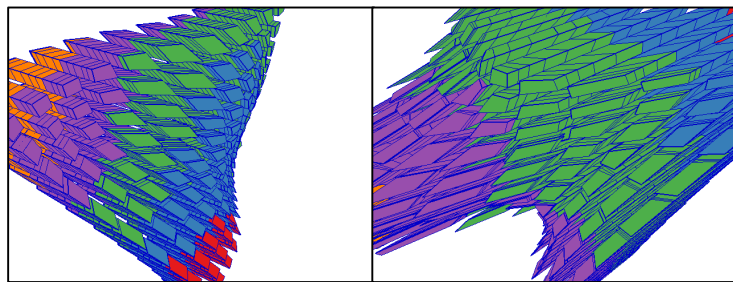


Figure 21 X & Y Angle, Z Exaggeration, X Angle, Y Angle, Number of Visible Cells

### **XY Displacement**

The top view has 12% more NVC value compared to base case. The 45-degree view has a 19% more visible cells. When optimizing with the X and Y angle parameter the results showed 9% more cells. The maximum correlation of the XY with the NVC was in the first case with an  $R^2$  value of .8 for the top view and the average  $R^2$  value is .45.

### **XYZ Displacement**

Top view has a gain of 16% while the 45-degree view has a 34%. The optimization for the X & Y camera angle has a gain of 19% and the NVC value of 1239. This constitute of 93%



of the dataset. The averaged correlation  $R^2$  value was .3 when identifying the optimal X & Y camera angle.

### **Overall Analysis**

As stated in the base case analysis, the high number of visible cells is due to the default displacement. This utility metric does provide a good indication on the performance of the detail-in-context method in terms of the degree of showing the data. In addition, Number of visible cells is a heuristic solution that gives an approximation results.

### **5.5.3 Face Conformal Energy Metric (FCE)**

This result of this metric depends on the shape of the dataset and the amount of variation applied to it. The goal of using this metric as an objective function is to minimize the change of the shape. In this case, the optimizer will search a solution space that has zero changes.

FCE metric did not present easy to relate values for both of the used cases. As a method that utilizes a base case to compare against, it does not provide direct relation. Thus, it presents the need for a metric that can provide easier understanding of the change to the data.

### **Gaussian parameter**

On the top view, the changes to the Gaussian parameter did not present any effect on the FCE metric on both cases due to the minimization function. On the 45-degree view, it has high correlation with an  $R^2$  value of .93 on the first case where on the second case the correlation is .79. On the 45-degree view, the maximum change was .8 and the average is .6. We expected that at particular angles and the shape of the data, the changes on the Gaussian parameter would impact the FCE metric.

### **Camera Distance**

In this experiment, the camera distance does not have an impact on the FCE metric from the top view. On the 45-degree view the average correlation is .47. The change of the minimal results was on the 45-degree view on average is 7.7. When adding the optimization for X & Y, the average maximum change reached 4.2. From these experiments, the camera distance has an impact on the shape due to the used default value for the Gaussian that would make a change based on a particular camera angle.

### **Z Axis Exaggeration**

This parameter changes the shape of the data and thus it has an impact. It has an  $R^2$  correlation value of .9 for case 2 and an average value of .44. This correlation is when optimizing for the camera angle. The average impact on FCE of 41.5.

### **XY Displacement**

The highest average  $R^2$  value is .3 for the top view. The XY displacement property has a high impact on the FCE results. Optimizing for the angle and XY displacement, the recorded FCE is 58.8 for the first case where the value was 93.3. This means on particular camera angle the XY displacement will have a high impact.

### **XYZ Displacement**

This property presented high impact on all experiments. The highest being the average FCE value of 83.9 when including the optimizing for the viewing angle. The top view FCE value is 58 and the FCE value for the 45-degree view is 62.1. There is no noted correlation value.

### **Overall Analysis**

Face Conformal Energy values does provide an indication on the change on the shape although the values are not easily comparable. The small changes are in fraction and the large changes reached to 93.

### **5.5.4 Ratio of Used Space (RUS)**

This is a design guideline metric with the objective to minimized wasted space.

#### **Gaussian parameter**

This parameter has a local change to the data and from the experiments it does not show large variation. The maximum change was from 40% to 50% when optimizing for Gaussian and X & Y angle which is similar to the RUS value of the base case. The first case did show an  $R^2$  correlation of .5 for the 45-degree view.

#### **Camera Distance**

This parameter has the biggest impact with 90% RUS value when optimizing for distance and X&Y angle. The rest of the configuration did show improved results that jumped from 40% to 60% and 70% RUS values. It also has the high averaged  $R^2$  correlation value of .94 for the 45-degree view.

#### **Z Axis Exaggeration**

This parameter showed an overall better correlation for the top and 45-degree view with  $R^2$  value of .99. The averaged results have of RUS is .7 for the top view, .6 for the 45-degree view and .8 for when optimizing for the viewing angle.

#### **XY Displacement**

In general, it had minimal impact on the result compared to the other parameter with 40% values of RUS for top and 45-degree view and .6 for the optimized X & Y angle. The 45-degree view had a  $R^2$  correlation value of .45.

#### **XYZ Displacement**

Is similar to XY displacement parameter in results and impact, the highest RUS value was 70% as seen in Figure 22. Also there are no noticeable correlation values.

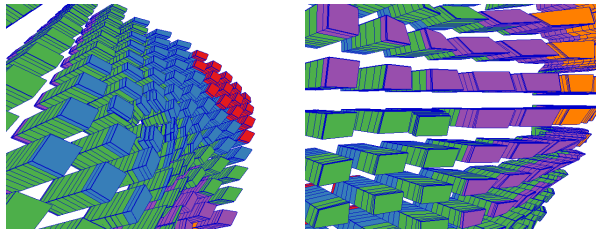


Figure 22 X & Y Angle, Camera Distance, X Angle, Y Angle, using Ratio of Used Space

## Overall Analysis

RUS as a metric provides information on how sparse is the displayed data. Ratio of used space does provide a good measure of the utilization of the available space.

### 5.5.5 Average Relative Change of Mean Curvature (RCMC)

The average relative change of mean curvature is a shape metric similar to FCE which is also used as minimization objective function. As this metric is based on a simple relative change equation, the results are relatively easier to interpret.

### Gaussian parameter

In this parameter experiments, only the 45-degree view did have an  $R^2$  correlation value of .85 on the average of the two cases. There has been no noticeable change in the recorded results. This is mainly due to the minimization function where the solution space only contains the possible parameter that produces zero changes.

### Camera Distance

There is no correlation between this parameter and the RCME. In addition, this parameter does not impact the shape. This is mainly due to the Camera distance does not impact the shape.

### Z Axis Exaggeration

This parameter does have a correlation with the 45-degree view on the second case with an  $R^2$  value of .6 and an average of .34. The maximum change is in the optimization camera

setup which is 40% relative change to the original shape. There is a maximum 10% shape change on both the top view and the 45-degree view.

### **XY Displacement**

This parameter has no noticeable correlation value. It has a minimal recorded shape change for the top view and 45-degree view with 10% RCMC value. When also optimizing for the X&Y angle, the maximum shape change is 40%.

### **XYZ Displacement**

This parameter has a minimal correlation with RCMC with a .25  $R^2$  value for the optimized camera angle and .31  $R^2$  value for the top view. Over all on all the experiment the minimal change was 30% and the top RCMC value was 50%.

### **Overall Analysis**

In general, RCMC provides a better measure in the sense that it has a clear degree of curvature change from the original shape to the modified shape in comparison to FCE metric. In the other hand, RCMC could not detect local changes such as the changes Gaussian parameter has on the shape which the FCE metric could.

## **5.5.6 Combined Ratio of Used Space & Average Relative Change of Mean**

### **Curvature**

This objective function is designed to capture the measurement of both selected aspects of this study, the relative shape metric, and the design guideline of maximizing the use of space.

### **Gaussian parameter**

This parameter has a high correlation with this objective function on the 45-degree view with an average  $R^2$  value of .93. Over all the used camera setups, minimum result value is

30% and the maximal output value is 40%. Figure 23 shows the optimized view using the X & Y angle.

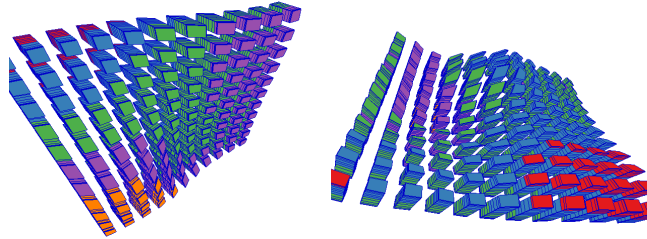


**Figure 23 X & Y Angle, The Gaussian parameter, X Angle, Y Angle, Combined Ratio of Used Space & Average Relative Change of Mean Curvature**

### **Camera Distance**

This camera property has a  $R^2$  correlation value of .97 on the 45-degree view. On the X&Y optimization value, it has an  $R^2$  value of .5. A value of .7 is the maximal recorded combined results.

### **Z Axis Exaggeration**

The correlation of this property is high on all camera setups. It has an  $R^2$  value of .97 on the top view and .98 on the 45-degree view, and .83 when optimizing for the X & Y angle. The maximal recorded change is .6 on the top view and 45-degree view in addition to .7  $R^2$  when optimizing for the camera angle.

### **XY Displacement**

The maximal correlation in this shape parameter is on the 45-degree view with an  $R^2$  value of .81. The maximal recorded change is .5, which is when looking for the impact of the camera angle with the X&Y displacement.

### **XYZ Displacement**

This parameter has a correlation on both the top view and the 45-degree with .96 and .95  $R^2$  values. The maximum-recorded result is .7 when also optimizing for the camera angle

with maximal impact and minimal recorded result is .4 on all experiments as seen in Figure 24 for both cases.

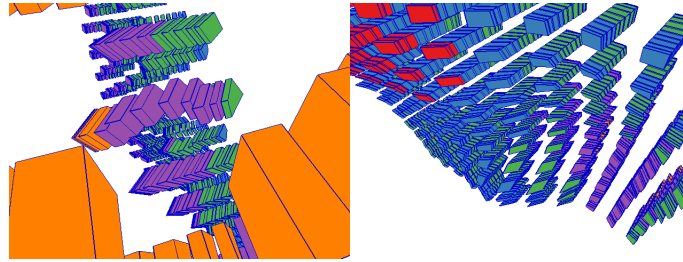


Figure 24 X & Y Angle, XYZ Displacement, X Angle, Y Angle, Combined Ratio of Used Space & Average Relative Change of Mean Curvature

### Overall Analysis

Combined RUS & RCMC provides a sense for both worlds and the measure did present a correlated value for both the shape a used space. The result of the combined metric does suffer from the issues presented of each of the single metrics. The shape metric as is will always minimize and as seen in the results it leads to minimal to almost no changes. On the other hand, the RUS metric maximizes the use of space and this can be on the cost of high values of shape changing parameters namely the  $Z$  exaggeration and XYZ displacement or close view of the results by minimizing the camera distance.

The relative shape change metric by itself will constantly minimize the changes without providing difference on the shape. However, the utilized space by itself focuses on utilizing all of the space. Combining these two metrics has produced a balance that was achieved by forcing specific weight values. Regarding the input parameters displacement and camera distance, which had the major impact on both the used space and the relative shape change.

Close up to the data will reduce the full picture. Having a measurement that can balance out the use of space and the minimization of shape changes can lead to an efficient use of space while maintaining a recognizable shape.

The used shape metric is one-dimensional and the shape of the data is much more complex. Any new shape metrics requires representing the data or the change of the data. FCE and RCMC does not distinguish if the change of the shape is distortion or exaggeration where as it is not too sensitive to displacement.

## 5.6 Summary of Results

This section highlights the major findings of the experiments. The first sub-section presents the highest correlation values between the input parameters and the objective functions. The second sub-section contains the results of the objective functions.

### 5.6.1 Highest Correlation Values

This sub-section focuses on the highest outcome of the objective functions based on the used input parameters. The following tables list the summary of the results per group experiment. Table 4 shows the summary of the highest correlation values between objective functions and input parameters.

**Table 4: Summary of highest correlation values between the objective function and input parameters**

Objective function	Properties	R <sup>2</sup> Value	SD
Number of Visible Cells	X&Y Displacement on top view	.45	0.37



Face Conformal Energy	The Gaussian on the 45-degree view	.8	0.0695
Ratio of Used Space	Camera Distance on the 45-degree view	.9	0.0105
	Z Exaggeration on top and 45-degree view	.99	.0005,.001
Average Relative Change of Mean Curvature	The Gaussian on the 45-degree view	.8	.0165
Combined Ratio of Used Space & Average Relative Change of Mean Curvature	The Gaussian on the top view	.93	.024
	Camera distance on the 45-degree view	.97	.0045
	Z Exaggeration on top/45 and arbitrary X & Y camera angle	.99, .98, and .83	.001,.011,0.037
	XYZ on top/45 degree-view	.96 and .95	.0295,.0435

## 5.6.2 Highest objective function results

The following Table 5 lists the objective functions and the input properties that have the highest obtained results.

**Table 5: Summary of highest results obtained from objective functions and input parameters**

Objective function	Properties	Maximum Change from base case
Number of Visible Cells	XYZ Displacement on 45-degree view	34%
Face Conformal Energy	XYZ Displacement on the 45-degree view	8300%
Ratio of Used Space	Camera Distance on optimized X & Y view	84%
	Z Exaggeration on optimized X & Y view	64.2%
Average Relative Change of Mean Curvature	XYZ Displacement on optimized X & Y view	500%

Combined Ratio of Used Space & Average Relative Change of Mean Curvature	Camera distance on optimized X & Y view	13.7%
	Z Exaggeration on optimized X & Y view	13.7%

### 5.6.3 Observation on the input parameters

This is an analysis of the used input parameters and the impact they have on the visualization method. The analysis starts with discussing the impact of the camera angle then it goes by each of the used parameters.

#### Camera X&Y Angle

Adding the camera x and y location does provide maximal values although not the best view to show the data. Camera angles have big range of impact on the results. The use of these parameters should be limited to an acceptable range. Some of the generated results do indeed maximize the objective function; however, some of the results show limited view of the full picture.

#### Gaussian Parameter

Gaussian parameter shows a local change around the center of focus and it is mainly impacted by the viewing angle. The highest impact this parameter has is when associated with the 45-degree view. This means to capitalize on the Gaussian parameters a specific camera angle has to be selected. This parameter also has a high correlation with both the shape metrics of the 45-degree view.

### **Camera Distance**

This camera parameter has the maximum impact on the RUS and the combined RUS and RCMC metrics. This is due to a close of the result would fill the available space and a faraway distance would reduce that.

### **Z Axis Exaggeration**

This shape parameter has a highest impact on the RUS metric. This is due to the exaggeration can fill the space on extreme case. However, the combination of the z axis exaggeration with RUS may or may not suit the user, as the optimal result tend to over exaggerate to fill the display.

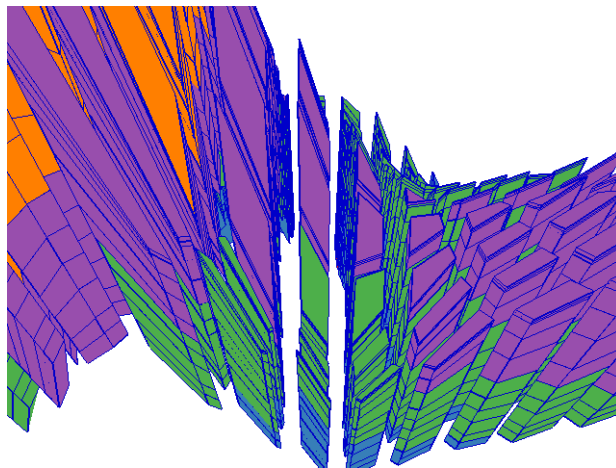


**Figure 25 Z Axis Exaggeration**

### **XY Displacement**

From the conducted experiments, there are minor impacts on the noticed on the used metrics. It has an  $R^2$  correlation value of .45 with the number of visible cells. Both of the shape metrics has seen changes using this parameter when optimizing for the view, the FCE has a change of 5800% and on the RCMC it has a change of 40%. On the combined RUS & RCMC it has a correlation of .5 on the top view, .88 on the 45-degree view, and .6

when optimizing the camera angles. However, it does not maximize this metric. From all of the used parameters this one has minimal impact with all of the used metrics.

### **XYZ Displacement**

In general, this parameter has highest impact on the NVC, FCE, and RCMC metrics. It has 19% more cells using number of visible cells metric compared to base. On the FCE metric is has an 8300% change compared to the base case. On the RCMC it has 50% change. On the combined metric of RUS and RCMC it has 70% change. On the RUS metric the maximum it produced is 45% more used space although it is not the maximum parameter.

## CHAPTER 6

### SURVEY & VALIDATION

As part of this research work, we have conducted a validation survey on multiple aspect of this study. There is a total of 12 questions used. The first aspect is on the validity of the general and specific used lens parameters. The second part is on the usefulness of the used metrics. The last question is a general research focuses on the importance of automated generation of visualizations. These questions are on a scale from ten (10) to one (1). Ten being high in score and one being low on score.

#### 6.1 Questionnaire

##### **Lens Parameter:**

1. Does camera distance have an impact on view?
2. Does Camera angle has an impact on view?
3. Is Exaggeration on the Z axis important?
4. Does the Displacement XY enhance the view?
5. Does Displacement XYZ enhance the view?
6. Does Distortion enhance the view?

##### **Metric parameter:**

7. Usefulness of Number of Visible Cells (NVC). Is showing more data beneficial?
8. Usefulness of Ratio of used space (RUS). Is maximizing used space beneficial?
9. Is absolute shape change analysis beneficial?
10. Is relative shape change analysis beneficial?
11. Does combining any metrics provide better information?

##### **General question:**

12. Is automating the view useful?

## **6.2 Survey results and Analysis**

Twenty (20) individuals who have used multiple reservoir visualization applications have conducted this surveyed. Four of these engineers have 8 years of experience and have developed simulation visualization applications. The rest of the participants have experience that range from 3 to 15 years in the field of visualization applications of reservoir simulation. In the experiment setup, we have presented a live demonstration of the lens in action with all various lens parameters and implemented metrics. Then the users answer the survey questions after seeing the lens in action. Figure 26 shows a complete analysis of the user survey.

## **6.3 Distance and Camera Angles**

On the lens parameters, the users have stated both camera distance and camera angle are important for 3D visualization. Camera distance scored 9.3 with SD of 1.1 and camera angle scored 9.5 with SD of .97. This re-indicate the importance of interactive navigation in visualization applications. The metric analysis has showed that both selection camera distance and angles is importance in order to have a full picture of the displayed data.

## **6.4 Z Axis Exaggeration**

The survey has indicated that the exaggeration of the z-axis is only specific to data type. Multiple users have stated that this only works on geological structure due to the scale of the data on the XY-axis differs from the Z-axis. The average score this parameter has is 6.85 with SD of 1.93. Typical reservoir thickness can varies from 50 feet to hundreds of feet whereas the areal scale can vary from few kilometers to 100 kilometers [134]. We have

anticipated the need for this parameter and used it in this research. This is due to the fact we have applied this lens on a hydrocarbon reservoir data. The experiment has presented that the use of exaggeration does show more cell. However, extreme exaggeration will block the view.

## **6.5 XY & XYZ Displacement Function**

We have anticipated that displacement on the XY and XYZ would have scored high value in the validation this is due to have the ability to show more data and being an important part of the visual access lens. However, from the survey, the XY displacement scored 6.12 with SD of 1.8 and XYZ displacement scored 5 with SD of 1.5. These scores were accompanied with comments such as displacement has to be limited, too many cells, and as long as there is a communication between the cells. The lowest rated values were three with a comment stating problem of physical properties and displacement gives wrong location. This indicates the importance of accurate representation of the actual data and thus any changes to the displacement should be minimized to reflect coherence. The highest rated value was eight (8) with a comment stating this is good for looking at hidden cells. The conducted experiment showed otherwise, the need of displacement would show more data at hand. Any displacement value will increase the number of visible cells. This indicates showing more data is not a high demand in visualization application.

## **6.6 Distortion Function**

The distortion function is the essence of the detail-in-focus lens, it has scored 7.1 in the validation survey with an SD of 2.2. It had mixed reviews, one of the comments were

impressive but not useful. The highest scored value was 10. The general feedback through the interview was positive. This is similar to what the metrics have showed, it does not add much when the data is displaced and it have a negative impact on the shape factor.

## **6.7 Number of Visible Cells (NVC)**

Regarding the metric questions, the overall results are from neutral to good. The number of visible cells (NVC) metric which translate to is more data visible data is good or not. The average received score from the reviewers is 6.9 with SD of 1.94. The reviewers' comments are it is not always good to view more data, if it can only show the important part, and it has to be in-combination with another metrics. The lowest score was one with a feedback of no and the highest score was 10. This mix of reviews on the metric was mainly focused around the concept of showing more data is not always good. This was not anticipated. However, the objective of this metric is to identify the performance of the lens of where it can deliver more information to the view. In the experiments, when optimizing for viewing more cells data the view is not always at suitable. This corresponds to Visual Emptiness research where less visible is more [108].

## **6.8 Ratio of Used Space (RUS)**

The general feedback of Proper use of space has scored an average of 6.9 and SD of 1.6. The reviewers' comments focused on view coherence and usability. During the demonstration, users stated that usage of space is not too critical as long as it does not clutter the view. Optimized for maximum space usage can cause clutter as the results from



the experiments shows Z axis exaggeration can fill the space. This means, any visualization lens should not fill the space fully to reduce clutter.

## **6.9 Curvature Analysis (FCE & RCMC)**

The surveyed users have stated that in day to day visual analysis the curvature analysis has no usage. The scored values for the Face Energy Conformal, which is an absolute value, is 4.85 with SD of 2.65. The RCMC metric slightly better as one surveyor stated relative is better than absolute for referencing with an average score of 5.8 and SD of 2.69. This is anticipated as this metric is designed to evaluate the degree of change the lens apply on the data for the purpose of visualization scientist to evaluate different lenses. From the experiments the use of the curvature analysis had little impact except on displacement as it has a global change.

## **6.10 Combined Metric (RUS & RCMC)**

The question regarding the combined metric got a score of 5.15 with SD of 2.58. The general feedback is that metrics has to be normalized and with weights. This has been reflected from the literature review and experiments as the combined metrics has to compromise on all participating fronts. This outcome is aligned with the experiments results as the combined metric has the minimal impact on the results of the experiments although, it has the most correlation with multiple lens properties as seen in Table 3. The minimal impact is due to the compromise the metric by selecting a single point from the pareto front [109].

## 6.11 View Automation

Last questions, is automating the generation of the best view useful has gotten a score of 8.5 with SD of 1.5. This indicated the need for a lens that can automate the visualization. The reviewers' comments focused on providing input, automation, and depending on implementation. The general feedback from the interviews states that it takes time to set the proper display to convey the information in the visualized data. This state the need to continuously investigate and propose solutions in this open research problem.

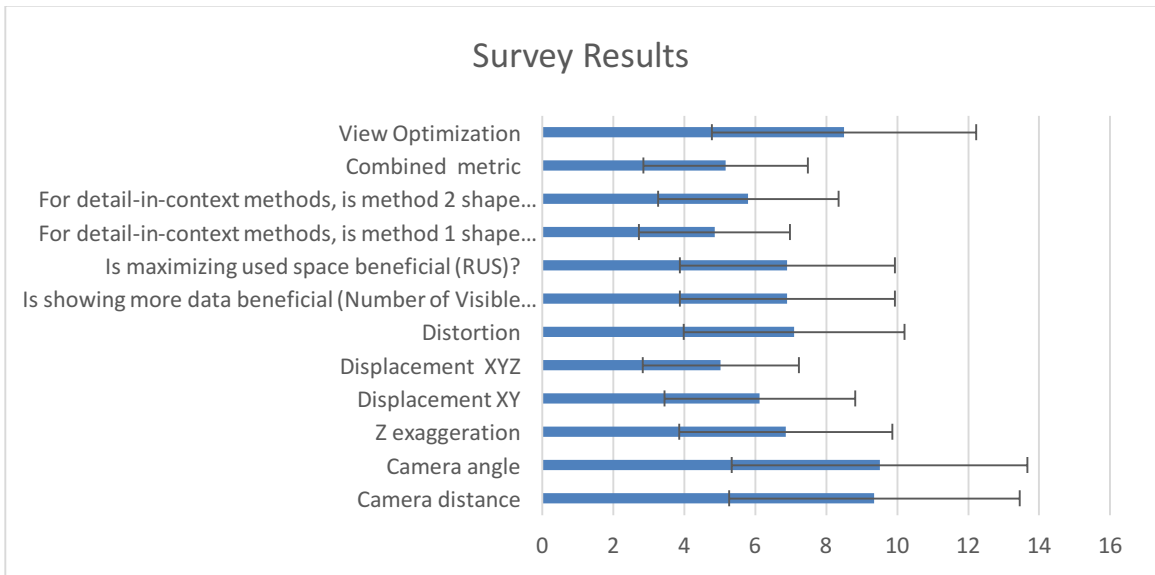


Figure 26 Survey Results

## CHAPTER 7

### CONCLUSION

The use of aesthetics metrics on visualization results has shown in this work to be descriptive and beneficial. The conducted experiments in this thesis work shows that the used input parameters can be optimized using the designed metrics as the objective functions. The implemented metrics provides indicative information on multiple aspects of the results of the fisheye method. First, is a utility metric that provides the number of visible cells (NVC). It provides the practical side of metrics and it is used to maximizing the visible cells. Second metric, Ratio of Used Space, is based on Tufte's guidelines where he stated that it is better to minimize white space. Third, Face Conformal Energy is a shape metric that provides the energy difference on a shape change. This is not easily relatable to base case as the values can go from 0 to more than 100%. The fourth metric is RCMC. This metric is a much easier to interpret because it provides the percentage of relative shape change to the base case. The fifth metric is combination of RUS and RCMC metrics which complement each other shortcomings as it provides a sense of shape change and used space. In this thesis work, five input parameters are evaluated against the metrics. We have identified that the XYZ Displacement, Z Axis Exaggeration and Camera Distance has the highest impact on the results of the output of the detail-in-context visualization.

The team have reduced the threat to validity by repeating the experiments to ensure the results are consistent. The research cover a limited set of default configuration for the selected parameters and matrices. In addition, the survey only covered experts in the field

of visualization of reservoir simulation models. These experts do not focus on the significance of improving the area of scientific visualization, their main focus is in visualization of multi-billion cell models.

The presented metrics is an attempt on using aesthetics and design guidelines to quantify the results of visualization methods. The field of aesthetics metrics is not new however applying it to 3D visualization is fairly new. However, these metrics represent a small sample of what can be achieved. This work opens many possibilities to customize metrics for specific type of data to be a basis of comparison for new visualization methods. The experiments in this covered a limited set of metrics to have a depth analysis on it. From the research, there can be many developed matrices that target different aspects of a visualization lens. Future work can take multiple directions; first direction is covering additional aesthetic metrics that are driven by perception theories, design guidelines or further sources. Second direction, is to evaluate alternative visualization lenses. Third direction is applying the same metrics on varies data types.

## References

- [1] T. A. DeFanti and M. D. Brown, "Visualization in scientific computing," *Adv. Comput.*, vol. 33, no. 1, pp. 247–305, 1991.
- [2] D. J. Cox, "Using the supercomputer to visualize higher dimensions: An artist's contribution to scientific visualization," *Leonardo*, vol. 41, no. 4, pp. 391–400, 2008.
- [3] A. H. Dogru, L. S. Fung, T. M. Al-Shaalán, U. Middyá, J. A. Pita, and others, "From Mega Cell to Giga Cell Reservoir Simulation," in *SPE Annual Technical Conference and Exhibition*, 2008.
- [4] B. Al-Harbi, A. Al-Darrab, A. S. Al-Zawawi, K. Al-Zamil, and others, "Advanced Visualization for Reservoir Simulation," in *SPE Saudi Arabia Section Technical Symposium and Exhibition*, 2013.
- [5] B. H. McCormick, T. A. DeFanti, and M. D. Brown, *Visualization in scientific computing*, vol. 7. IEEE COMPUTER SOC 10662 LOS VAQUEROS CIRCLE, PO BOX 3014, LOS ALAMITOS, CA 90720-1264, 1987.
- [6] C. Johnson, "Top scientific visualization research problems," *Comput. Graph. Appl. IEEE*, vol. 24, no. 4, pp. 13–17, 2004.
- [7] D. A. Norman, *Emotional design: Why we love (or hate) everyday things*. Basic books, 2004.
- [8] C. Bennett, J. Ryall, L. Spalteholz, and A. Gooch, "The Aesthetics of Graph Visualization.," in *Computational Aesthetics*, 2007, pp. 57–64.
- [9] M. S. T. Carpendale, D. J. Cowperthwaite, and F. D. Fracchia, "Distortion viewing techniques for 3-dimensional data," in *Information Visualization '96, Proceedings IEEE Symposium on*, 1996, pp. 46–53.
- [10] S. K. Card, J. D. Mackinlay, and B. Shneiderman, *Readings in information visualization: using vision to think*. Morgan Kaufmann, 1999.
- [11] M. Friendly and D. J. Denis, "Milestones in the history of thematic cartography, statistical graphics, and data visualization," *URL Httpwww Datavis Camilestones*, 2001.
- [12] K. L. Smith, S. Moriarty, K. Kenney, and G. Barbatsis, *Handbook of visual communication: Theory, methods, and media*. Routledge, 2004.
- [13] J. J. Thomas, K. Cook, and others, "A visual analytics agenda," *Comput. Graph. Appl. IEEE*, vol. 26, no. 1, pp. 10–13, 2006.
- [14] R. Burkhard and M. Meier, "Tube map: Evaluation of a visual metaphor for interfunctional communication of complex projects," in *Proceedings of I-Know*, 2004, vol. 4, pp. 449–456.
- [15] J. S. Yi, Y. ah Kang, J. T. Stasko, and J. A. Jacko, "Toward a deeper understanding of the role of interaction in information visualization," *Vis. Comput. Graph. IEEE Trans. On*, vol. 13, no. 6, pp. 1224–1231, 2007.
- [16] C. Tominski, S. Gladisch, U. Kister, R. Dachzelt, and H. Schumann, "A survey on interactive lenses in visualization," *EuroVis State---Art Rep.*, pp. 43–62, 2014.
- [17] L. J. Durlofsky, "Upscaling of geocellular models for reservoir flow simulation: a review of recent progress," in *7th International Forum on Reservoir Simulation Bñhl/Baden-Baden, Germany*, 2003, pp. 23–27.

- [18] Y.-J. Chiang and C. T. Silva, "I/O optimal isosurface extraction," in *Visualization '97., Proceedings*, 1997, pp. 293–300.
- [19] G. Volpe, "Streamlines and streamribbons in aerodynamics," in *27th Aerospace Sciences Meeting, Reno, NV*, 1989, pp. 89–0140.
- [20] S. Born, A. Wiebel, J. Friedrich, G. Scheuermann, and D. Bartz, "Illustrative stream surfaces," *Vis. Comput. Graph. IEEE Trans. On*, vol. 16, no. 6, pp. 1329–1338, 2010.
- [21] M. Hummel, C. Garth, B. Hamann, H. Hagen, K. Joy, and others, "Iris: Illustrative rendering for integral surfaces," *Vis. Comput. Graph. IEEE Trans. On*, vol. 16, no. 6, pp. 1319–1328, 2010.
- [22] S. Born, A. Wiebel, J. Friedrich, G. Scheuermann, and D. Bartz, "Illustrative stream surfaces," *Vis. Comput. Graph. IEEE Trans. On*, vol. 16, no. 6, pp. 1329–1338, 2010.
- [23] J. D. D. W. T. Ertl, "Interactive Cutaway Illustrations."
- [24] J. D. D. W. T. Ertl, "Transparency in Interactive Technical Illustrations."
- [25] S. K. Feiner and D. D. Seligmann, "Cutaways and ghosting: satisfying visibility constraints in dynamic 3D illustrations," *Vis. Comput.*, vol. 8, no. 5–6, pp. 292–302, 1992.
- [26] M. Burns and A. Finkelstein, "Adaptive cutaways for comprehensible rendering of polygonal scenes," in *ACM Transactions on Graphics (TOG)*, 2008, vol. 27, p. 154.
- [27] C. Coffin and T. Höllerer, "Interactive perspective cut-away views for general 3D scenes," in *3D User Interfaces, 2006. 3DUI 2006. IEEE Symposium on*, 2006, pp. 25–28.
- [28] W. Li, L. Ritter, M. Agrawala, B. Curless, and D. Salesin, "Interactive cutaway illustrations of complex 3D models," in *ACM Transactions on Graphics (TOG)*, 2007, vol. 26, p. 31.
- [29] M. Tatzgern, D. Kalkofen, and D. Schmalstieg, "Compact explosion diagrams," in *Proceedings of the 8th International Symposium on Non-Photorealistic Animation and Rendering*, 2010, pp. 17–26.
- [30] I. Viola, A. Kanitsar, and M. E. Groller, "Importance-driven volume rendering," in *Proceedings of the conference on Visualization '04*, 2004, pp. 139–146.
- [31] I. Viola, M. Feixas, M. Sbert, and M. E. Gröller, "Importance-driven focus of attention," *Vis. Comput. Graph. IEEE Trans. On*, vol. 12, no. 5, pp. 933–940, 2006.
- [32] N. Elmqvist, U. Assarsson, and P. Tsigas, "Dynamic Transparency for 3D Visualization: Design and Evaluation," *Int. J. Virtual Real.*, vol. 1, no. 8, pp. 65–78, 2009.
- [33] J. Kruger, J. Schneider, and R. Westermann, "Clearview: An interactive context preserving hotspot visualization technique," *Vis. Comput. Graph. IEEE Trans. On*, vol. 12, no. 5, pp. 941–948, 2006.
- [34] M. Agrawala, D. Phan, J. Heiser, J. Haymaker, J. Klingner, P. Hanrahan, and B. Tversky, "Designing effective step-by-step assembly instructions," in *ACM Transactions on Graphics (TOG)*, 2003, vol. 22, pp. 828–837.
- [35] W. Li, M. Agrawala, and D. Salesin, "Interactive image-based exploded view diagrams," in *Proceedings of the 2004 Graphics Interface Conference*, 2004, pp. 203–212.

- [36] S. Bruckner and M. E. Groller, “Exploded views for volume data,” *Vis. Comput. Graph. IEEE Trans. On*, vol. 12, no. 5, pp. 1077–1084, 2006.
- [37] J. H. Peery and E. H. Herron, “Three-Phase Reservoir Simulation,” *J. Pet. Technol.*, vol. 21, no. 02, pp. 211–220, Feb. 1969.
- [38] S. Islam, S. Dipankar, D. Silver, and M. Chen, “Spatial and temporal splitting of scalar fields in volume graphics,” in *Volume Visualization and Graphics, 2004 IEEE Symposium on*, 2004, pp. 87–94.
- [39] S. Islam, D. Silver, and M. Chen, “Volume splitting and its applications,” *Vis. Comput. Graph. IEEE Trans. On*, vol. 13, no. 2, pp. 193–203, 2007.
- [40] M. J. McGuffin, L. Tancau, and R. Balakrishnan, “Using deformations for browsing volumetric data,” in *Visualization, 2003. VIS 2003. IEEE*, 2003, pp. 401–408.
- [41] A. Brambilla, I. Viola, and H. Hauser, “A hierarchical splitting scheme to reveal insight into highly self-occluded integral surfaces,” 2012.
- [42] M. Sarkar and M. H. Brown, “Graphical fisheye views,” *Commun. ACM*, vol. 37, no. 12, pp. 73–83, 1994.
- [43] C. D. Correa, D. Silver, and M. Chen, “Illustrative deformation for data exploration,” *Vis. Comput. Graph. IEEE Trans. On*, vol. 13, no. 6, pp. 1320–1327, 2007.
- [44] T. A. Keahey, “Visualization of high-dimensional clusters using nonlinear magnification,” in *Electronic Imaging ’99*, 1999, pp. 228–235.
- [45] A. Brambilla, R. Carnecky, R. Peikert, I. Viola, and H. Hauser, “Illustrative flow visualization: State of the art, trends and challenges,” *Visibility-Oriented Vis. Des. Flow Illus.*, 2012.
- [46] B. Cabral and L. C. Leedom, “Imaging vector fields using line integral convolution,” in *Proceedings of the 20th annual conference on Computer graphics and interactive techniques*, 1993, pp. 263–270.
- [47] R. Crawfis, N. Max, and B. Becker, “Vector field visualization,” *IEEE Comput. Graph. Appl.*, no. 5, pp. 50–56, 1994.
- [48] M. Oohigashi, V. Čingoski, K. Kaneda, and H. Yamashita, “A new method for 3-D vector field visualization utilizing streamlines and volume rendering techniques,” *Magn. IEEE Trans. On*, vol. 34, no. 5, pp. 3435–3438, 1998.
- [49] C.-K. Chen, S. Yan, H. Yu, N. Max, and K.-L. Ma, “An illustrative visualization framework for 3d vector fields,” in *Computer Graphics Forum*, 2011, vol. 30, pp. 1941–1951.
- [50] P. Eliasson, J. Ooppelstrup, and A. Rizzi, “STREAM 3D: Computer graphics program for streamline visualization,” *Adv. Eng. Softw. 1978*, vol. 11, no. 4, pp. 162–168, 1989.
- [51] C. Garth, H. Krishnan, X. Tricoche, K. Joy, and others, “Generation of accurate integral surfaces in time-dependent vector fields,” *Vis. Comput. Graph. IEEE Trans. On*, vol. 14, no. 6, pp. 1404–1411, 2008.
- [52] M. Schlemmer, I. Hotz, B. Hamann, F. Morr, and H. Hagen, “Priority Streamlines: A context-based Visualization of Flow Fields,” in *EuroVis*, 2007, pp. 227–234.
- [53] S. Bruckner, S. Grimm, A. Kanitsar, and M. E. Gröller, “Illustrative context-preserving volume rendering,” in *EuroVis*, 2005, pp. 69–76.

- [54] S. Bruckner, S. Grimm, A. Kanitsar, and M. E. Groller, "Illustrative context-preserving exploration of volume data," *Vis. Comput. Graph. IEEE Trans. On*, vol. 12, no. 6, pp. 1559–1569, 2006.
- [55] F. de Moura Pinto and C. M. Freitas, "Importance-aware composition for illustrative volume rendering," in *Graphics, Patterns and Images (SIBGRAPI), 2010 23rd SIBGRAPI Conference on*, 2010, pp. 134–141.
- [56] C. Appert, O. Chapuis, and E. Pietriga, "High-precision magnification lenses," in *Proceedings of the SIGCHI Conference on Human Factors in Computing Systems*, 2010, pp. 273–282.
- [57] P. Cignoni, C. Montani, and R. Scopigno, "MagicSphere: an insight tool for 3D data visualization," in *Computer Graphics Forum*, 1994, vol. 13, pp. 317–328.
- [58] E. A. Bier, M. C. Stone, K. Pier, W. Buxton, and T. D. DeRose, "Toolglass and magic lenses: the see-through interface," in *Proceedings of the 20th annual conference on Computer graphics and interactive techniques*, 1993, pp. 73–80.
- [59] J. Viega, M. J. Conway, G. Williams, and R. Pausch, "3D magic lenses," in *Proceedings of the 9th annual ACM symposium on User interface software and technology*, 1996, pp. 51–58.
- [60] L. Wang, Y. Zhao, K. Mueller, and A. Kaufman, "The magic volume lens: An interactive focus+ context technique for volume rendering," in *Visualization, 2005. VIS 05. IEEE*, 2005, pp. 367–374.
- [61] E. Mendez, D. Kalkofen, and D. Schmalstieg, "Interactive context-driven visualization tools for augmented reality," in *Proceedings of the 5th IEEE and ACM International Symposium on Mixed and Augmented Reality*, 2006, pp. 209–218.
- [62] T. Ropinski and K. Hinrichs, "Real-time rendering of 3D magic lenses having arbitrary convex shapes," 2004.
- [63] Y. Yang, J. X. Chen, and M. Beheshti, "Nonlinear perspective projections and magic lenses: 3D view deformation," *Comput. Graph. Appl. IEEE*, vol. 25, no. 1, pp. 76–84, 2005.
- [64] C. D. Shaw, J. A. Hall, D. S. Ebert, and D. A. Roberts, "Interactive lens visualization techniques," in *Proceedings of the conference on Visualization '99: celebrating ten years*, 1999, pp. 155–160.
- [65] E. LaMar, B. Hamann, K. Joy, and others, "A magnification lens for interactive volume visualization," in *Computer Graphics and Applications, 2001. Proceedings. Ninth Pacific Conference on*, 2001, pp. 223–232.
- [66] C. Pindat, E. Pietriga, O. Chapuis, and C. Puech, "Drilling into complex 3D models with gimlenses," in *Proceedings of the 19th ACM Symposium on Virtual Reality Software and Technology*, 2013, pp. 223–230.
- [67] G. Volpe, "Streamlines and streamribbons in aerodynamics," in *27th Aerospace Sciences Meeting, Reno, NV*, 1989, pp. 89–0140.
- [68] O. Mattausch, T. Theu\sl, H. Hauser, and E. Gröller, "Strategies for interactive exploration of 3D flow using evenly-spaced illuminated streamlines," in *Proceedings of the 19th spring conference on Computer graphics*, 2003, pp. 213–222.
- [69] A. Fuhrmann and E. Gröller, "Real-time techniques for 3D flow visualization," in *Proceedings of the conference on Visualization '98*, 1998, pp. 305–312.



- [70] N. Elmqvist, “BalloonProbe: Reducing occlusion in 3D using interactive space distortion,” in *Proceedings of the ACM symposium on Virtual reality software and technology*, 2005, pp. 134–137.
- [71] J. Brosz, S. Carpendale, and M. A. Nacenta, “The undistort lens,” in *Computer Graphics Forum*, 2011, vol. 30, pp. 881–890.
- [72] Y.-S. Wang, T.-Y. Lee, and C.-L. Tai, “Focus+ context visualization with distortion minimization,” *Vis. Comput. Graph. IEEE Trans. On*, vol. 14, no. 6, pp. 1731–1738, 2008.
- [73] X. Zhao, W. Zeng, X. D. Gu, A. E. Kaufman, W. Xu, and K. Mueller, “Conformal magnifier: A focus+ context technique with local shape preservation,” *Vis. Comput. Graph. IEEE Trans. On*, vol. 18, no. 11, pp. 1928–1941, 2012.
- [74] Y. Luo, J. A. I. Guitián, E. Gobbetti, and F. Marton, “Context preserving focal probes for exploration of volumetric medical datasets,” in *Modelling the Physiological Human*, Springer, 2009, pp. 187–198.
- [75] M. Cohen and K. Brodlie, “Focus and context for volume visualization,” in *Theory and Practice of Computer Graphics, 2004. Proceedings*, 2004, pp. 32–39.
- [76] D. Winch, P. Calder, and R. Smith, “(Focus+ context) 3: distortion-oriented displays in three dimensions,” in *User Interface Conference, 2000. AUIC 2000. First Australasian*, 2000, pp. 126–133.
- [77] C. D. Correa, D. Silver, and M. Chen, “Illustrative deformation for data exploration,” *Vis. Comput. Graph. IEEE Trans. On*, vol. 13, no. 6, pp. 1320–1327, 2007.
- [78] Y.-S. Wang, C. Wang, T.-Y. Lee, and K.-L. Ma, “Feature-preserving volume data reduction and focus+ context visualization,” *Vis. Comput. Graph. IEEE Trans. On*, vol. 17, no. 2, pp. 171–181, 2011.
- [79] H. Doleisch, M. Gasser, and H. Hauser, “Interactive feature specification for focus+ context visualization of complex simulation data,” in *VisSym*, 2003, vol. 3, pp. 239–248.
- [80] H. Piringer, R. Kosara, and H. Hauser, “Interactive focus+ context visualization with linked 2d/3d scatterplots,” in *Coordinated and Multiple Views in Exploratory Visualization, 2004. Proceedings. Second International Conference on*, 2004, pp. 49–60.
- [81] H. Doleisch, “SimVis: Interactive visual analysis of large and time-dependent 3D simulation data,” in *Proceedings of the 39th conference on Winter simulation: 40 years! The best is yet to come*, 2007, pp. 712–720.
- [82] M. S. T. Carpendale, D. J. Cowperthwaite, and F. D. Fracchia, “Extending distortion viewing from 2D to 3D,” *Comput. Graph. Appl. IEEE*, vol. 17, no. 4, pp. 42–51, 1997.
- [83] D. A. Norman, *Emotional design: Why we love (or hate) everyday things*. Basic books, 2004.
- [84] D. A. Norman, *The design of everyday things: Revised and expanded edition*. Basic books, 2013.
- [85] I. Biederman, “Recognition-by-components: a theory of human image understanding,” *Psychol. Rev.*, vol. 94, no. 2, p. 115, 1987.
- [86] D. Bernstein, *Essentials of psychology*. Cengage Learning, 2013.

- [87] D. A. Norman, *Emotional design: Why we love (or hate) everyday things*. Basic books, 2004.
- [88] H. Stevenson, *Emergence: The gestalt approach to change*. 2010.
- [89] B. Gillam, "The perception of spatial layout from static optical information," *Percept. Space Motion*, pp. 23–67, 1995.
- [90] G. Humphrey, "The Psychology of the Gestalt.," *J. Educ. Psychol.*, vol. 15, no. 7, p. 401, 1924.
- [91] G. Humphrey, "The Psychology of the Gestalt.," *J. Educ. Psychol.*, vol. 15, no. 7, p. 401, 1924.
- [92] P. Goolkasian and A. Bojko, "Location constancy and its effect on visual selection," *Spat. Vis.*, vol. 14, no. 2, pp. 175–199, 2001.
- [93] H. Stevenson, *Emergence: The gestalt approach to change*. 2010.
- [94] S. Lehar, "Gestalt isomorphism and the primacy of subjective conscious experience: A Gestalt Bubble model," *Behav. Brain Sci.*, vol. 26, no. 04, pp. 375–408, 2003.
- [95] J. Wolfe, K. Kluender, D. Levi, L. Bartoshuk, R. Herz, R. Klatzky, and S. Lederman, "Sensation and Perception," in *Sensation and Perception*, 2nd ed., Sinauer Associates, 2008.
- [96] S. Plous, *The psychology of judgment and decision making*. McGraw-Hill Book Company, 1993.
- [97] R. J. Corsini, *The dictionary of psychology*. Psychology Press, 1999.
- [98] L. Wang, J. Giesen, K. T. McDonnell, P. Zolliker, and K. Mueller, "Color design for illustrative visualization," *Vis. Comput. Graph. IEEE Trans. On*, vol. 14, no. 6, pp. 1739–1754, 2008.
- [99] C. Bennett, J. Ryall, L. Spalteholz, and A. Gooch, "The Aesthetics of Graph Visualization.," in *Computational Aesthetics*, 2007, pp. 57–64.
- [100] K. Wong and D. Sun, "On evaluating the layout of UML diagrams for program comprehension," *Softw. Qual. J.*, vol. 14, no. 3, pp. 233–259, 2006.
- [101] F. Linghammar, "Usability and Aesthetics: is beautiful more usable," 2007.
- [102] B. Yost, Y. Haciahmetoglu, and C. North, "Beyond visual acuity: the perceptual scalability of information visualizations for large displays," in *Proceedings of the SIGCHI conference on Human factors in computing systems*, 2007, pp. 101–110.
- [103] H. C. Purchase, D. Carrington, and J.-A. Allder, "Empirical evaluation of aesthetics-based graph layout," *Empir. Softw. Eng.*, vol. 7, no. 3, pp. 233–255, 2002.
- [104] C. Johnson, "Top scientific visualization research problems," *Comput. Graph. Appl. IEEE*, vol. 24, no. 4, pp. 13–17, 2004.
- [105] E. R. Tufte and P. R. Graves-Morris, *The visual display of quantitative information*, vol. 2. Graphics press Cheshire, CT, 1983.
- [106] E. R. Tufte, "Envisioning information.," *Optom. Vis. Sci.*, vol. 68, no. 4, pp. 322–324, 1991.
- [107] C. Ware, "Information Visualization: Perception for Design," 2004.
- [108] D. Mortelmans, "Visualizing emptiness," *Vis. Anthropol.*, vol. 18, no. 1, pp. 19–45, 2005.
- [109] W. Huang, M. L. Huang, and C.-C. Lin, "Evaluating overall quality of graph visualizations based on aesthetics aggregation," *Inf. Sci.*, vol. 330, pp. 444–454, 2016.

- [110] R. Tamassia, G. Di Battista, and C. Batini, "Automatic graph drawing and readability of diagrams," *Syst. Man Cybern. IEEE Trans. On*, vol. 18, no. 1, pp. 61–79, 1988.
- [111] G. Di Battista, P. Eades, R. Tamassia, and I. G. Tollis, "Algorithms for drawing graphs: an annotated bibliography," *Comput. Geom.*, vol. 4, no. 5, pp. 235–282, 1994.
- [112] I. Herman, G. Melançon, and M. S. Marshall, "Graph visualization and navigation in information visualization: A survey," *Vis. Comput. Graph. IEEE Trans. On*, vol. 6, no. 1, pp. 24–43, 2000.
- [113] I. Tollis, P. Eades, G. Di Battista, and L. Tollis, *Graph drawing: algorithms for the visualization of graphs*, vol. 1. Prentice Hall New York, 1998.
- [114] K. Wong and D. Sun, "On evaluating the layout of UML diagrams for program comprehension," *Softw. Qual. J.*, vol. 14, no. 3, pp. 233–259, 2006.
- [115] R. Davidson and D. Harel, "Drawing graphs nicely using simulated annealing," *ACM Trans. Graph. TOG*, vol. 15, no. 4, pp. 301–331, 1996.
- [116] D. Harel, "On the aesthetics of diagrams," in *Mathematics of Program Construction*, 1998, pp. 1–5.
- [117] C. Wetherell and A. Shannon, "Tidy drawings of trees," *Softw. Eng. IEEE Trans. On*, no. 5, pp. 514–520, 1979.
- [118] H. C. Purchase, "Metrics for graph drawing aesthetics," *J. Vis. Lang. Comput.*, vol. 13, no. 5, pp. 501–516, 2002.
- [119] D. Harel, "On the aesthetics of diagrams," in *Mathematics of Program Construction*, 1998, pp. 1–5.
- [120] M. Taylor and P. Rodgers, "Applying graphical design techniques to graph visualisation," in *Information Visualisation, 2005. Proceedings. Ninth International Conference on*, 2005, pp. 651–656.
- [121] D. Baum, "Introducing aesthetics to software visualization."
- [122] W. Huang, P. Eades, S.-H. Hong, and C.-C. Lin, "Improving force-directed graph drawings by making compromises between aesthetics," in *Visual Languages and Human-Centric Computing (VL/HCC), 2010 IEEE Symposium on*, 2010, pp. 176–183.
- [123] C. Papadopoulos and C. Voglis, "Untangling graphs representing spatial relationships driven by drawing aesthetics," in *Proceedings of the 17th Panhellenic Conference on Informatics*, 2013, pp. 158–165.
- [124] F. Beck, M. Burch, and S. Diehl, "Towards an aesthetic dimensions framework for dynamic graph visualisations," in *Information Visualisation, 2009 13th International Conference*, 2009, pp. 592–597.
- [125] A. Žilinskas and A. Varoneckas, "On multi-objective optimization aided drawing of special graphs," *Appl. Math. Comput.*, vol. 255, pp. 105–113, 2015.
- [126] B. Al-Harbi, A. Al-Darrab, A. S. Al-Zawawi, K. Al-Zamil, and others, "Advanced Visualization for Reservoir Simulation," in *SPE Saudi Arabia Section Technical Symposium and Exhibition*, 2013.
- [127] M. S. T. Carpendale, D. J. Cowperthwaite, and F. D. Fracchia, "Extending distortion viewing from 2D to 3D," *Comput. Graph. Appl. IEEE*, vol. 17, no. 4, pp. 42–51, 1997.

- [128] “Welcome to PyGMO — PyGMO 1.1.7dev documentation.” [Online]. Available: <http://esa.github.io/pygmo/>. [Accessed: 07-Apr-2016].
- [129] W. Griffin, Y. Wang, D. Berrios, and M. Olano, “Real-time GPU surface curvature estimation on deforming meshes and volumetric data sets,” *Vis. Comput. Graph. IEEE Trans. On*, vol. 18, no. 10, pp. 1603–1613, 2012.
- [130] M. Eigensatz, R. W. Sumner, and M. Pauly, “Curvature-Domain Shape Processing,” in *Computer Graphics Forum*, 2008, vol. 27, pp. 241–250.
- [131] M. Eigensatz and M. Pauly, “Positional, Metric, and Curvature Control for Constraint-Based Surface Deformation,” in *Computer Graphics Forum*, 2009, vol. 28, pp. 551–558.
- [132] J. Amanatides, A. Woo, and others, “A fast voxel traversal algorithm for ray tracing,” in *Eurographics*, 1987, vol. 87, p. 10.
- [133] E. R. Tufte and P. R. Graves-Morris, *The visual display of quantitative information*, vol. 2. Graphics press Cheshire, CT, 1983.
- [134] T. Ahmed and others, *Reservoir engineering handbook*. Gulf Professional Publishing, 2006.

## APPENDIX

### The Gaussian parameter & Number of Visible Cells

View	Top	45	X & Y Angle		
Input	Gaussian	Gaussian	Gaussian	X Angle	Y Angle
Case 1	-inf	-inf	0.028	0.001	0.003
Case 2	-inf	-inf	0.023	0.001	0.003
Avg	-inf	-inf	0.025	0.001	0.003

**Table 6: The Gaussian parameter & Number of Visible Cells Correlation per experiment**

	Top		45		X & Y Angle	
	Min	Max	Min	Max	Min	Max
Case 1	669.0	669.0	650.0	650.0	671.0	984.0
Case 2	647.0	647.0	700.0	700.0	633.0	1178.0
Avg	658.0	658.0	675.0	675.0	652.0	1081.0

**Table 7: The Gaussian parameter & Number of Visible Cells Min Max per experiment**

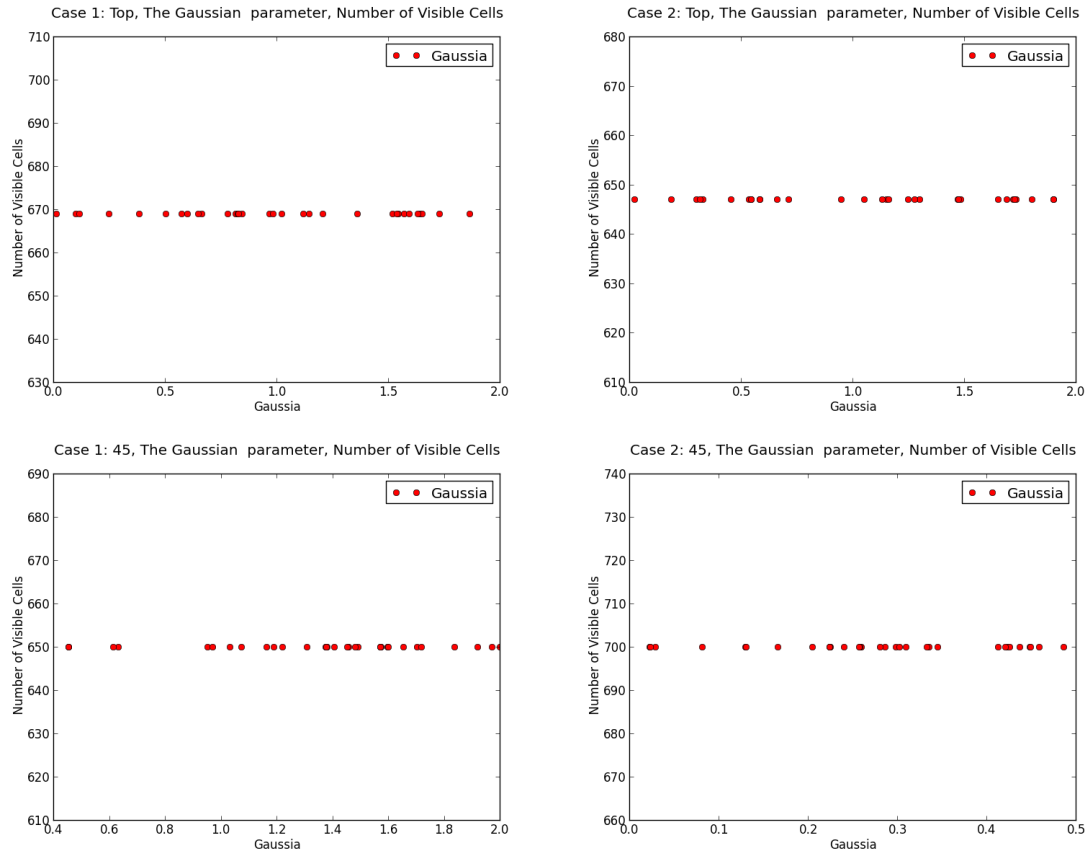


Figure 27: Top & 45: The Gaussian parameter & Number of Visible Cells

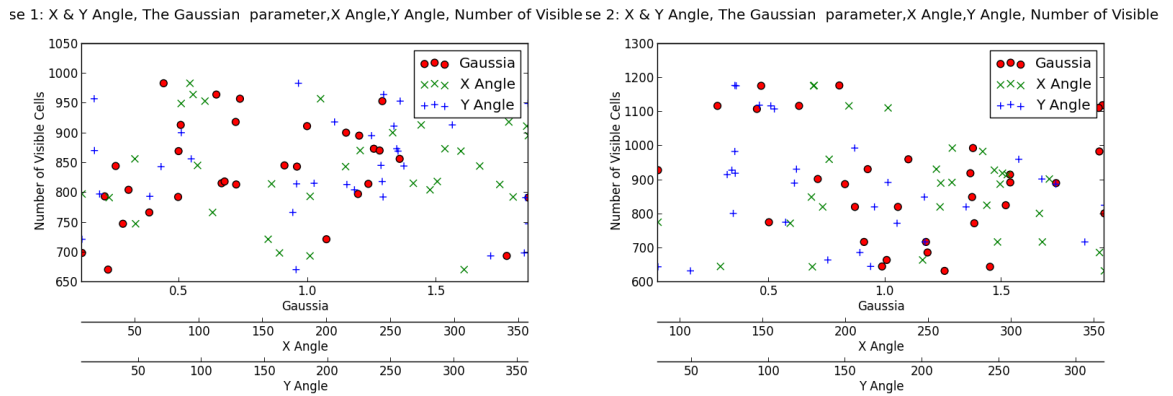


Figure 28: X & Y Angles The Gaussian parameter & Number of Visible Cells

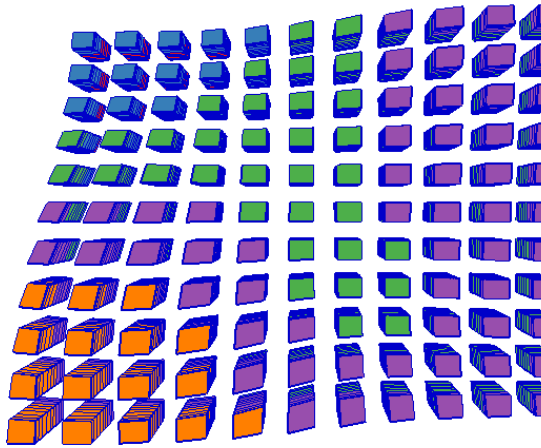


Figure 29: 3D Case 1: Top, The Gaussian parameter, Number of Visible Cells

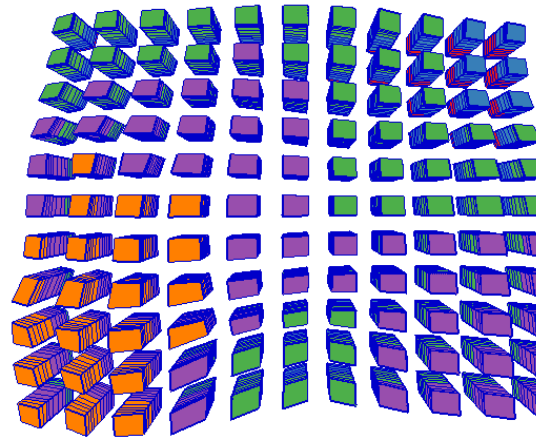


Figure 30: 3D Case 2: Top, The Gaussian parameter, Number of Visible Cells

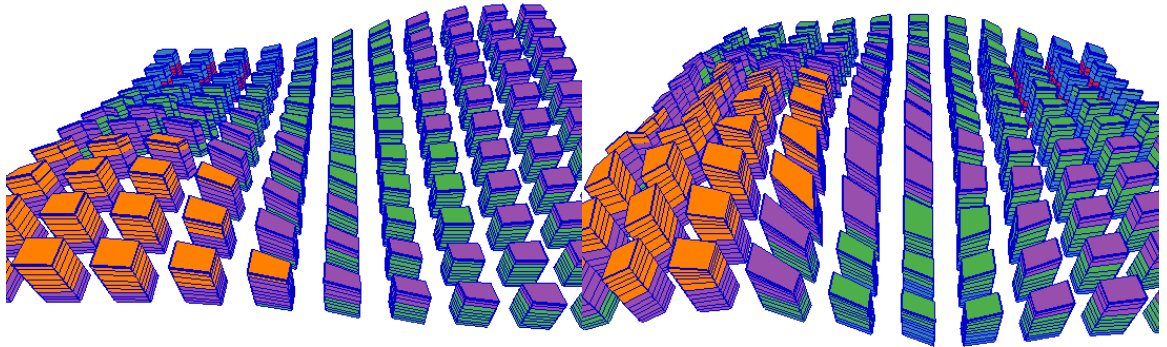


Figure 31: 3D Case 1: 45, The Gaussian parameter, Number of Visible Cells

Figure 32: 3D Case 2: 45, The Gaussian parameter, Number of Visible Cells

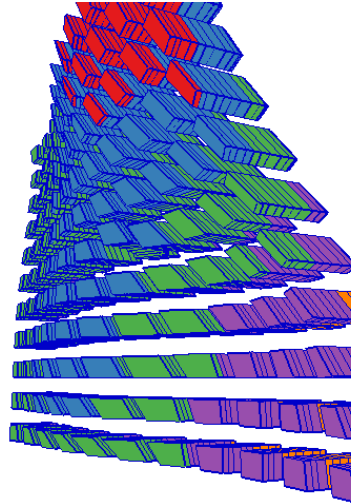


Figure 33: 3D Case 1: X & Y Angle, The Gaussian parameter, X Angle, Y Angle, Number of Visible Cells

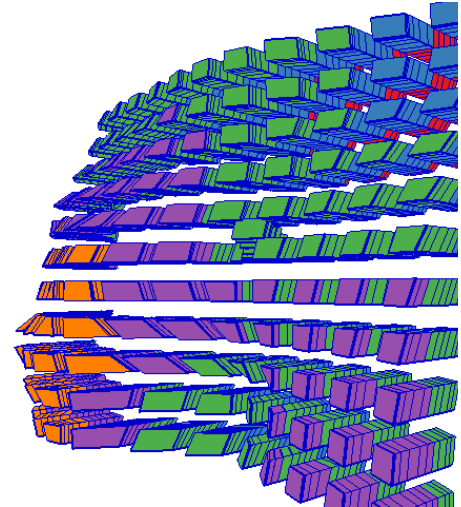


Figure 34: 3D Case 2: X & Y Angle, The Gaussian parameter, X Angle, Y Angle, Number of Visible Cells

### Camera Distance & Number of Visible Cells

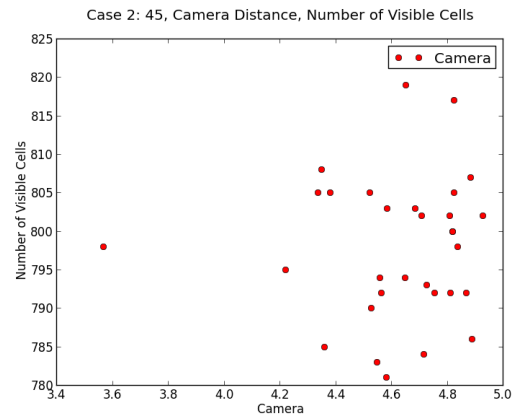
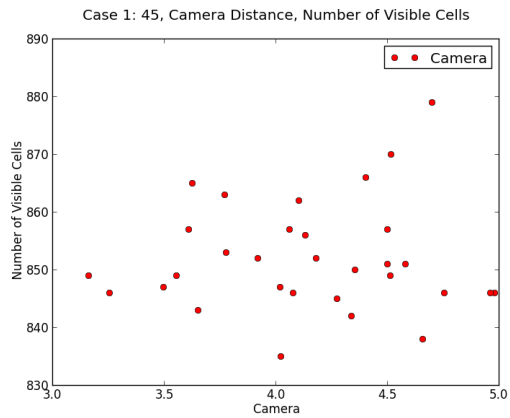
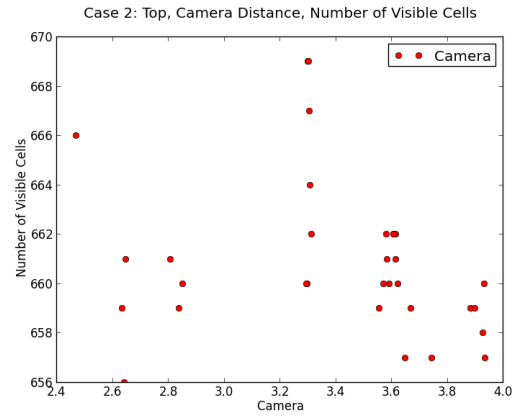
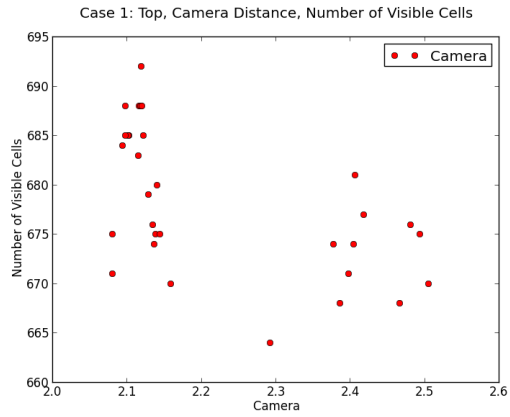
View	Top	45	X & Y Angle		
Input	Camera	Camera	Camera	X Angle	Y Angle
Case 1	0.322	0.025	0.058	0.171	0.087
Case 2	0.048	0.005	0.007	0.062	0.068
Avg	0.185	0.015	0.033	0.117	0.078

Table 8: Camera Distance & Number of Visible Cells Correlation per experiment

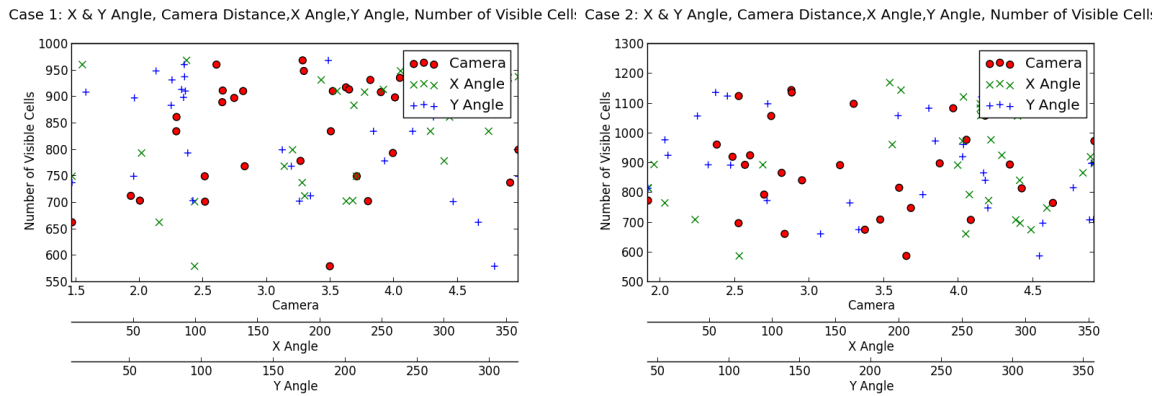
	Top		45		X & Y Angle	
	Min	Max	Min	Max	Min	Max
Case 1	664.0	692.0	835.0	888.0	580.0	969.0
Case 2	656.0	669.0	781.0	822.0	588.0	1170.0
Avg	660.0	680.5	808.0	855.0	584.0	1069.5

Table 9: Camera Distance & Number of Visible Cells Min Max per experiment





**Figure 35: Top & 45: Camera Distance & Number of Visible Cells**



**Figure 36: X & Y Angles Camera Distance & Number of Visible Cells**

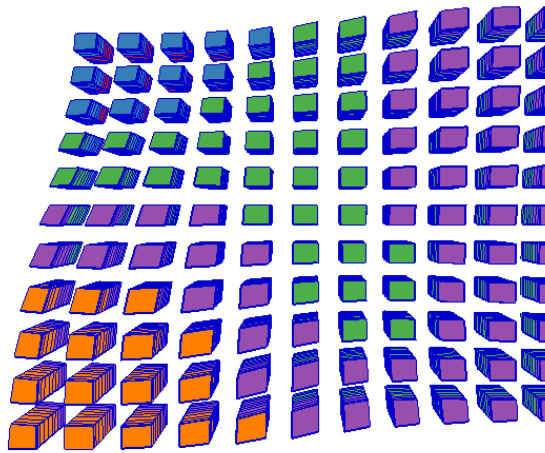


Figure 37: 3D Case 1: Top, Camera Distance, Number of Visible Cells

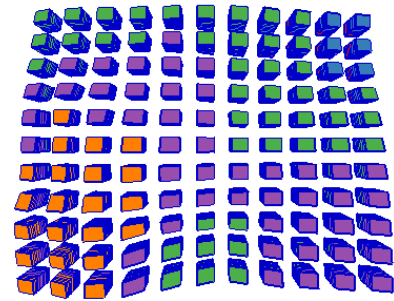


Figure 38: 3D Case 2: Top, Camera Distance, Number of Visible Cells

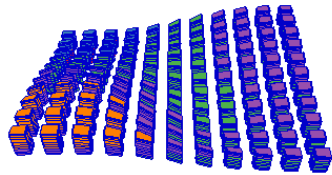


Figure 39: 3D Case 1: 45, Camera Distance, Number of Visible Cells

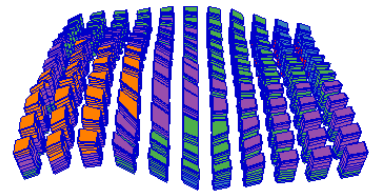


Figure 40: 3D Case 2: 45, Camera Distance, Number of Visible Cells

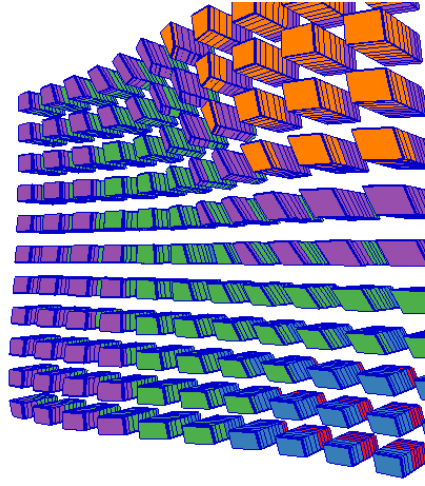


Figure 41: 3D Case 1: X & Y Angle, Camera Distance, X Angle, Y Angle, Number of Visible Cells

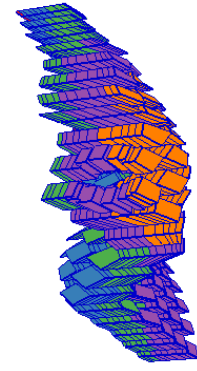


Figure 42: 3D Case 2: X & Y Angle, Camera Distance, X Angle, Y Angle, Number of Visible Cells

### Z Exaggeration & Number of Visible Cells

View	Top	45	X & Y Angle		
Input	Z Exagg	Z Exagg	Z Exagg	X Angle	Y Angle
Case 1	0.057	0.058	0.018	0.001	0.025
Case 2	0.114	0.110	0.323	0.002	0.018
Avg	0.086	0.084	0.171	0.002	0.021

Table 10: Z Exaggeration & Number of Visible Cells Correlation per experiment

	Top		45		X & Y Angle	
	Min	Max	Min	Max	Min	Max
Case 1	717.0	739.0	817.0	882.0	658.0	1006.0
Case 2	718.0	733.0	913.0	1010.0	689.0	1183.0
Avg	717.5	736.0	865.0	946.0	673.5	1094.5

Table 11: Z Exaggeration & Number of Visible Cells Min Max per experiment

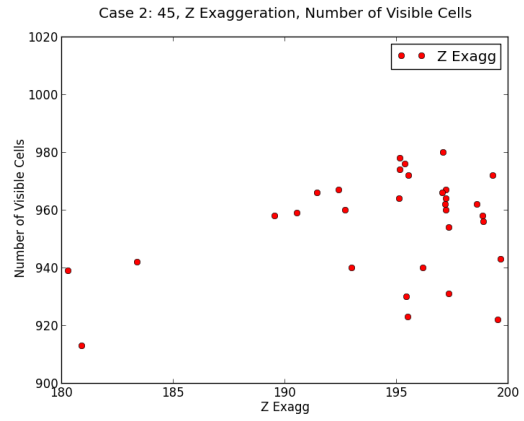
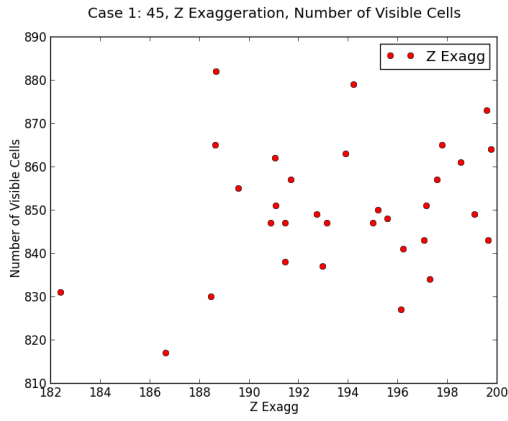
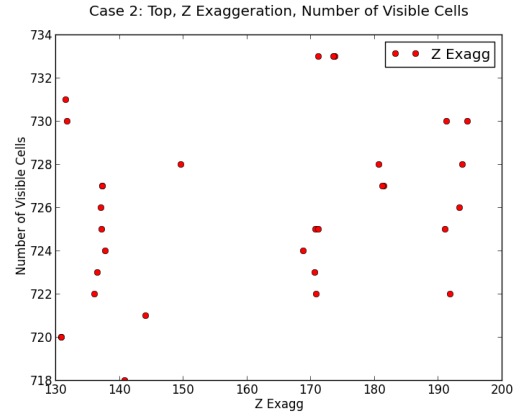
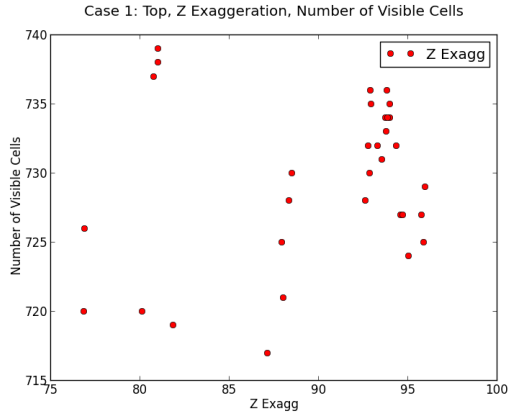


Figure 43: Top & 45: Z Exaggeration & Number of Visible Cells

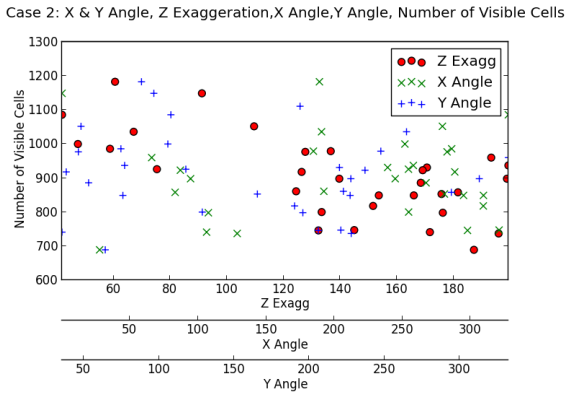
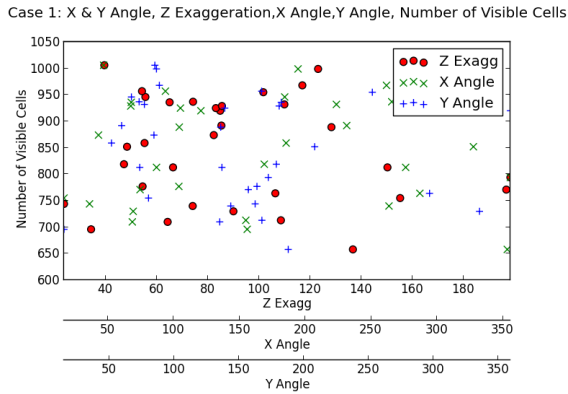


Figure 44: X & Y Angles Z Exaggeration & Number of Visible Cells

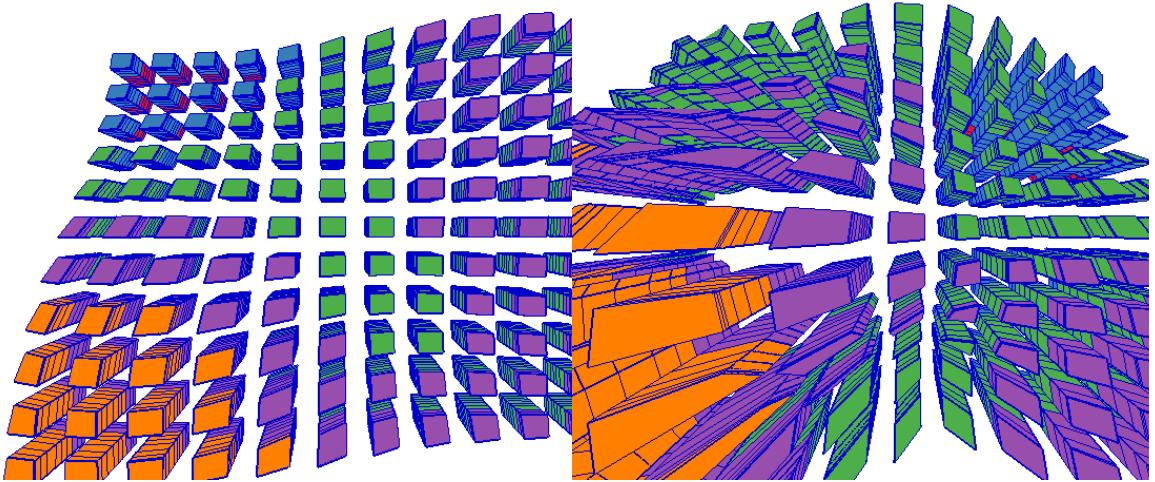


Figure 45: 3D Case 1: Top, Z Exaggeration, Number of Visible Cells

Figure 46: 3D Case 2: Top, Z Exaggeration, Number of Visible Cells

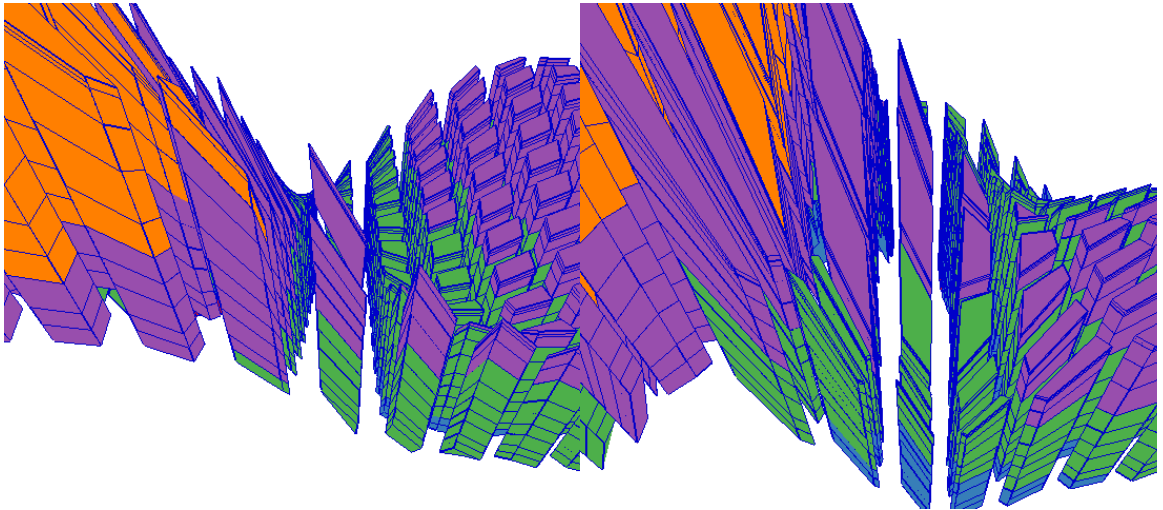


Figure 47: 3D Case 1: 45, Z Exaggeration, Number of Visible Cells

Figure 48: 3D Case 2: 45, Z Exaggeration, Number of Visible Cells

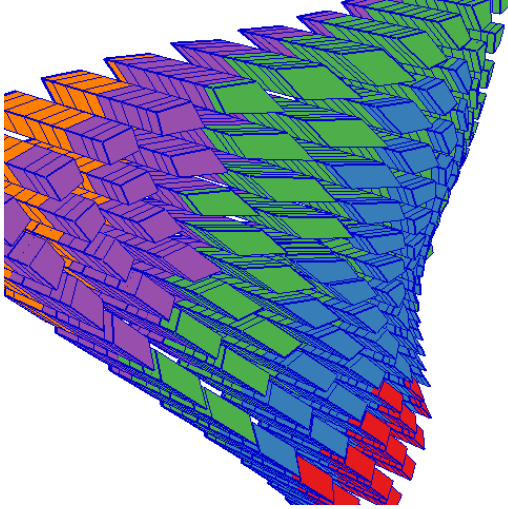


Figure 49: 3D Case 1: X & Y Angle, Z Exaggeration, X Angle, Y Angle, Number of Visible Cells

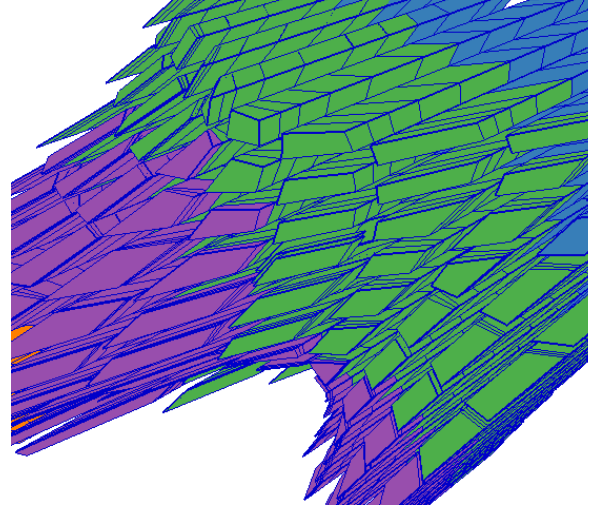


Figure 50: 3D Case 2: X & Y Angle, Z Exaggeration, X Angle, Y Angle, Number of Visible Cells

### XY Displacement & Number of Visible Cells

View	Top	45	X & Y Angle		
Input	XY Disp	XY Disp	XY Disp	X Angle	Y Angle
Case 1	0.822	0.029	0.187	0.128	0.150
Case 2	0.082	0.046	0.213	0.019	0.010
Avg	0.452	0.037	0.200	0.073	0.080

Table 12: XY Displacement & Number of Visible Cells Correlation per experiment

	Top		45		X & Y Angle	
	Min	Max	Min	Max	Min	Max
Case 1	738.0	770.0	792.0	839.0	507.0	1151.0
Case 2	694.0	716.0	678.0	775.0	537.0	1115.0
Avg	716.0	743.0	735.0	807.0	522.0	1133.0

Table 13: XY Displacement & Number of Visible Cells Min Max per experiment

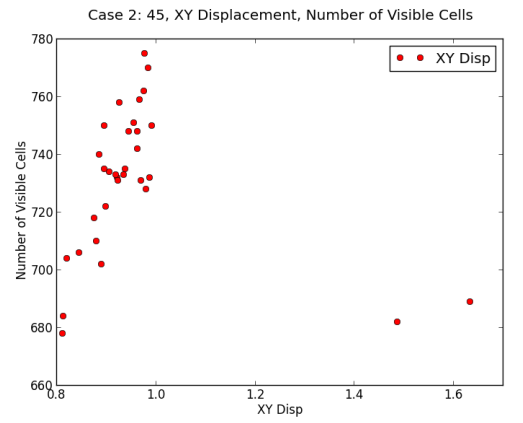
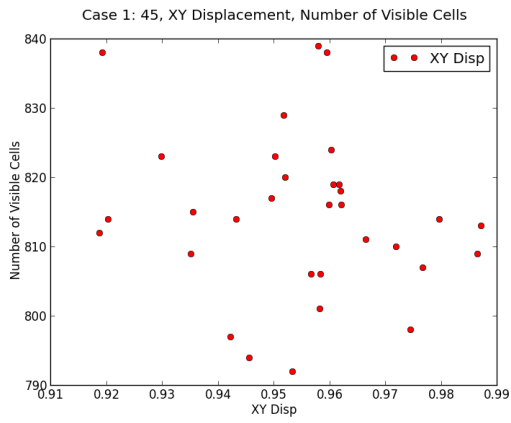
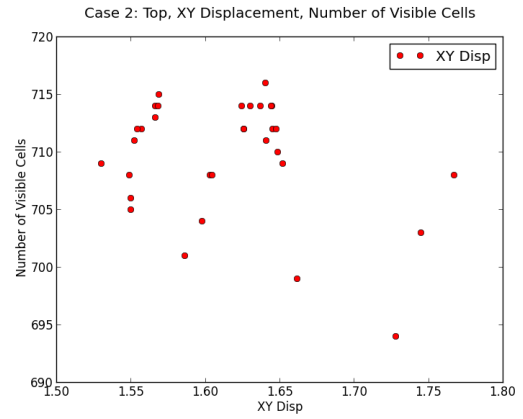
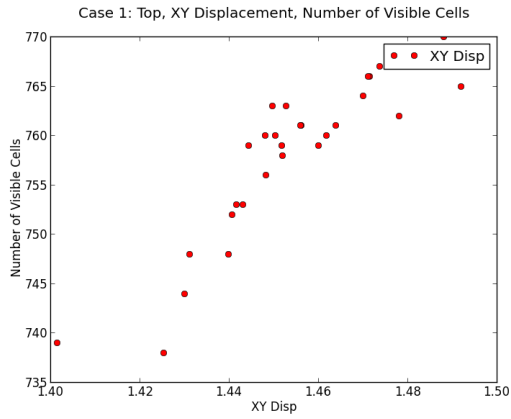


**Figure 51: Top & 45: XY Displacement & Number of Visible Cells**

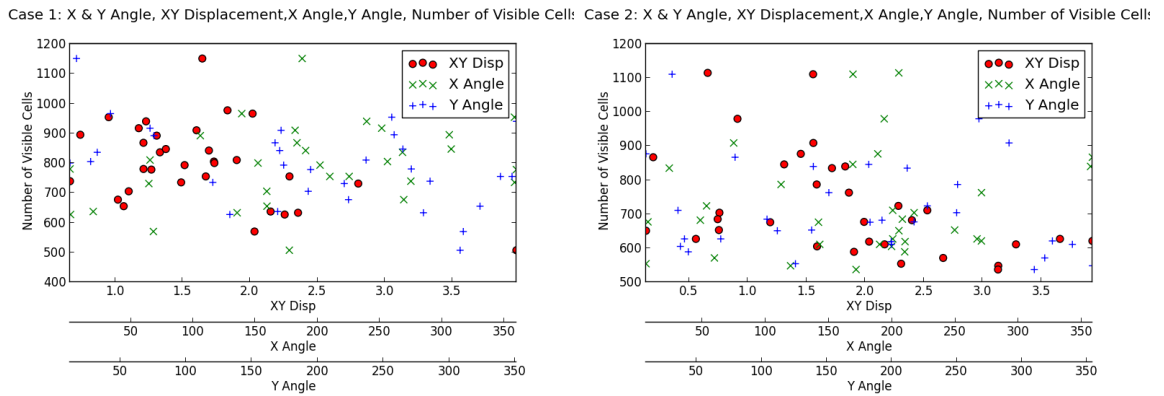


**Figure 52: X & Y Angles XY Displacement & Number of Visible Cells**

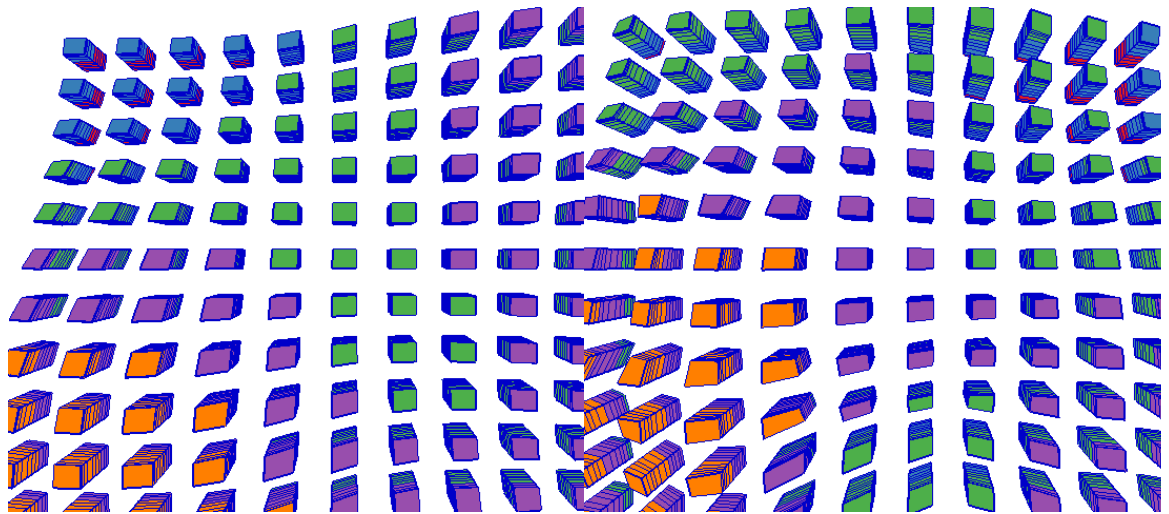


Figure 53: 3D Case 1: Top, XY Displacement, Number of Visible Cells

Figure 54: 3D Case 2: Top, XY Displacement, Number of Visible Cells

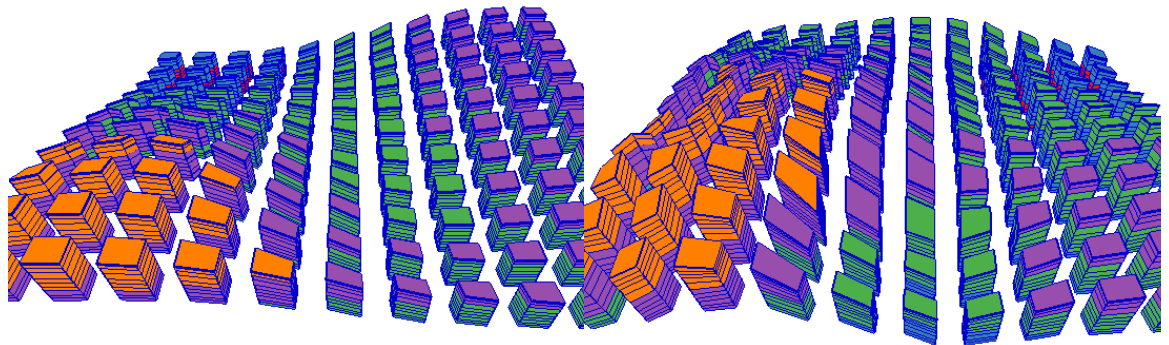


Figure 55: 3D Case 1: 45, XY Displacement, Number of Visible Cells

Figure 56: 3D Case 2: 45, XY Displacement, Number of Visible Cells



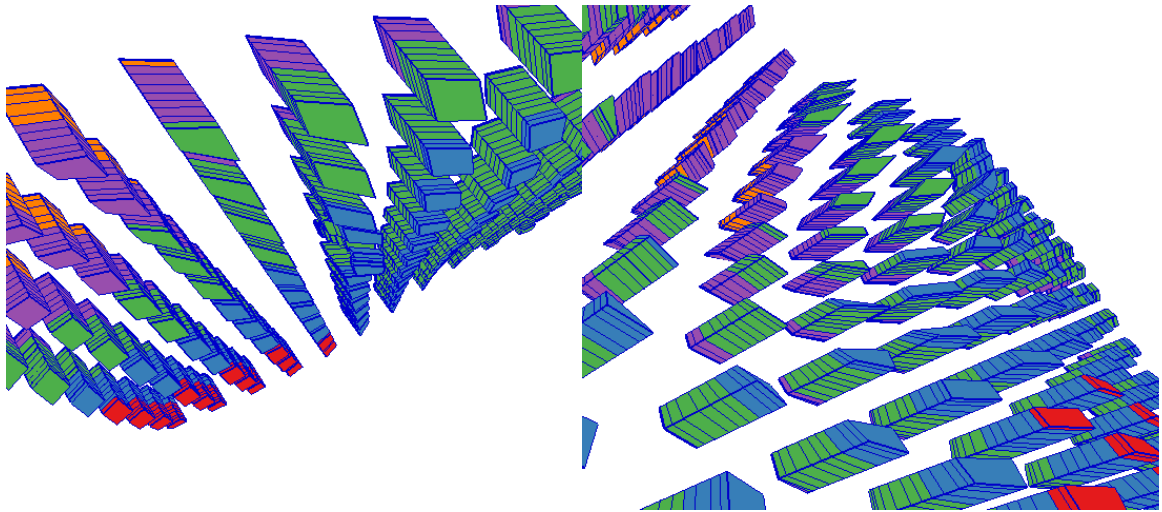


Figure 57: 3D Case 1: X & Y Angle, XYZ Displacement, X Angle, Y Angle, Number of Visible Cells

Figure 58: 3D Case 2: X & Y Angle, XYZ Displacement, X Angle, Y Angle, Number of Visible Cells

### XYZ Displacement & Number of Visible Cells

View	Top	45	X & Y Angle		
Input	XYZ Dis	XYZ Dis	XYZ Dis	X Angle	Y Angle
Case 1	0.145	0.300	0.373	0.011	0.023
Case 2	0.001	0.002	0.274	0.000	0.056
Avg	0.073	0.151	0.323	0.006	0.040

Table 14: XYZ Displacement & Number of Visible Cells Correlation per experiment

	Top		45		X & Y Angle	
	Min	Max	Min	Max	Min	Max
Case 1	704.0	726.0	778.0	873.0	623.0	1235.0
Case 2	798.0	816.0	880.0	932.0	717.0	1243.0
Avg	751.0	771.0	829.0	902.5	670.0	1239.0

Table 15: XYZ Displacement & Number of Visible Cells Min Max per experiment

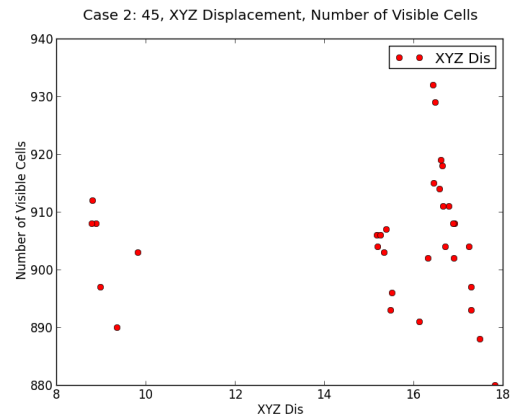
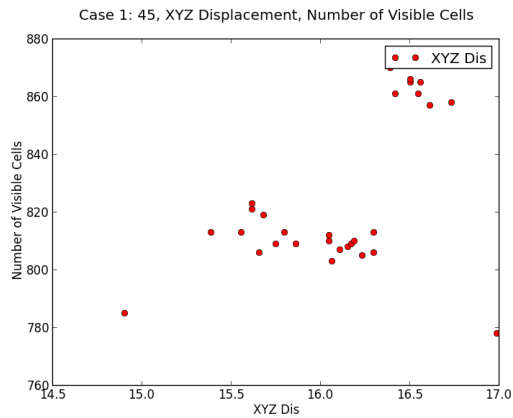
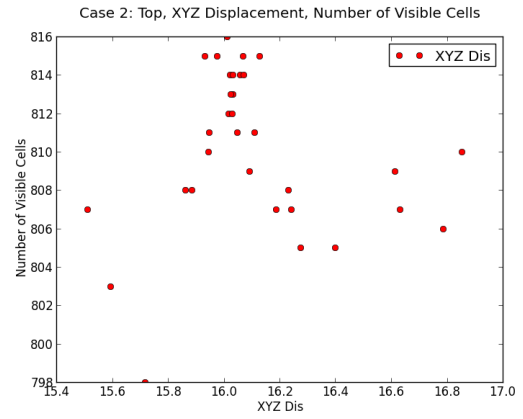
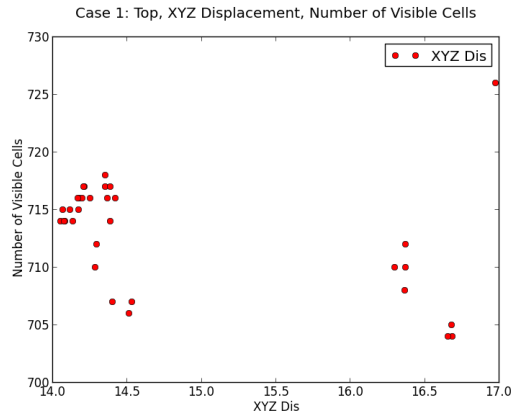


**Figure 59: Top & 45: XYZ Displacement & Number of Visible Cells**

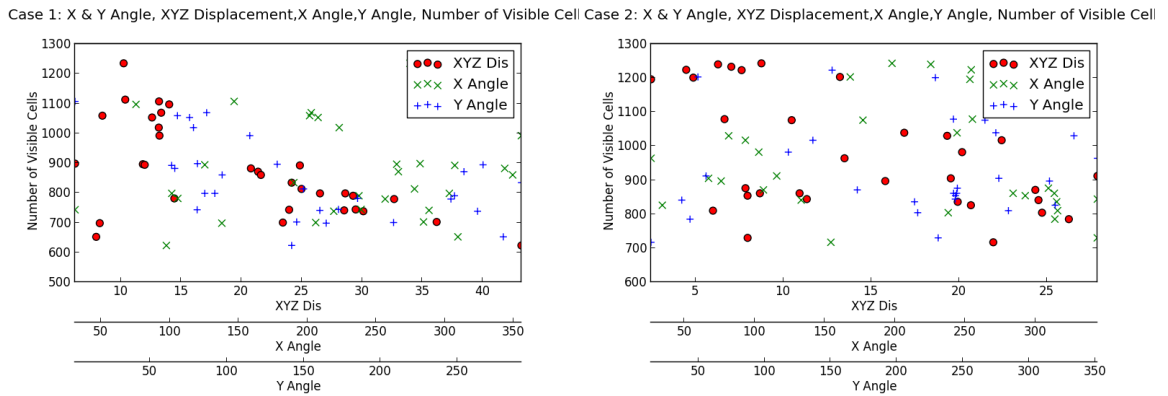


**Figure 60: X & Y Angles XYZ Displacement & Number of Visible Cells**

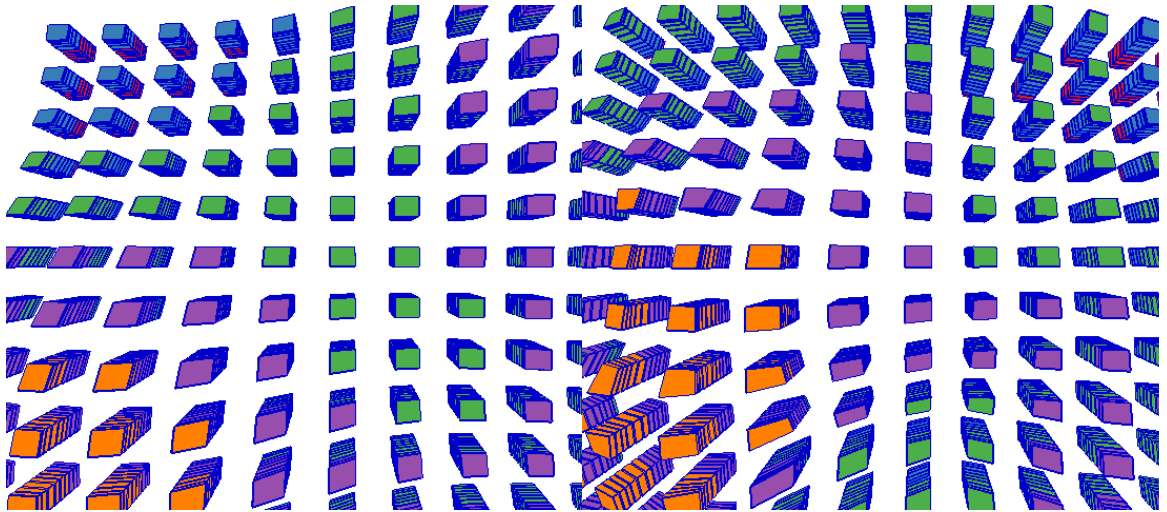


**Figure 61: 3D Case 1: Top, XYZ Displacement, Number of Visible Cells**

**Figure 62: 3D Case 2: Top, XYZ Displacement, Number of Visible Cells**

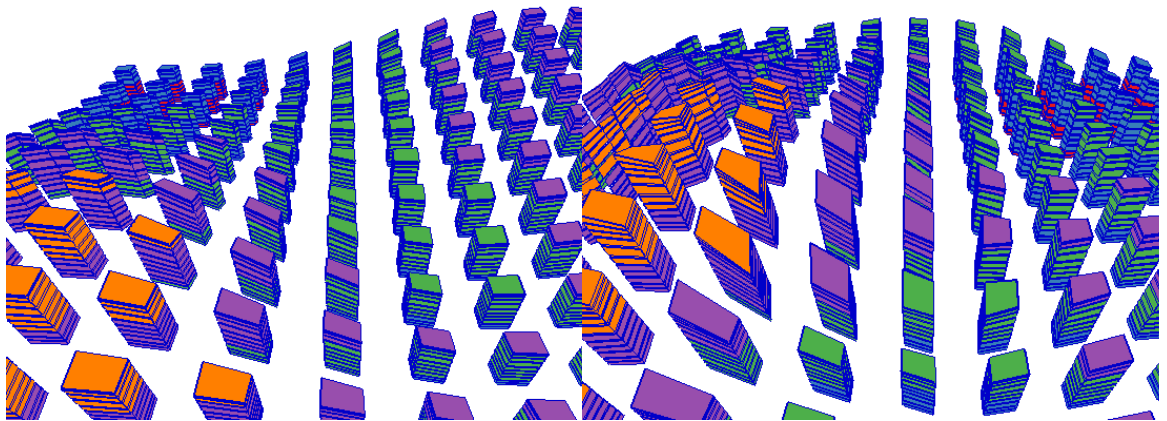


**Figure 63: 3D Case 1: 45, XYZ Displacement, Number of Visible Cells**

**Figure 64: 3D Case 2: 45, XYZ Displacement, Number of Visible Cells**

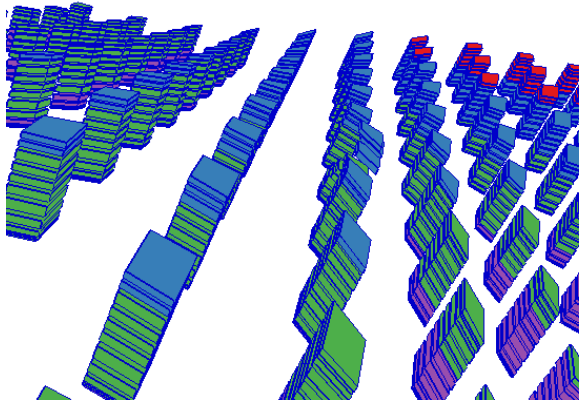


**Figure 65: 3D Case 1: X & Y Angle, XYZ  
Displacement, X Angle, Y Angle, Number of Visible  
Cells**

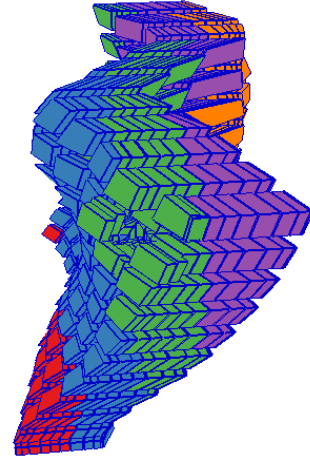


**Figure 66: 3D Case 2: X & Y Angle, XYZ  
Displacement, X Angle, Y Angle, Number of Visible  
Cells**

### The Gaussian parameter & Face Conformal Energy

View	Top	45	X & Y Angle		
Input	Gaussian	Gaussian	Gaussian	X Angle	Y Angle
Case 1	nan	0.932	nan	nan	nan
Case 2	nan	0.793	nan	nan	nan
Avg	nan	0.862	nan	nan	nan

**Table 16: The Gaussian parameter & Face Conformal Energy Correlation per experiment**

	Top		45		X & Y Angle	
	Min	Max	Min	Max	Min	Max
Case 1	0.0	0.0	0.0	0.4	0.0	0.0
Case 2	0.0	0.0	0.0	0.8	0.0	0.0
Avg	0.0	0.0	0.0	0.6	0.0	0.0

**Table 17: The Gaussian parameter & Face Conformal Energy Min Max per experiment**

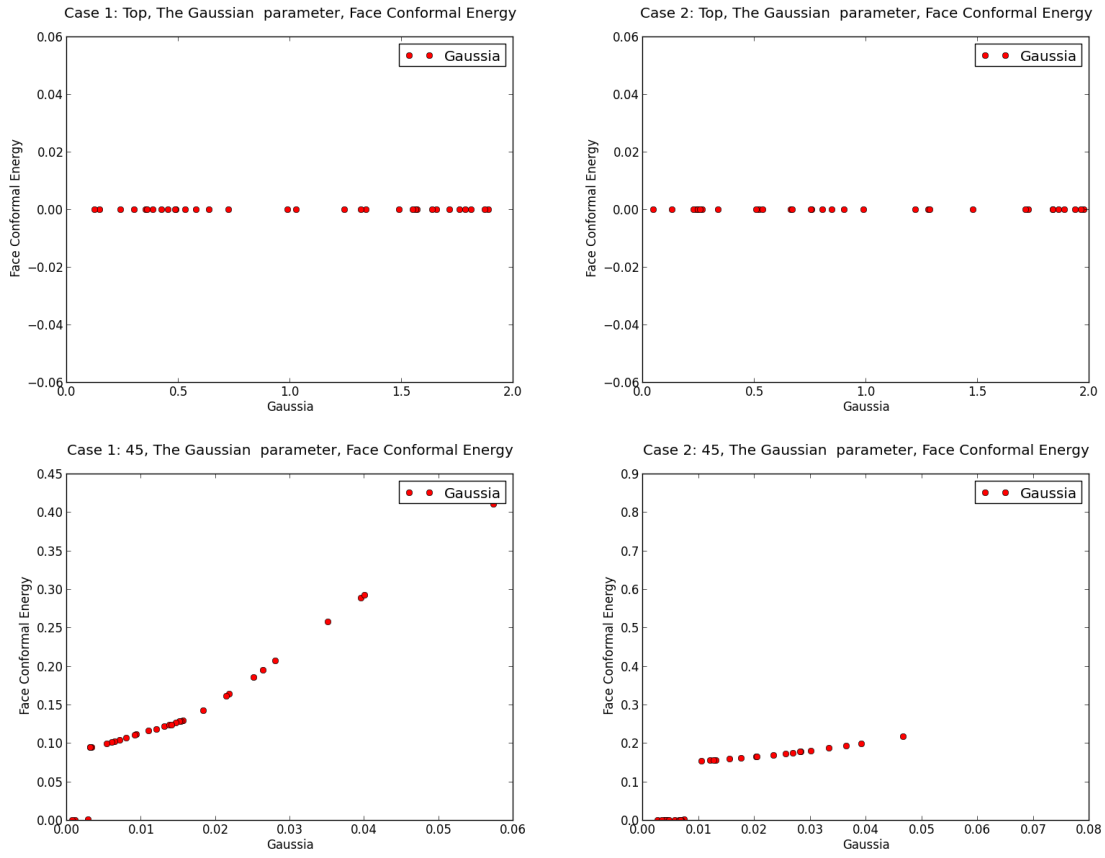


Figure 67: Top & 45: The Gaussian parameter & Face Conformal Energy

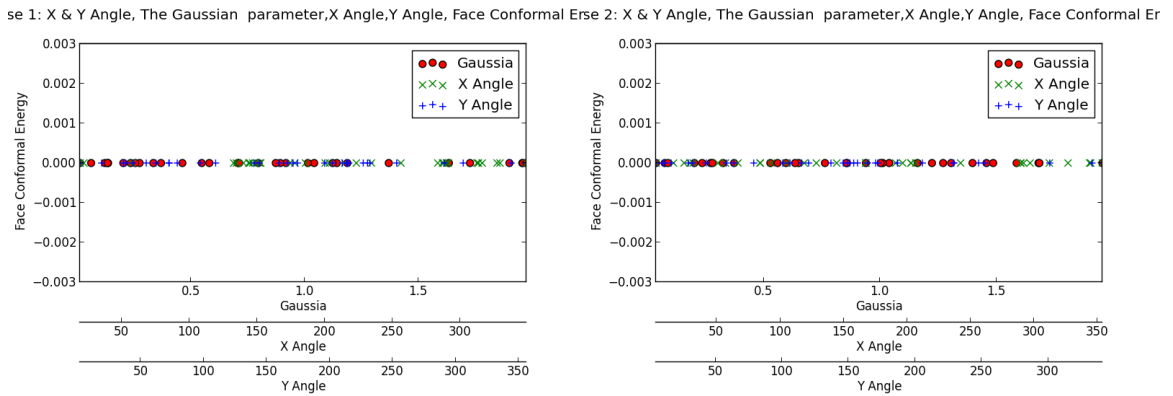


Figure 68: X & Y Angles The Gaussian parameter & Face Conformal Energy

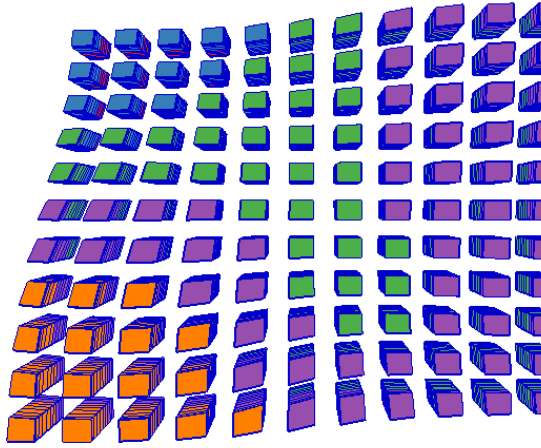


Figure 69: 3D Case 1: Top, The Gaussian parameter, Face Conformal Energy

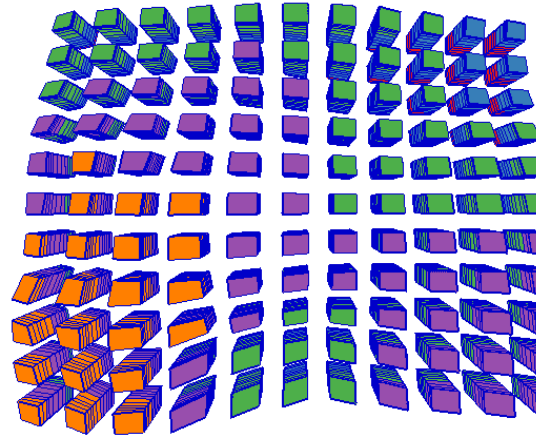


Figure 70: 3D Case 2: Top, The Gaussian parameter, Face Conformal Energy

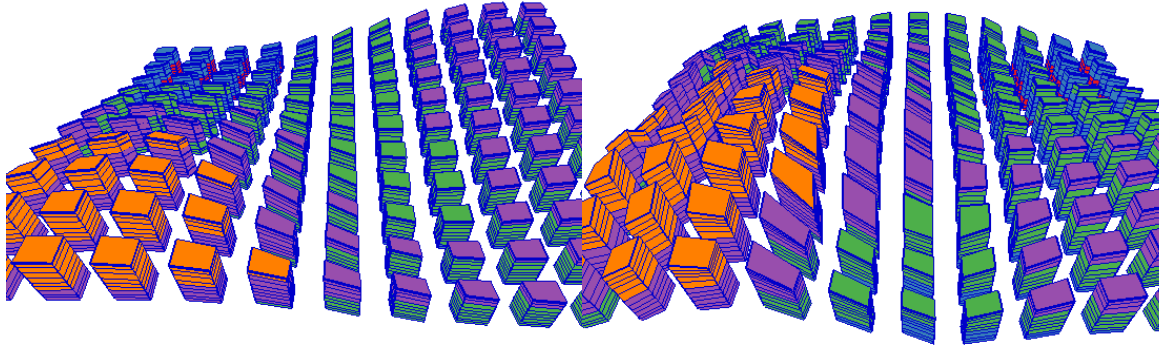


Figure 71: 3D Case 1: 45, The Gaussian parameter, Face Conformal Energy

Figure 72: 3D Case 2: 45, The Gaussian parameter, Face Conformal Energy

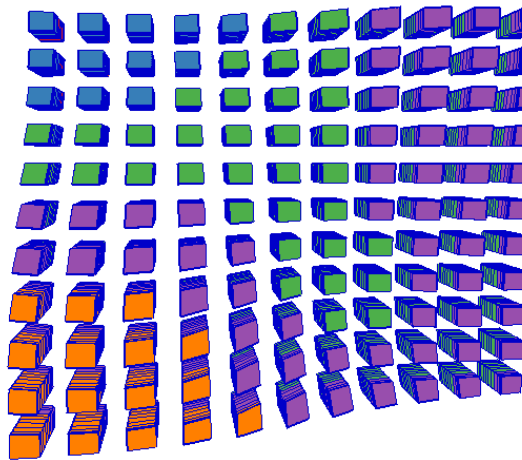


Figure 73: 3D Case 1: X & Y Angle, The Gaussian parameter, X Angle, Y Angle, Face Conformal Energy

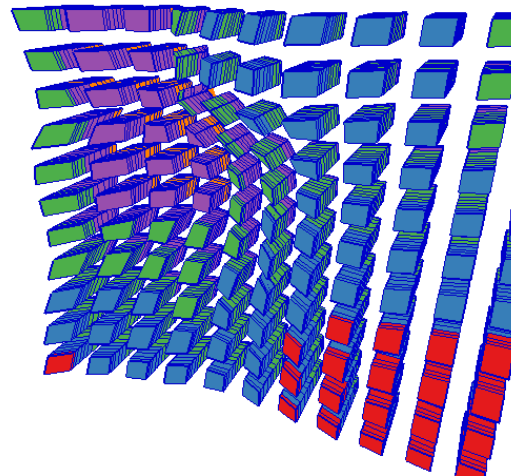


Figure 74: 3D Case 2: X & Y Angle, The Gaussian parameter, X Angle, Y Angle, Face Conformal Energy

### Camera Distance & Face Conformal Energy

View	Top	45	X & Y Angle		
Input	Camera	Camera	Camera	X Angle	Y Angle
Case 1	nan	0.342	0.001	0.020	0.000
Case 2	nan	0.553	nan	nan	nan
Avg	nan	0.447	nan	nan	nan

Table 18: Camera Distance & Face Conformal Energy Correlation per experiment

	Top		45		X & Y Angle	
	Min	Max	Min	Max	Min	Max
Case 1	0.0	0.0	8.6	8.6	0.0	8.4
Case 2	0.0	0.0	6.7	6.7	0.0	0.0
Avg	0.0	0.0	7.7	7.7	0.0	4.2

Table 19: Camera Distance & Face Conformal Energy Min Max per experiment

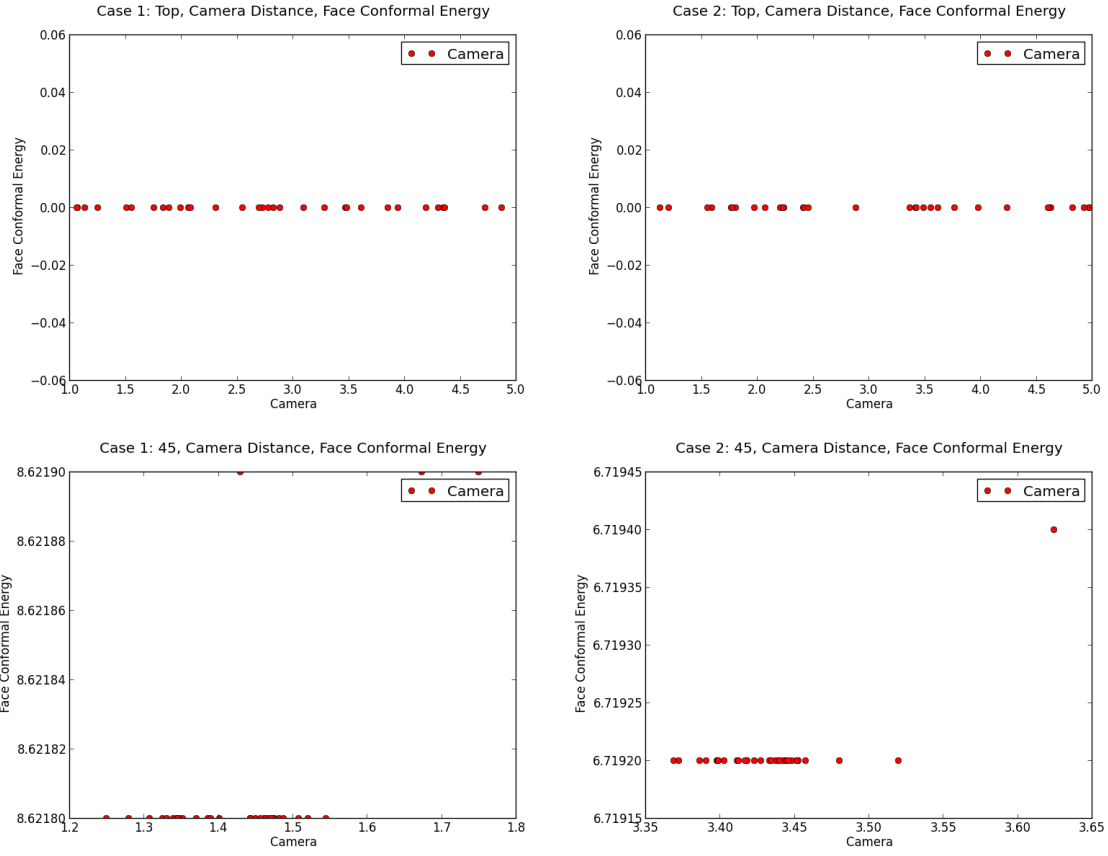


**Figure 75: Top & 45: Camera Distance & Face Conformal Energy**

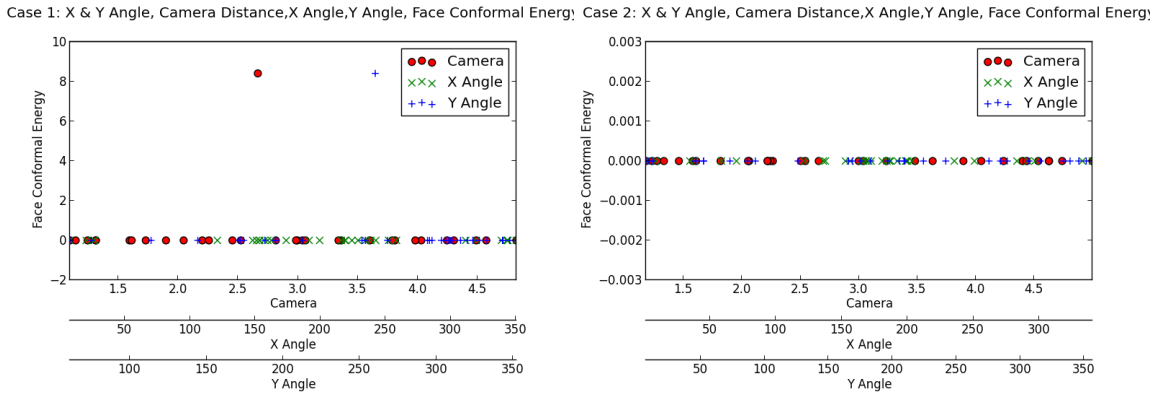


**Figure 76: X & Y Angles Camera Distance & Face Conformal Energy**



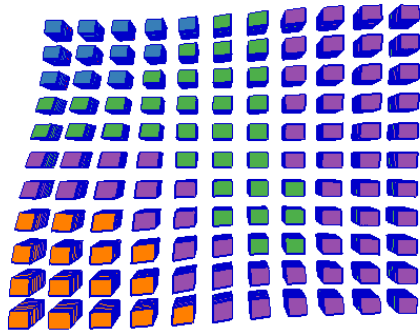


Figure 77: 3D Case 1: Top, Camera Distance, Face Conformal Energy

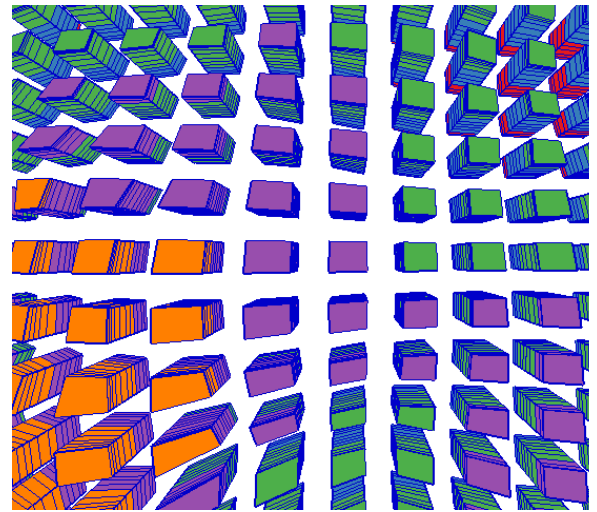


Figure 78: 3D Case 2: Top, Camera Distance, Face Conformal Energy

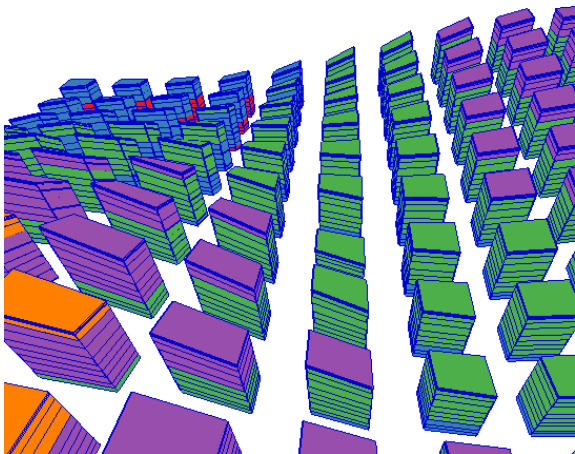


Figure 79: 3D Case 1: 45, Camera Distance, Face Conformal Energy

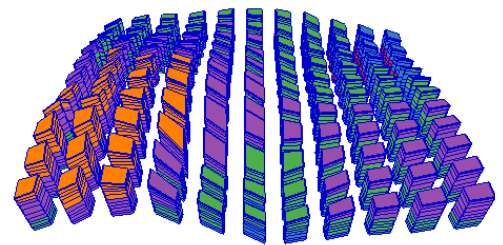


Figure 80: 3D Case 2: 45, Camera Distance, Face Conformal Energy

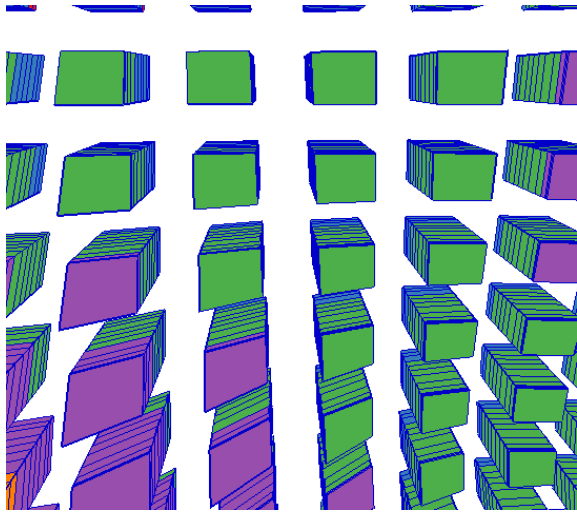


Figure 81: 3D Case 1: X & Y Angle, Camera Distance, X Angle, Y Angle, Face Conformal Energy

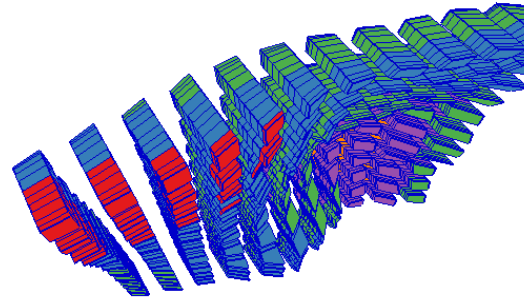


Figure 82: 3D Case 2: X & Y Angle, Camera Distance, X Angle, Y Angle, Face Conformal Energy

## Z Exaggeration & Face Conformal Energy

View	Top	45	X & Y Angle		
Input	Z Exagg	Z Exagg	Z Exagg	X Angle	Y Angle
Case 1	0.407	0.180	0.034	0.014	0.100
Case 2	0.158	0.387	0.852	0.002	0.028
Avg	0.282	0.283	0.443	0.008	0.064

Table 20: Z Exaggeration & Face Conformal Energy Correlation per experiment

	Top		45		X & Y Angle	
	Min	Max	Min	Max	Min	Max
Case 1	0.1	5.4	8.6	13.5	0.4	20.2
Case 2	0.0	1.3	5.8	9.5	0.0	62.8
Avg	0.0	3.3	7.2	11.5	0.2	41.5

Table 21: Z Exaggeration & Face Conformal Energy Min Max per experiment

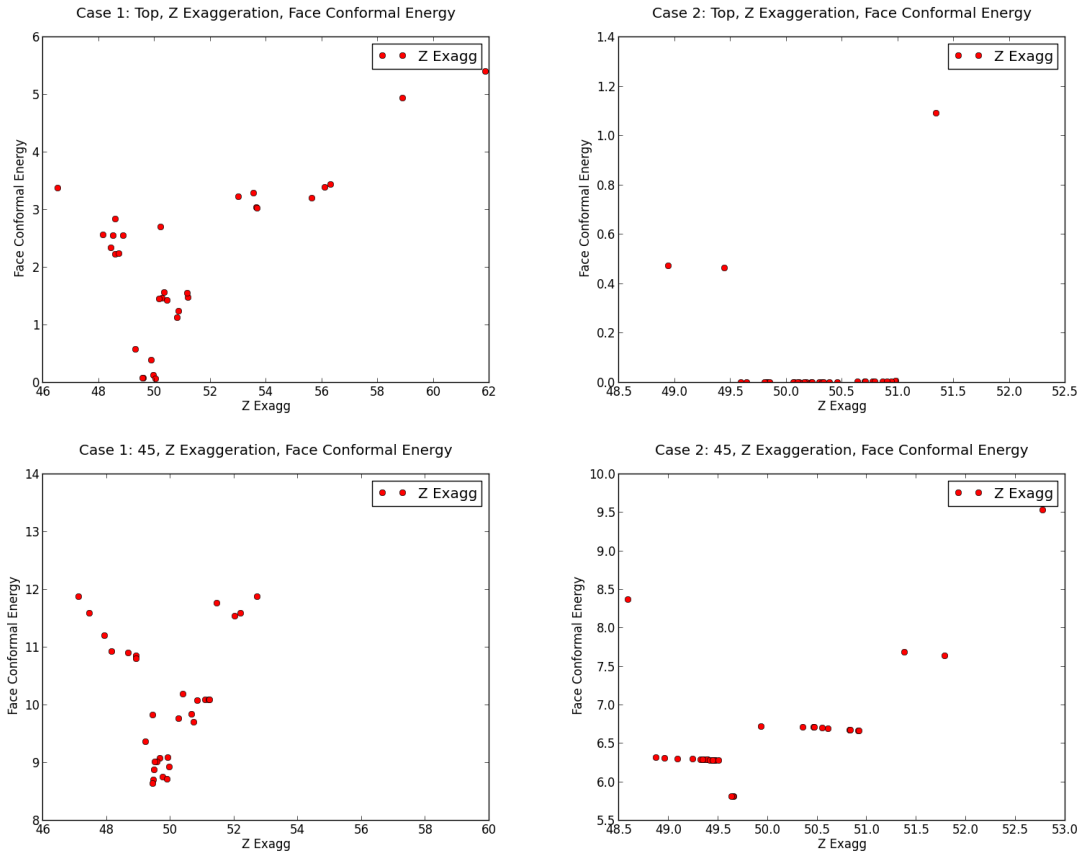


**Figure 83: Top & 45: Z Exaggeration & Face Conformal Energy**

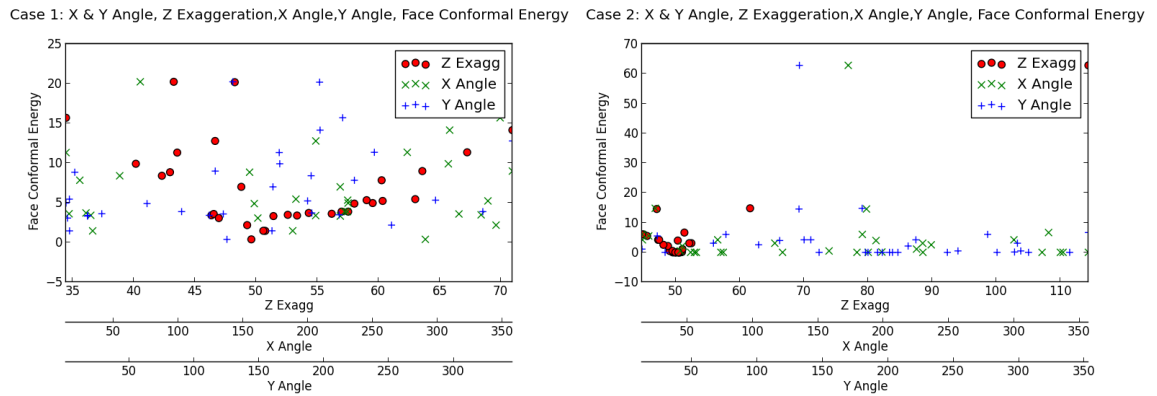


**Figure 84: X & Y Angles Z Exaggeration & Face Conformal Energy**

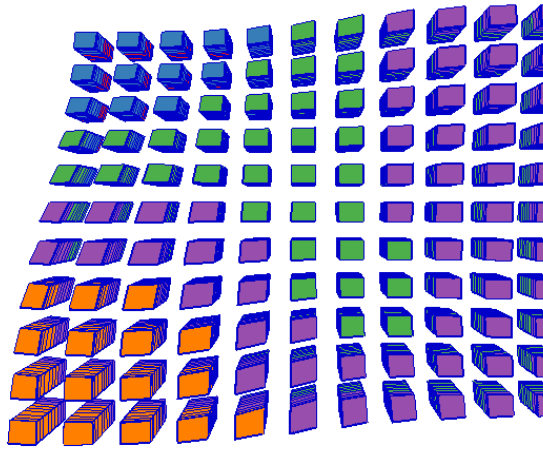


Figure 85: 3D Case 1: Top, Z Exaggeration, Face Conformal Energy

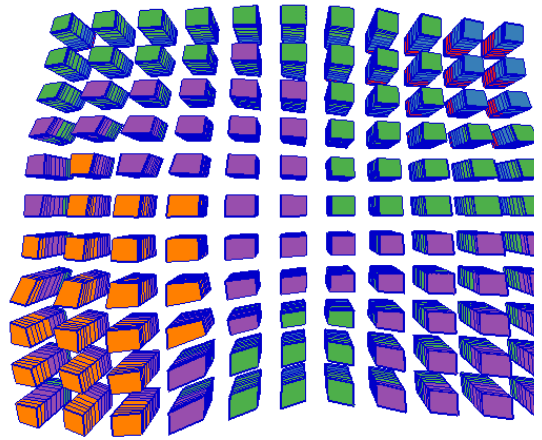


Figure 86: 3D Case 2: Top, Z Exaggeration, Face Conformal Energy

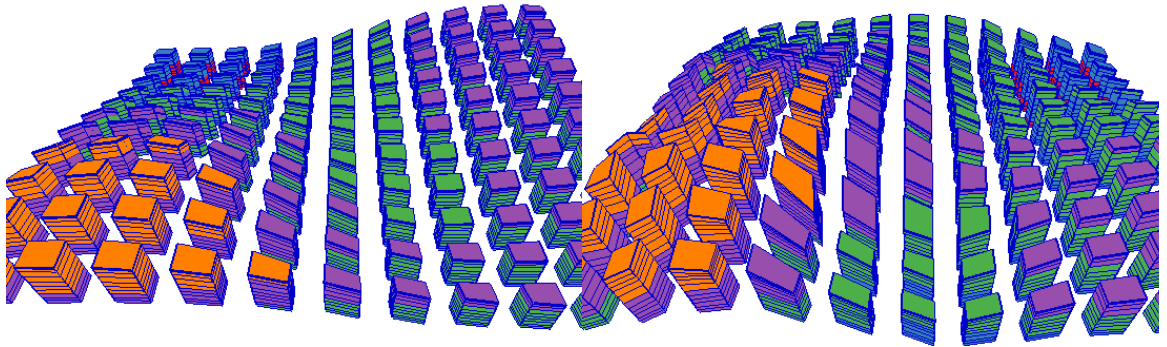


Figure 87: 3D Case 1: 45, Z Exaggeration, Face Conformal Energy

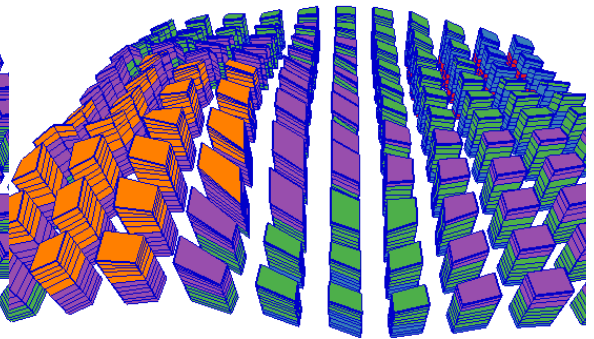


Figure 88: 3D Case 2: 45, Z Exaggeration, Face Conformal Energy

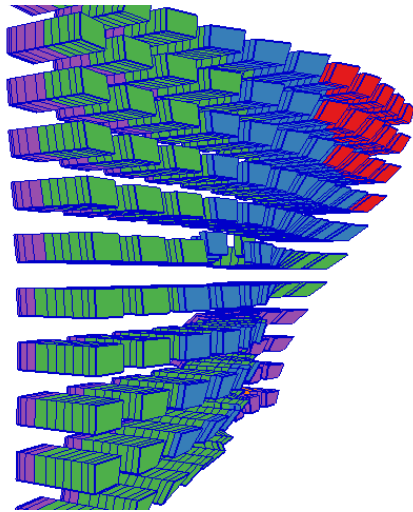


Figure 89: 3D Case 1: X & Y Angle, Z Exaggeration, X Angle, Y Angle, Face Conformal Energy

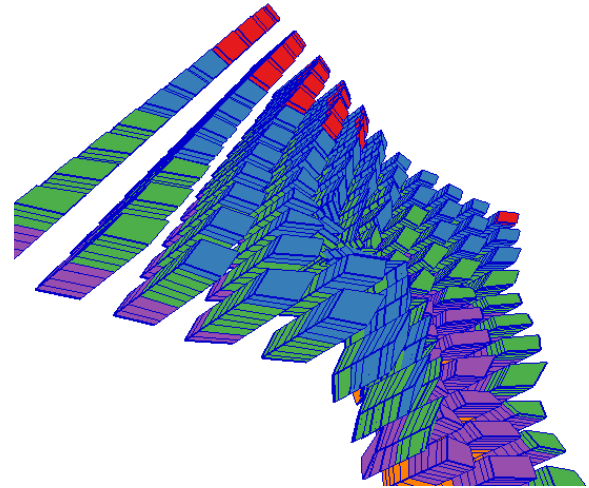


Figure 90: 3D Case 2: X & Y Angle, Z Exaggeration, X Angle, Y Angle, Face Conformal Energy

### XY Displacement & Face Conformal Energy

View	Top	45	X & Y Angle		
Input	XY Disp	XY Disp	XY Disp	X Angle	Y Angle
Case 1	0.630	0.008	0.040	0.014	0.041
Case 2	0.006	0.466	0.380	0.023	0.009
Avg	0.318	0.237	0.210	0.019	0.025

Table 22: XY Displacement & Face Conformal Energy Correlation per experiment

	Top		45		X & Y Angle	
	Min	Max	Min	Max	Min	Max
Case 1	0.0	4.6	8.6	21.6	1.9	93.3
Case 2	0.0	4.9	5.9	8.3	0.0	24.3
Avg	0.0	4.7	7.3	15.0	1.0	58.8

Table 23: XY Displacement & Face Conformal Energy Min Max per experiment

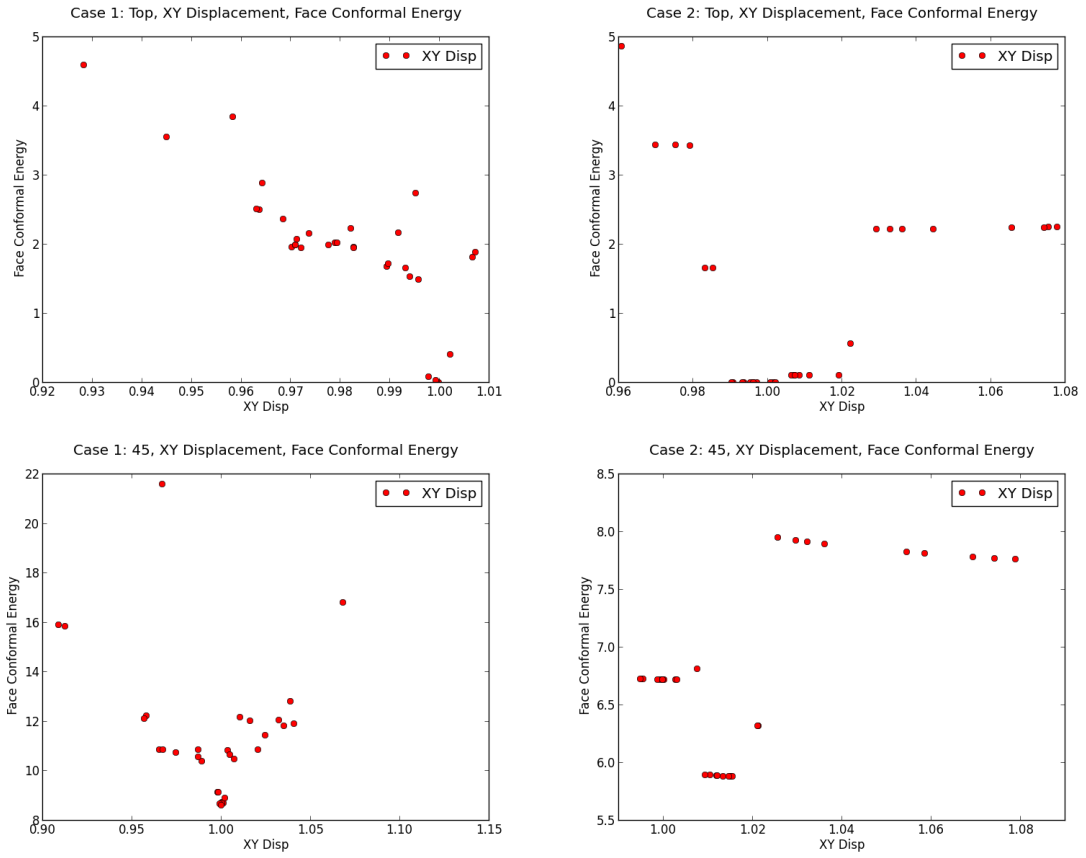


**Figure 91: Top & 45: XY Displacement & Face Conformal Energy**

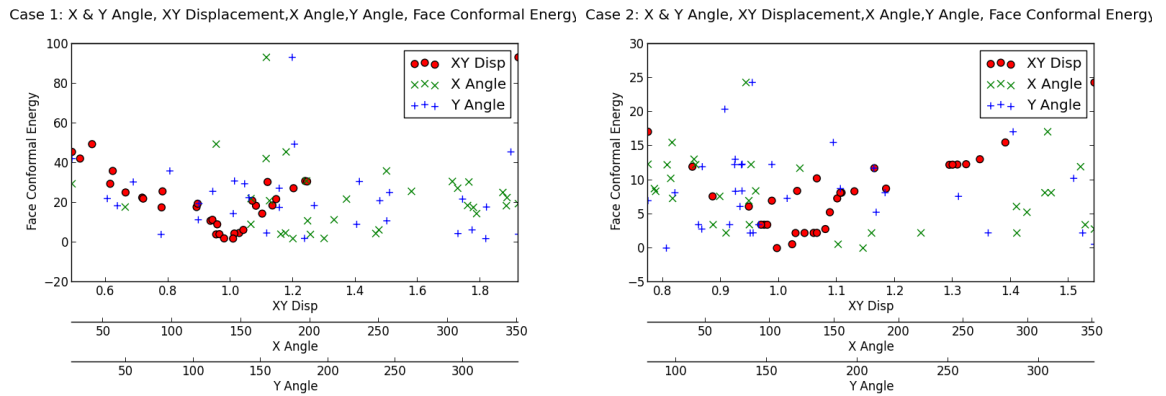


**Figure 92: X & Y Angles XY Displacement & Face Conformal Energy**

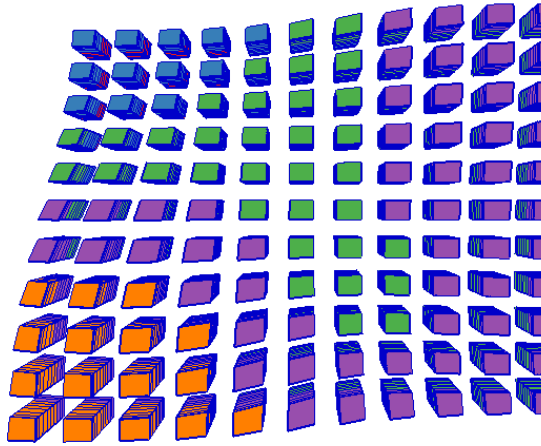


Figure 93: 3D Case 1: Top, XY Displacement, Face Conformal Energy

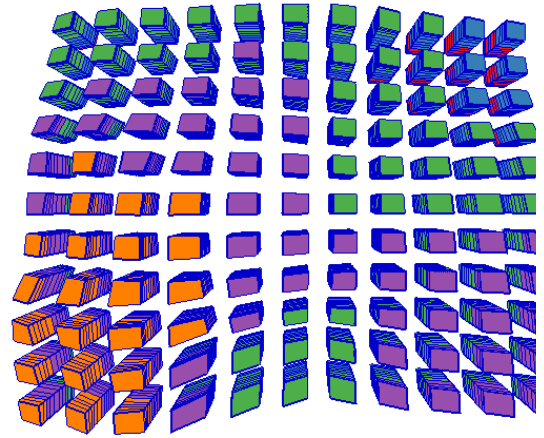


Figure 94: 3D Case 2: Top, XY Displacement, Face Conformal Energy

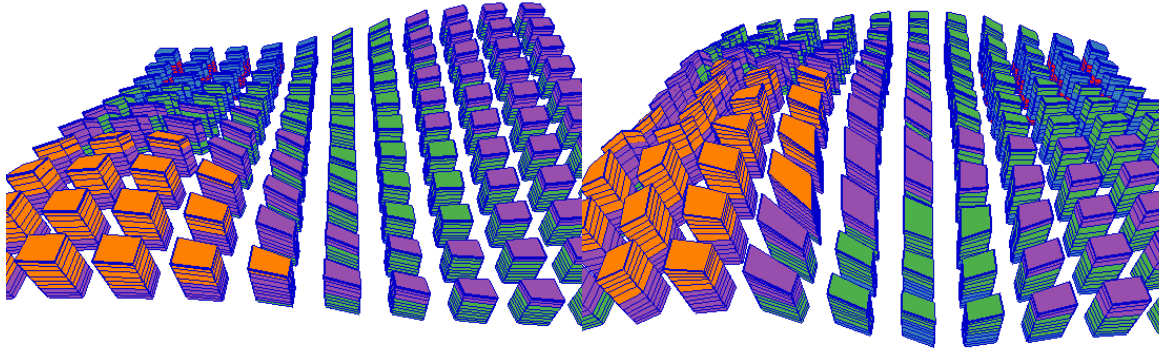


Figure 95: 3D Case 1: 45, XY Displacement, Face Conformal Energy

Figure 96: 3D Case 2: 45, XY Displacement, Face Conformal Energy

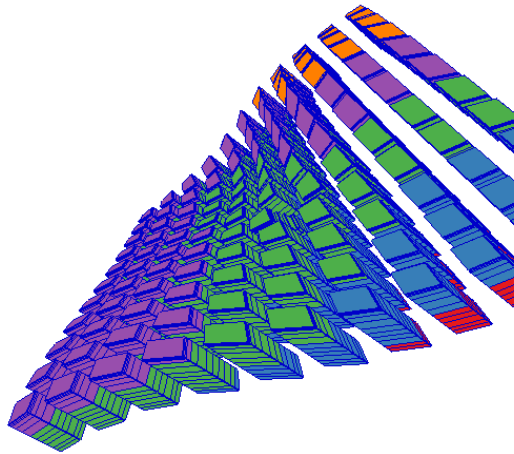


Figure 97: 3D Case 1: X & Y Angle, XY Displacement, X Angle, Y Angle, Face Conformal Energy

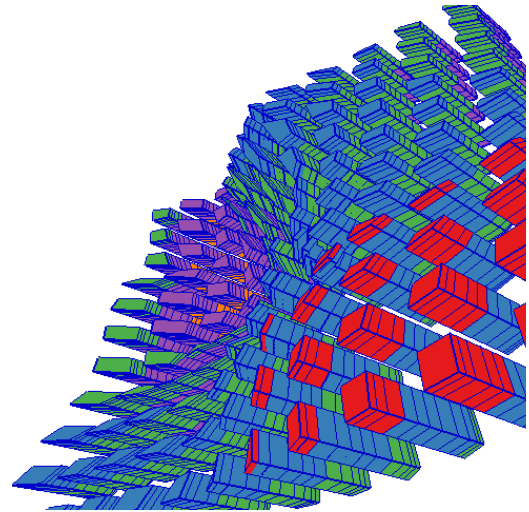


Figure 98: 3D Case 2: X & Y Angle, XY Displacement, X Angle, Y Angle, Face Conformal Energy

### XYZ Displacement & Face Conformal Energy

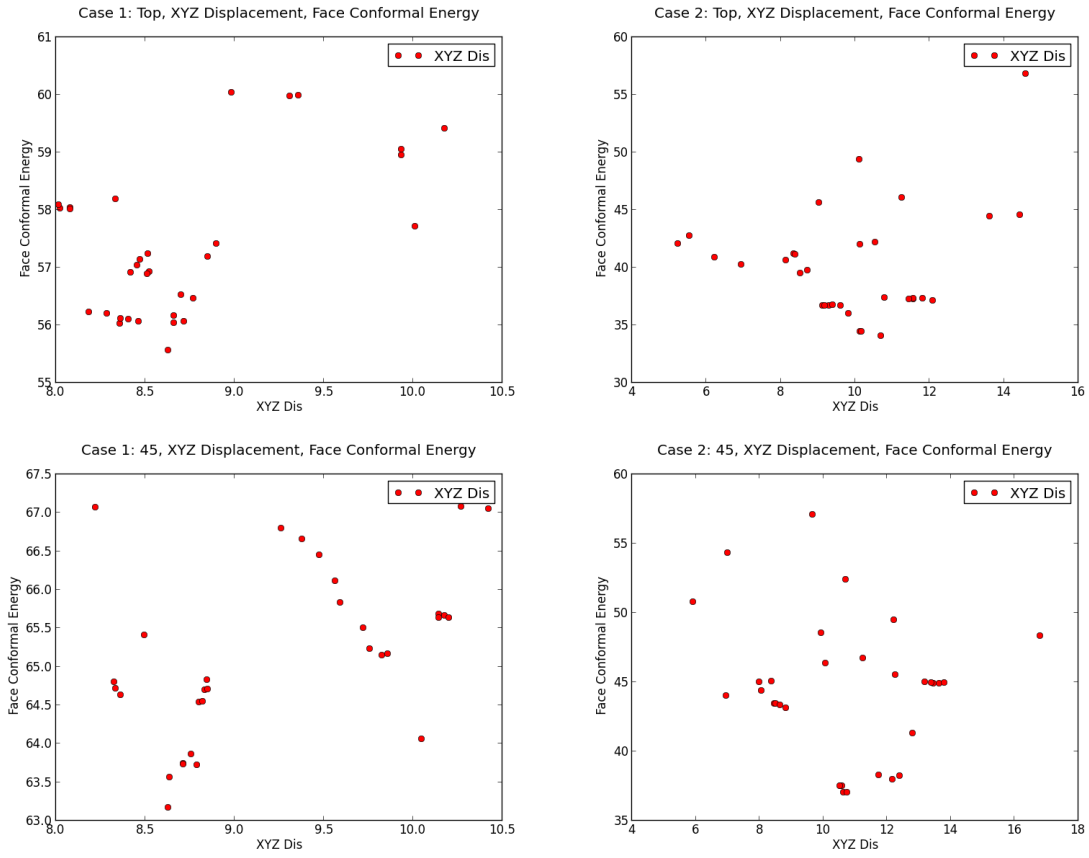
View	Top	45	X & Y Angle		
Input	XYZ Dis	XYZ Dis	XYZ Dis	X Angle	Y Angle
Case 1	0.283	0.240	0.005	0.120	0.034
Case 2	0.044	0.028	0.000	0.019	0.015
Avg	0.163	0.134	0.003	0.069	0.025

Table 24: XYZ Displacement & Face Conformal Energy Correlation per experiment

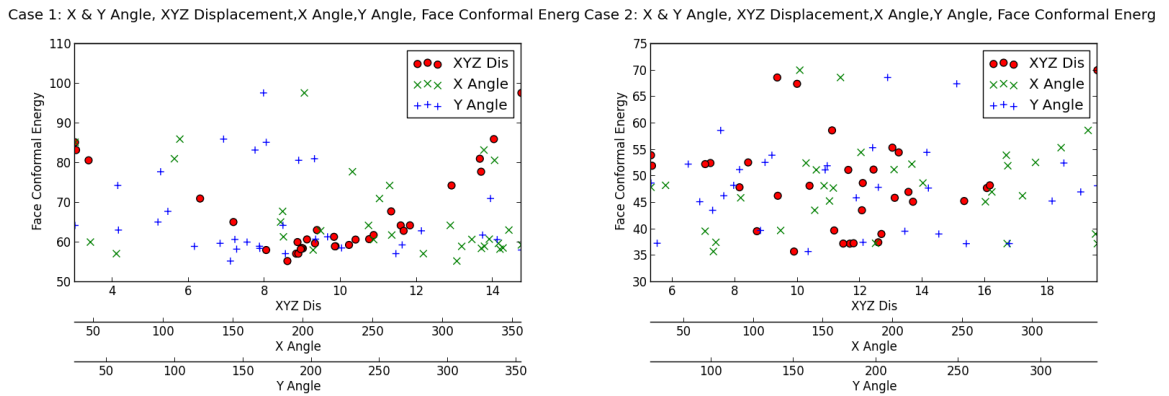
	Top		45		X & Y Angle	
	Min	Max	Min	Max	Min	Max
Case 1	55.6	60.0	63.2	67.1	55.3	97.7
Case 2	34.1	56.8	37.0	57.1	35.8	70.0
Avg	44.8	58.4	50.1	62.1	45.5	83.9

Table 25: XYZ Displacement & Face Conformal Energy Min Max per experiment





**Figure 99: Top & 45: XYZ Displacement & Face Conformal Energy**



**Figure 100: X & Y Angles XYZ Displacement & Face Conformal Energy**

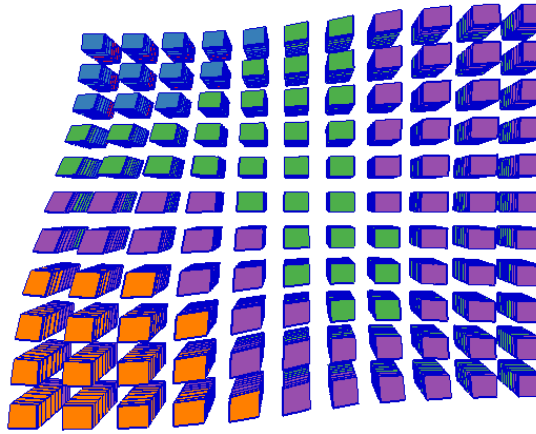


Figure 101: 3D Case 1: Top, XYZ Displacement, Face Conformal Energy

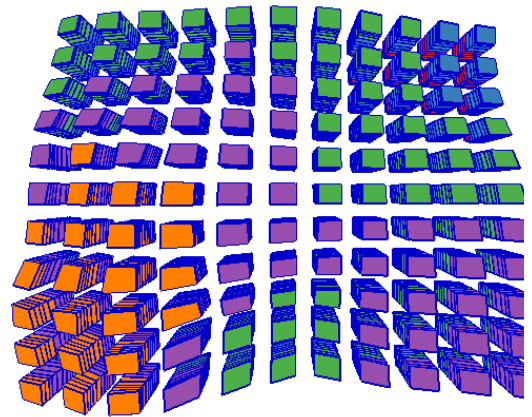


Figure 102: 3D Case 2: Top, XYZ Displacement, Face Conformal Energy

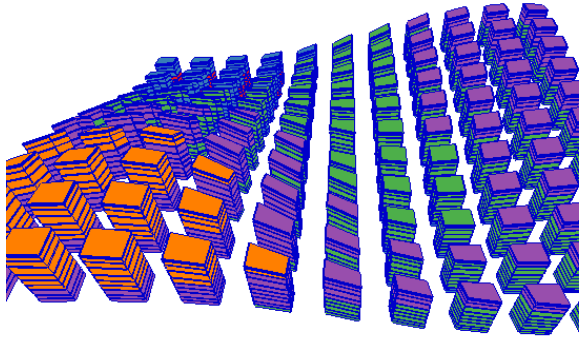


Figure 103: 3D Case 1: 45, XYZ Displacement, Face Conformal Energy

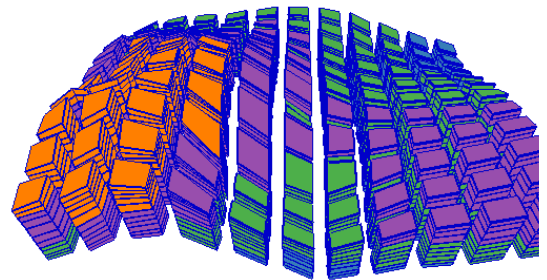


Figure 104: 3D Case 2: 45, XYZ Displacement, Face Conformal Energy

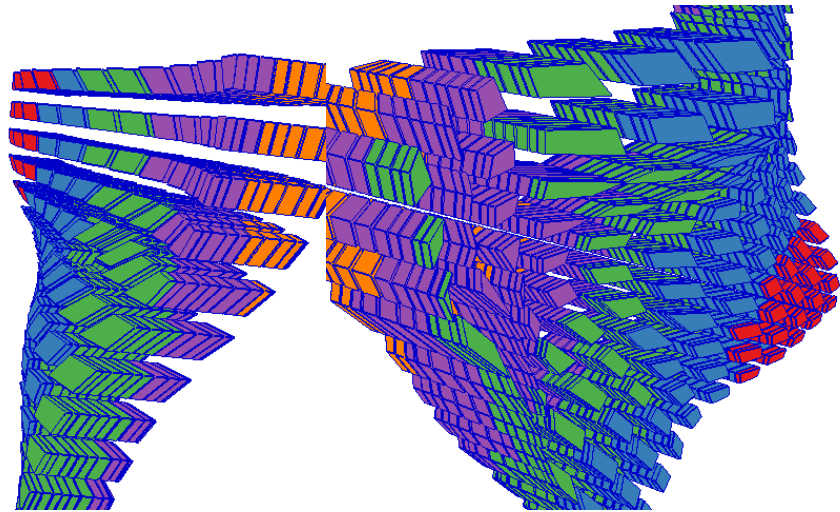


Figure 105: 3D Case 1: X & Y Angle, XYZ  
Displacement, X Angle, Y Angle, Face Conformal  
Energy

Figure 106: 3D Case 2: X & Y Angle, XYZ  
Displacement, X Angle, Y Angle, Face Conformal  
Energy

### The Gaussian parameter & Ratio of Used Space

View	Top	45	X & Y Angle		
Input	Gaussian	Gaussian	Gaussian	X Angle	Y Angle
Case 1	-inf	0.508	0.001	0.102	0.144
Case 2	-inf	-inf	0.044	0.241	0.015
Avg	-inf	-inf	0.023	0.171	0.079

Table 26: The Gaussian parameter & Ratio of Used Space Correlation per experiment

	Top		45		X & Y Angle	
	Min	Max	Min	Max	Min	Max
Case 1	0.4	0.4	0.4	0.4	0.4	0.5
Case 2	0.4	0.4	0.4	0.4	0.4	0.5
Avg	0.4	0.4	0.4	0.4	0.4	0.5

Table 27: The Gaussian parameter & Ratio of Used Space Min Max per experiment

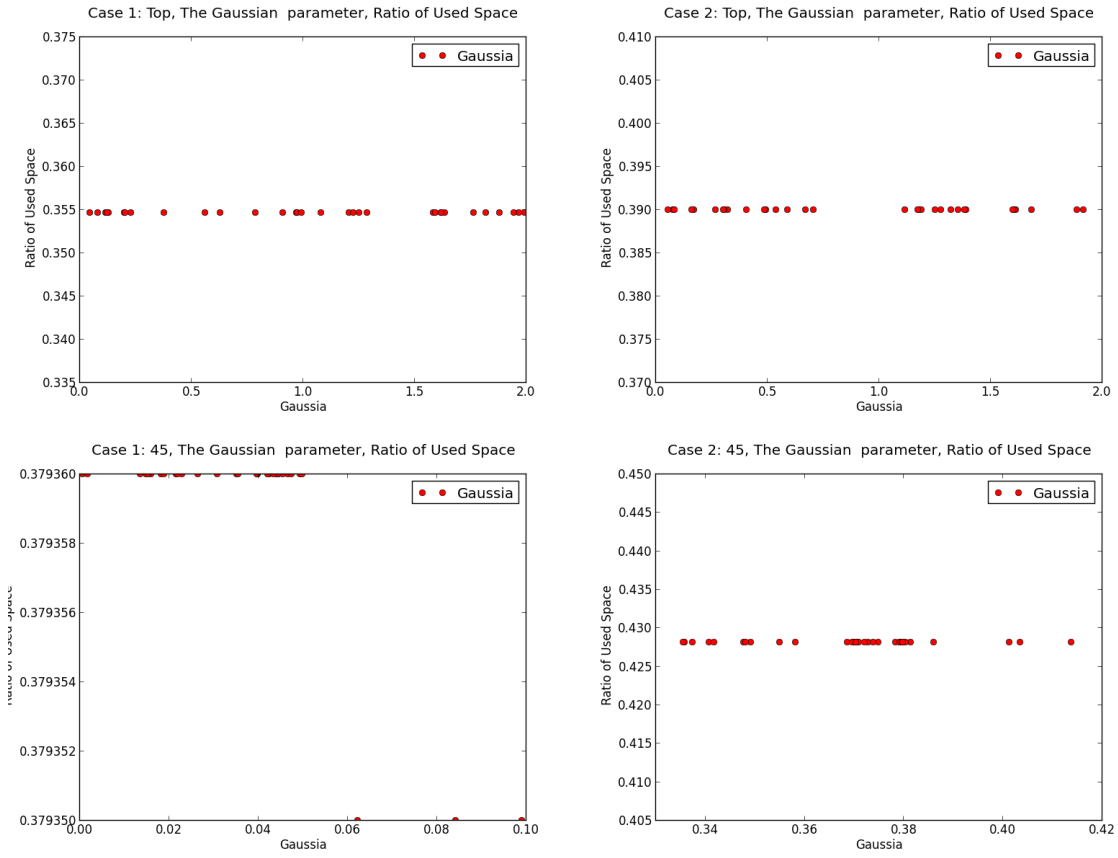


**Figure 107: Top & 45: The Gaussian parameter & Ratio of Used Space**

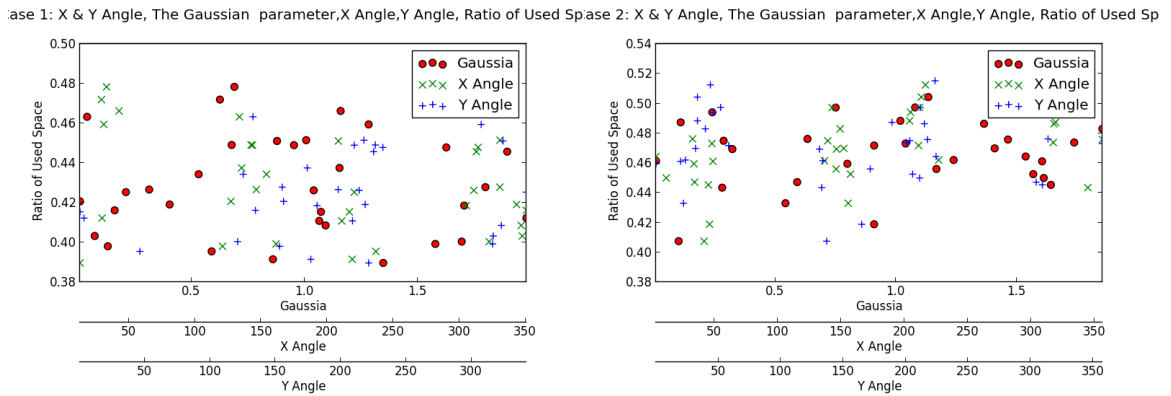


**Figure 108: X & Y Angles The Gaussian parameter & Ratio of Used Space**

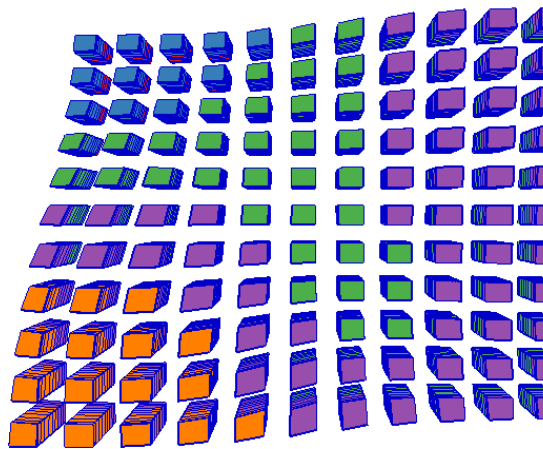


Figure 109: 3D Case 1: Top, The Gaussian parameter, Ratio of Used Space

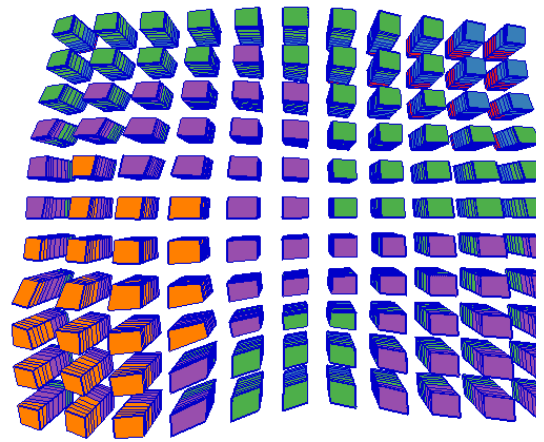


Figure 110: 3D Case 2: Top, The Gaussian parameter, Ratio of Used Space

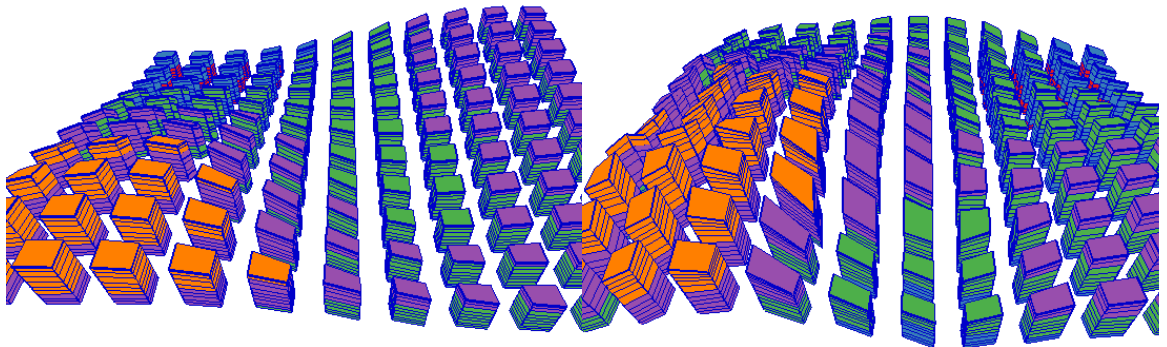


Figure 111: 3D Case 1: 45, The Gaussian parameter, Ratio of Used Space

Figure 112: 3D Case 2: 45, The Gaussian parameter, Ratio of Used Space

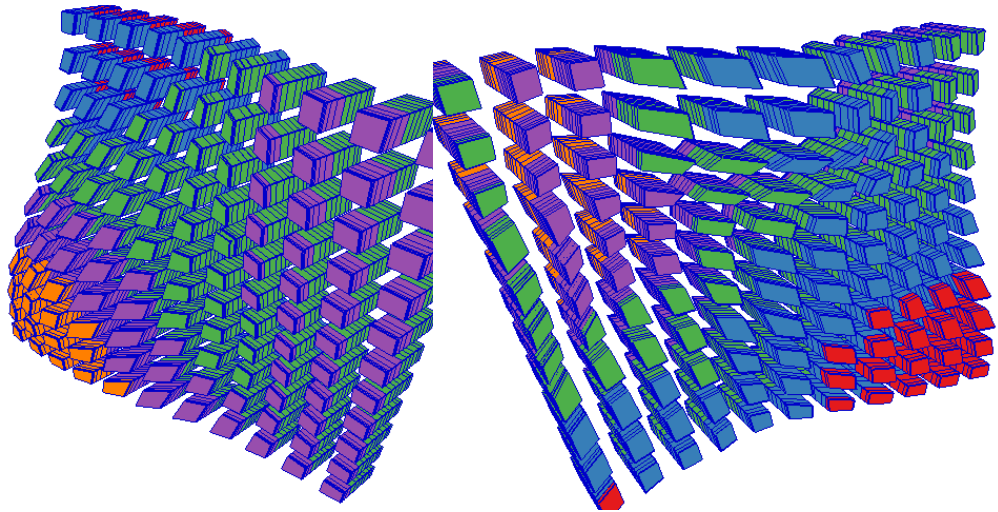


Figure 113: 3D Case 1: X & Y Angle, The Gaussian parameter, X Angle, Y Angle, Ratio of Used Space

Figure 114: 3D Case 2: X & Y Angle, The Gaussian parameter, X Angle, Y Angle, Ratio of Used Space

### Camera Distance & Ratio of Used Space

View	Top	45	X & Y Angle		
Input	Camera	Camera	Camera	X Angle	Y Angle
Case 1	0.116	0.936	0.214	0.014	0.010
Case 2	0.014	0.957	0.360	0.004	0.023
Avg	0.065	0.946	0.287	0.009	0.016

Table 28: Camera Distance & Ratio of Used Space Correlation per experiment

	Top		45		X & Y Angle	
	Min	Max	Min	Max	Min	Max
Case 1	0.6	0.6	0.7	0.7	0.6	0.9
Case 2	0.7	0.7	0.7	0.7	0.6	0.9
Avg	0.6	0.6	0.7	0.7	0.6	0.9

Table 29: Camera Distance & Ratio of Used Space Min Max per experiment

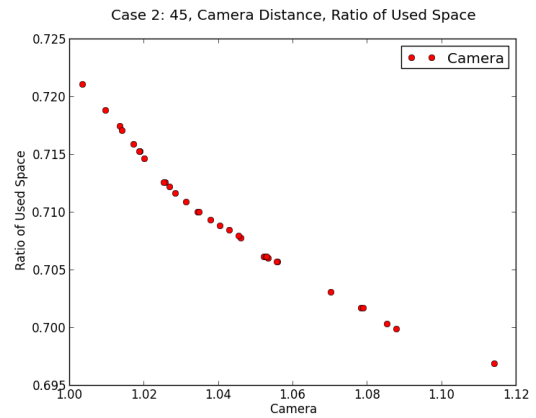
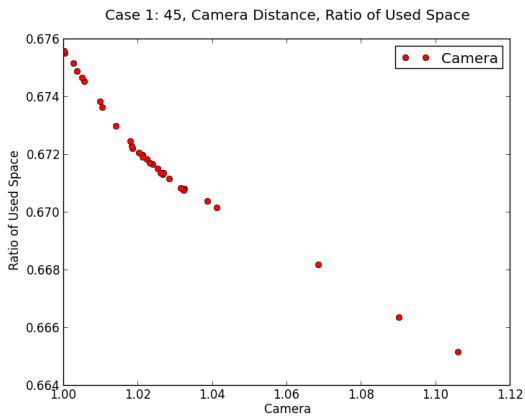
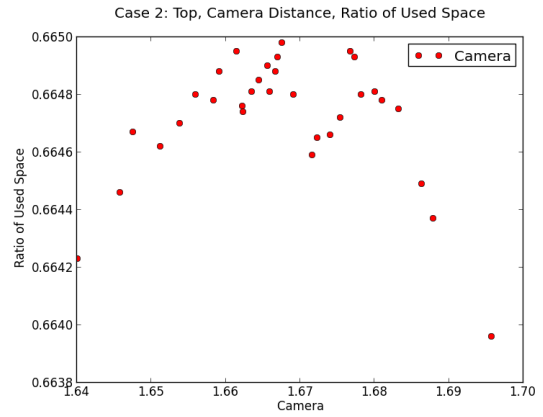
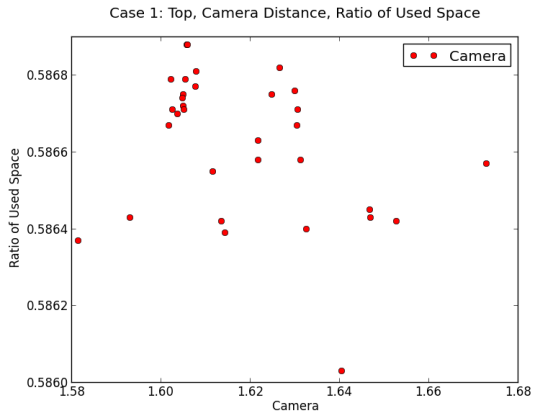


**Figure 115: Top & 45: Camera Distance & Ratio of Used Space**

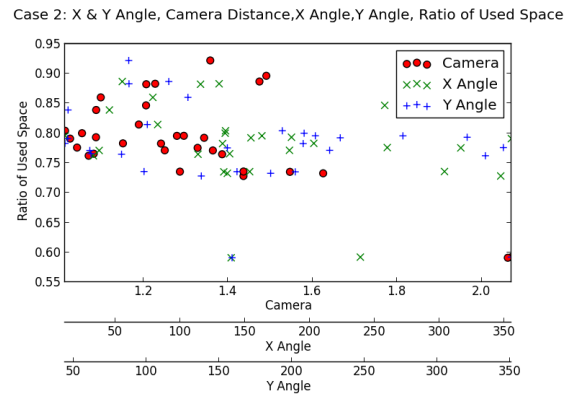
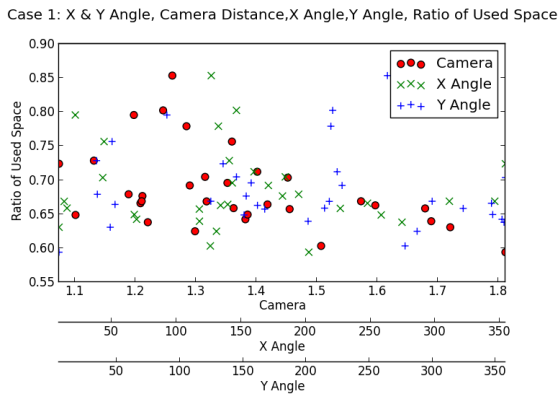


**Figure 116: X & Y Angles Camera Distance & Ratio of Used Space**

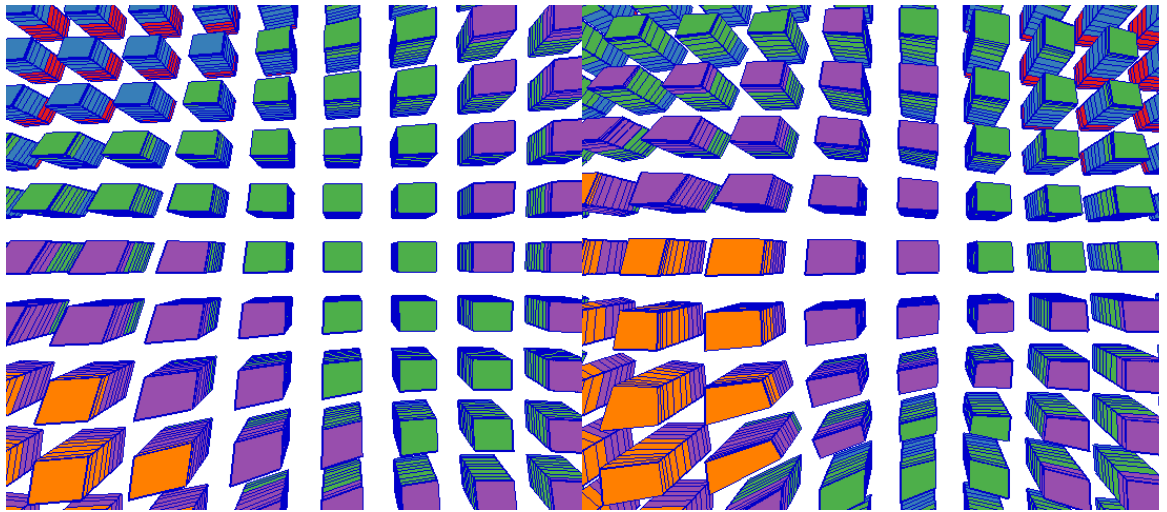


Figure 117: 3D Case 1: Top, Camera Distance, Ratio of Used Space

Figure 118: 3D Case 2: Top, Camera Distance, Ratio of Used Space

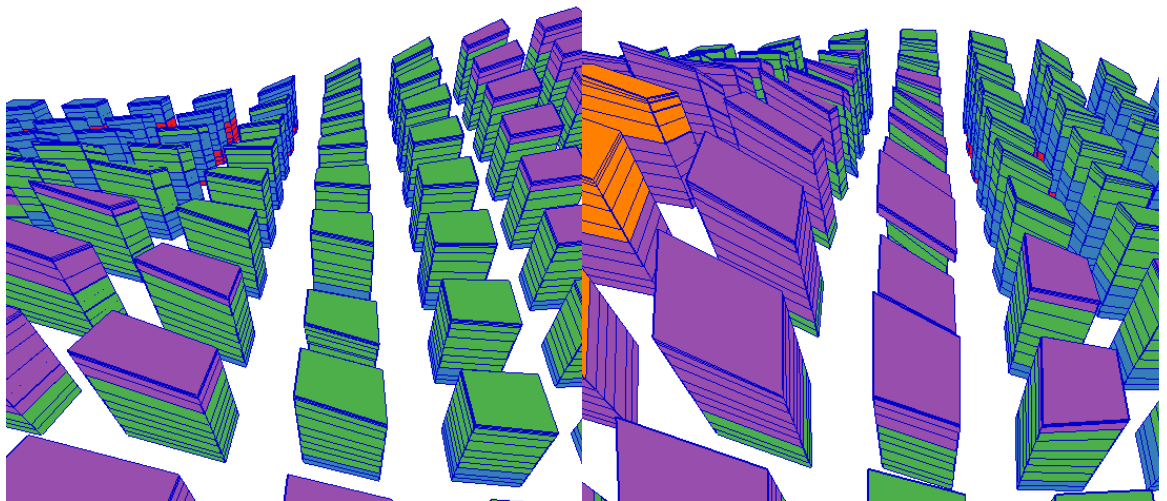


Figure 119: 3D Case 1: 45, Camera Distance, Ratio of Used Space

Figure 120: 3D Case 2: 45, Camera Distance, Ratio of Used Space



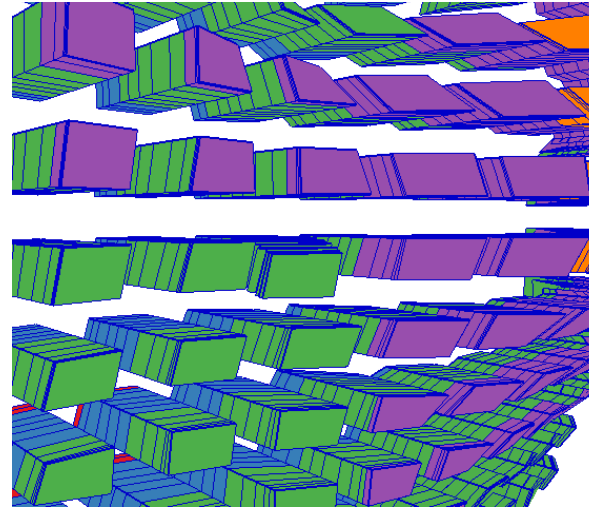
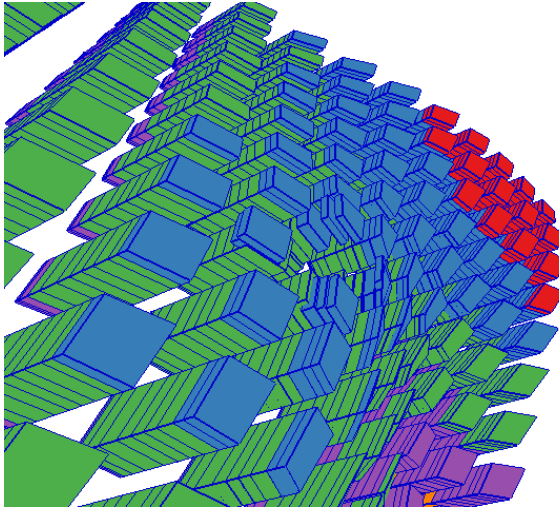


Figure 121: 3D Case 1: X & Y Angle, Camera Distance, X Angle, Y Angle, Ratio of Used Space

Figure 122: 3D Case 2: X & Y Angle, Camera Distance, X Angle, Y Angle, Ratio of Used Space

### Z Exaggeration & Ratio of Used Space

View	Top	45	X & Y Angle		
Input	Z Exagg	Z Exagg	Z Exagg	X Angle	Y Angle
Case 1	0.997	0.997	0.108	0.114	0.055
Case 2	0.998	0.999	0.339	0.062	0.002
Avg	0.998	0.998	0.224	0.088	0.029

Table 30: Z Exaggeration & Ratio of Used Space Correlation per experiment

	Top		45		X & Y Angle	
	Min	Max	Min	Max	Min	Max
Case 1	0.7	0.7	0.6	0.6	0.6	0.7
Case 2	0.7	0.7	0.7	0.7	0.6	0.8
Avg	0.7	0.7	0.6	0.6	0.6	0.8

Table 31: Z Exaggeration & Ratio of Used Space Min Max per experiment

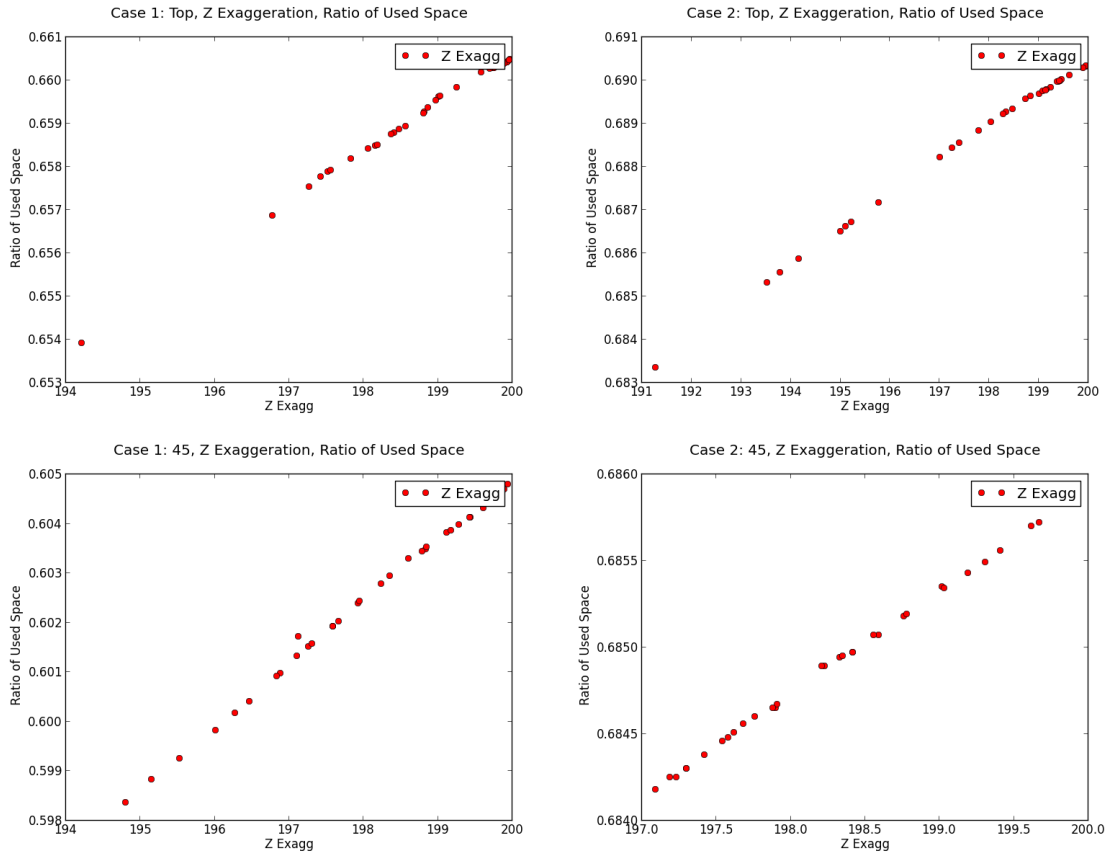


**Figure 123: Top & 45: Z Exaggeration & Ratio of Used Space**

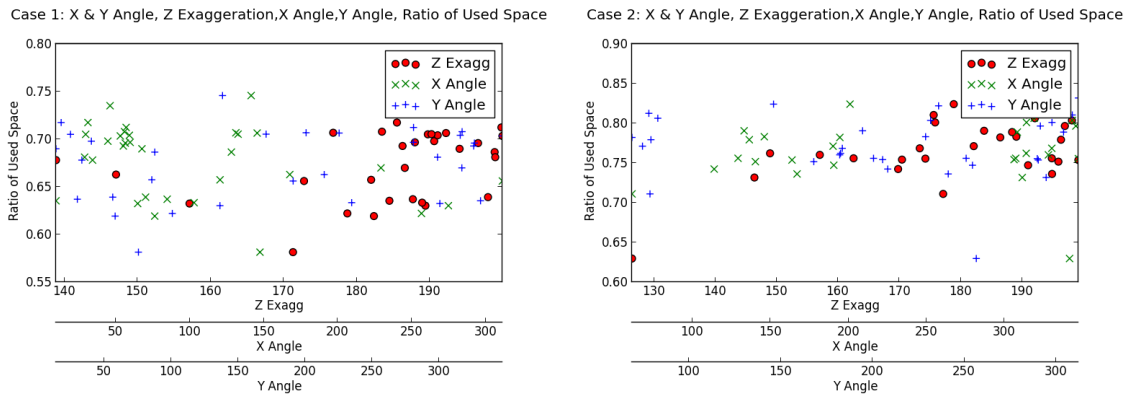


**Figure 124: X & Y Angles Z Exaggeration & Ratio of Used Space**

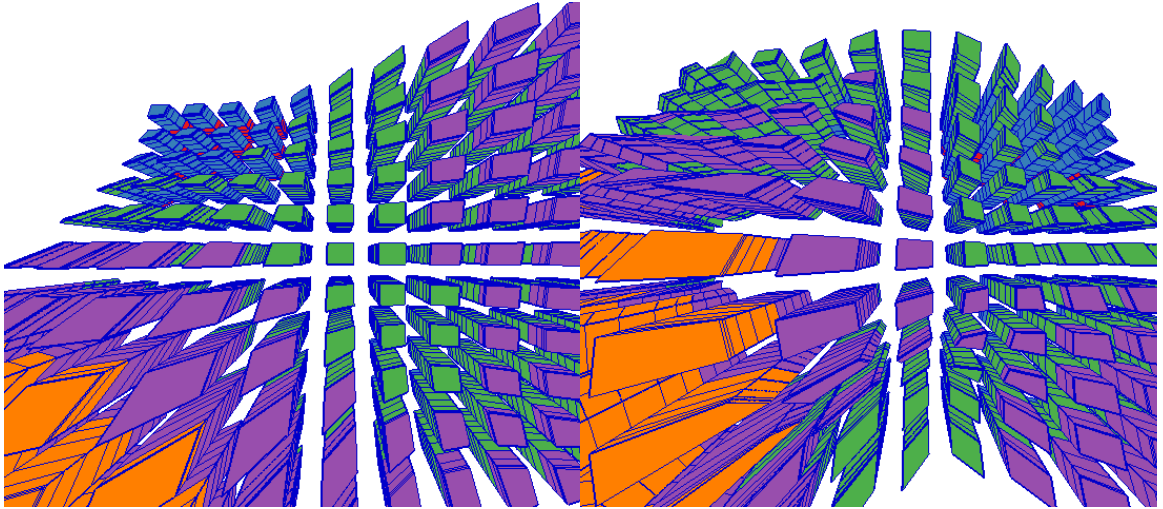


Figure 125: 3D Case 1: Top, Z Exaggeration, Ratio of Used Space

Figure 126: 3D Case 2: Top, Z Exaggeration, Ratio of Used Space

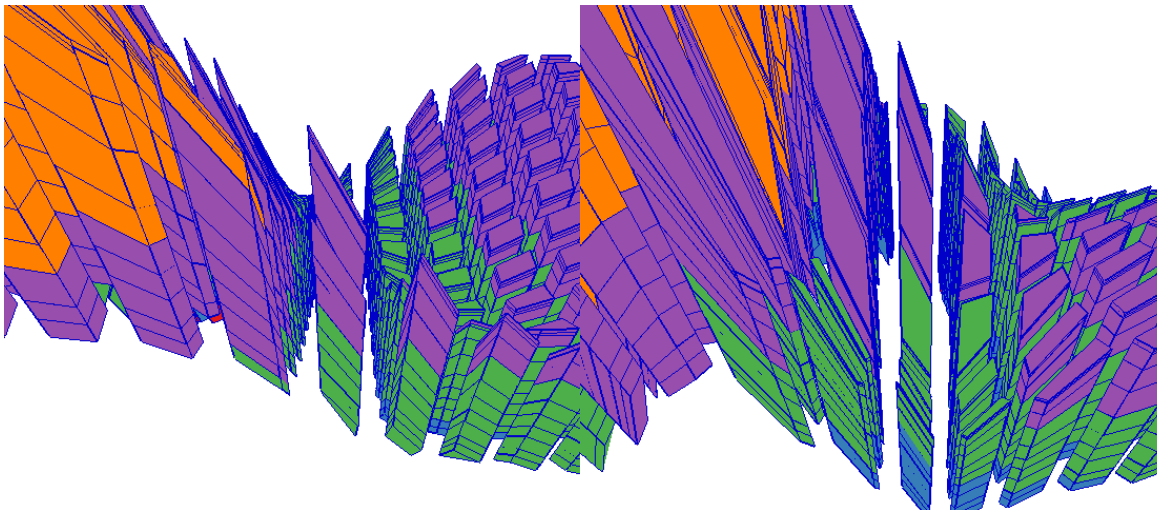


Figure 127: 3D Case 1: 45, Z Exaggeration, Ratio of Used Space

Figure 128: 3D Case 2: 45, Z Exaggeration, Ratio of Used Space

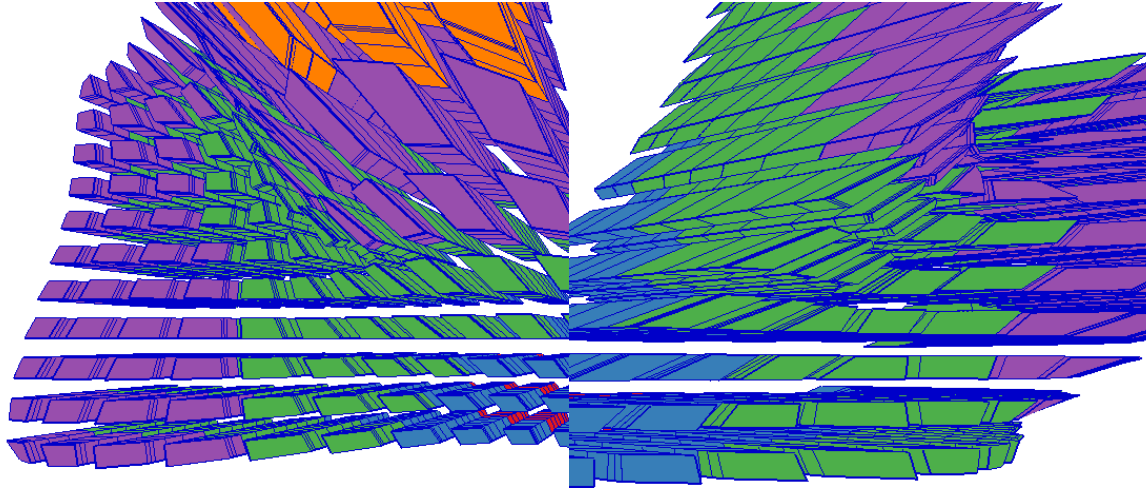


Figure 129: 3D Case 1: X & Y Angle, Z  
Exaggeration, X Angle, Y Angle, Ratio of Used Space

Figure 130: 3D Case 2: X & Y Angle, Z  
Exaggeration, X Angle, Y Angle, Ratio of Used Space

### XY Displacement & Ratio of Used Space

View	Top	45	X & Y Angle		
Input	XY Disp	XY Disp	XY Disp	X Angle	Y Angle
Case 1	0.197	0.435	0.150	0.001	0.024
Case 2	0.087	0.460	0.169	0.099	0.153
Avg	0.142	0.448	0.160	0.050	0.088

Table 32: XY Displacement & Ratio of Used Space Correlation per experiment

	Top		45		X & Y Angle	
	Min	Max	Min	Max	Min	Max
Case 1	0.4	0.4	0.4	0.4	0.3	0.5
Case 2	0.4	0.4	0.5	0.5	0.4	0.7
Avg	0.4	0.4	0.4	0.4	0.4	0.6

Table 33: XY Displacement & Ratio of Used Space Min Max per experiment

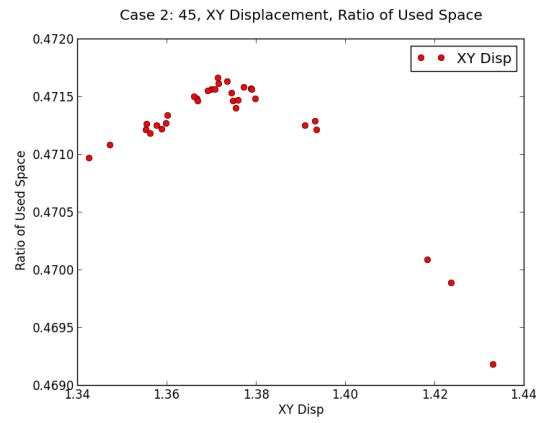
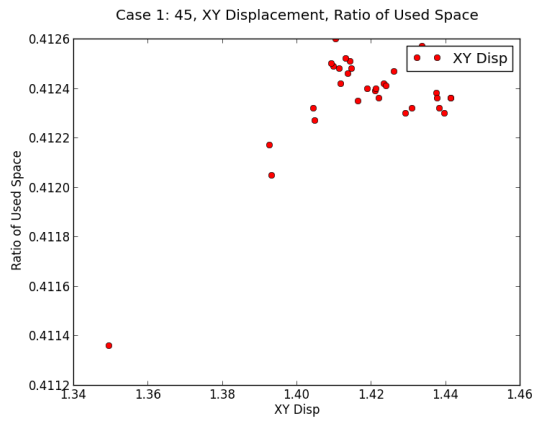
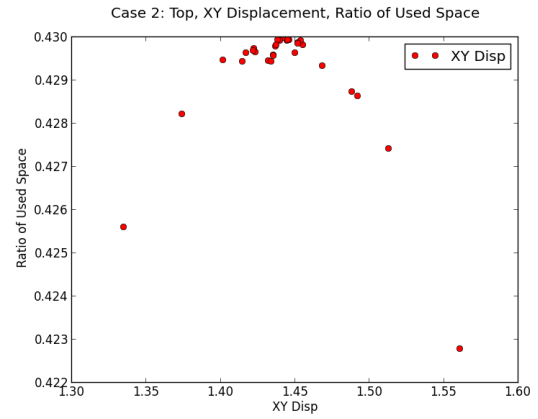
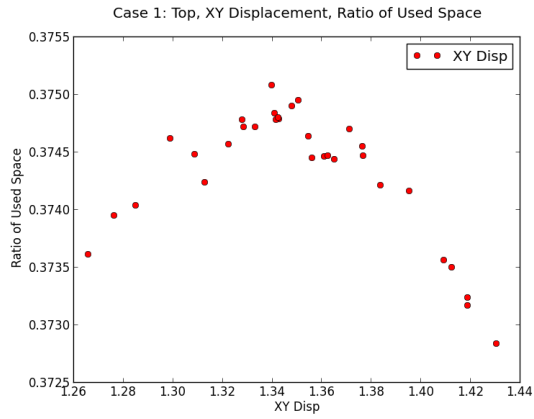


**Figure 131: Top & 45: XY Displacement & Ratio of Used Space**

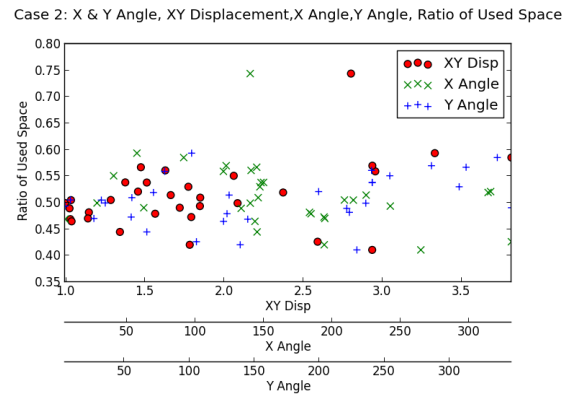
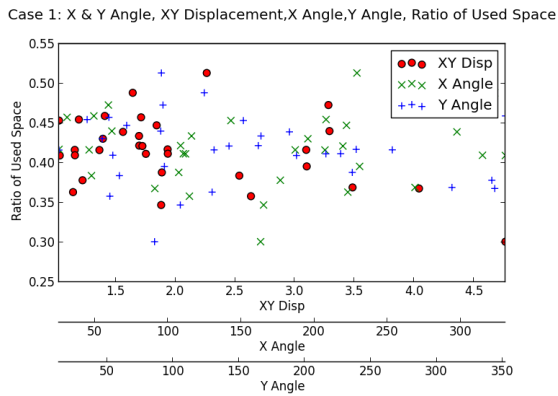


**Figure 132: X & Y Angles XY Displacement & Ratio of Used Space**

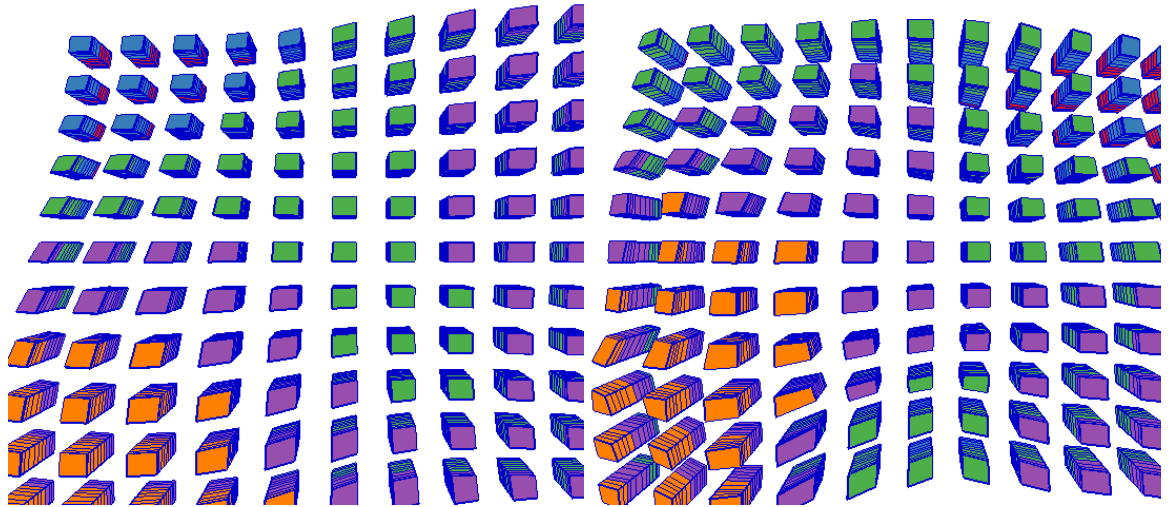


Figure 133: 3D Case 1: Top, XY Displacement, Ratio of Used Space

Figure 134: 3D Case 2: Top, XY Displacement, Ratio of Used Space

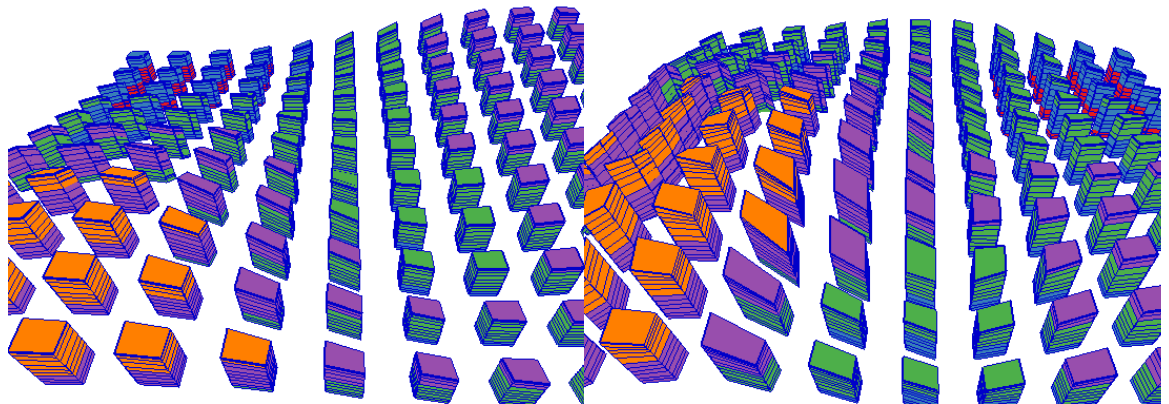


Figure 135: 3D Case 1: 45, XY Displacement, Ratio of Used Space

Figure 136: 3D Case 2: 45, XY Displacement, Ratio of Used Space

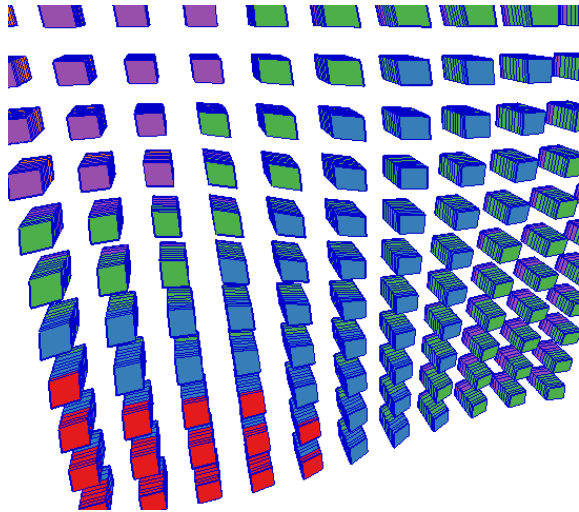


Figure 137: 3D Case 1: X & Y Angle, XY Displacement, X Angle, Y Angle, Ratio of Used Space

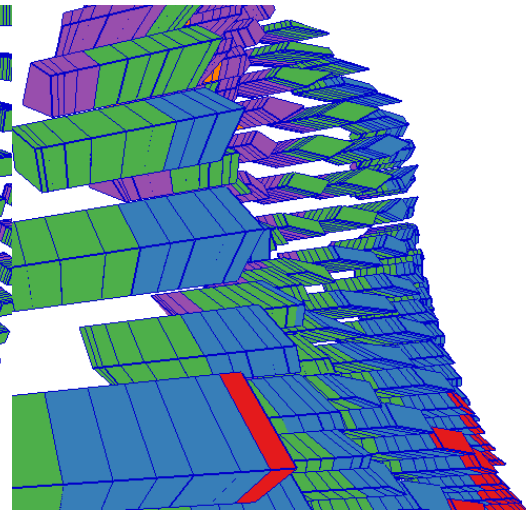


Figure 138: 3D Case 2: X & Y Angle, XY Displacement, X Angle, Y Angle, Ratio of Used Space

### XYZ Displacement & Ratio of Used Space

View	Top	45	X & Y Angle		
Input	XYZ Dis	XYZ Dis	XYZ Dis	X Angle	Y Angle
Case 1	0.028	0.168	0.004	0.002	0.072
Case 2	0.134	0.110	0.005	0.001	0.017
Avg	0.081	0.139	0.005	0.001	0.045

Table 34: XYZ Displacement & Ratio of Used Space Correlation per experiment

	Top		45		X & Y Angle	
	Min	Max	Min	Max	Min	Max
Case 1	0.4	0.4	0.5	0.5	0.4	0.7
Case 2	0.5	0.5	0.5	0.5	0.5	0.6
Avg	0.5	0.5	0.5	0.5	0.4	0.7

Table 35: XYZ Displacement & Ratio of Used Space Min Max per experiment

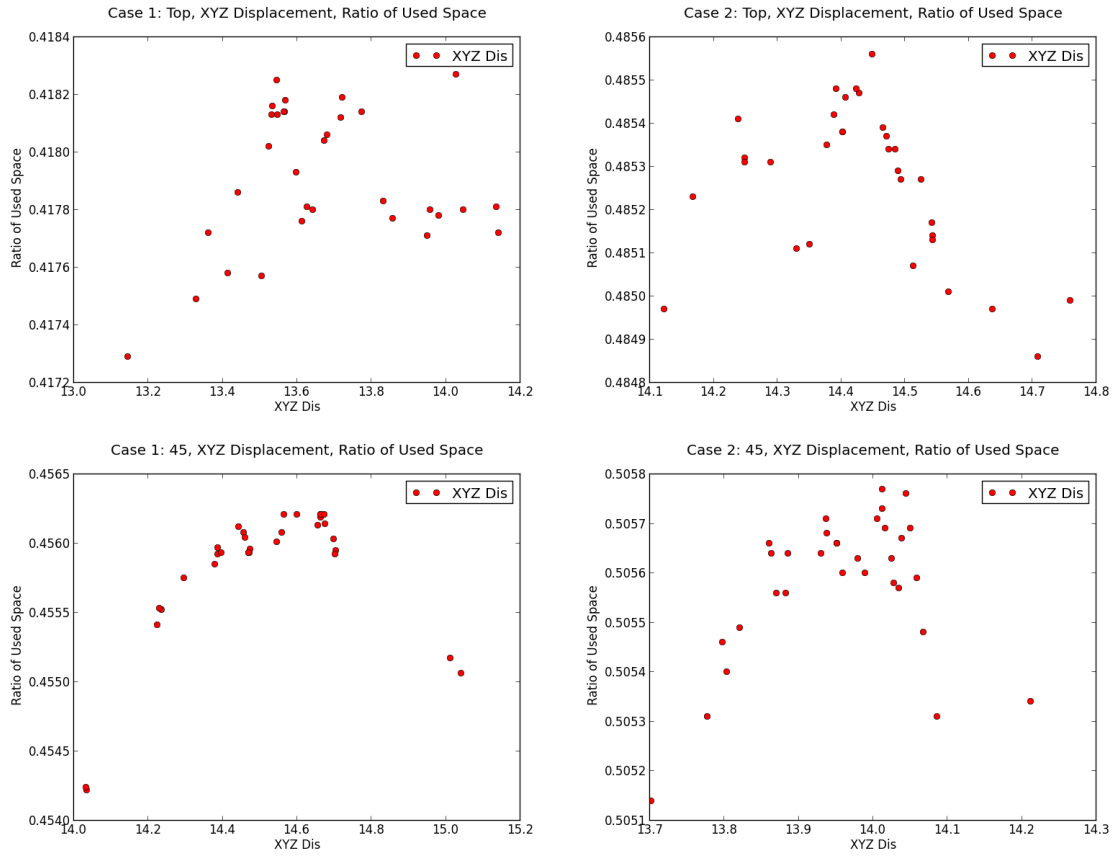


**Figure 139: Top & 45: XYZ Displacement & Ratio of Used Space**

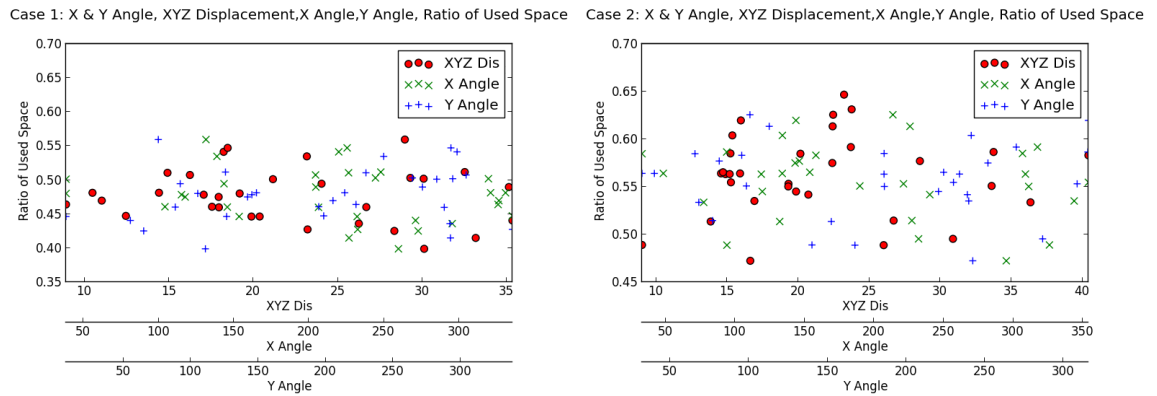


**Figure 140: X & Y Angles XYZ Displacement & Ratio of Used Space**



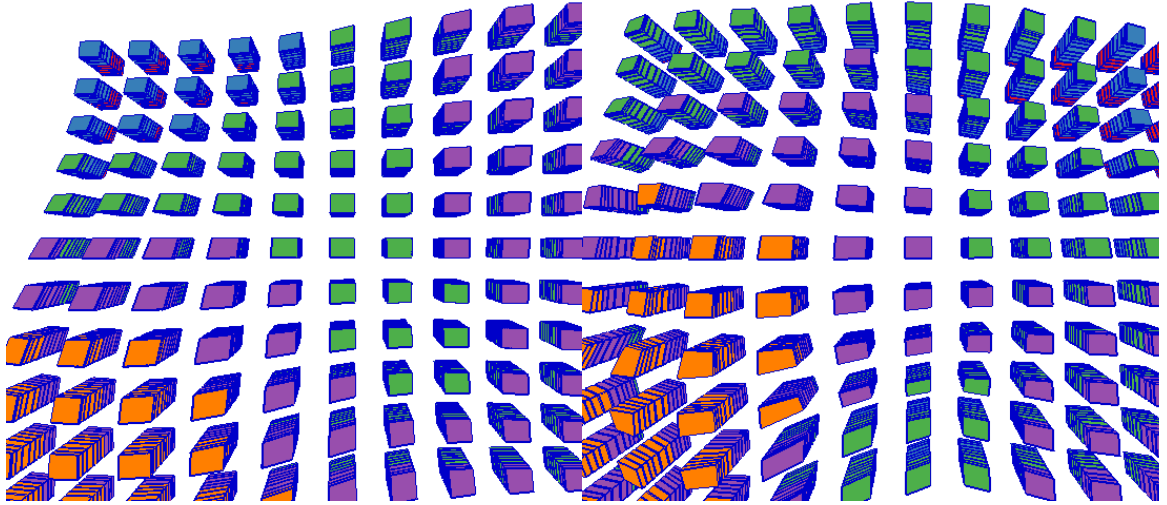


Figure 141: 3D Case 1: Top, XYZ Displacement, Ratio of Used Space

Figure 142: 3D Case 2: Top, XYZ Displacement, Ratio of Used Space

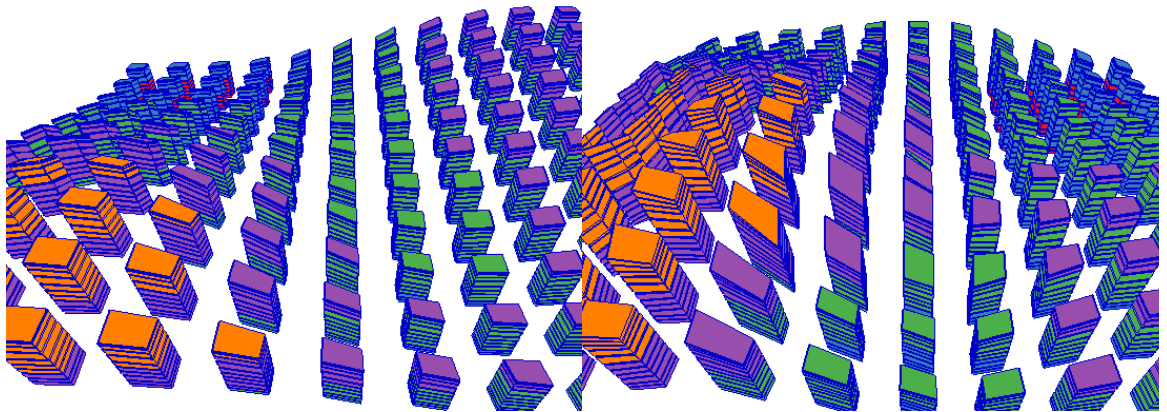


Figure 143: 3D Case 1: 45, XYZ Displacement, Ratio of Used Space

Figure 144: 3D Case 2: 45, XYZ Displacement, Ratio of Used Space

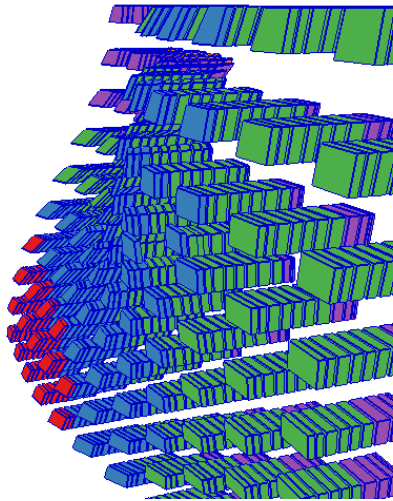


Figure 145: 3D Case 1: X & Y Angle, XYZ  
Displacement, X Angle, Y Angle, Ratio of Used Space

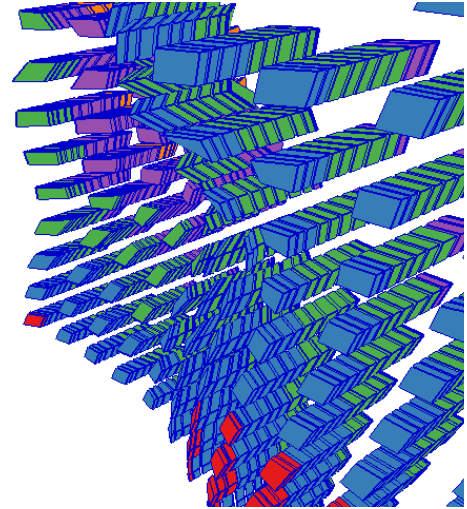


Figure 146: 3D Case 2: X & Y Angle, XYZ  
Displacement, X Angle, Y Angle, Ratio of Used Space

### The Gaussian parameter & Average Relative Change of Mean Curvature

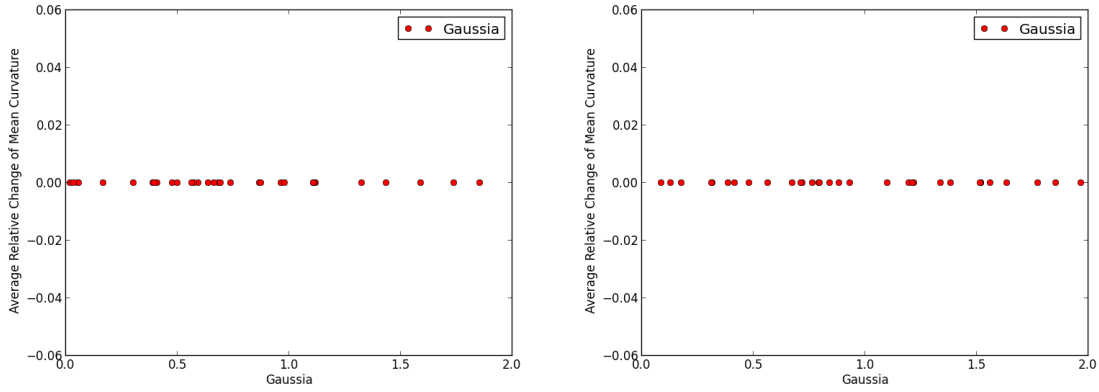
View	Top	45	X & Y Angle		
Input	Gaussian	Gaussian	Gaussian	X Angle	Y Angle
Case 1	nan	0.837	nan	nan	nan
Case 2	nan	0.870	nan	nan	nan
Avg	nan	0.853	nan	nan	nan

Table 36: The Gaussian parameter & Average Relative Change of Mean Curvature Correlation per experiment

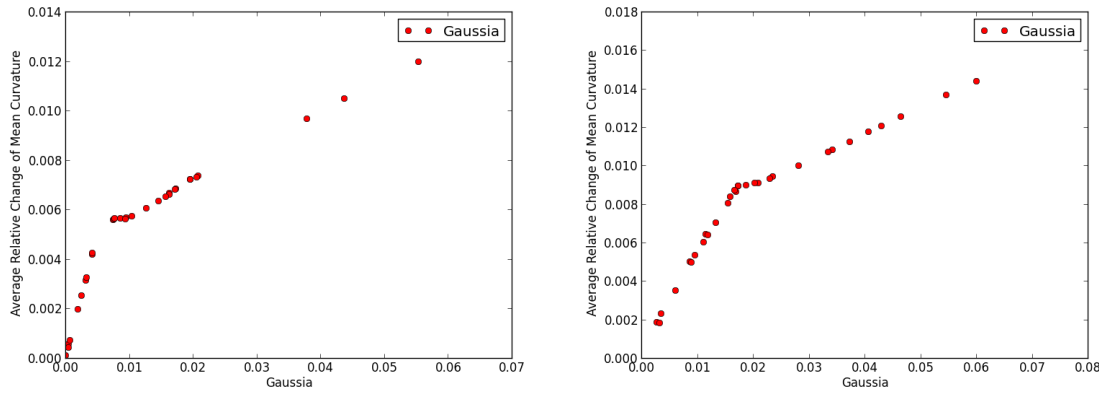
	Top		45		X & Y Angle	
	Min	Max	Min	Max	Min	Max
Case 1	0.0	0.0	0.0	0.0	0.0	0.0
Case 2	0.0	0.0	0.0	0.0	0.0	0.0
Avg	0.0	0.0	0.0	0.0	0.0	0.0

Table 37: The Gaussian parameter & Average Relative Change of Mean Curvature Min Max per experiment

Case 1: Top, The Gaussian parameter, Average Relative Change of Mean Curvature Case 2: Top, The Gaussian parameter, Average Relative Change of Mean Curvature



Case 1: 45, The Gaussian parameter, Average Relative Change of Mean Curvature Case 2: 45, The Gaussian parameter, Average Relative Change of Mean Curvature



**Figure 147: Top & 45: The Gaussian parameter & Average Relative Change of Mean Curvature**

Angle, The Gaussian parameter, X Angle, Y Angle, Average Relative Change of I Angle, The Gaussian parameter, X Angle, Y Angle, Average Relative Change of I

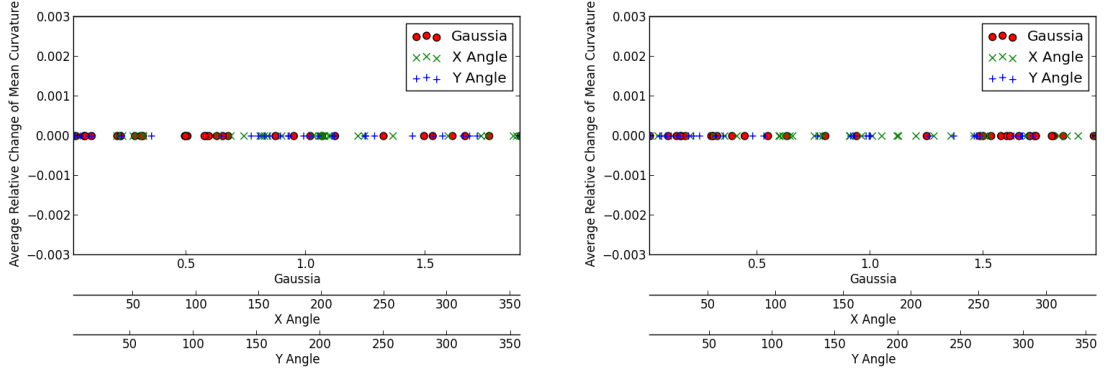


**Figure 148: X & Y Angles The Gaussian parameter & Average Relative Change of Mean Curvature**

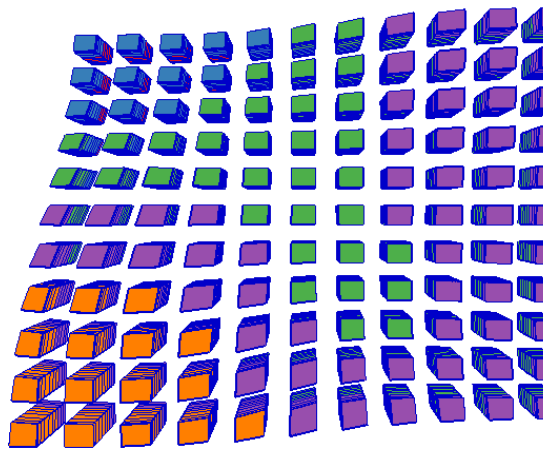


Figure 149: 3D Case 1: Top, The Gaussian parameter, Average Relative Change of Mean Curvature

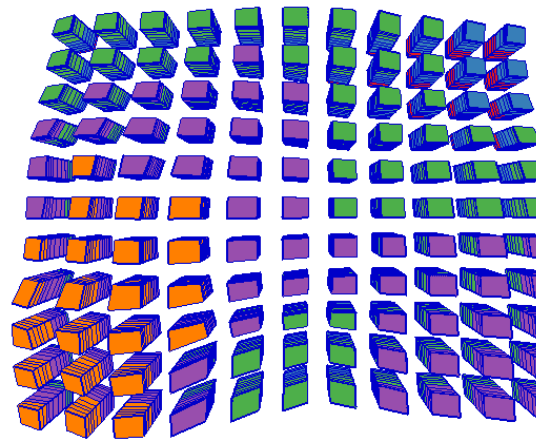


Figure 150: 3D Case 2: Top, The Gaussian parameter, Average Relative Change of Mean Curvature

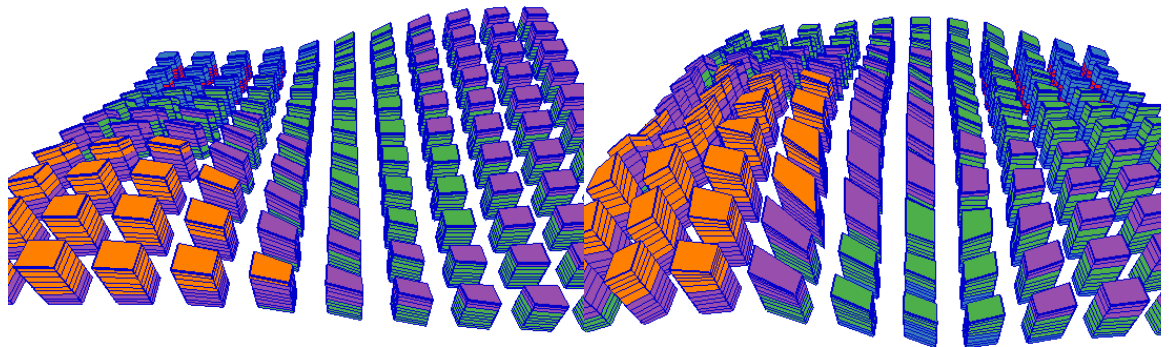


Figure 151: 3D Case 1: 45, The Gaussian parameter, Average Relative Change of Mean Curvature

Figure 152: 3D Case 2: 45, The Gaussian parameter, Average Relative Change of Mean Curvature

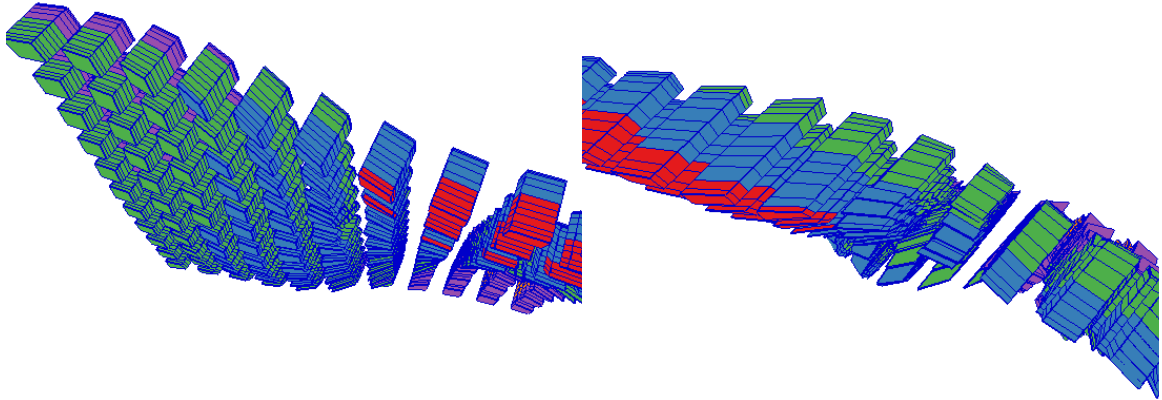


Figure 153: 3D Case 1: X & Y Angle, The Gaussian parameter, X Angle, Y Angle, Average Relative Change of Mean Curvature

Figure 154: 3D Case 2: X & Y Angle, The Gaussian parameter, X Angle, Y Angle, Average Relative Change of Mean Curvature

### Camera Distance & Average Relative Change of Mean Curvature

View	Top	45	X & Y Angle		
Input	Camera	Camera	Camera	X Angle	Y Angle
Case 1	nan	-inf	0.013	0.038	0.030
Case 2	nan	0.002	nan	nan	nan
Avg	nan	-inf	nan	nan	nan

Table 38: Camera Distance & Average Relative Change of Mean Curvature Correlation per experiment

	Top		45		X & Y Angle	
	Min	Max	Min	Max	Min	Max
Case 1	0.0	0.0	0.0	0.0	0.0	0.0
Case 2	0.0	0.0	0.0	0.0	0.0	0.0
Avg	0.0	0.0	0.0	0.0	0.0	0.0

Table 39: Camera Distance & Average Relative Change of Mean Curvature Min Max per experiment

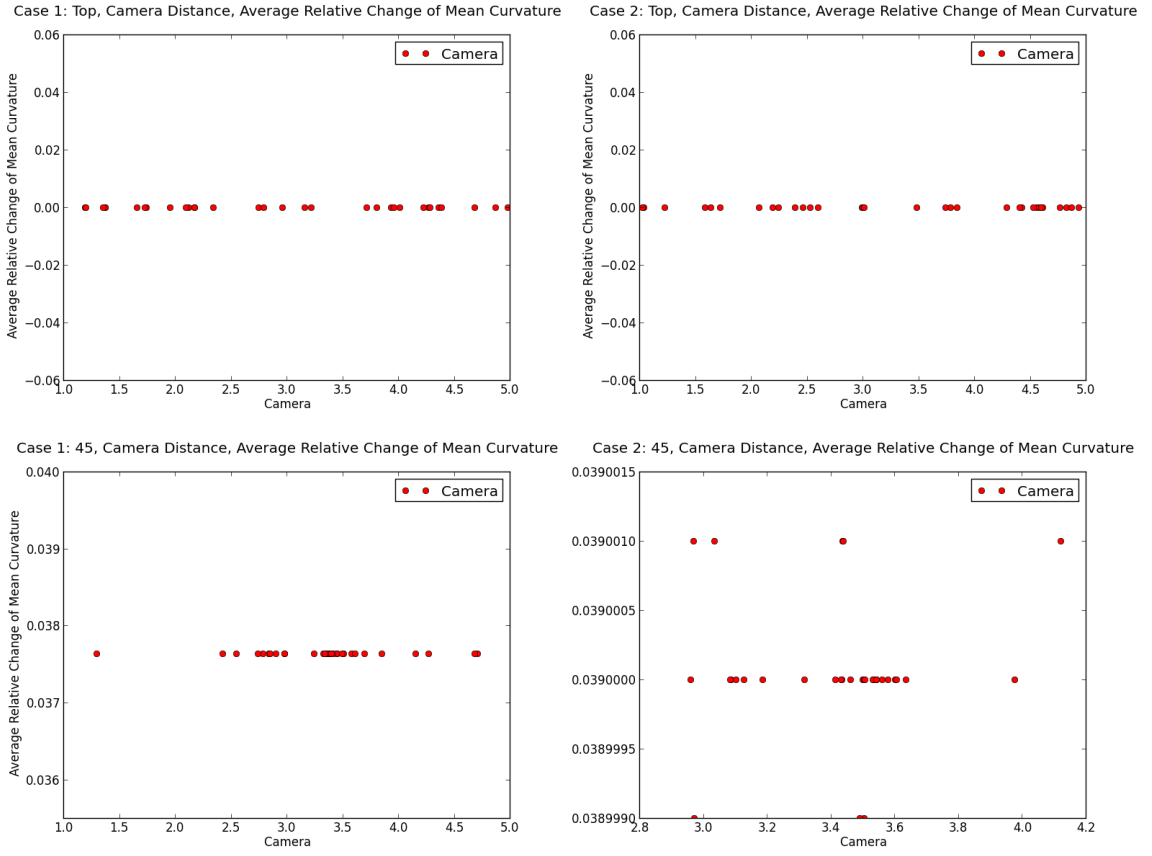


**Figure 155: Top & 45: Camera Distance & Average Relative Change of Mean Curvature**

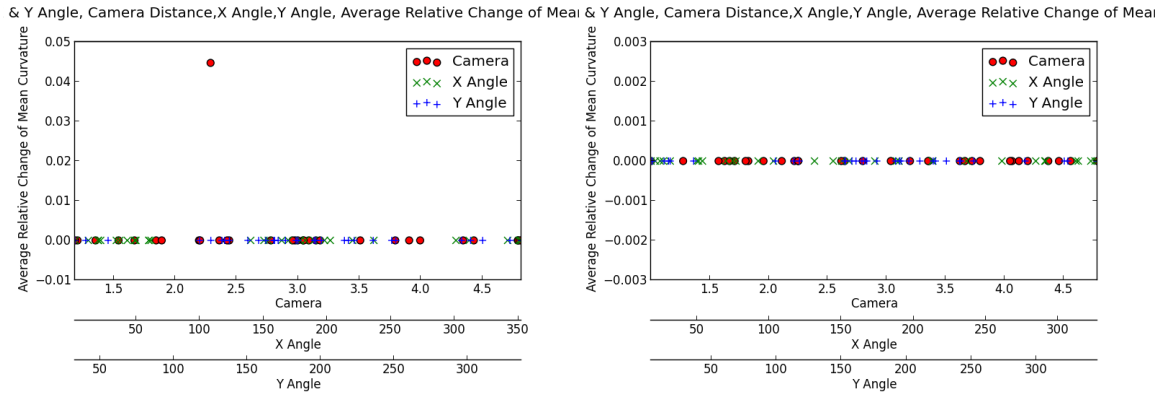


**Figure 156: X & Y Angles Camera Distance & Average Relative Change of Mean Curvature**

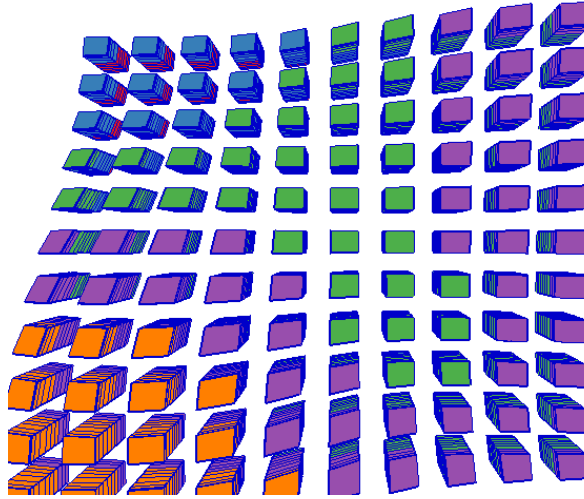


Figure 157: 3D Case 1: Top, Camera Distance, Average Relative Change of Mean Curvature

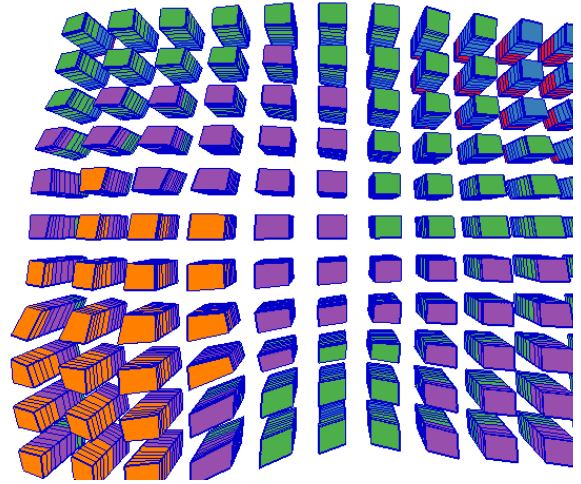


Figure 158: 3D Case 2: Top, Camera Distance, Average Relative Change of Mean Curvature

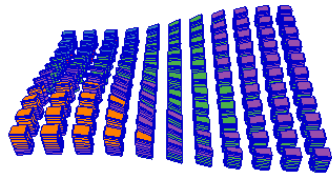


Figure 159: 3D Case 1: 45, Camera Distance, Average Relative Change of Mean Curvature

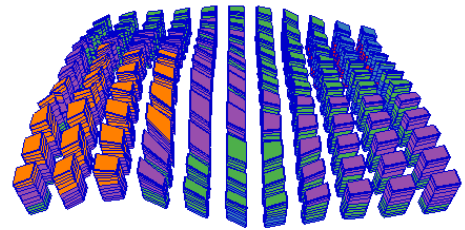


Figure 160: 3D Case 2: 45, Camera Distance, Average Relative Change of Mean Curvature

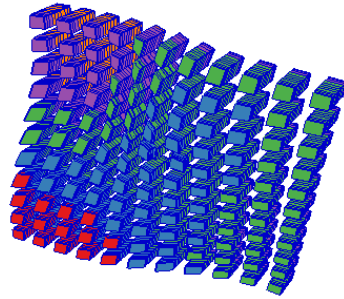


Figure 161: 3D Case 1: X & Y Angle, Camera Distance, X Angle, Y Angle, Average Relative Change of Mean Curvature

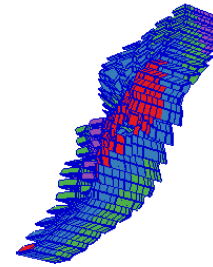


Figure 162: 3D Case 2: X & Y Angle, Camera Distance, X Angle, Y Angle, Average Relative Change of Mean Curvature

### Z Exaggeration & Average Relative Change of Mean Curvature

View	Top	45	X & Y Angle		
Input	Z Exagg	Z Exagg	Z Exagg	X Angle	Y Angle
Case 1	0.110	0.090	0.628	0.031	0.001
Case 2	0.267	0.077	0.069	0.031	0.021
Avg	0.189	0.084	0.348	0.031	0.011

Table 40: Z Exaggeration & Average Relative Change of Mean Curvature Correlation per experiment

	Top		45		X & Y Angle	
	Min	Max	Min	Max	Min	Max
Case 1	0.0	0.0	0.0	0.1	0.0	0.5
Case 2	0.0	0.1	0.0	0.1	0.0	0.3
Avg	0.0	0.1	0.0	0.1	0.0	0.4

Table 41: Z Exaggeration & Average Relative Change of Mean Curvature Min Max per experiment



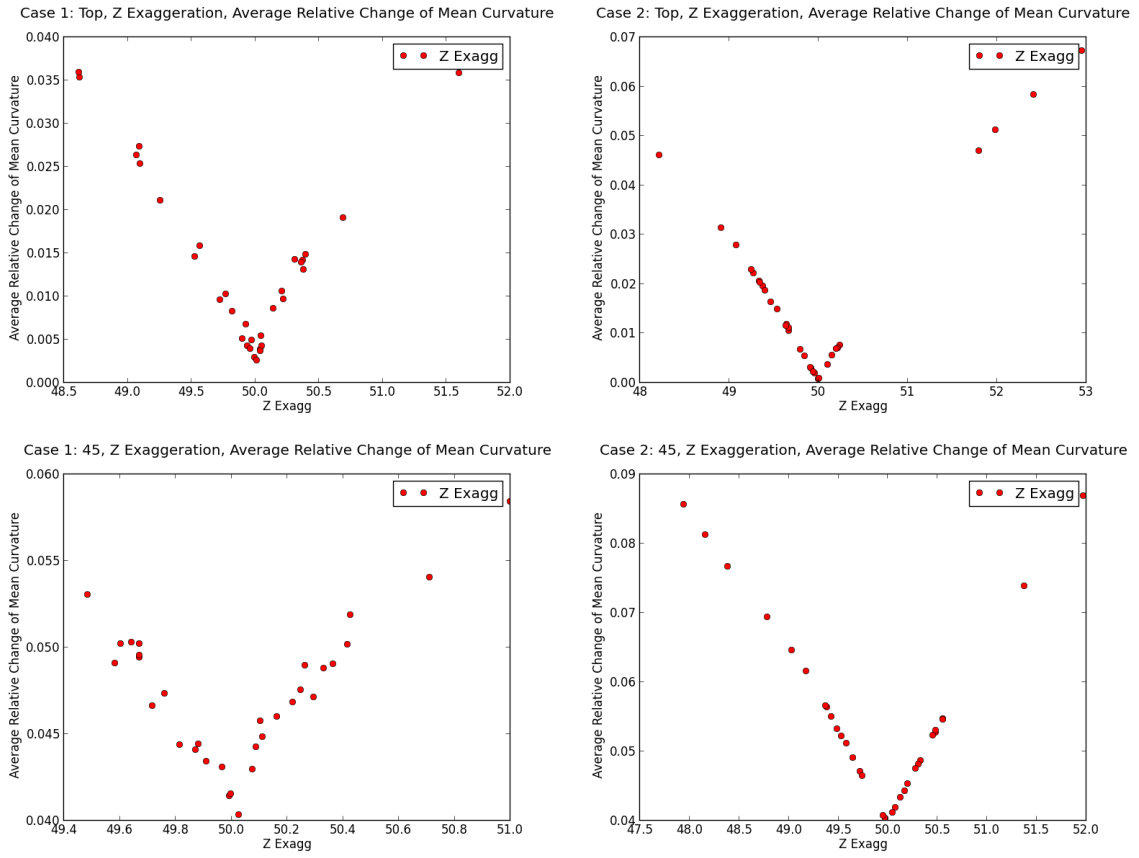


Figure 163: Top & 45: Z Exaggeration & Average Relative Change of Mean Curvature

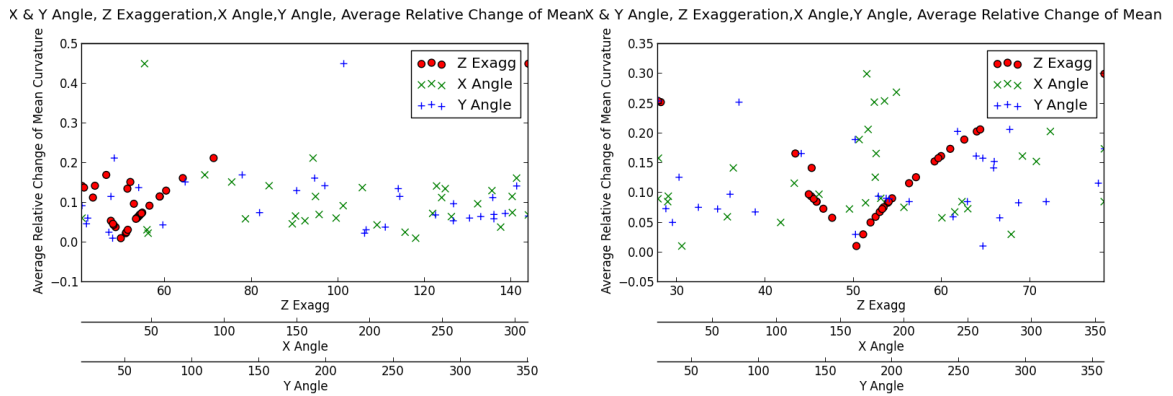


Figure 164: X & Y Angles Z Exaggeration & Average Relative Change of Mean Curvature

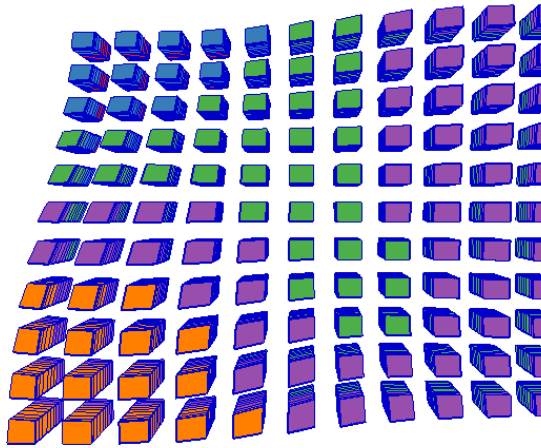


Figure 165: 3D Case 1: Top, Z Exaggeration, Average Relative Change of Mean Curvature

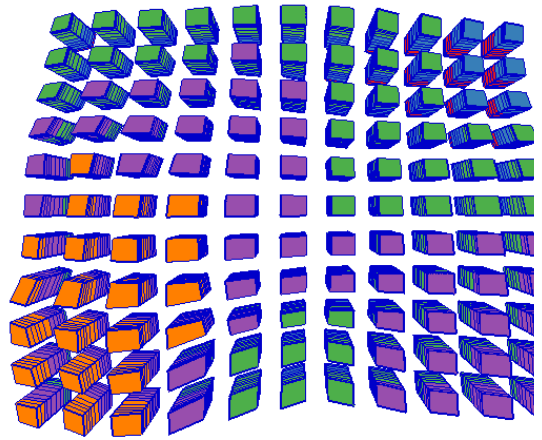


Figure 166: 3D Case 2: Top, Z Exaggeration, Average Relative Change of Mean Curvature

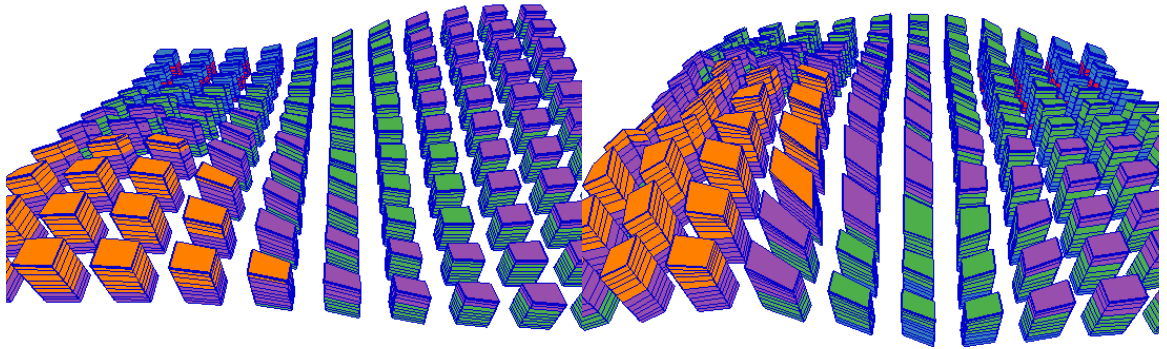
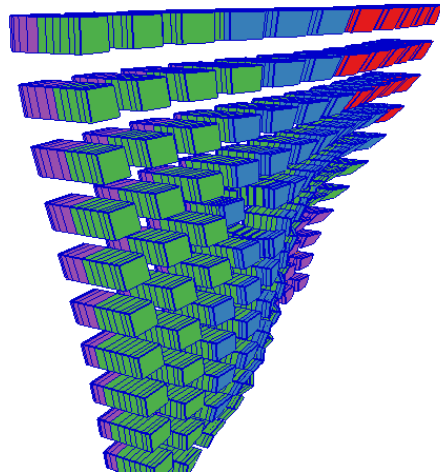
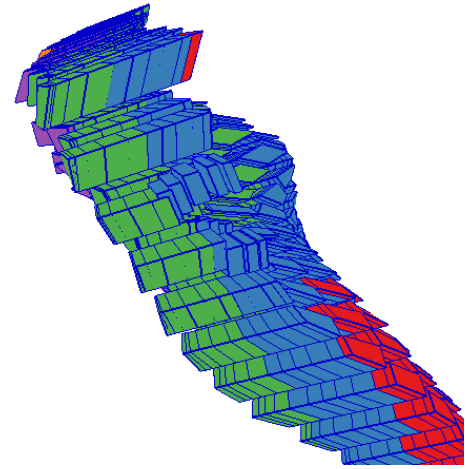


Figure 167: 3D Case 1: 45, Z Exaggeration, Average Relative Change of Mean Curvature

Figure 168: 3D Case 2: 45, Z Exaggeration, Average Relative Change of Mean Curvature



**Figure 169: 3D Case 1: X & Y Angle, Z Exaggeration, X Angle, Y Angle, Average Relative Change of Mean Curvature**



**Figure 170: 3D Case 2: X & Y Angle, Z Exaggeration, X Angle, Y Angle, Average Relative Change of Mean Curvature**

### XY Displacement & Average Relative Change of Mean Curvature

View	Top	45	X & Y Angle		
Input	XY Disp	XY Disp	XY Disp	X Angle	Y Angle
Case 1	0.009	0.059	0.017	0.005	0.041
Case 2	0.000	0.075	0.020	0.014	0.005
Avg	0.005	0.067	0.018	0.009	0.023

**Table 42: XY Displacement & Average Relative Change of Mean Curvature Correlation per experiment**

	Top		45		X & Y Angle	
	Min	Max	Min	Max	Min	Max
Case 1	0.0	0.1	0.0	0.1	0.0	0.5
Case 2	0.0	0.0	0.0	0.1	0.0	0.3
Avg	0.0	0.1	0.0	0.1	0.0	0.4

**Table 43: XY Displacement & Average Relative Change of Mean Curvature Min Max per experiment**

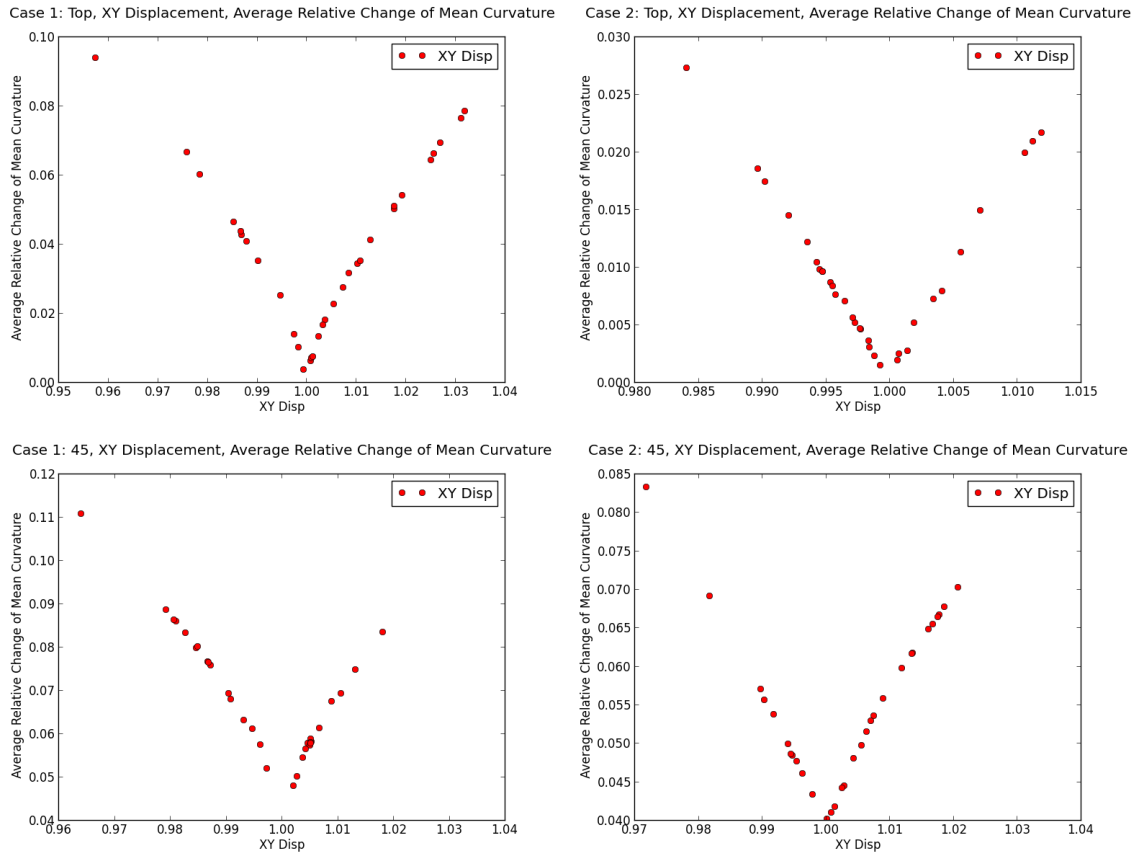


**Figure 171: Top & 45: XY Displacement & Average Relative Change of Mean Curvature**

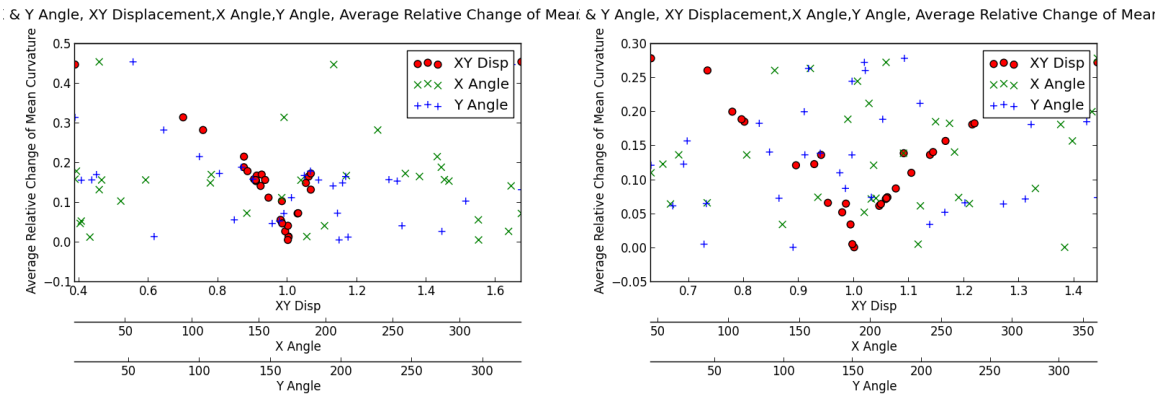


**Figure 172: X & Y Angles XY Displacement & Average Relative Change of Mean Curvature**

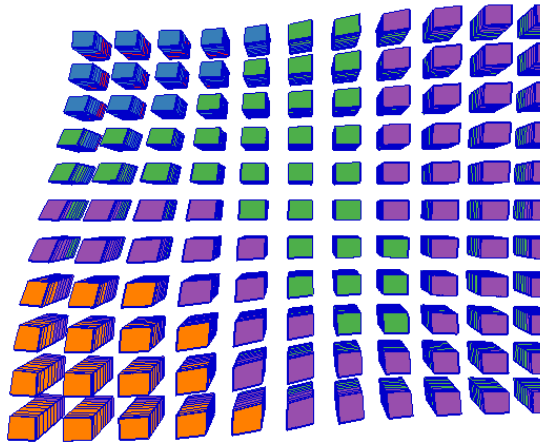


**Figure 173: 3D Case 1: Top, XY Displacement, Average Relative Change of Mean Curvature**

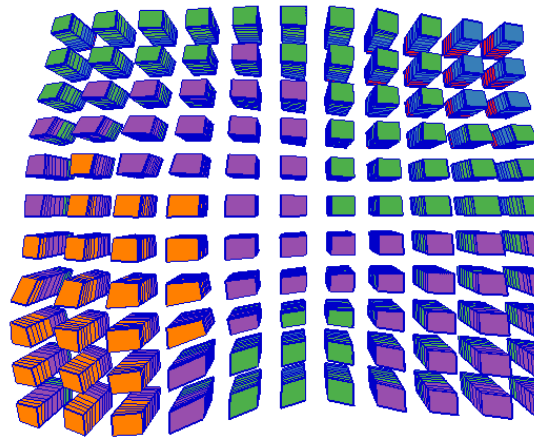


**Figure 174: 3D Case 2: Top, XY Displacement, Average Relative Change of Mean Curvature**

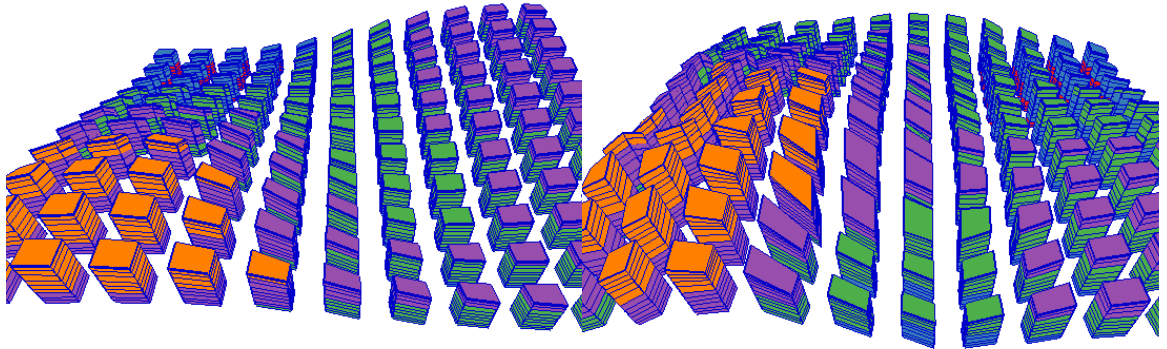


**Figure 175: 3D Case 1: 45, XY Displacement, Average Relative Change of Mean Curvature**

**Figure 176: 3D Case 2: 45, XY Displacement, Average Relative Change of Mean Curvature**

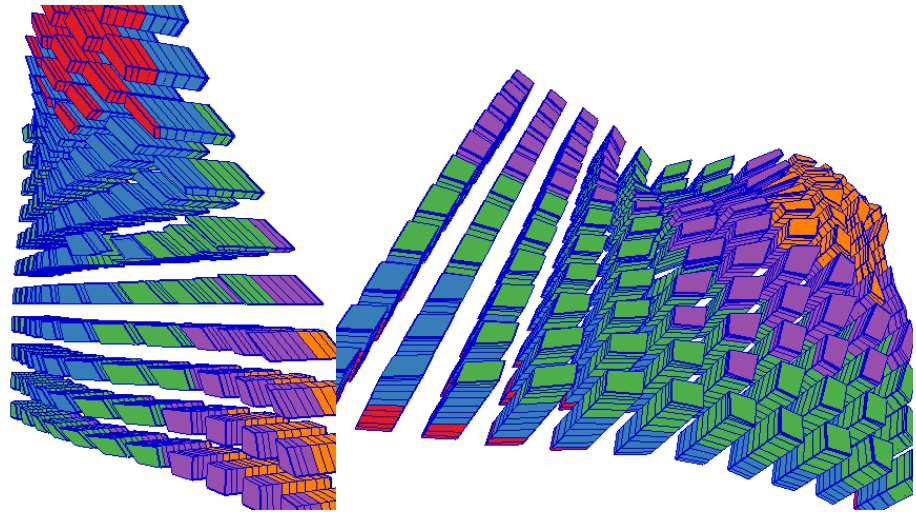


**Figure 177: 3D Case 1: X & Y Angle, XY Displacement, X Angle, Y Angle, Average Relative Change of Mean Curvature**

**Figure 178: 3D Case 2: X & Y Angle, XY Displacement, X Angle, Y Angle, Average Relative Change of Mean Curvature**

### XYZ Displacement & Average Relative Change of Mean Curvature

View	Top	45	X & Y Angle		
Input	XYZ Dis	XYZ Dis	XYZ Dis	X Angle	Y Angle
Case 1	0.221	0.068	0.000	0.009	0.003
Case 2	0.399	0.018	0.516	0.004	0.001
Avg	0.310	0.043	0.258	0.006	0.002

**Table 44: XYZ Displacement & Average Relative Change of Mean Curvature Correlation per experiment**

	Top		45		X & Y Angle	
	Min	Max	Min	Max	Min	Max
Case 1	0.4	0.4	0.4	0.4	0.4	0.5
Case 2	0.3	0.3	0.3	0.3	0.3	0.5
Avg	0.3	0.4	0.4	0.4	0.3	0.5

**Table 45: XYZ Displacement & Average Relative Change of Mean Curvature Min Max per experiment**

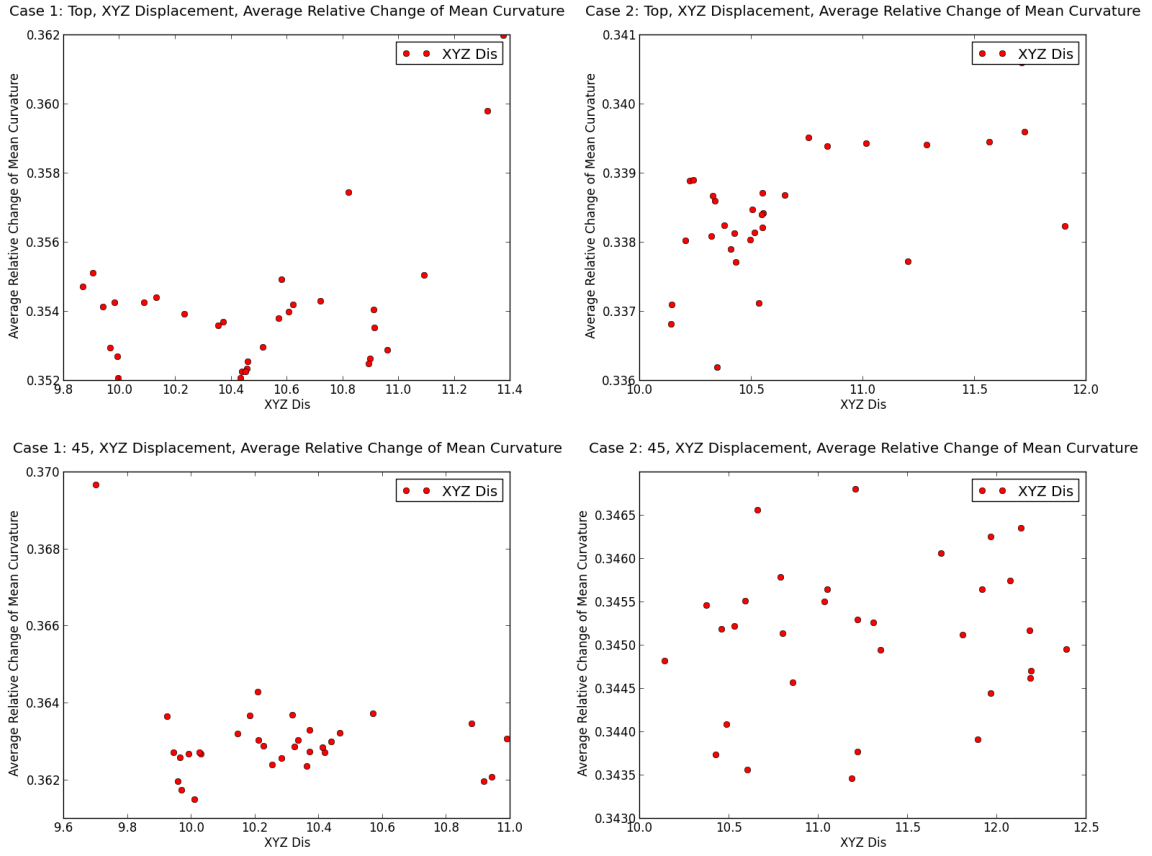


**Figure 179: Top & 45: XYZ Displacement & Average Relative Change of Mean Curvature**

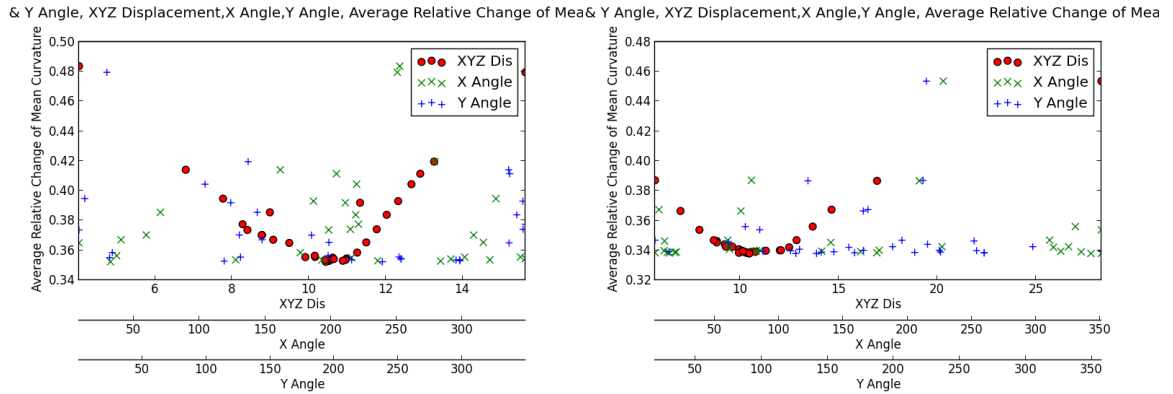


**Figure 180: X & Y Angles XYZ Displacement & Average Relative Change of Mean Curvature**

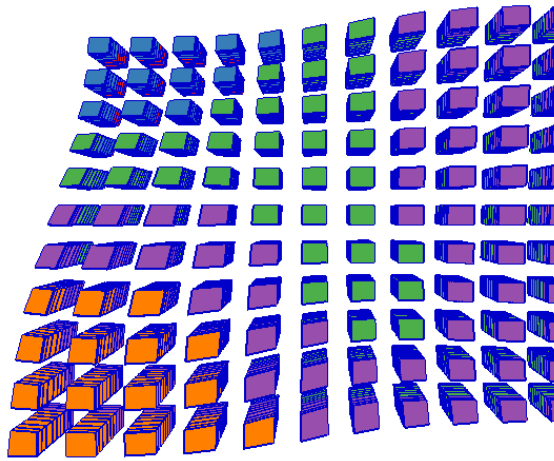


Figure 181: 3D Case 1: Top, XYZ Displacement, Average Relative Change of Mean Curvature

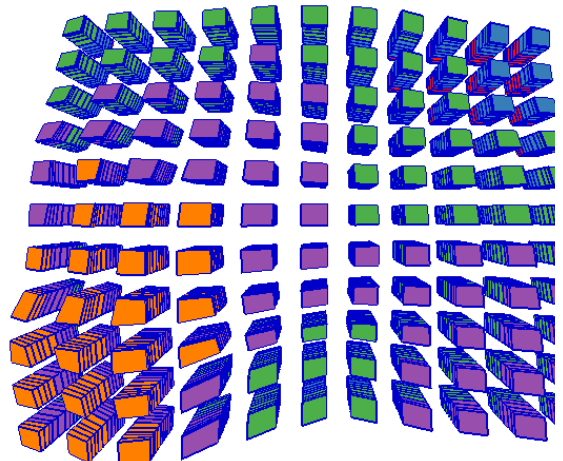


Figure 182: 3D Case 2: Top, XYZ Displacement, Average Relative Change of Mean Curvature

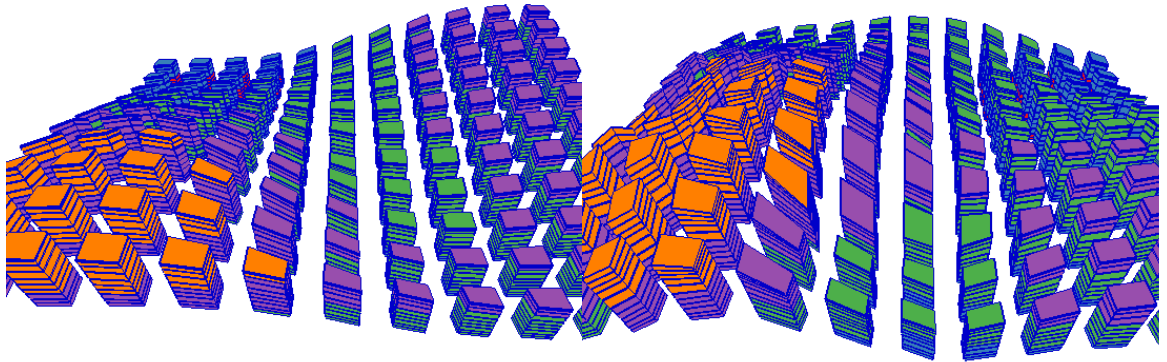


Figure 183: 3D Case 1: 45, XYZ Displacement, Average Relative Change of Mean Curvature

Figure 184: 3D Case 2: 45, XYZ Displacement, Average Relative Change of Mean Curvature



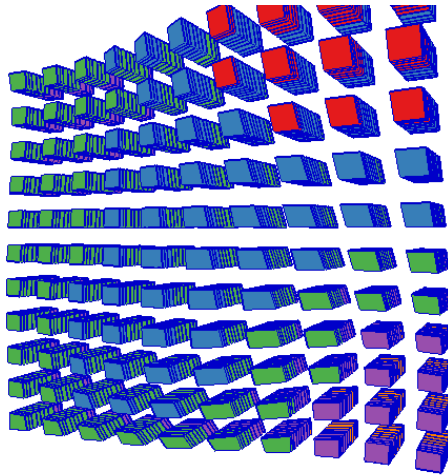


Figure 185: 3D Case 1: X & Y Angle, XYZ Displacement, X Angle, Y Angle, Average Relative Change of Mean Curvature



Figure 186: 3D Case 2: X & Y Angle, XYZ Displacement, X Angle, Y Angle, Average Relative Change of Mean Curvature

### The Gaussian parameter & Combined Ratio of Used Space & Average Relative Change of Mean Curvature

View	Top	45	X & Y Angle		
Input	Gaussian	Gaussian	Gaussian	X Angle	Y Angle
Case 1	-inf	0.962	0.001	0.173	0.000
Case 2	-inf	0.914	0.056	0.047	0.058
Avg	-inf	0.938	0.029	0.110	0.029

Table 46: The Gaussian parameter & Combined Ratio of Used Space & Average Relative Change of Mean Curvature Correlation per experiment

	Top		45		X & Y Angle	
	Min	Max	Min	Max	Min	Max
Case 1	0.2	0.2	0.3	0.3	0.3	0.3
Case 2	0.3	0.3	0.3	0.3	0.3	0.4
Avg	0.3	0.3	0.3	0.3	0.3	0.4

**Table 47: The Gaussian parameter & Combined Ratio of Used Space & Average Relative Change of Mean Curvature Min Max per experiment**

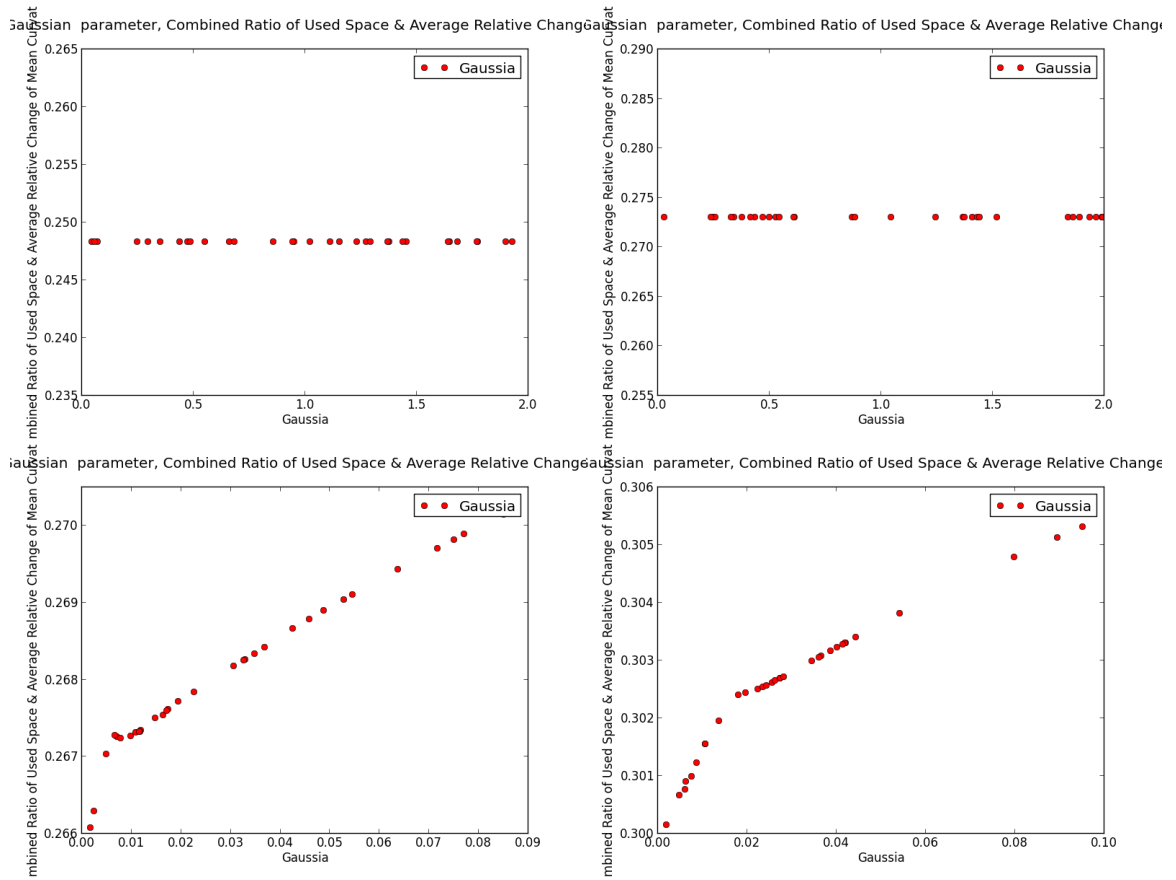


**Figure 187: Top & 45: The Gaussian parameter & Combined Ratio of Used Space & Average Relative Change of Mean Curvature**

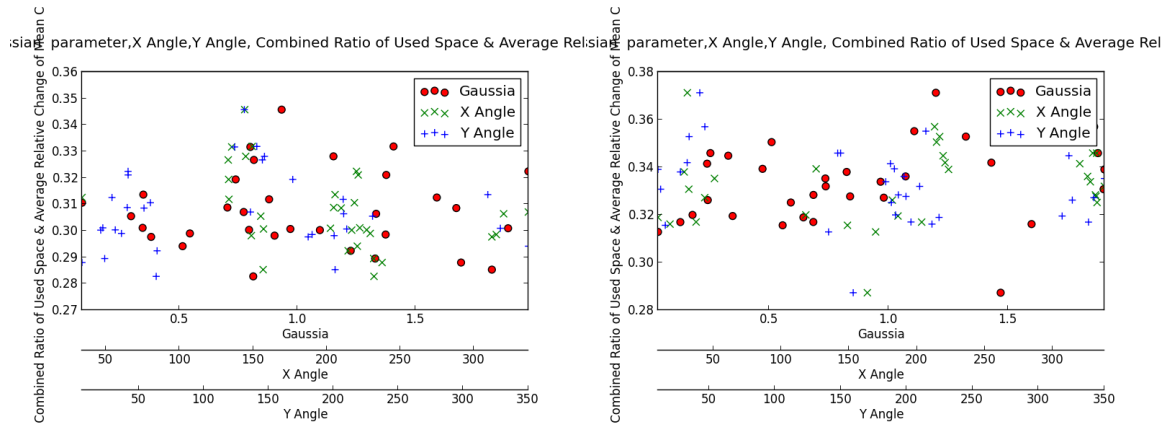


**Figure 188: X & Y Angles The Gaussian parameter & Combined Ratio of Used Space & Average Relative Change of Mean Curvature**

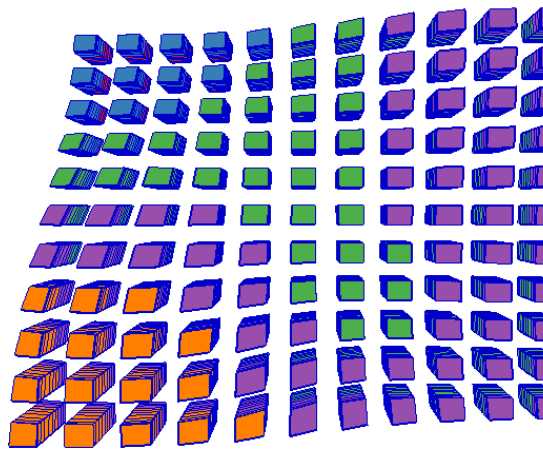


**Figure 189: 3D Case 1: Top, The Gaussian parameter, Combined Ratio of Used Space & Average Relative Change of Mean Curvature**

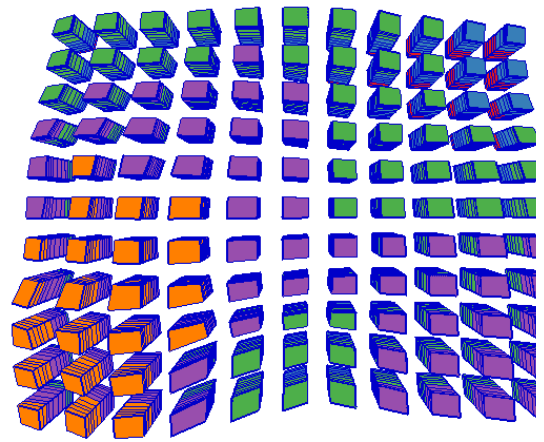


**Figure 190: 3D Case 2: Top, The Gaussian parameter, Combined Ratio of Used Space & Average Relative Change of Mean Curvature**

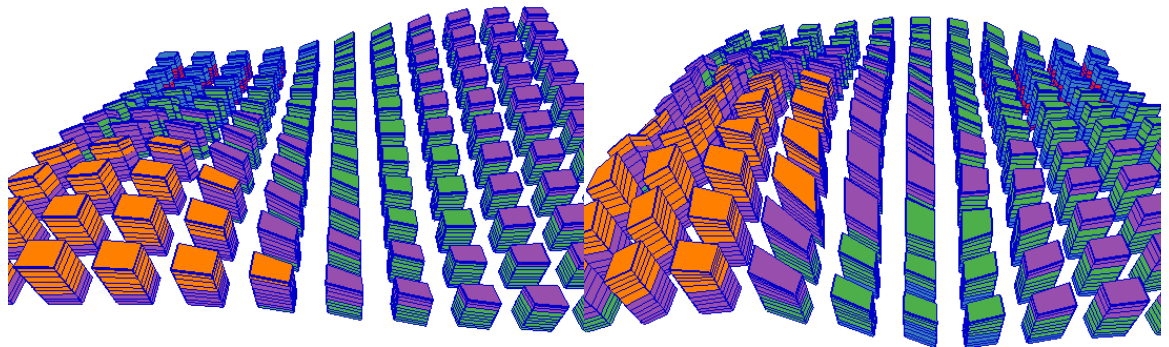


**Figure 191: 3D Case 1: 45, The Gaussian parameter, Combined Ratio of Used Space & Average Relative Change of Mean Curvature**

**Figure 192: 3D Case 2: 45, The Gaussian parameter, Combined Ratio of Used Space & Average Relative Change of Mean Curvature**

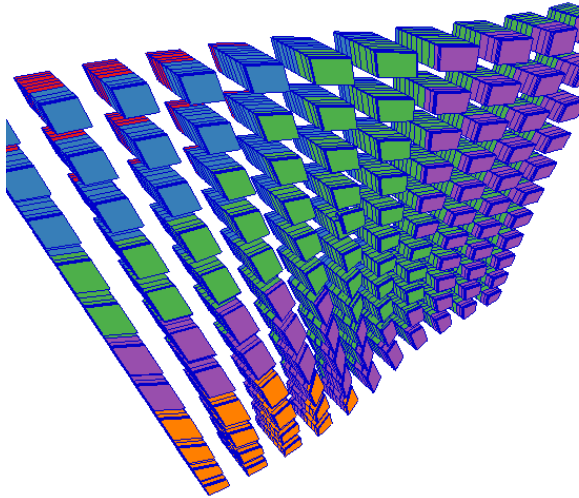


**Figure 193: 3D Case 1: X & Y Angle, The Gaussian parameter, X Angle, Y Angle, Combined Ratio of Used Space & Average Relative Change of Mean Curvature**

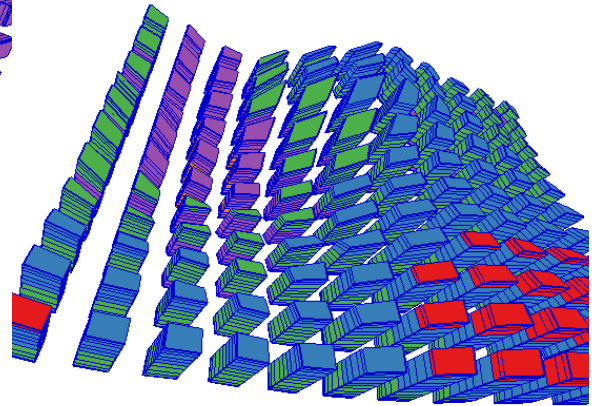


**Figure 194: 3D Case 2: X & Y Angle, The Gaussian parameter, X Angle, Y Angle, Combined Ratio of Used Space & Average Relative Change of Mean Curvature**

### Camera Distance & Combined Ratio of Used Space & Average Relative Change of Mean Curvature

View	Top	45	X & Y Angle		
Input	Camera	Camera	Camera	X Angle	Y Angle
Case 1	0.078	0.976	0.369	0.187	0.070
Case 2	0.240	0.967	0.653	0.004	0.006
Avg	0.159	0.971	0.511	0.096	0.038

**Table 48: Camera Distance & Combined Ratio of Used Space & Average Relative Change of Mean Curvature Correlation per experiment**

	Top		45		X & Y Angle	
	Min	Max	Min	Max	Min	Max
Case 1	0.4	0.4	0.5	0.5	0.4	0.6
Case 2	0.5	0.5	0.5	0.5	0.2	0.7
Avg	0.4	0.4	0.5	0.5	0.3	0.7

**Table 49: Camera Distance & Combined Ratio of Used Space & Average Relative Change of Mean Curvature Min Max per experiment**

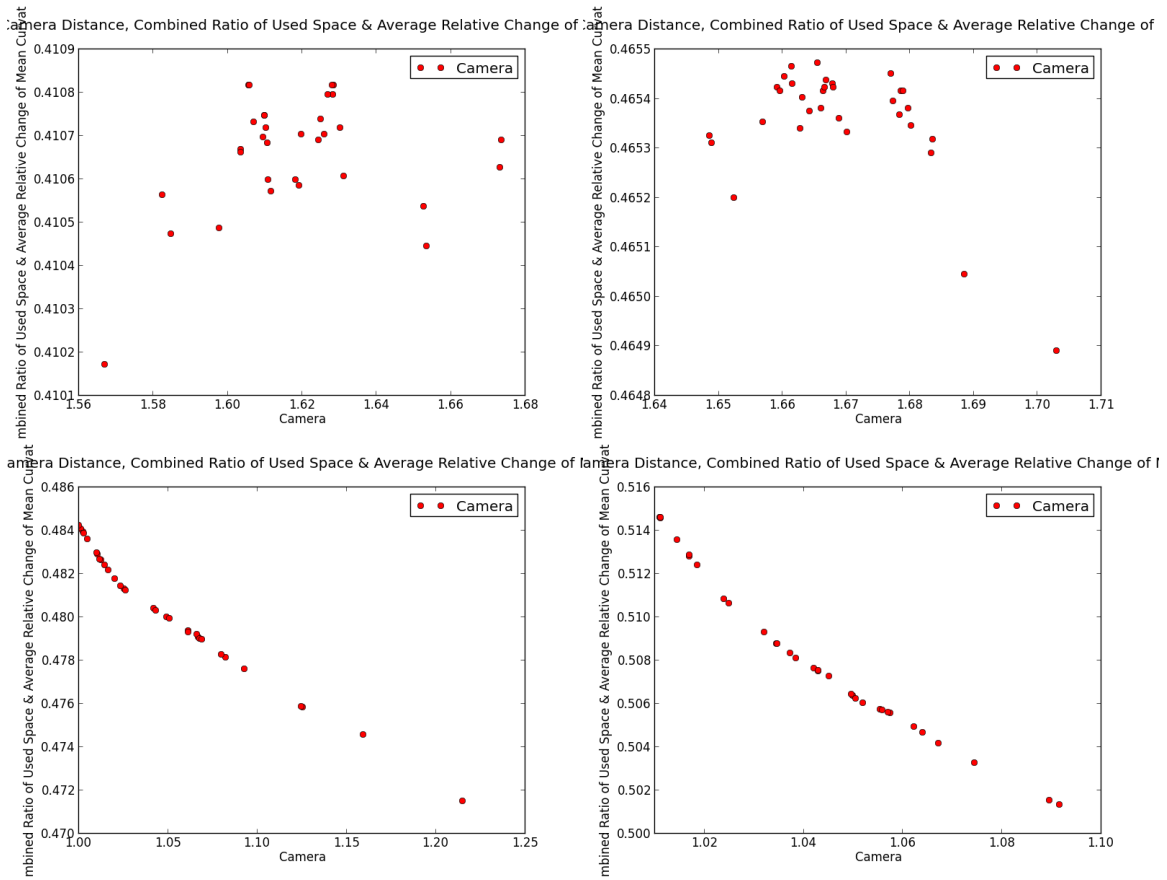


**Figure 195: Top & 45: Camera Distance & Combined Ratio of Used Space & Average Relative Change of Mean Curvature**

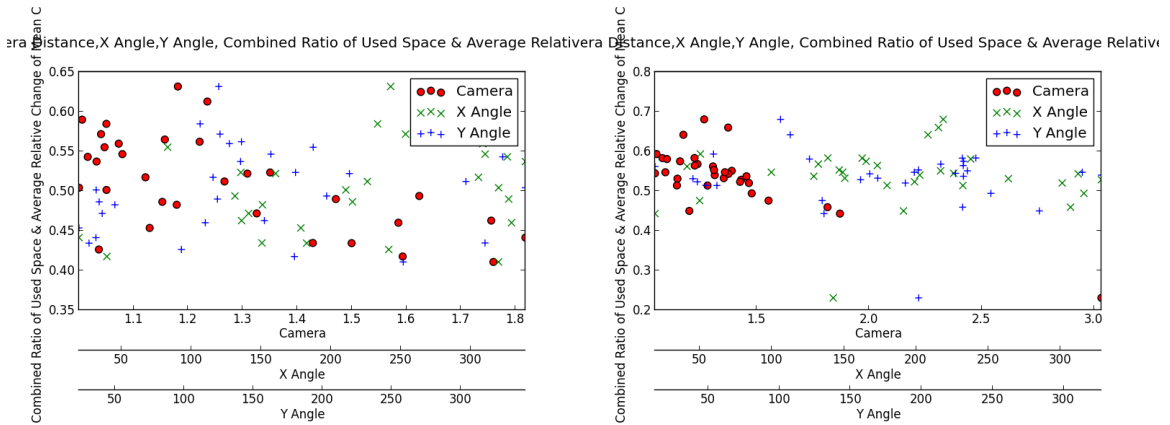


**Figure 196: X & Y Angles Camera Distance & Combined Ratio of Used Space & Average Relative Change of Mean Curvature**

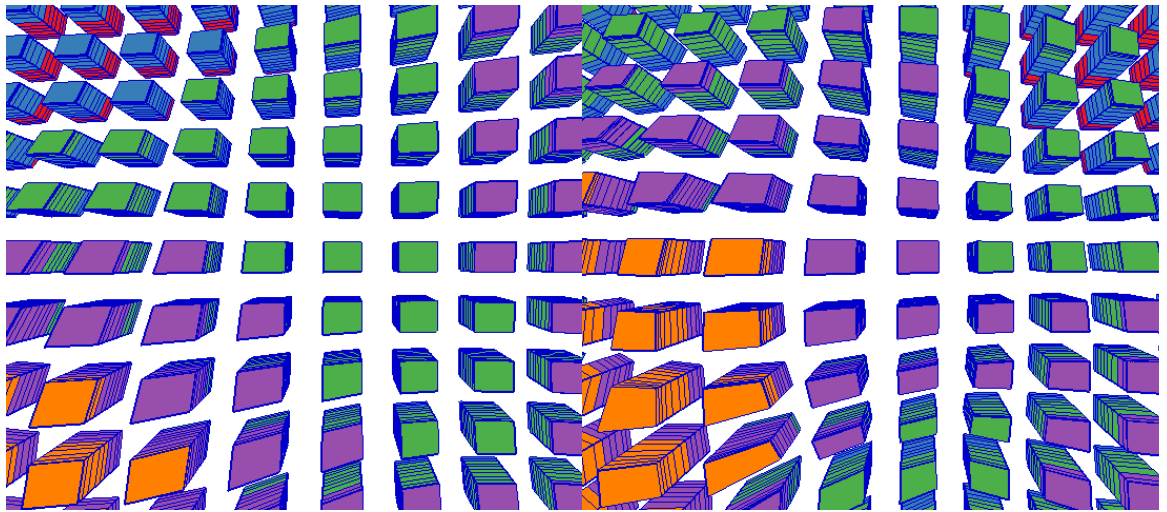


**Figure 197: 3D Case 1: Top, Camera Distance,  
Combined Ratio of Used Space & Average Relative  
Change of Mean Curvature**

**Figure 198: 3D Case 2: Top, Camera Distance,  
Combined Ratio of Used Space & Average Relative  
Change of Mean Curvature**

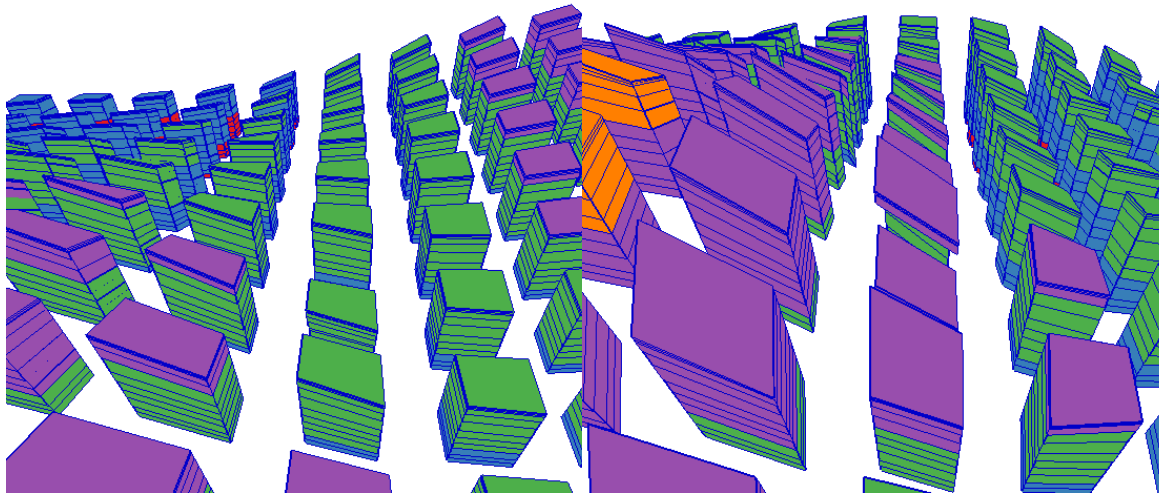


**Figure 199: 3D Case 1: 45, Camera Distance,  
Combined Ratio of Used Space & Average Relative  
Change of Mean Curvature**

**Figure 200: 3D Case 2: 45, Camera Distance,  
Combined Ratio of Used Space & Average Relative  
Change of Mean Curvature**

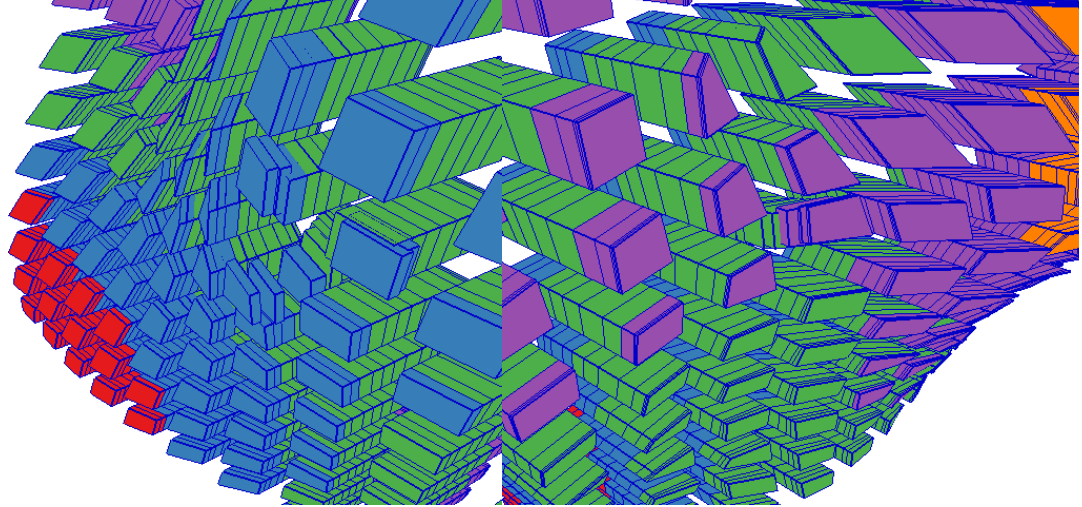


Figure 201: 3D Case 1: X & Y Angle, Camera Distance, X Angle, Y Angle, Combined Ratio of Used Space & Average Relative Change of Mean Curvature

Figure 202: 3D Case 2: X & Y Angle, Camera Distance, X Angle, Y Angle, Combined Ratio of Used Space & Average Relative Change of Mean Curvature

### Z Exaggeration & Combined Ratio of Used Space & Average Relative Change of Mean Curvature

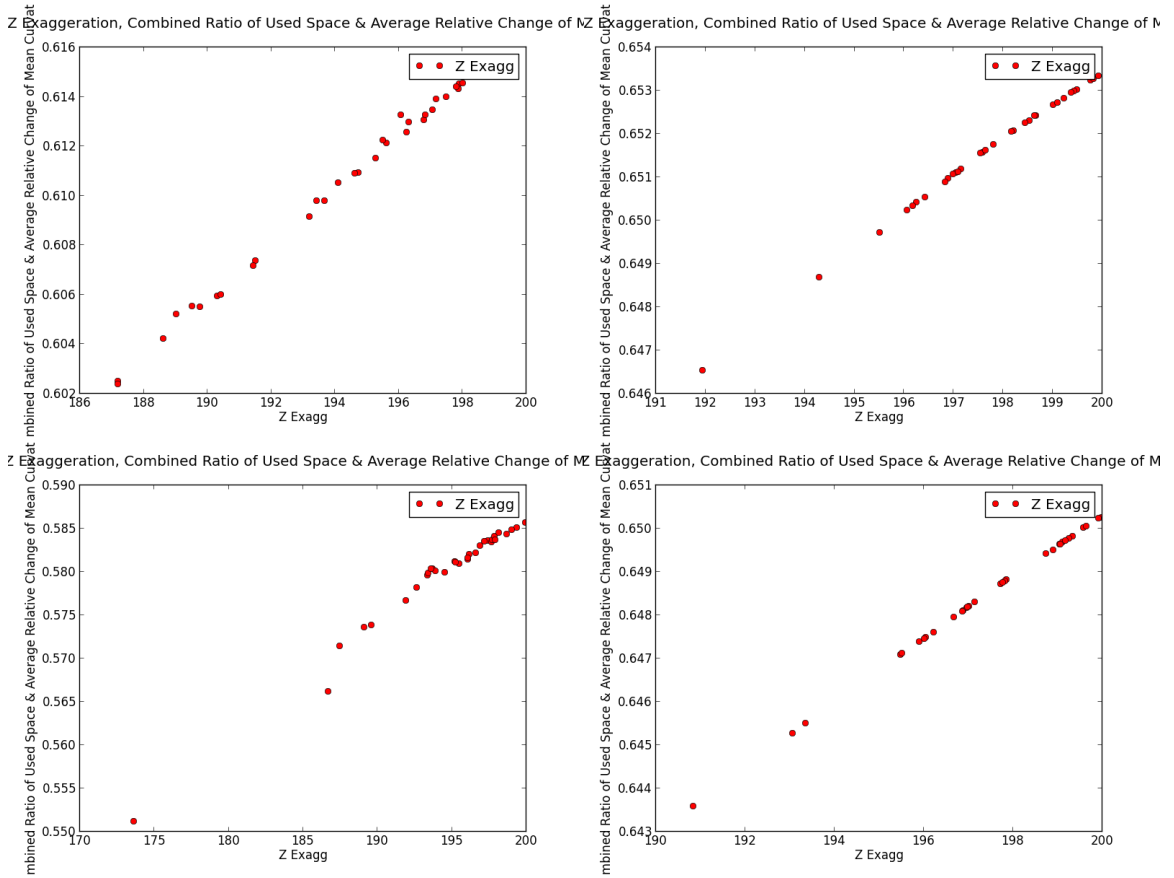
View	Top	45	X & Y Angle		
Input	Z Exagg	Z Exagg	Z Exagg	X Angle	Y Angle
Case 1	0.996	0.977	0.797	0.044	0.009
Case 2	0.998	0.999	0.871	0.002	0.014
Avg	0.997	0.988	0.834	0.023	0.011

Table 50: Z Exaggeration & Combined Ratio of Used Space & Average Relative Change of Mean Curvature Correlation per experiment

	Top		45		X & Y Angle	
	Min	Max	Min	Max	Min	Max
Case 1	0.6	0.6	0.6	0.6	0.3	0.7
Case 2	0.6	0.7	0.6	0.7	0.3	0.8
Avg	0.6	0.6	0.6	0.6	0.3	0.7



**Table 51: Z Exaggeration & Combined Ratio of Used Space & Average Relative Change of Mean Curvature Min Max per experiment**



**Figure 203: Top & 45: Z Exaggeration & Combined Ratio of Used Space & Average Relative Change of Mean Curvature**

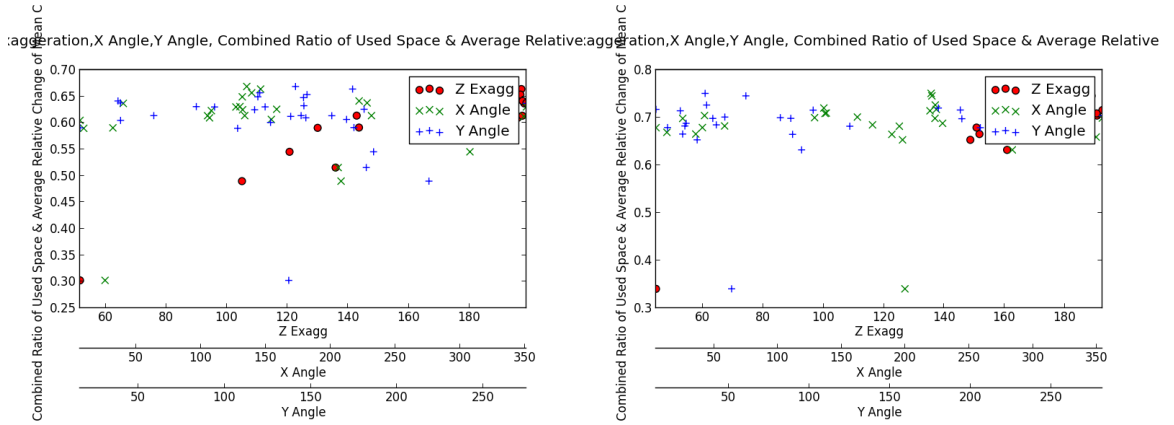


**Figure 204: X & Y Angles Z Exaggeration & Combined Ratio of Used Space & Average Relative Change of Mean Curvature**



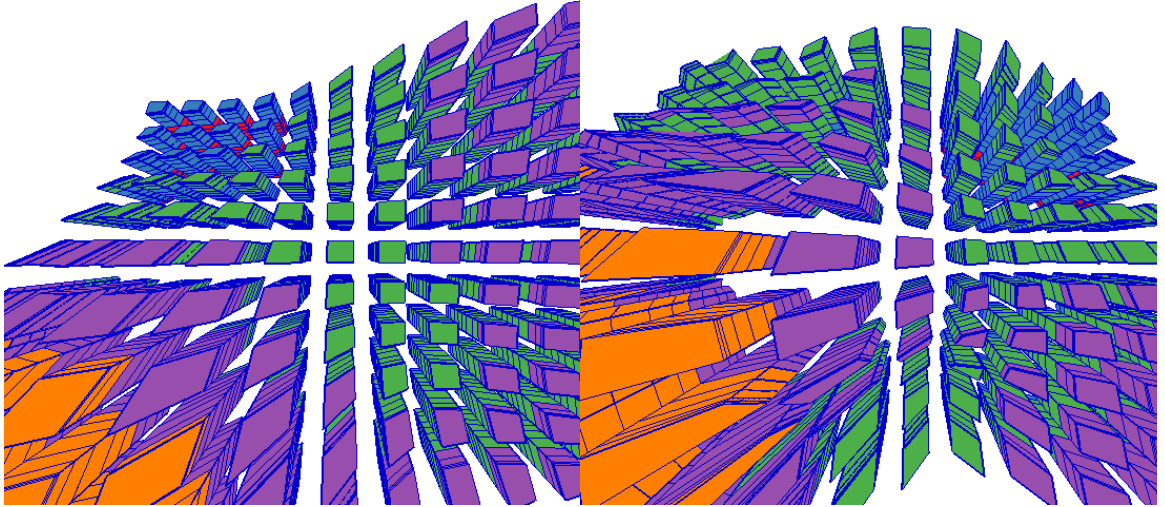


**Figure 205: 3D Case 1: Top, Z Exaggeration,  
Combined Ratio of Used Space & Average Relative  
Change of Mean Curvature**

**Figure 206: 3D Case 2: Top, Z Exaggeration,  
Combined Ratio of Used Space & Average Relative  
Change of Mean Curvature**

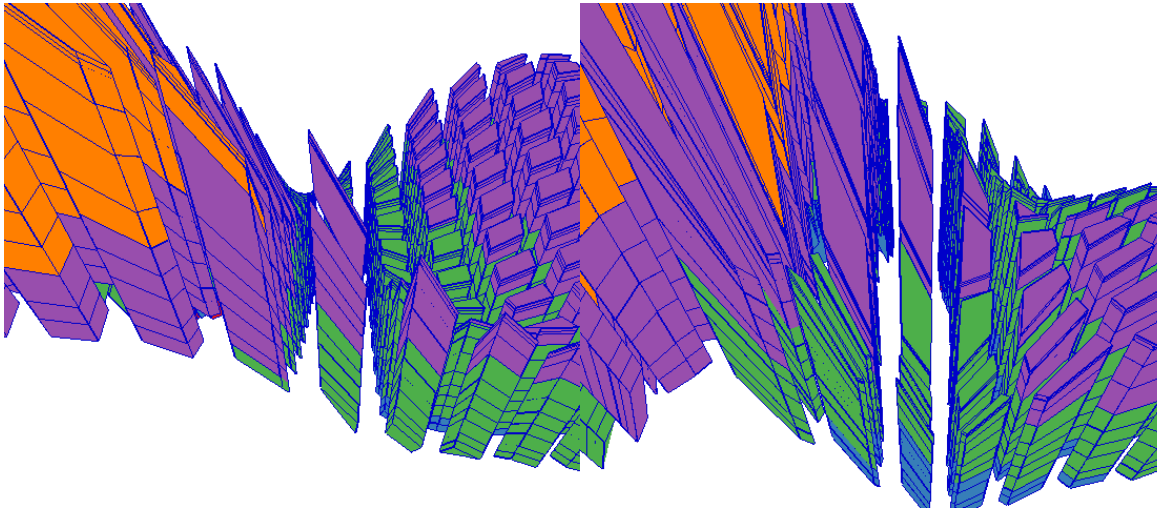


**Figure 207: 3D Case 1: 45, Z Exaggeration,  
Combined Ratio of Used Space & Average Relative  
Change of Mean Curvature**

**Figure 208: 3D Case 2: 45, Z Exaggeration,  
Combined Ratio of Used Space & Average Relative  
Change of Mean Curvature**

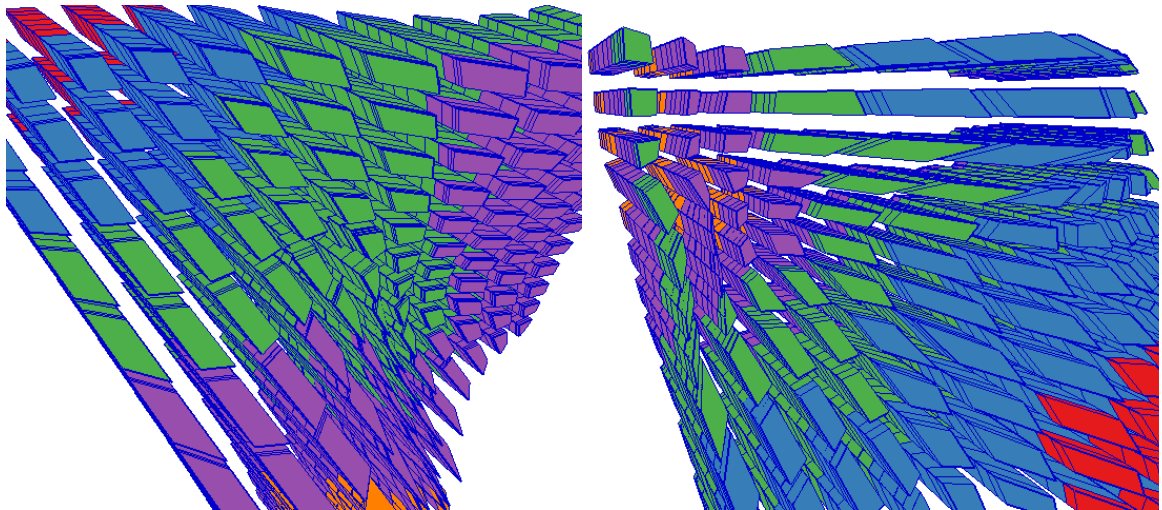


**Figure 209: 3D Case 1: X & Y Angle, Z Exaggeration, X Angle, Y Angle, Combined Ratio of Used Space & Average Relative Change of Mean Curvature**

**Figure 210: 3D Case 2: X & Y Angle, Z Exaggeration, X Angle, Y Angle, Combined Ratio of Used Space & Average Relative Change of Mean Curvature**

### **XY Displacement & Combined Ratio of Used Space & Average Relative Change of Mean Curvature**

View	Top	45	X & Y Angle		
Input	XY Disp	XY Disp	XY Disp	X Angle	Y Angle
Case 1	0.265	0.776	0.684	0.000	0.000
Case 2	0.810	0.986	0.566	0.049	0.111
Avg	0.537	0.881	0.625	0.025	0.056

**Table 52: XY Displacement & Combined Ratio of Used Space & Average Relative Change of Mean Curvature Correlation per experiment**

	Top		45		X & Y Angle	
	Min	Max	Min	Max	Min	Max
Case 1	0.2	0.3	0.3	0.3	0.3	0.5
Case 2	0.3	0.3	0.3	0.4	0.2	0.5
Avg	0.3	0.3	0.3	0.3	0.2	0.5

**Table 53: XY Displacement & Combined Ratio of Used Space & Average Relative Change of Mean Curvature Min Max per experiment**

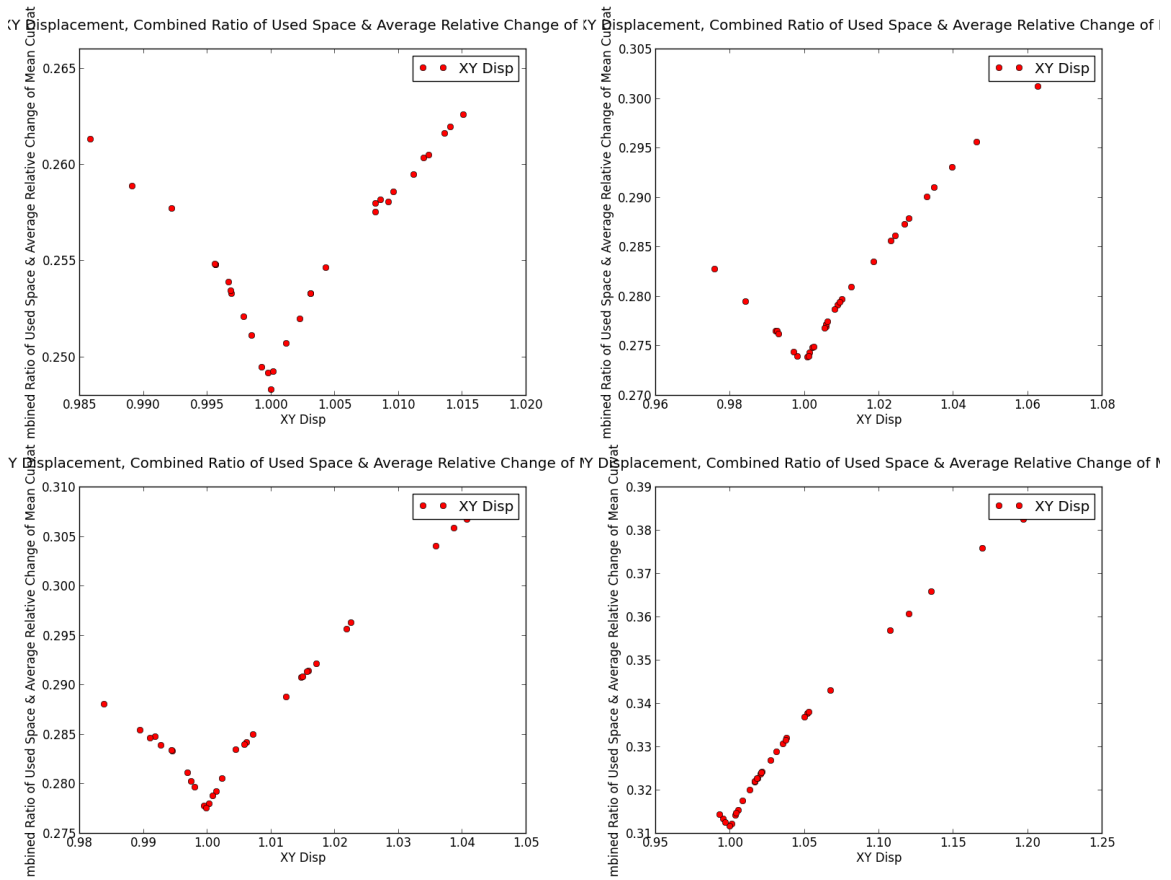


**Figure 211: Top & 45: XY Displacement & Combined Ratio of Used Space & Average Relative Change of Mean Curvature**

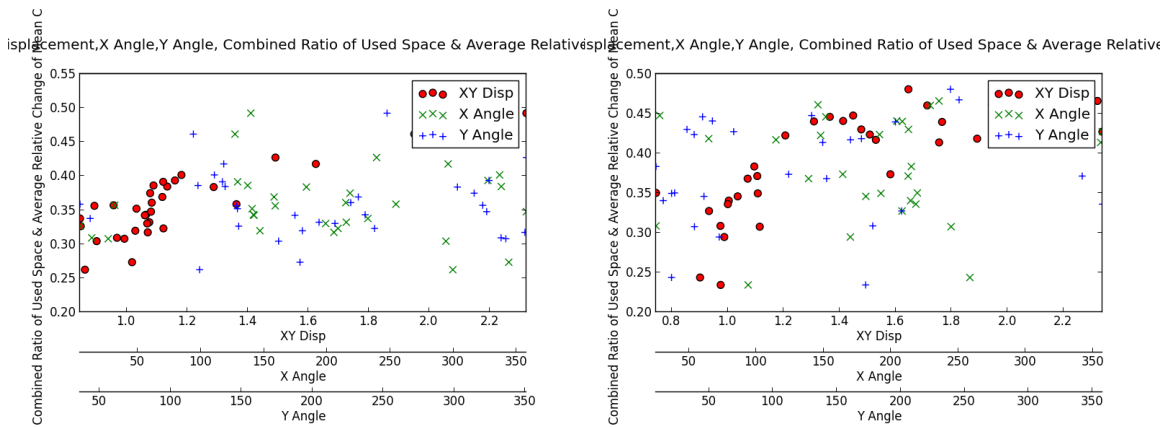


**Figure 212: X & Y Angles XY Displacement & Combined Ratio of Used Space & Average Relative Change of Mean Curvature**

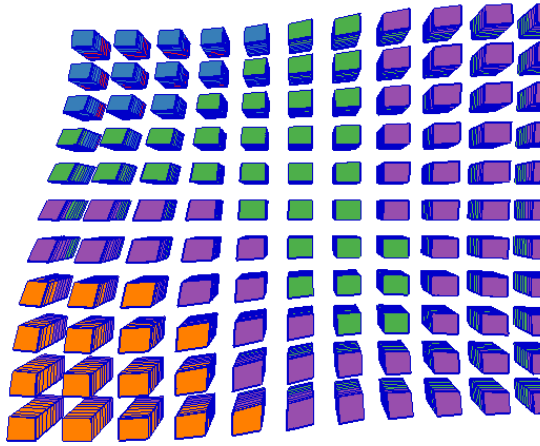


**Figure 213: 3D Case 1: Top, XY Displacement, Combined Ratio of Used Space & Average Relative Change of Mean Curvature**

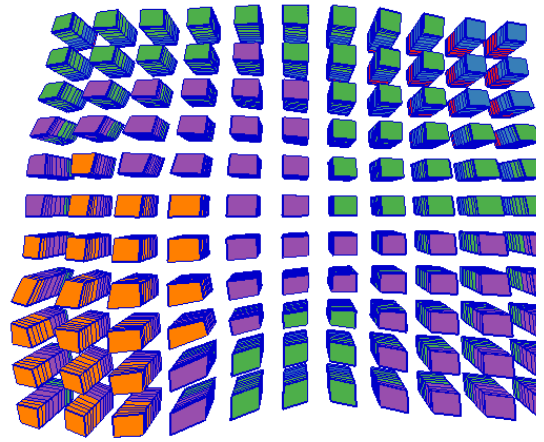


**Figure 214: 3D Case 2: Top, XY Displacement, Combined Ratio of Used Space & Average Relative Change of Mean Curvature**

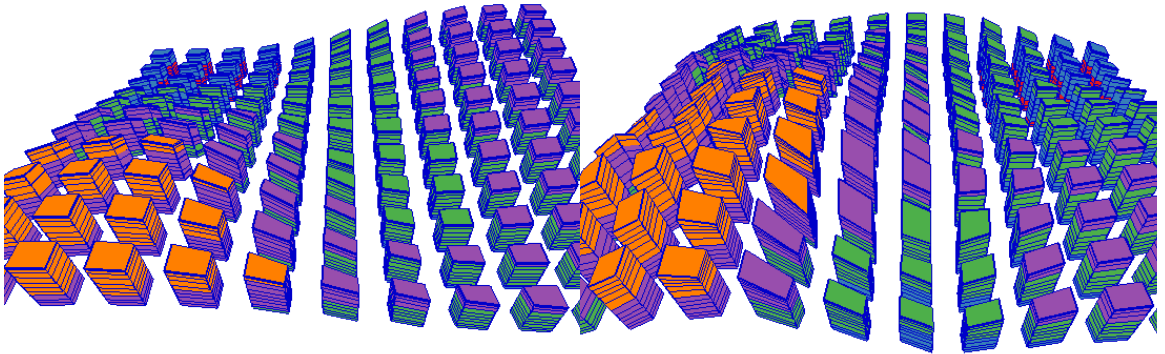


**Figure 215: 3D Case 1: 45, XY Displacement, Combined Ratio of Used Space & Average Relative Change of Mean Curvature**

**Figure 216: 3D Case 2: 45, XY Displacement, Combined Ratio of Used Space & Average Relative Change of Mean Curvature**

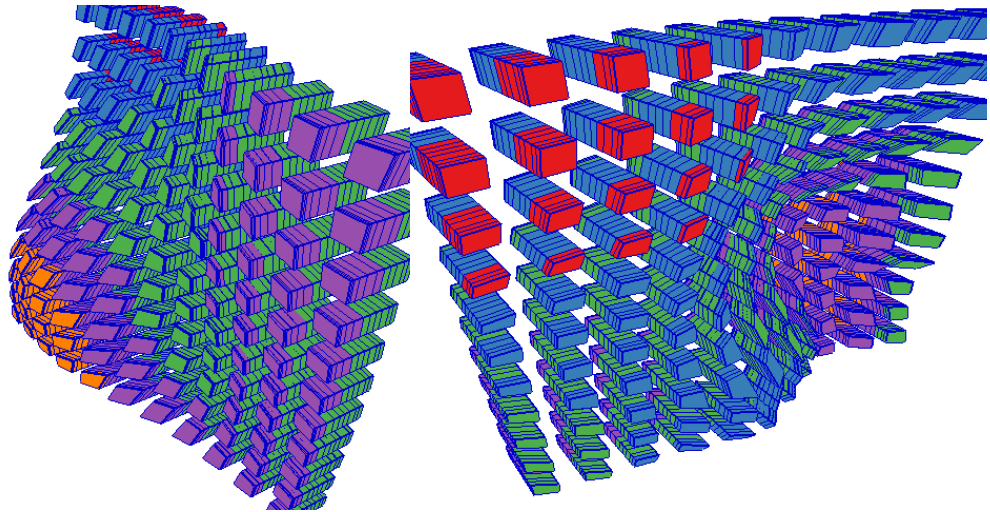


**Figure 217: 3D Case 1: X & Y Angle, XY Displacement, X Angle, Y Angle, Combined Ratio of Used Space & Average Relative Change of Mean Curvature**

**Figure 218: 3D Case 2: X & Y Angle, XY Displacement, X Angle, Y Angle, Combined Ratio of Used Space & Average Relative Change of Mean Curvature**

### XYZ Displacement & Combined Ratio of Used Space & Average Relative Change of Mean Curvature

View	Top	45	X & Y Angle		
Input	XYZ Dis	XYZ Dis	XYZ Dis	X Angle	Y Angle
Case 1	0.992	0.994	0.326	0.000	0.007
Case 2	0.933	0.907	0.117	0.015	0.070
Avg	0.962	0.950	0.222	0.007	0.038

**Table 54: XYZ Displacement & Combined Ratio of Used Space & Average Relative Change of Mean Curvature Correlation per experiment**

	Top		45		X & Y Angle	
	Min	Max	Min	Max	Min	Max
Case 1	0.4	0.4	0.4	0.4	0.4	0.6
Case 2	0.4	0.4	0.5	0.5	0.5	0.7
Avg	0.4	0.4	0.4	0.5	0.4	0.7

**Table 55: XYZ Displacement & Combined Ratio of Used Space & Average Relative Change of Mean Curvature Min Max per experiment**

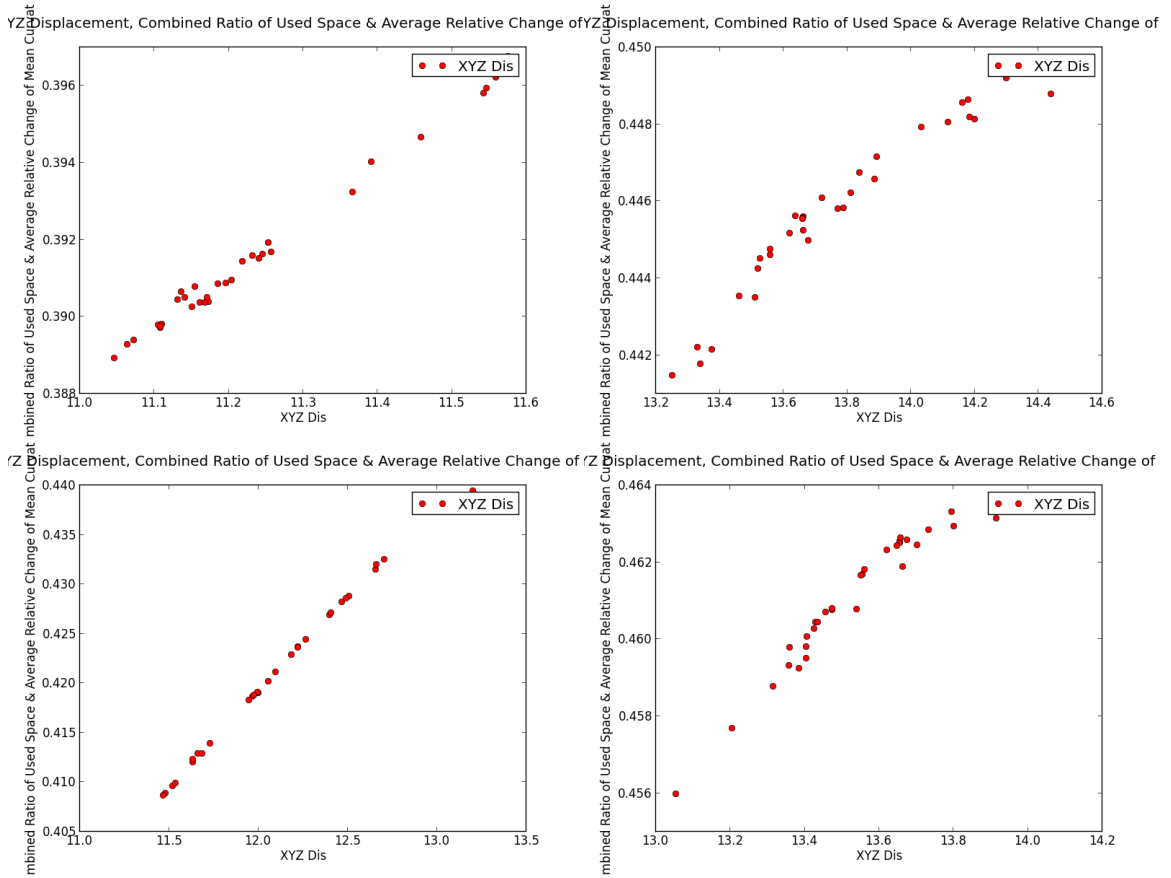


**Figure 219: Top & 45: XYZ Displacement & Combined Ratio of Used Space & Average Relative Change of Mean Curvature**

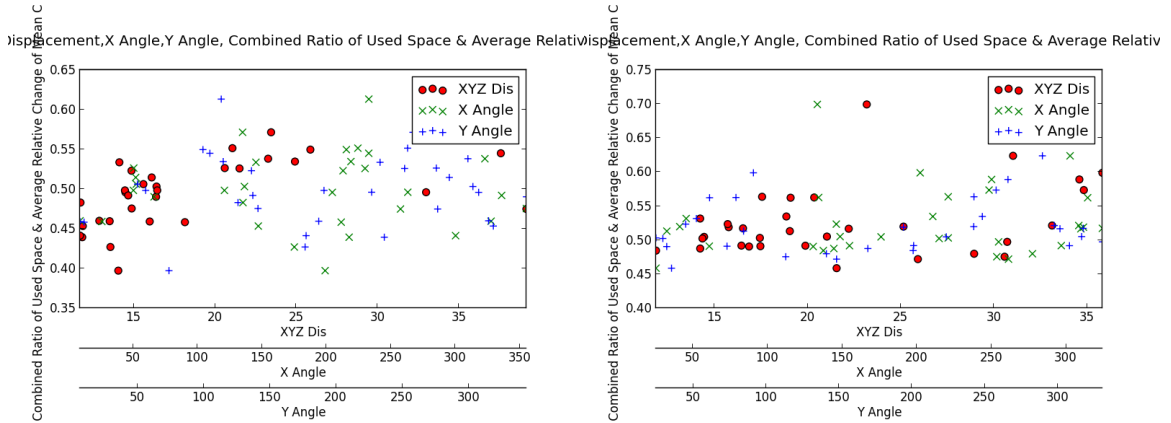


**Figure 220: X & Y Angles XYZ Displacement & Combined Ratio of Used Space & Average Relative Change of Mean Curvature**



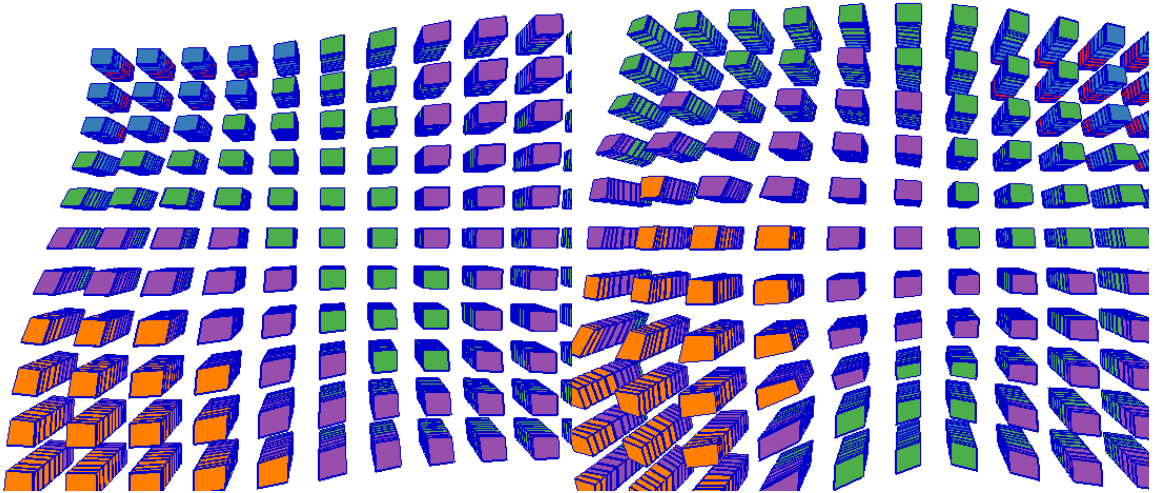


**Figure 221: 3D Case 1: Top, XYZ Displacement, Combined Ratio of Used Space & Average Relative Change of Mean Curvature**

**Figure 222: 3D Case 2: Top, XYZ Displacement, Combined Ratio of Used Space & Average Relative Change of Mean Curvature**

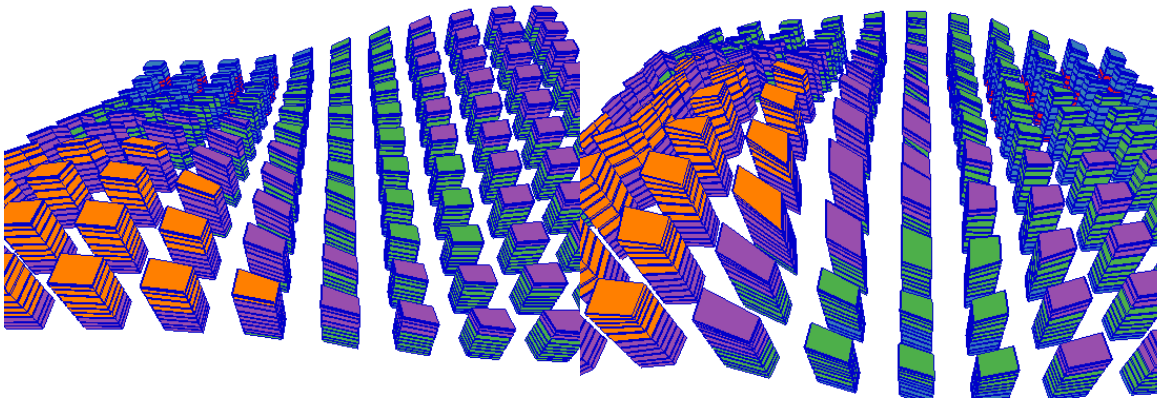


**Figure 223: 3D Case 1: 45, XYZ Displacement, Combined Ratio of Used Space & Average Relative Change of Mean Curvature**

**Figure 224: 3D Case 2: 45, XYZ Displacement, Combined Ratio of Used Space & Average Relative Change of Mean Curvature**

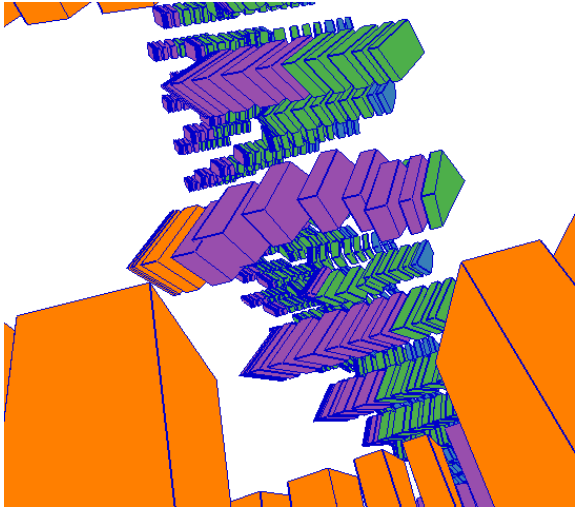


**Figure 225: 3D Case 1: X & Y Angle, XYZ Displacement, X Angle, Y Angle, Combined Ratio of Used Space & Average Relative Change of Mean Curvature**

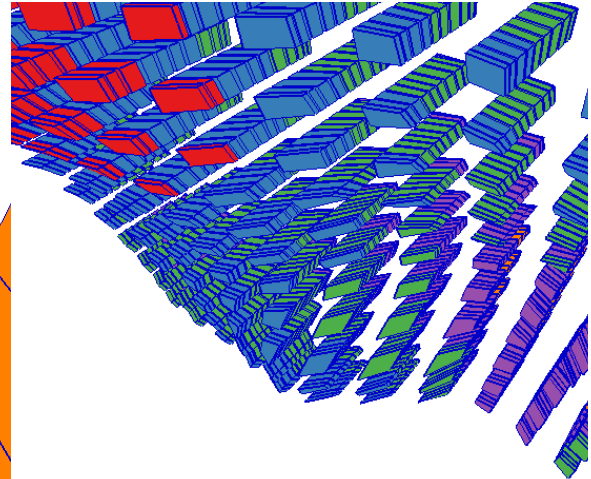


**Figure 226: 3D Case 2: X & Y Angle, XYZ Displacement, X Angle, Y Angle, Combined Ratio of Used Space & Average Relative Change of Mean Curvature**



## Vitae

Name :Badr Muhammad Al Harbi

Nationality :Saudi

Date of Birth :10/23/1977

Academic Background :Earned a Bachelor of Science (BS): Computer Engineering from King Fahd University of Petroleum and Minerals (KFUPM), Dhahran, Saudi Arabia, in June 2001

Papers :Al-Harbi, Badr, Ali Alturki, and Adel Ahmed. "An Application of Measuring Aesthetics in Visualization." International Conference on Cooperative Design, Visualization and Engineering. Springer International Publishing, 2016.

Email :badrharbi@gmail.com